Photodegradation of Wool and Wool Blend Fabrics in Relation to Their Use in Automotive Upholstery

A thesis submitted to the
University of Manchester Institute of Science and Technology
for the degree of
Doctor of Philosophy
in the
Faculty of Technology

December 1995

Dianne C. Jones

Department of Textiles

Dedicated to the memory of my father

Abstract

The aim of this study was to investigate the photostability of wool, relative to its performance in automotive upholstery. The rate of photoyellowing, phototendering and dye fading of wool was examined under automotive environmental conditions. The application of a UV absorber, Cibafast W, was found to have a short term protective effect. A range of 100% wool and wool blend fabrics were developed and tested for lightfastness and wear performance. Photostabilized wool blend fabrics reach car manufacturers lightfastness standards depending on the blend percentage used. Material specifications can have a considerable effect on fabric performance. Both lightfastness and abrasion resistance of wool fabrics improve with increasing mean wool fibre diameter. Wool / polyester blends have a pilling tendency making them unacceptable for automotive use, whereas wool / nylon blends have superior abrasion resistance both before and after light exposure. Factors such as fabric lamination and the application of surface treatments increase the rate of photodegradation.

A number of analytical techniques were used to investigate the effect of light exposure on the physicochemical properties of wool. Using X-ray Photoelectron Spectroscopy (XPS), the rate of surface photooxidation of wool was found to occur at more than twice the rate for nylon and polyester fabrics. Cystine residues in the epicuticle are rapidly oxidised on initial exposure to light and the application of Cibafast W gives no significant protection to the outermost surface of undyed or dyed wool. Static Secondary Ion Mass Spectrometry (SSIMS) indicates changes in the relative concentrations of bound fatty acids of the wool epicuticle following light exposure, with photooxidation of the main component 18-methyleicosanoic acid implicated. Using the techniques of FT-Raman and FT-IR spectroscopy the rate of bulk cystine photooxidation was followed by examining decreases in the disulphide bond signal and increases in bands assigned to the oxidation products of cystine. These techniques suggest that disulphide bond cleavage is accompanied by changes in structural conformation of the fibre which may involve a loss in α-helical content. FT-IR and FT-Raman analysis show that Cibafast W gives significant protection to cystine residues in the bulk and inner surface of undyed and dyed wool. Considerable changes in the surface morphology of light degraded wool were found using Scanning Electron Microscopy (SEM) and Atomic Force Microscopy (AFM). Light induced surface migration of photostabilizers in polyester and nylon fabrics was detected using XPS, but in wool this migratory behaviour is still unproven.

Declaration

No portion of the work referred to in this thesis has been submitted in support of an application for another degree or qualification of this or any other university or other institution of learning.

Dianne C. Jones

December 1995

Acknowledgements

I would first like to thank my supervisors Dr. Chris Carr and Dr. Bill Cooke for their help and advice throughout this research project. I would sincerely like to thank Guilford Automotive for their financial support of this project. My gratitude also goes to the International Wool Secretariat for sponsorship during the first year of research and the supply of materials throughout the project. I am very grateful for the help given by many of the technical staff at Guilford Automotive, in particular the project supervisors David Marriott, Mike Taylor and the late Mike Kowalski. I am indebted to David Pearson for his support and commitment to the research project.

I would like to thank the many members of staff in the Department of Textiles at UMIST who have given me help and advice. For technical assistance I would like to acknowledge the help of Trevor Jones, Jean Walton, Les Downes, Don Burnham and Alison Harvey. I would particularly like to thank Stuart Reyner for sorting out all those impossible computer problems. This list would not be complete without thanking Ken Walker and Steve Smith for providing me with the much needed cups of tea.

I would like to thank Dr. John Vickerman of the Department of Chemistry at UMIST for access to XPS instrumentation, and particularly Alex Henderson for his expert advice. I must also thank Dr. John Walton in the Department of Corrosion for AFM analysis.

My thanks also go to various people within many different organisations for their help and advice during this research. In particular Dr. David James at Nicolet Instruments and Dr. Shaun Smith, Peter Duffield, Barry Greenwood and Brian Maston at the International Wool Secretariat.

Finally I would like to thank my family for their support and encouragement. I would dearly like to thank Mark for his patience, understanding and the household chores!

Contents

Chapter 1

Introduction

1.1 Automotive Fabrics: Requirements and Considerations

In the early years of car production, seats were covered with leather or heavily milled woollen fabrics. However, as the motor industry expanded there was a need for a consistent product which could be mass produced to known levels of performance. PVC was used during the 1960's, but its poor tactile quality and impermeability led to the use of woven and warp knitted Nylon 6 fabrics during the early 1970's. The proportion of glazed areas increased with changes in car exterior design, subjecting upholstery fabrics to greater amounts of light. The poor light stability of Nylon 6 significantly reduced its performance and eventually led to its replacement by polyester by the 1980's. The high light stability of dyed polyester means it remains as the main fibre in current use. A variety of woven and knitted fabric structures are used, usually laminated to a polyester or polyether urethane foam backing. Consumer demand for greater comfort and luxury of interior styling has led some manufacturers to seek alternatives to man-made fibres, with particular interest in wool. There is caution however, due to the unproven performance of wool to current automotive standards and in service. A need to determine information on the performance of wool under these conditions initiated this study.

Automotive manufacturers demand stringent performance and quality standards for upholstery fabrics. The appearance, hand and physical performance of fabrics must remain unchanged for the greater part of the life span of the vehicle. This is difficult to achieve since automotive fabrics must often face abrasive, tensile and compressional forces under severe environmental conditions. Photodegradation of fibres occurs during exposure to the high energy UV region of the spectrum. This region is divided into UV-A (400-320 nm), UV-B (320-280 nm) and UV-C (> 280 nm). Wavelengths below 290 nm do not reach the earth due to filtering by atmospheric ozone, the intensity and distribution of the UVB component is variable with season and location[1]. Automotive side and rear window glass filters wavelengths below 310 nm, laminated glass used in windscreens filters light below 340 nm [2]. However, the radiant energy is still sufficient to cause chemical and structural changes in fibres leading to a

reduction in the physical integrity of fabrics. Exposure to light causes discolouration of fabrics due to yellowing of the fibres and the fading of dyestuffs. Photodegradation is accelerated by the elevated temperatures often encountered in enclosed vehicles. Fabric surface temperatures of over 100°C have been recorded in vehicles in Australia[3] . An increase in humidity generally increases the rate of photodegradation of many fibres[4].

In order to anticipate in-service performance of fabrics, automotive manufacturers have developed comprehensive laboratory testing programmes involving a large number of specialised test methods. Of particular importance is light fastness performance, abrasion resistance, tensile strength and flammability. Accelerated light fastness testing is carried out using xenon light sources in enclosed chambers with controlled temperature and humidity levels[5]. Fabrics are subjected to specified levels of radiant exposure and then measured for changes in colour, strength and abrasion resistance. Abrasion resistance is tested using accelerated methods such as Martindale, Taber and Stoll. Fabrics must reach a specified number of abrasion cycles and are judged on structural integrity and appearance retention. New textile products must be engineered in order to meet these standards, the correct choice of fibre type, dyestuff, fabric structure and finishing route is critical. Natural fibres pose a difficulty to this engineering approach since the variation in their inherent physical and chemical properties make the useful lifetime of fabrics more difficult to predict.

1.2 The Chemistry and Morphology of Wool

Wool belongs to the class of fibrous proteins known as keratins. Keratins are defined as insoluble crosslinked proteins containing a sulphur content of at least 2%, present mainly in the amino acid cystine[6]. Fibres can show significant variation in their physical and chemical properties depending on the breed of sheep and their diet, health and climate during growth. The wool fibre is cylindrical, it tapers gradually from root to tip and has a spiral crimped form, the number of crimps ranging from 0-12 per cm. Fibre diameters can range between 15 μm for merino wool to over 50 μm for coarser breeds. Fibre lengths vary from 30 cm in coarse wool to 8 cm in finer breeds.

1.2.1 The Polymer System

The structural units which form the polymer chains in wool are the α-amino acids, the general formula is shown in Figure 1.1. All amino acids contain carboxyl and amino groups but are characterised by the nature of their side chain groups (R). Eighteen different amino acids have been identified in wool, differing in the size and chemical nature of their side chains. Those with non-polar hydrocarbon side chains, alanine, glycine, isoleucine, leucine, valine and phenylalanine have low chemical reactivity and vary in hydrophobic character. Serine, threonine and tyrosine have a polar hydroxyl group in their side chains and are chemically more reactive. There are two sulphur-containing amino acids, methionine and cystine and two heterocyclic residues, proline and tryptophan, Figure 1.1. The most reactive side chains are those which contain acidic or basic groups. Aspartic acid and glutamic acid have carboxyl functional groups in their side chains. Arginine, lysine and histidine have basic side chains containing guanidyl, amino and glyoxalyl functional groups respectively. The concentration of these amino acids in wool can be variable and depends on factors such as breed of sheep, diet, health and climate during growth.

Proteins are formed on condensation of amino acids at their carboxyl and amino groups so that amino acids are linked in sequences by amide, or peptide links. The -NHCHRCO- repeating units are known as peptide groups, and polymer chains consisting of a large number of amino acids are termed polypeptides. A large proportion of the polypeptide chains in wool exist in helical configuration known as α- keratin, which has an axial repeat length of 0.51 nm. This helical configuration is stabilised by hydrogen bonds which form between the peptide -CO- and -NH- within adjacent turns of the helix. On stretching the fibre, the relaxed helical configuration is extended to a more linear sheet structure known as β-keratin.

The alignment of polypeptide chains in wool is such that a number of important interpolymer crosslinks are formed between reactive amino acid groups in adjacent chains. These crosslinks are mainly responsible for the mechanical properties of the fibre such as tensile strength and elasticity. Covalent disulphide bonds form between adjacent polypeptide chains via crosslinking of two cysteine residues to form one cystine residue, Figure 1.1. These interpolymer disulphide bonds are responsible for the physical stability of wool and are particularly important in resisting conformational changes in the fibre. Intrapolymer disulphide bonds may form within the same polymer chain. Salt linkages are also formed between the acidic and basic side chains in adjacent polypeptide chains. Links may form between the

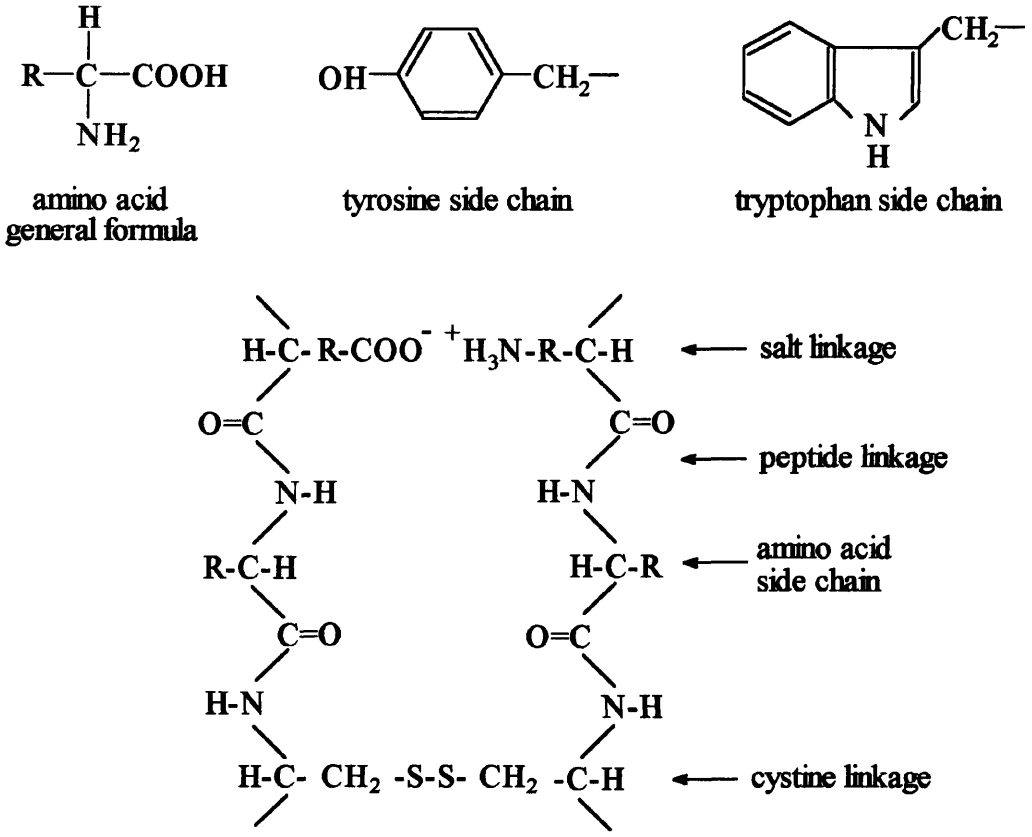

Figure 1.1 The polymer system of wool

ε–amino group of lysine and the γ-carboxyl group of glutamic acid, or less commonly to the β-carboxyl group of aspartic acid. Hydrogen bonding is a particularly important feature of wool, bonds can form between the peptide -CO- and -NH- groups in adjacent chains, or between side chain hydroxyl groups. Hydrophobic interactions may also occur between adjacent non-polar side groups such as phenylalanine, alanine, valine and leucine.

The ordered α-keratin and β-keratin structures are found regularly packed in the crystalline regions which make up 30-40% of the fibre. These crystalline regions are embedded in an amorphous matrix which is highly crosslinked. Three distinct fractions of keratinous proteins have been identified in wool. The distribution of these proteins varies between the morphological components causing regions of the fibre to differ in their physical and chemical properties. Low sulphur proteins make up 58% of the fibre and have an average sulphur content of 1.5%. They are rich in glutamic acid, lysine, aspartic acid, leucine and arginine and are mainly found in the crystalline regions since they are the only group with α-helical character[7,8]. High sulphur proteins make up 18% of the fibre with a sulphur content of 5% and are rich in cystine, serine, proline and threonine [8]. Ultrahigh sulphur proteins make up 8% with

a sulphur content of 8%[9]. The high sulphur proteins contribute to the amorphous regions of the fibre. In addition there are high glycine / tyrosine proteins which can vary in concentration from 1% in coarse breeds to 12% in Merino wool[10] . They have a low sulphur content in the range 0.5-2%[11]. There are also non-keratinous proteins which make up 17% of the fibre mass. They are low in cystine and are easily degraded since they are only slightly crosslinked. In wool they are found as a network structure embedded in the keratinous proteins and are the chemical and physical weak regions of the fibre[12].

1.2.2 Fibre Morphology

The Cuticle

The cuticle forms the outermost surface of the fibre representing approximately 10% of the total fibre mass and is responsible for much of the fibre's chemical and physical properties[13]. It is particularly rich in cystine, serine and proline and may be more amorphous than the rest of the fibre[14]. The cuticle is less extensible than the cortex due to the high degree of disulphide crosslinking. The cuticle consists of a single layer of flattened cells which vary in thickness from 0.5 - 0.9 μm depending on breed. The cells overlap to give a characteristic scale pattern with their free ends directed towards the fibre tip. The cuticle is divided into three distinct layers with differing chemical properties. The epicuticle is the outermost layer, it is a thin hydrophobic membrane approximately 2-4 nm thick[15] and it surrounds each cuticle cell individually[16] . It consists of keratinous proteins and is estimated to have a cystine crosslink content of 6% and a high lysine content [15]. The epicuticle has an exterior lipid layer called the F-layer which consists mainly of a C_{21} fatty acid bound to the surface protein by thioester linkages[17] [18]. It is thought to be responsible for the hydrophobic nature of wool. Beneath the epicuticle is the exocuticle which represents about 60% of the cuticle[19] . It contains high sulphur proteins and is estimated to have a cystine crosslink content of 10%, about twice the density of the fibre as a whole [19]. The uppermost layer adjacent to the epicuticle is called the A-layer and is approximately 30-50 nm thick [19]. The A-layer is even more highly crosslinked having a higher sulphur content than the rest of the exocuticle. Studies of wear damaged wool show that this layer is the most resistant to degradation due to the high degree of disulphide crosslinking [12]. Below the exocuticle is the amorphous endocuticle which makes up about 40% of the cuticle [19]. It contains non-keratinous proteins and has the lowest cystine crosslink content of the cuticle of 1.6% [19]. This layer is mechanically the weakest of the cuticle, it is

often found to be the place of initial cleavage during wear, reflecting the low degree of crosslinking [12].

The cuticle is held to the cortex by a cementing layer known as the cell membrane complex, which contains lipids, chemically resistant membranes and a material known as intercellular cement which contains non-keratinous proteins rich in high glycine, tyrosine and phenylalanine[20]. The cell membrane complex also cements the overlapping cuticle cells together and surrounds individual cortical cells. The chemical nature of the three types of cell membrane complex is thought to be different[21].

The Cortex

The cortex makes up the bulk of the fibre and consists of long spindle shaped cells aligned with the fibre axis. The cortex is divided into two distinct regions, the orthocortex and paracortex which show a distinct bilateral segmentation in fine wool fibres, but are more randomly distributed in coarse fibres[22]. Both regions are made up of a number of macrofibrils surrounded by an intermacrofibrillar matrix. In the orthocortex, the macrofibrils are smaller and more distinct, whereas in the paracortex the macrofibrils are more randomly distributed and poorly defined in structure. The macrofibrils contain hundreds of crystalline microfibrils which are thought to consist mainly of α-helical low sulphur proteins[23] but may also contain a proportion of high sulphur proteins[24]. The microfibrils are packed in an amorphous intermicrofibrillar matrix made up of high sulphur and high glycine / tyrosine proteins[25]. In the orthocortex, the microfibrils are tightly packed in the macrofibrils and form whorl-like arrangements[26]. In the paracortex the microfibrils are less densely packed and are more randomly arranged. The paracortex is more rigid and chemically resistant than the orthocortex due to a higher proportion of intermicrofibrillar matrix which is rich in high sulphur proteins. The paracortex has a cystine crosslink concentration of 7.7% compared to 6.1%[27] for the orthocortex. The orthocortex has a higher concentration of low sulphur proteins due to the higher content of α-helical microfibrils. It may also be richer in high glycine / tyrosine proteins[28]

1.2.3 Disulphide Bond Oxidation

The disulphide bonds of cystine are one of the most susceptible oxidation sites in wool. Since they are of prime importance to the integrity of the polymer system their chemical reactivity will be considered briefly. The extent of oxidation depends on the nature of the oxidising

species, for example whether it is a chemical agent or oxygen attack during light or heat exposure. Chemical oxidising agents are often used to alter the properties of wool by specific modification of the disulphide bonds. The final oxidation product of cystine is cysteic acid (sulphonic acid) and its concentration provides a measure of the extent of disulphide bond oxidation. If mild conditions of oxidation are used, or if oxidising agents are used under neutral or acidic conditions then intermediate oxidation products are formed. These products are decomposed in alkaline solutions, unstable under the conditions of acid hydrolysis and decompose to cystine and cysteic acid under hydrolytical conditions making their detection difficult.

Three possible pathways have been identified for the oxidation of disulphides, paths (1) and (2) involving S-S fission and path (3) involving C-S fission. The main intermediate products are shown in Figure 1.2 although other intermediate products may be possible between each step[29] . In paths (1) and (2), two moles of cysteic acid are produced whereas in path (3) one mole of cysteic acid and one mole of H_2SO_4 are produced. In path (1) the disulphide bond remains intact during stepwise oxidation, this pathway can only be expected during oxidation under non-hydrolytical conditions, for example photooxidation. Paths (2) and (3) are favoured under hydrolytical conditions. The end product, cysteic acid, is stable to acids, alkalis, oxidising and reducing agents, but severe treatments with oxidising agents may cause decomposition. The intermediate oxidation products cystine-S-monoxide (i), cystine-S,S-dioxide (ii), cysteine sulphinic acid (iv) and cysteine-S-sulphonic acid (vi) have been detected in various quantities in oxidised wool depending on treatment and conditions[30] [31].

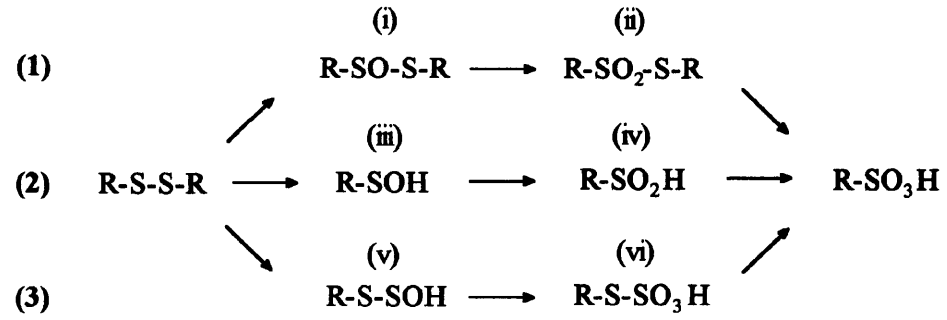

Figure 1.2 Oxidation pathways for disulphides such as cystine [29]

1.3 Photochemistry of Polymer Systems

1.3.1 Introduction to Photochemical Processes

Absorption of Radiation

The Grotthus-Draper law states that, *only light absorbed by a molecule can induce a photochemical change within it.* It is necessary that the system contains chromophores which are able to accept energy and any light passing through the system which is not absorbed will not initiate reaction. The development of quantum theory gave the Stark-Einstein law; *A molecule undergoing photochemical change does so through the absorption of a single quantum of light.* Absorption of a quantum of radiation by a chromophore raises it from an initial lower energy state, known as the ground state ($\mathbf{E}_0$), to a higher energy excited state ($\mathbf{E}_1$). The energy required for this transition must be equal to the photon energy ($\mathbf{E}\ (h\nu)$)[32].

$$\mathbf{E}\ (h\nu) = \mathbf{E}_1 - \mathbf{E}_0 \qquad [1.1]$$

If the photon has the correct energy, absorption can only occur if the electronic transition causes a property known as the transition dipole moment to have non-zero values and therefore be an 'allowed' transition. During an electronic transition there is a redistribution of charge in the molecule, if there is a difference in magnitude of the dipole moment of the ground state molecule compared to the excited state then a transition dipole moment is induced. The transition dipole moment is therefore a measure of the magnitude and direction of charge during a transition. The intensity of absorption of light of specific frequency by a chromophore is related to the square of the transition dipole moment.

The electronic energy states of molecules have discrete energy levels specific to the molecule. Associated with each electronic state are a number of vibrational and rotational energy levels. Transitions between electronic states occur during the absorption of UV and visible light via the promotion of electrons from molecular orbitals of lower to higher energy. In ground state organic molecules, the molecular orbitals most populated by valence electrons are the σ, π bonding orbitals and the *n* non-bonding orbitals. Ground state organic molecules also contain higher energy molecular orbitals which are sparsely populated by electrons, these are the σ^* and π^* antibonding orbitals. Absorption of UV or visible light promotes an electron from one of the σ, π or *n* orbitals to the higher energy antibonding orbitals σ^* or π^*. In ground state molecules each molecular orbital can contain up to two electrons with opposed spins. This

state, in which all the electrons in molecular orbitals are spin paired, is known as the ground singlet state of the molecule (S_0) . In most cases, electronic transitions occur from the ground singlet state and electrons are promoted to higher energy orbitals without a change in their direction of spin. The excited state populated in this case is known as a singlet excited state and may take a number of discrete values (S_1 ...S_n). In addition there is a second type of excited state which is usually populated by energy transitions from the singlet excited state. This state contains pairs of electrons with parallel spin directions and is known as the triplet excited state (T_1 ...T_n). It is of lower energy than the equivalent singlet excited state.

The nature of the transition which takes place between two molecular orbitals depends on the energy of the incident light and the absorbing chromophore involved. The electronic transitions and absorption wavelengths of some simple chromophores are shown in Figure 1.3. It can be seen that the energy supplied by near UV radiation is sufficient only to excite certain ($\eta \rightarrow \pi^*$) and ($\pi \rightarrow \pi^*$) transitions and also the ($\eta \rightarrow \sigma^*$) transition of peroxides. Chromophores of particular interest in polymer systems are C=O, aromatic molecules, peroxides and unsaturated groups.

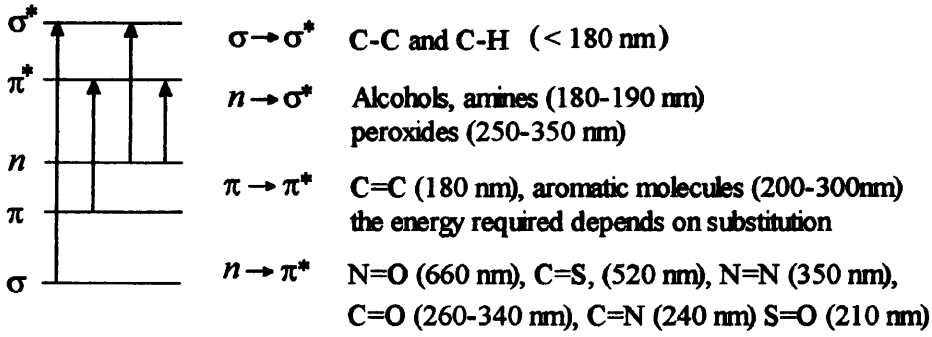

Figure 1.3 Electronic energy transitions of some simple chromophores

De-excitation Processes

The electronically excited molecule is unstable and it must find a pathway to dissipate the excess energy and return to the ground state. There are a number of harmless photophysical processes which do not alter the chemical nature of the absorbing molecule. The excited molecule may release its energy by emission of a photon as the electron returns from the higher excited state to the ground state. This is called fluorescence if the transition is from the first singlet excited state to the ground state ($S_1 \rightarrow S_0$). Phosphorescent emission occurs when the first triplet excited state returns to the ground singlet state involving an inversion of

electron spin ($T_1 \rightarrow S_0$). Fluorescent emission always occurs at longer wavelengths than the original absorption wavelength due to vibrational energy loss from the singlet excited state before emission occurs. Phosphorescence always occurs at longer wavelengths than fluorescence due to the lower energy of T_1 state compared to the S_1 state.

Non-radiative transitions may occur between electronic states within the same molecule. They rely on the overlap of electronic states in the molecule allowing energy to be passed from one to another. Internal conversion involves the direct transfer of energy between electronic states of the same spin multiplicity ($S_1 \rightarrow S_0$), the energy is lost as heat to return to the ground state. Intersystem crossing is a similar process, but in this case energy is transferred between states of differing spin multiplicity for example ($S_1 \rightarrow T_1$). or ($T_1 \rightarrow S_0$). Intersystem crossing from the first singlet excited state to the first triplet excited state is an important mechanism since the triplet excited state has a longer lifetime and is often more chemically reactive.

Energy may be dissipated by photochemical processes in which the molecule may fragment, rearrange or react with another molecule leading to a change in its chemical nature. These processes are important since they lead to the degradation of materials. Excitation energy from singlet or triplet state molecules may be transferred to other molecules. This process is important in many polymer systems since energy can be supplied to reactive molecules which cannot themselves absorb incident radiation. For transfer to occur, the excited state of the acceptor molecule must be lower in energy than the excited state of the donor. Also, the emission spectrum of donor and absorption spectrum of the acceptor must overlap. Transfer may occur by radiative processes in which a photon emitted from the donor is reabsorbed by the acceptor, which can occur over large molecular distances. It more commonly occurs by non-radiative processes involving direct electron exchange between the donor and acceptor molecular orbitals providing they are sufficiently close to overlap. Non radiative energy transfer can also take place between molecules over longer intermolecular distances up to 10 nm through dipole-dipole interactions.

1.3.2 Photochemical Processes in Polymers

Exposure of many natural and synthetic polymers to sunlight reduces their useful lifetime due to losses in tensile properties, discolouration, surface cracking and erosion. Incident radiation is unattenuated at the fibre surface and therefore surface degradation is particularly extensive.

Scission of bonds forming the main polymer backbone reduces the average relative molecular mass and leads to losses in mechanical and physical properties. In addition, photochemical reactions leading to the formation of new visible light absorbing chromophores is responsible for the discolouration of certain polymers, particularly wool. The photochemical processes leading to the degradation of polymers are complex and depend on the polymer structure and chemistry. In order for a polymer system to absorb UV light it must contain appropriate chromophores. Some polymers absorb light via specific chromophores which form part of the polymer repeat unit, for example the ester carbonyl groups in polyesters or the aromatic amino acids in wool. Others, such as polyamides do not contain groups inherent to their repeating units which can absorb light above 290 nm. The rapid photooxidation of these polymers is attributed to impurities situated in the polymer chain or side groups, with the rate of degradation often dependent on impurity concentration. These impurities are typically peroxides, hydroperoxides, carbonyl groups, α,β-unsaturated carbonyl groups, -C=C- unsaturations, aromatic groups and metallic impurities. These can be introduced during polymerization or they may be oxidation products formed during processing or storage. There are a large number of photochemical pathways through which the absorbing chromophores may dissipate their energy[32].

Those processes leading to the rupture of bonds integral to the polymer structure are of particular concern. Dissociation of bonds forming the polymer backbone is responsible for the phototendering of fibres. The energy of light between 290 - 400 nm is equivalent to 413 - 300 kJ mol^{-1} which is in the range of many single bond energies, for example the (C-C) bond energy is typically 350 kJ mol^{-1} . However, near UV light above 290 nm is of insufficient energy to be absorbed directly by C-C or amide groups forming the backbone of wool and nylon polymers. Energy may be supplied for the dissociation of these bonds by energy transfer from absorbing chromophores to sites on the polymer chain or side groups. Free radicals formed on dissociation of absorbing chromophores or subsequent reactions involving the excited chromophores, may attack the polymer backbone leading to chain scission. For many polymers these secondary processes leading to breakdown of the polymer chain have not been fully established.

In many polymer systems carbonyl groups present as impurities in the polymer chain are often the site of main chain cleavage. These groups strongly absorb near UV light and the photoexcited carbonyl triplet state is highly reactive and may undergo two reactions known as

the Norrish Type I and Type II processes. These involve chain scission adjacent to the electronically excited carbonyl group. The Norrish I process involves the formation of alkyl radicals, Figure 1.4 (i) whereas in the Norrish II process unsaturated groups are formed.

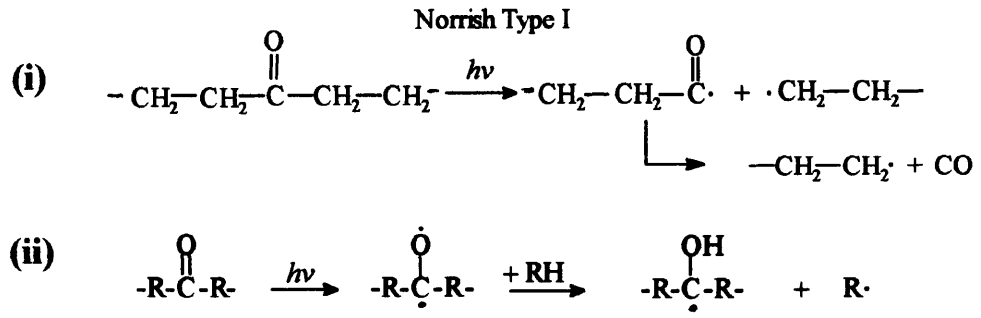

Figure 1.4 Reactions involving the photoexcited carbonyl chromophore

The triplet excited state carbonyl chromophore may also initiate free radical reactions. The reduction in negative charge over the oxygen atom due to the $(n \rightarrow \pi^*)$ transition causes hydrogen abstraction by the photoexcited carbonyl group, Figure 1.4 (ii). Hydrogen abstraction is usually from C-H groups in neighbouring molecules and the alkyl radical formed may then enter a number of reactions.

Photooxidation is the most important process leading to the degradation of polymers on exposure to near UV radiation. Photooxidation leads to increases in the concentrations of aldehydes, ketones, and carboxylic acid groups in polymers. The rate of accumulation of these groups during exposure is often used as an index of photodegradation. There are two mechanisms of photooxidation, both processes are initiated by a photoexcited species, usually in its triplet state (Sens(T_1)), which may be inherent to the substrate or may be present as an impurity. Type I process is illustrated in Figure 1.5. It involves hydrogen abstraction from sites on the polymer chain by a photoexcited chromophore or by free radical attack. Alkyl radicals are then formed (I) which react with molecular oxygen to form peroxy radicals (II). Hydrogen abstraction by peroxy radicals follows to form hydroperoxide groups (III) and also generates further alkyl radicals. Hydroperoxides absorb weakly in the near UV region causing cleavage of the O-O bonds to form alkoxy (IV) and hydroxyl radicals which are efficient hydrogen abstracting species. High temperatures during exposure will accelerate hydroperoxide decomposition. Alkoxy radicals may undergo chain scission with the formation of carbonyl

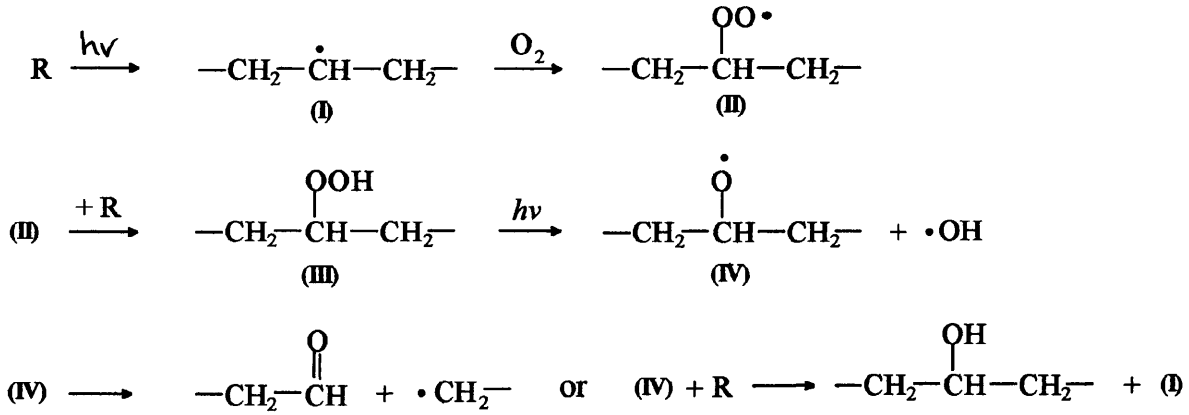

Figure 1.5 Type I photooxidation process in polymers

end groups or they may abstract hydrogen atoms from adjacent polymer chains. The generation of one radical can therefore lead to an autooxidative chain process.

This mechanism is thought to be responsible for the degradation of many polymers during near UV light exposure in the presence of oxygen. The rate and extent of this process is determined by the ease of oxygen permeation into the polymer and is usually confined to the more mobile amorphous regions Photooxidation is often restricted to the surface layers but this is often sufficient to cause a reduction in the useful lifetime of many polymers since surface cracks and pitting may propagate into the polymer bulk if stressed. Interpolymer crosslinks may also form between radical species on adjacent polymer chains, providing they are sufficiently close. This produces a rigid three dimensional structure causing brittleness and lowering extensibility.

The Type II photooxidation process involves quenching of the triplet state photoexcited chromophore by molecular oxygen and is shown in Figure 1.6. The ground state of O_2 molecule is unusual in that its two highest energy electrons are in unpaired orbitals with parallel spins, making it a triplet state ($O_2(T_0)$). Energy transfer can take place between the triplet excited state chromophore to triplet ground state oxygen to produce singlet excited oxygen ($O_2(S_1)$). Singlet excited oxygen[33] is much more reactive than the ground state, and since the energy gap between the ground state and singlet excited state is small, many compounds are capable of acting as sensitizers. These include carbonyl groups, aromatic groups and dyes. Singlet oxygen is capable of directly oxidising organic substrates by attacking electron rich sites. In particular C=C groups in polymers are attacked by singlet oxygen and hydroperoxides are formed. Singlet oxygen may also abstract hydrogen atoms from certain functional groups, depending on the strength of the bond to hydrogen. In

particular it may abstract hydrogen from OH groups in polymers to generate alkoxy and hydroperoxide radicals. Singlet oxygen can also react with disulphides, indoles, phenols and amines. Singlet oxygen may therefore act as an initiator of the autooxidative Type I process.

$$Sens(S_0) \xrightarrow{h\nu} Sens(S_1) \longrightarrow Sens(T_1)$$

$$Sens(T_1) + O_2(T_0) \longrightarrow Sens(S_0) + O_2^*(S_1)\ ,\quad O_2^*(S_1) + \quad RH \longrightarrow ROOH$$

Figure 1.6 Type II photooxidation process in polymers

1.3.3 Photochemistry of Wool

Exposure of wool to sunlight in air causes both colour changes and losses in physical properties such as tensile strength, elasticity and abrasion resistance. Bleaching occurs on exposure to blue light whereas near UV wavelengths cause wool to yellow. The rate of yellowing is increased if wool has been chemically bleached or treated with fluorescent whitening agents. The yellowing and bleaching tendencies of wool reduce the colour stability of dyed fabrics. The chromophores responsible for the initial yellowness of wool and those responsible for photoyellowing are unknown.

Phototendering of wool on exposure to near UV light drastically alters the physical and mechanical properties of fibres and fabrics. This is accompanied by the embrittlement of fibres giving fabric surfaces a harsher handle. Phototendering is attributed to the photo-oxidation of cystine to cysteic acid which cleaves the disulphide crosslinks responsible for much of the stability of the fibre. The large decreases in strength loss are also attributed to rupture of the polymer backbone[34]. Studies of the photodegradation of wool have tried to elucidate the mechanisms and species involved in the yellowing and tendering of the fibre. These studies are reviewed in Chapter 3. This section briefly describes the principal sites of quantum absorption and the pathways leading to the dissipation of energy in the fibre.

Wool contains chromophores inherent to its polymer structure which absorb wavelengths below 310 nm. This absorption is due to the ($\pi \rightarrow \pi^*$) transition of the ring systems of the aromatic amino acids tryptophan and tyrosine. Wool also has a broad absorption of unknown origin that extends over the region 320-400 nm. The species involved may be the chromophores responsible for the natural yellowness of wool[35] . Tryptophan oxidation

products such as N'-formylkynurenine (NFK) may be responsible (see section 3.1.1). Since the high energy UV wavelengths are absorbed by tryptophan and tyrosine, the pathways leading to the dissipation of this energy in the fibre are important. Studies have shown that in wool and other proteins, the energy absorbed by tyrosine is transferred to tryptophan, either by singlet-singlet or triplet-triplet processes[36] [37]. The energy held by tryptophan may be dissipated by a number of pathways. It has not been established if significant energy is lost through internal conversion from the singlet excited state of tryptophan. Emission of fluorescence from the singlet excited state has been estimated to account for 8% of the energy lost from tryptophan [37]. The singlet excited state of tryptophan can also be quenched by the disulphide bonds in wool. Reduction of the disulphide bonds in wool has been found to increase tryptophan fluorescence[38]. These bonds may also quench the singlet state of tyrosine residues, therefore reducing the amount of energy transferred to tryptophan. The quenching efficiency of the disulphide bonds may depend on their location in relation to tryptophan residues in the fibre. There may be an increased probability of quenching in regions of the fibre with high disulphide crosslinking density such as the cuticle. This quenching action by the disulphide bonds may photosensitize them to subsequent oxidation.

The main de-excitation pathway of tryptophan in wool involves intersystem crossing to the triplet state of tryptophan [35] [39]. It has been shown that in the absence of oxygen, tryptophan is highly labile and decomposes readily but under ambient conditions the primary reaction of the triplet state is with atmospheric oxygen [35]. Two reactions are possible, the first involves electron exchange energy transfer to produce the reactive singlet oxygen species. The second involves the direct oxidation of tryptophan to produce oxidation products.

$$TRP^{*}(T_1) + O_2(T_0) \rightarrow TRP(S_0) + O_2^{*}(S_1)$$
$$TRP^{*}(T_1) + O_2(T_0) \rightarrow \text{Tryptophan Oxidation Products}$$

On irradiation of wool at 310 nm 15 times the amount of oxygen was consumed relative to the amount of tryptophan destroyed, implying that tryptophan reacts with oxygen to form singlet excited oxygen. The deactivation of tryptophan by reaction with oxygen will depend on the accessibility of the residues in the wool fibre [39]. In crystalline regions, where oxygen may have restricted permeability, radiative decay or energy transfer to neighbouring molecules is more likely. The accessibility of the tryptophan residues in wool to oxygen is of importance if singlet oxygen formation is considered to be the main route leading to the photodegradation of wool.

A repeating cycle of tryptophan excitation and deactivation would create large quantities of singlet oxygen in wool, but other photoexcited species may also sensitize singlet oxygen formation. The triplet excited state of the unidentified absorbing species is also formed during exposure of wool. On irradiation of wool at 365 nm, large quantities of oxygen were produced and it was suggested that this species also sensitises singlet oxygen formation [35]. The tryptophan oxidation product, NFK has been shown to sensitize singlet oxygen formation on exposure to light above 320 nm[40] . Direct evidence has been recently obtained for the formation of singlet oxygen in UV irradiated wool[41]. Singlet oxygen exhibits weak luminescence at 1270 nm. During laser irradiation of wool in air at 350 nm this luminescence was detected. Surprisingly, during irradiation at 265 nm which should excite the tryptophan triplet state, no singlet oxygen emission was detected in wool. The study suggested that the yield of triplet state of tryptophan is low or its reaction with ground state oxygen may not involve singlet oxygen formation. This study implies that it is the unidentified species absorbing around 350 nm that is the main generator of singlet oxygen in wool rather than tryptophan. If singlet oxygen is considered to be the primary reactive species in irradiated wool then the nature of reaction of this species with other amino acids or with groups in the polymer backbone is important. Photooxidation of tryptophan, tyrosine, methionine, histidine[42] [43] and also cystine[44] in solution studies has been shown to proceed by reaction with singlet oxygen. This attack by singlet oxygen is thought to extend to proteins containing these amino acids.

1.3.4 Photochemistry of Nylon 66 [45]

Light below 290 nm is absorbed by the amide carbonyl chromophore and this leads to direct photolysis of the amide bonds (1), Figure 1.7. The radical species formed may then abstract hydrogen atoms from adjacent polymer chains to form carbonyl and primary amine terminated end groups (2), (3). The radical sites formed on the polymer chains following hydrogen abstraction may be involved in crosslinking in the absence of oxygen. The methylene groups adjacent to the -NH- groups on the polymer chains have been implicated as the most susceptible sites of hydrogen abstraction by radical species in polyamides. In the presence of oxygen the Type 1 autooxidative mechanism may then proceed at these sites involving the formation and dissociation of hydroperoxide groups (4).

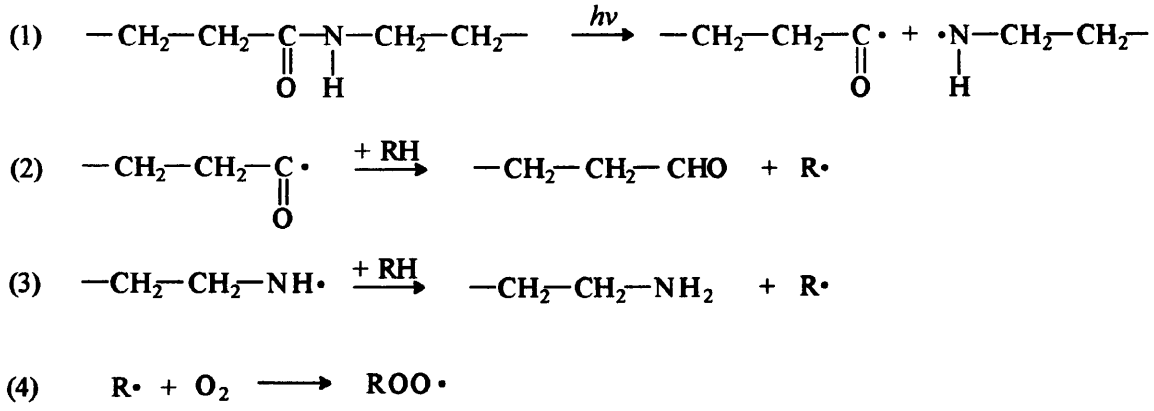

Figure 1.7 Photooxidation of nylon 66 via amide carbonyl absorption below 290 nm

The amide group does not absorb UV wavelengths above 300 nm and it is thought that photooxidation of nylon occurs via a free radical chain mechanism with impurity chromophores being the photoinitiators. The primary sites of absorption are thought to be impurity groups such as hydroperoxides and α,β-unsaturated carbonyl groups[46]. Phosphorescence emission from polyamides has been attributed to the presence of these carbonyl species. If these groups are present as impurities in the polymer backbone they may initiate Norrish I and II cleavage of the polymer chain and form radicals which are then sites for oxidation. Hydrogen abstraction at methylene groups on the polymer chain by the photoexcited carbonyl group may occur to initiate free radical processes. Photodecomposition of peroxide and hydroperoxide groups present as impurities would further generate radical species. All radical species which are accessible for oxidation may then follow the Type I autooxidation process shown in Figure 1.5.

Phototendering of delustred polyamide is most rapid on exposure to wavelengths between 340-350 nm, which is the absorption maximum for the anatase form of titanium dioxide[47]. Photoyellowing of polyamides is also a problem. In one study this has been attributed to the formation of pyrrole type compounds which requires the presence of amine-terminated chain ends and therefore relies on amide bond scission[48].

1.3.5 Photochemistry of Polyester[49 50]

In polyester, the ester carbonyl group is responsible for absorption between 290-320 nm and chain scission is predominant. Figure 1.8 (i) shows the possible points of initial chain scission at the ester group and the primary products which are carbon dioxide, carbon monoxide and

carboxylic and phenolic groups. Chain scission is thought to occur primarily by route (1) forming carboxylic end groups, the rate of formation of these groups is often used as an indicator of the extent of photodegradation. This process has been found to be relatively inefficient, which may be due to the rigidity of the polymer, or the ability to dissipate energy via the aromatic groups. Of greater significance in polyester, on exposure to light above 320 nm, is the presence of impurity hydroperoxide groups attached to sites on the polymer backbone, Figure 1.8 (ii). The influence of impurity groups in the degradation of polyester is illustrated by the fact that delustred polyester absorbs light above 320 nm due to titanium dioxide pigment, and is much less photostable than bright polyester[51]. The photostability of delustred polyester significantly improves after dyeing with disperse dyes[51].

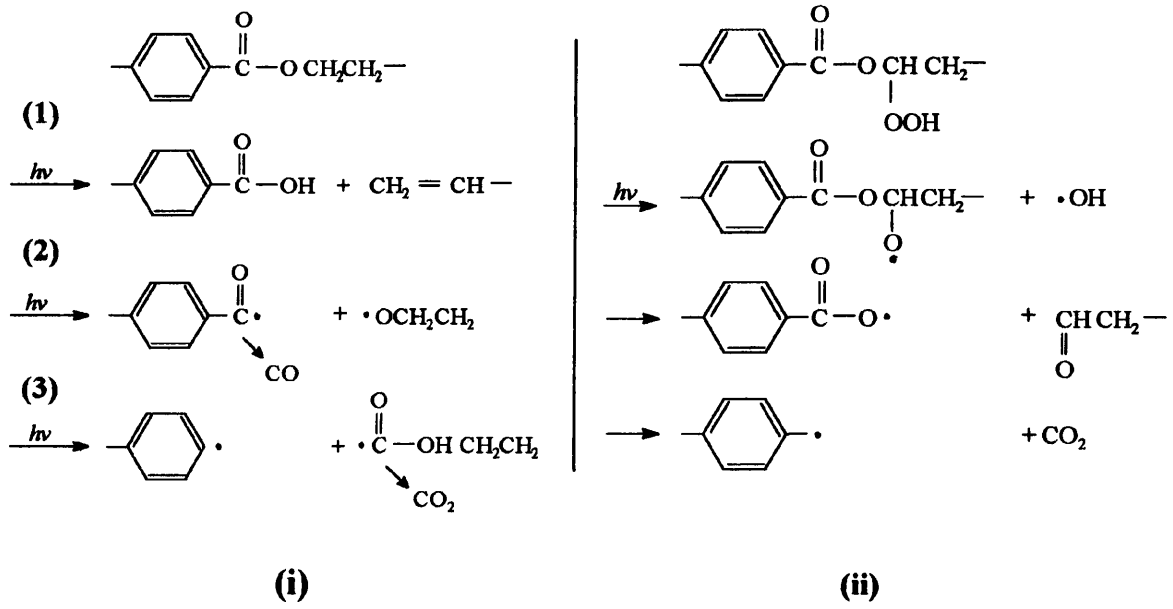

(i) (ii)

Figure 1.8 Photochemical reactions of polyester

1.4 Photostabilization of Polymers

Most commercial polymers require some form of stabilisation to protect against photooxidation during use. A variety of different products have been applied to polymers, a number of which have also been extended for use on wool and are reviewed in section 3.3.2. This section briefly discusses the mode of stabilisation of the various classes of stabiliser in relation to polymer systems in general. The main classes of stabilisers used for polymers are UV screeners, UV absorbers, excited state quenchers and antioxidants. The stabiliser must

have a high stability to light and show limited degradation itself during exposure. It is important that it does not react photochemically with the polymer and in many cases colour imparted by stabilisers is undesirable. In some cases a combination of stabiliser classes are used which together act synergistically. This is typical of certain combinations of UV absorbers and antioxidants. There are also examples of products which act antagonistically.

UV screeners function by limiting the amount of light entering the polymer by reflecting the incident radiation. Inorganic pigments may be applied as surface coatings or incorporated into the bulk of the fibre, for example magnesium oxide and calcium oxide are used in plastics and reflect wavelengths between 300-400 nm. The anatase form of titanium dioxide has a reflectance over 340 nm. One of the most successful UV screeners is carbon black dispersed in the polymer at concentrations of 2-5%. It also functions as a UV absorber and excited state quencher. Although it is an efficient stabiliser, its drawback for many applications is the undesirable colouration.

UV absorbers act by preventing photosensitive sites in polymers from absorbing damaging wavelengths. Those used on textiles are prepared as water soluble derivatives since they need to be monomolecularly dispersed in the fibre for maximum effectiveness. They may be applied by exhaustion with dyestuffs or padded onto fabrics as after treatments. Unlike screeners, the compounds must be able to preferentially absorb damaging wavelengths and therefore compounds must have UV absorption characteristics similar to the polymer. The absorber must deactivate the absorbed energy by photophysical processes which do not sensitize polymer degradation. For compounds which are deactivated by radiative process there is the risk that the energy may be reabsorbed by the polymer. Most of the commercial UV absorbers function by converting the UV energy into vibrational or thermal energy since they have high rates of internal conversion. The most common compounds are the 2-hydroxybenzophenones, 2-hydroxyphenylbenzotriazoles and 2-hydroxyphenyl-S-triazines. All these compounds contain a six-membered intramolecular hydrogen-bonded ring in which a phenolic group is hydrogen bonded to a heteroatom such as oxygen or nitrogen. One mechanism proposed for dissipation of absorbed energy involves the reversible formation of this ring giving two tautomeric forms due to proton transfer along the intramolecular hydrogen bond[52]. This mechanism is shown below for a typical sulphonated 2-hydroxyphenylbenzotriazole absorber in Figure 1.9 (i) and (ii).

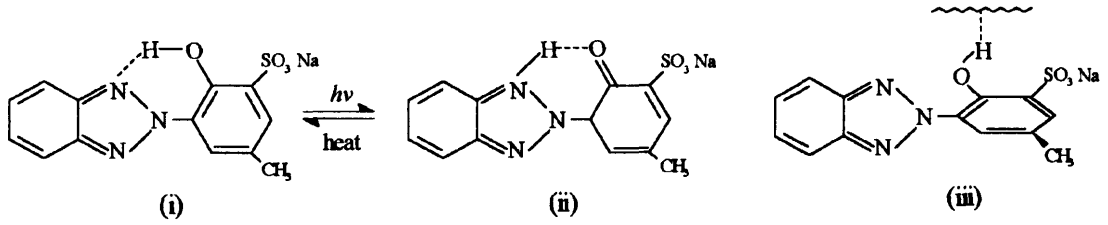

Figure 1.9 Hydrogen bonded forms of a sulphonated 2-hydroxyphenylbenzotriazole absorber

The effectiveness of these products relies on the strength and integrity of the intramolecular hydrogen bond. Modification of the structure of these compounds which prevent the formation of the intramolecular hydrogen bond severely inhibit effectiveness. Polar fibre environments may disrupt this structure due to intermolecular hydrogen bond formation between the substrate and absorber as shown in Figure 1.9 (iii). In polyamide fibres these products have been found to be ineffective and may accelerate degradation. It is claimed that the protective effect provided by these absorbers on certain substrates can not be explained by their UV absorption capacity alone and that they may also function as excited state quenchers.

Excited state quenchers function by deactivating photoexcited chromophores in the polymer before they can enter into chemical reactions. They usually do not absorb UV light directly but accept absorbed energy from excited states in the polymer. The energy level of the quencher must be lower than the chromophore. Chelates of the transition metals, particularly nickel are the most successful quenchers. Energy transfer may occur over long range or short range collisional distances. For short range energy transfer it is necessary for quenchers to have some mobility in the polymer. Since metal chelates have low mobility in the polymer it is thought that they function by long range energy transfer processes. Nickel chelates may also function by acting as singlet oxygen quenchers.

Antioxidants function by inhibiting chain propagation by radical scavenging and by decomposing hydroperoxides to non-radical products. For hydroperoxides, the first electronic excited state is dissociative and therefore excited state quenchers are ineffective. Preventative antioxidants function by decomposing hydroperoxides to non-radical products. Transition metal dithiocarbamates, particularly those of nickel, cobalt, copper and zinc, are effective hydroperoxide decomposers. Chain breaking antioxidants function by trapping or stabilising radical species before they can cause hydrogen abstraction of the polymer. The most important class are those which can donate labile hydrogen atoms to radicals such as hindered phenols and secondary amines. Hindered amines have been particularly successful in polymers and they

may function by a number of mechanisms. The amine group may donate its hydrogen atom to radical species. It may then be oxidised itself to give nitroxyl radicals which are effective polymer macroradical scavengers. Hindered amines have been found to act synergistically with certain UV absorbers.

1.5 Photostability of Dyestuffs [53] [54]

Dyestuffs for use on automotive textiles must have a high hot lightfastness and only certain dyes classes with only a limited number of dyes within each class reach the required standards. The rate of degradation of a particular dyestuff depends on many factors, such as the nature of the textile substrate and the spectral distribution and relative intensity of the incident light. In general, the rate of fading is accelerated by an increase in temperature and humidity, water may act as a plasticiser to promote the diffusion of oxygen. The physical state of the substrate is important since dyes fade at a faster rate on finer fibres due to the increased surface area to bulk ratio.

Many studies have tried to find a correlation between dye structure and lightfastness but no general link has been found. Photochemical reactions of the excited dye lead to the breakdown of the dye structure and the formation of differently coloured or colourless products. The photoexcited dye may dissipate energy by a number of processes, but the reactive state of the dye is generally thought to be the triplet state due to its longer lifetime. Reversible photochemical reactions may take place such as photochromism which involves *cis-trans* isomerization about azo bonds. Irreversible photochemical reactions lead to the degradation of the dye and therefore fading. Photooxidation of the dye molecule is generally believed to be the main reaction leading to the fading of most dyestuffs, this may take place by Type I and Type II processes. In some cases photoreductive degradation of the dye occurs, often in protein substrates. If a dye is in close contact with a substrate that readily donates hydrogen, or if the substrate is more easily oxidised than the dye, then reductive fading is favoured. The substituents on the dye molecule are believed to have a large effect on the fastness properties of dyes. A particular substituent may increase or decrease the electron density around the reaction site and therefore increase the ease of oxidation or increase the ease of reduction respectively.

Since most dyeings involve trichromatic mixtures of dyes, the fastness properties of the dyestuff combination is important and this cannot be predicted from the fastness properties of the individual dyes. Catalytic fading of dyes involves the rapid fading of one component of a dye mixture. This causes off-tone fading of fabrics. This may occur due to transfer of energy from certain photosensitizing dyes, impurities or additives. Lightfastness may be increased with an increase in concentration of the dye on the fabric and increased aggregation of the dye in the substrate (see section 3.3.1). The application of photoprotective agents to dyed fabrics may also improve lightfastness.

Apart from the photochemical processes leading to the fading of dyestuffs, there is a second problem involving interactions of the photoexcited dye with the substrate. Dye-sensitized phototendering of polymers can occur particularly with dyes based on the anthraquinone structure, such as vat dyes. Accelerated phototendering of the dyed substrate occurs in the presence of oxygen and can be accelerated by water. Certain orange and yellow dyes are particularly harmful but there is no general correlation between chemical structure and degree of tendering. Two theories have developed to explain photosensitized tendering of polymers. The first involves hydrogen abstraction from the polymer by the photoexcited dye, reducing the dye but also leaving a free radical site on the polymer which is attacked by oxygen[55]. This process will depend on the nature of the substrate and the availability of neighbouring hydrogen donors. The second and most favoured mechanism is that the dye itself is responsible for singlet oxygen production due to quenching of the triplet state of the dye by molecular oxygen[56]. Singlet oxygen may then directly oxidise the polymer especially if the dye and polymer are in intimate contact.

Chapter 2

Introduction to Analytical Techniques

2.1 Vibrational Spectroscopy[57 58]

2.1.1 Introduction to Infrared Spectroscopy

Infrared radiation excites transitions between vibrational energy levels of molecules. Harmonic vibrations of molecules involve each atom in the molecule vibrating at the same frequency, with each atom passing through its equilibrium position simultaneously. These are known as normal modes of vibration. Since vibrational energy levels are quantised, only those frequencies of infrared radiation which match the harmonic vibrational frequencies of the molecule can be absorbed. If infrared radiation of appropriate energy is supplied to a molecule, energy can only be absorbed if the molecular vibration causes a change in the magnitude of the dipole moment of the molecule. If the vibration causes a periodic change in the magnitude of the dipole moment it can be acted upon by an electric field of a photon of the same frequency and absorption will occur. If the photon frequency does not match the oscillation frequency of the dipole moment associated with a particular molecular vibration, then absorption will not take place. The greater the magnitude of change in dipole moment associated with a particular vibration, the more effectively the photon energy can be transferred to the molecule to activate the vibration and therefore absorption will be more intense. The intensity of an infra red absorption band is proportional to the square of the change in dipole moment with respect to the change in the normal co-ordinate of the molecular vibration $(\delta\mu / \delta Q)^2$. A diatomic molecule only has one normal mode of vibration involving the symmetric stretching of the bond between the two atoms. In polyatomic molecules there are a large number of vibrations which involve all the atoms in the molecule or specific groups of atoms within it. These may involve symmetric and antisymmetic stretching of bonds, and the bending, rocking and twisting of atoms about bonds. Only some of the possible vibrations may be activated by infrared energy, depending on whether the particular vibration causes a change in the dipole moment. In molecules which contain a centre of symmetry in their ground states, such as H_2 or CO_2 no dipole moment exists. For any vibrational mode of the molecule which retains the centre of symmetry, the dipole moment will remain zero and infrared absorption will not

occur. For example the symmetric stretching of the CO_2 molecule is infrared inactive. The CO_2 molecule also has antisymmetric stretching and bending vibrations; in both modes a change in dipole moment occurs allowing infrared radiation of appropriate frequency to be absorbed. Therefore in molecules which possess a centre of symmetry at equilibrium, vibrations which retain this centre of symmetry will be infrared-inactive, those which remove the centre of symmetry will be active. Unsymmetric molecules may contain axes or planes of symmetry, vibrations of the molecule along these axes which retain the axis symmetry will be inactive.

An infrared spectrum plots the intensity of absorption by a sample against the frequency of absorption which is expressed in reciprocal wavelength, termed wavenumbers (cm^{-1}). There are three regions, the most useful and informative is the mid infrared which spans from 4,000 cm^{-1} to 400 cm^{-1} (2.5 - 25 μm) and contains the fundamental vibrational modes. The near infrared spans from 9,000 cm^{-1} to 4,000 cm^{-1} and contains mainly harmonic overtones of the fundamental frequencies above 2,000 cm^{-1} in the mid infrared spectrum. The far infrared from 400 cm^{-1} to 50 cm^{-1} has broad bands due to inorganic and metal compounds. In the mid infrared, qualitative analysis is possible by comparing the absorption frequencies to molecular vibrational frequencies. In non-linear molecules there are 3N-6 independent normal modes of vibration, in the case of linear molecules there are 3N-5 modes. In simple molecules it is possible to calculate mathematically the frequencies of the normal modes of vibration from the atomic masses, force constants of bonds and geometry of the molecule. Not all of the possible vibrational frequencies may be infrared active, but the absorption wavenumbers can be calculated. In complex molecules the number of possible vibrations becomes large and difficult to calculate. An infrared spectrum often contains many bands of uncertain assignment at frequencies below 1500 cm^{-1} . These are due to vibrations involving the whole molecule and they are difficult to interpret. The position, intensity and number of vibrational frequencies in this region is unique to each particular molecule and it can therefore be used as a molecular fingerprint. However, the vibrations of certain functional groups within a molecule are localised and appear at characteristic group frequencies in the infrared spectrum. Interpretation of infrared spectra is usually carried out empirically with reference to group frequencies, for example X-H, C=O, C=C, S=O, C-N. The stretching vibration of the C=O group gives a strong band located in the region 1900 -1550 cm^{-1} its precise position depends

on the nature of substituents, it is particularly sensitive to electronegative substituents which weaken the C=O force constant.

Quantitative analysis is possible since the intensity of an absorption band is related to the concentration of the component or components giving rise to the absorption band. This is described by the Beer-Lambert Law which relates the spectral absorbance (A) to the thickness of the sample (l) and the concentration of the species being measured (C), where K is the absorption coefficient of the species.

$$A = K\,l\,C \qquad [2.1]$$

This describes a linear relationship, but in practice there are many sources of error, such as sample thickness which limits the use of absolute concentration values. Usually quantitative analysis is carried out by measuring the absorbance of a band of interest relative to another unrelated band in the spectrum or by using an internal standard of known concentration.

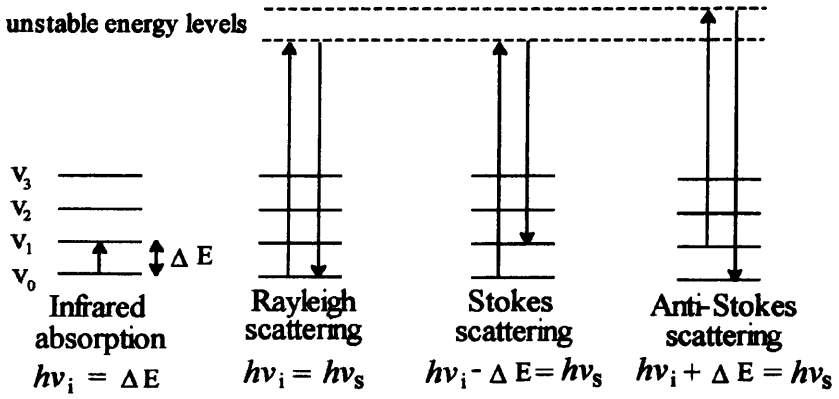

Figure 2.1 Comparison of infrared absorption, Rayleigh and Raman scattering

2.1.2 Introduction to Raman Spectroscopy

Electromagnetic radiation may be absorbed, transmitted or scattered by a molecule. If a molecule scatters a photon elastically so that energy is not lost to the molecule, it is known as Rayleigh scattering. Rayleigh scattering therefore occurs at the same frequency as the incident radiation. In 1928, C.V. Raman proved that there was also a second type of scattering[59]. He observed that weak scattering could occur from molecules at frequencies not present in the incident light. In other words, incident photons were inelastically scattered from molecules as a result of an exchange of energy between the molecule and photon. In Raman spectroscopy, the sample is irradiated with high energy monochromatic laser light. The frequency of the

laser is usually higher than the vibrational frequencies of molecules, but lower than the electronic frequencies. On irradiation, the incident photon ($h\nu_i$) interacts with the molecule in its ground vibrational state (v_0) and raises it to an unstable high energy level, or virtual state as illustrated in Figure 2.1. Energy is immediately lost from this unstable state by emission of a photon ($h\nu_s$) as the molecule returns to the ground state. Rayleigh scattering occurs if the molecule returns to the ground state so that the incident and scattered photon have the same energy. The excited molecule may return to its first vibrational energy level (v_1) rather than to the ground state. The emitted photon will then be lower in energy than the incident photon, by an amount equal to the difference between the ground and first vibrational energy levels (ΔE). This process is known as Stokes scattering. Alternatively, a photon may be scattered from a molecule which is already in its first vibrationally excited state. As the molecule returns to the ground state from its higher unstable state, the emitted photon contains excess energy equal to the difference between the first vibrationally excited state and the ground state. This is known as anti-Stokes scattering. Since the Boltzman distribution function predicts that at ambient temperature most molecules exist in the ground vibrational state, Stokes scattering is much more intense than anti-Stokes scattering. It is the frequencies of Stokes scattering which are usually measured in Raman spectroscopy from which the vibrational frequencies of molecules (ΔE) can be calculated. The Raman spectrum is then a plot of scattering intensity as a function of vibrational frequency expressed in wavenumbers.

Figure 2.1 shows that Raman scattering involves transitions between the molecular vibrational energy levels also excited by direct absorption in infrared spectroscopy. The selection rules for the two, however, are quite different which means that certain vibrations which are infrared inactive may be active in Raman spectroscopy and vice versa. In order for a molecular vibration to be Raman active there must be a change in the polarizability of the molecule during the vibration. If a molecule is placed in an electric field the electrons will be displaced relative to the protons causing an induced dipole moment. Polarizability (α) is a measure of the extent to which the electron cloud can be displaced or deformed relative to the nucleus by the electric field of the photon. Its magnitude is defined in equation [2.2] by the induced dipole moment (μ) created when a molecule is placed in the electric field divided by the strength of the electric field (E).

$$\alpha = \mu / E \qquad [2.2]$$

In heteronuclear and homonuclear diatomic molecules, as the bond length stretches and contracts during a vibration, the electron cloud of the molecule alters its shape as the electrons are displaced relative to the nuclei. This allows energy to be transferred to the molecule from a photon of appropriate frequency to excite the molecular vibration. Polyatomic molecules may have modes of vibration which are infrared inactive due to symmetry properties, but are Raman active for example the symmetric stretch of CO_2 . In contrast the asymmetric stretch of CO_2 which is infrared active is not Raman active since the polarizability does not change during the vibration. This gives rise to a selection rule which states that in a molecule with a centre of symmetry, those vibrations which are symmetrical about the centre of symmetry are Raman active and infrared inactive. Those vibrations which are not centrosymmetric are Raman inactive and usually infrared active.

Qualitatively, the information in a Raman spectrum is similar to an infrared spectrum and therefore the two techniques can be thought of as being complementary. Functional groups common to both spectra occur at approximately similar frequencies. Raman spectroscopy is particularly useful in providing information on non-polar groupings and homonuclear diatomic molecules such as C-C, S-S, N=N, which are all inactive in infrared spectroscopy. It gives strong bands for C=C stretching modes, particularly for symmetric vibrational modes of aromatic rings. There is a linear relationship between the intensity of a Raman band and the concentration of the species responsible. Raman scattering intensity at a particular wavelength is an absolute value and not expressed as a ratio of the original incident intensity as for infrared spectroscopy. Since the source of Raman scattering is the sample itself, the intensity of scattering depends on the position of the sample and the concentration of material impinging on the laser. Therefore, a direct comparison between the intensity of Raman bands between samples cannot be made. It is more usual to compare band intensities relative to other bands in the spectrum, or to include an internal standard of known concentration in each sample and normalise spectra against this standard.

2.1.3 Instrumentation

2.1.3.1 Fourier Transform Spectroscopy

A typical instrument for Infrared or Raman spectroscopy requires a source of incident radiation, a method of splitting transmitted or scattered radiation from the sample into its

component wavelengths and a detector to measure the intensity of each wavelength component. Conventional dispersive instruments use diffraction gratings to split the transmitted radiation into its individual wavelengths, each wavelength component being analysed one at a time. These instruments have now been superseded by Fourier Transform (FT) instruments in which each component wavelength of the spectrum is collected simultaneously. Polychromatic radiation from the source enters an interferometer and passes through a beamsplitter which splits the beam in half. One half of the beam is transmitted through the beamsplitter to a movable mirror, the other half is reflected from the beamsplitter to a fixed mirror. Both beams are reflected from these mirrors and recombine at the beamsplitter. Constructive or destructive interference takes place as the wavelength components recombine depending on the position of the movable mirror. For monochromatic radiation the signal intensity as a function of mirror displacement is a cosine function. In the case of polychromatic radiation, there is a summation of the individual cosine functions generated for each wavelength component and the total signal response as a function of mirror position is known as an interferogram. In the case of FT-IR spectroscopy this modulated infrared beam then passes through the sample and the transmitted frequencies appear to the detector in the form of an interferogram, a summation of the wavelength intensities of the transmitted light. The interferogram is unscrambled and converted into a spectrum using a Fourier Transform which calculates the amplitude of each component wavelength present in the interferogram. Since all wavelength components impinge on the detector simultaneously, there is a high signal to noise ratio, and acquisition time is much quicker. This also ensures that resolution and energy throughput are constant across the entire spectrum. In dispersive instruments a loss of energy occurs at the dispersing elements, making weak signals difficult to detect. FT instruments do not contain these elements and the light throughput is typically 40 times greater than dispersive instruments making microsampling possible and weaker signals easier to detect.

2.1.3.2 FT-IR Spectroscopy

In FT-IR spectroscopy the source of polychromatic infrared radiation is usually a solid material heated to emit blackbody radiation. After passing through the interferometer the modulated beam is reflected by a mirroring system and focused on the sample where selective absorption takes place. Those frequencies transmitted or reflected by the sample are focused

onto the detector and this response is converted into a single beam spectrum. This spectrum is ratioed against a reference spectrum of the original incident intensity at each wavelength producing an infrared spectrum of % transmission or % reflectance as a function of wavenumber. This referencing process also subtracts the absorbance contributions from water and CO_2 molecules present in the air from the sample spectrum.

Samples must be of appropriate thickness to allow sufficient energy of the incident beam to be transmitted. This often poses a problem for the analysis of textile samples. Fibres can be ground with an infrared transparent medium such as KBr and pressed into transparent discs. Alternatively powdered or finely cut fibres can be mixed with KBr and the diffuse reflectance from the sample is analysed. The development of microspectroscopy allows selected areas of fibres to be analysed using a conventional microscope with an infrared objective. One method has gained particular popularity for the FT-IR analysis of textile samples since it is non-destructive. This is attenuated total reflectance spectroscopy.

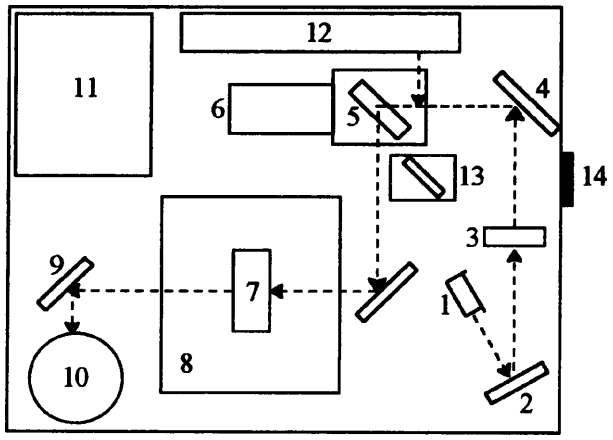

1 Mid Infrared source
2 Mirror
3 Aperture
4 Parabolic mirror
5 Beamsplitter
6 Interferometer
7 Sample accessory
8 Sample compartment
9 Detector mirror
10 Liquid nitrogen cooled detector
11 Power supply
12 HeNe Laser
13 Slide mirror(diverts beam to port)
14 Beam port to microscope attachment

Figure 2.2 Diagram of Nicolet (750) FT-IR spectrometer used in this study

2.1.3.3 Attenuated Total Reflectance (ATR) Spectroscopy[60]

This technique allows the surface of materials to be analysed, the principle of the technique is illustrated in Figure 2.3. A transmitting crystal of high refractive index (n_1) is placed in contact with two sample surfaces of lower refractive index (n_2). The incident infrared radiation is totally internally reflected within the crystal, and therefore traverse along the axis of the crystal provided that the angle of incidence of the radiation into the crystal (θ) is adjusted such that

$\sin\theta > n_2 / n_1$. At each reflectance point on the crystal / surface interface an evanescent wave of the same frequency as the incident beam is generated which extends a few microns into the sample surface. The evanescent wave is attenuated at wavelengths which the sample absorbs, the transmitted portion of the evanescent wave re-enters the crystal. After multiple internal reflections the infrared beam exits the crystal and is focussed onto the detector. To ensure spectral reproducibility and high signal to noise ratio, the sample must be in close contact with the crystal. Crystal materials must be of high refractive index and transparent in the infrared region of interest. Thallium bromide/iodide (KRS-5) or germanium are typical crystal materials.

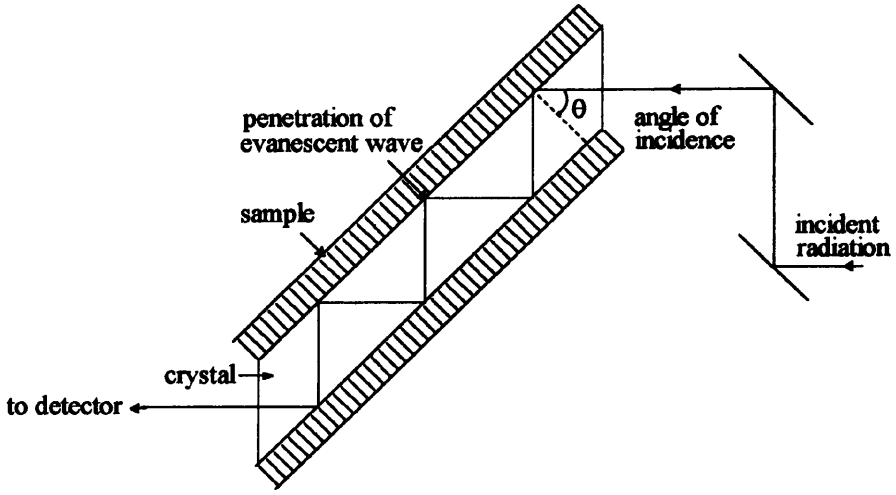

Figure 2.3 Diagram of Attenuated Total Reflectance accessory used in this study

2.1.3.4 FT-Raman Spectroscopy

Raman scattering is an inefficient process, approximately 10^{-6} of the incident intensity only appears as Raman scattering. Intense incident sources are needed, such as lasers, in order to excite sufficient Raman scattering in combination with highly sensitive detectors. The dispersive technique uses visible frequency lasers, often at wavelengths which are sufficient to excite electronic transitions of molecules risking sample degradation. Fluorescence from samples can be excited by the visible laser frequencies. This can mask the weak Raman signals causing vibrational information to be obscured by a high intensity background. Most FT-Raman instruments use near infrared laser frequencies, typically 1.064μm (9398 cm^{-1}) which is less energetic and does not excite fluorescence. The sample is irradiated in a dark

enclosed chamber and the backscattered radiation from the sample is collected by a series of mirrors which direct it to the interferometer. Therefore, in contrast to FT-IR instruments the incident source is monochromatic, and it is the polychromatic radiation scattered from the sample which is modulated by the interferometer before passing to the detector. Before the scattered wavelengths enter the interferometer it is essential that the Rayleigh scattering from the sample is filtered. This strong scattering, which is 1000 times stronger than Raman scattering, if not attenuated, will be distributed as noise throughout the spectrum. Highly sensitive near-infrared detectors are used to measure Raman scattering.

In Raman spectroscopy, as the concentration of material on which the laser impinges increases the scattering intensity increases. For FT-IR an increase in sample concentration past a certain point will restrict transmission of the infrared radiation. Therefore in Raman spectroscopy sampling is much simpler and samples can be of any thickness, transparent or opaque, they only require positioning in the path of the laser for analysis. Powder and liquid samples can be investigated in NMR tubes. Raman microspectroscopy allows selected areas of individual fibres to be analysed. Since water and glass are inefficient Raman scatterers they can be used as an aid to sampling. The limiting factor in Raman spectroscopy is the inherent Raman scattering efficiency of the material itself, sampling methods can do little to improve signal intensity from a weak Raman scatterer.

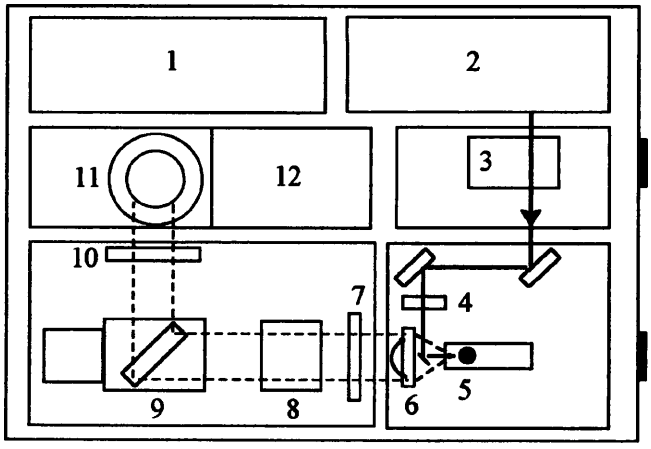

1 Power supply
2 Nd YAG Laser
3 Laser & white light power meter
4 Focusing lens
5 Sample
6 Collimating lens
7 Filter
8 Polarizer (optional)
9 Interferometer
10 Filter
11 Liquid nitrogen cooled detector
12 Electronics & power supplies

Figure 2.4 Diagram of a Nicolet (950) FT-Raman spectrometer used in this study

2.2 X-Ray Photoelectron Spectroscopy (XPS) [61 62]

2.2.1 Introduction to XPS

In photoelectron spectroscopy, a sample (solid, liquid, or gas) is irradiated with high energy radiation (X-rays, UV rays) under ultra high vacuum conditions. This leads to the ejection of electrons, known as photoelectrons, from the sample surface. These photoelectrons are counted and sorted according to their kinetic energies in an electron energy analyser. An incident photon of energy $h\nu$ interacts with an electron in an atom or molecule which has a binding energy E_B . If the energy of $h\nu > E_B$, then the electron will be ejected with a kinetic energy E_K. The binding energy of the electron can be calculated using equation [2.3]

$$E_B = h\nu - E_K - \Phi \qquad [2.3]$$

Φ is the work function of the surface, or the energy required to remove the photoelectron from the surface. X-rays have energy sufficient to eject electrons from core atomic orbitals (typically of wavelength 0.99 nm with photon energy of 1253.6 eV). The binding energy of each core electron is characteristic of the individual element to which it was bound and of the particular atomic orbital from which it was ejected. In XPS the core electron binding energies of elements commonly encountered are in the range 100 eV - 2000 eV.

The spectrum is a plot of the number of photoelectrons ejected as a function of binding energy or kinetic energy of the photoelectron. The peaks in the spectrum therefore correspond to the elements present in the surface of the sample. There may be more than one band present in the spectrum for a particular element, since the incident X-ray energy may be sufficient to ionise electrons in a number of core orbitals. Since the energies of atomic orbitals are quantised and specific for each element, bands are discrete and in most cases there is little overlap between peaks.

The incident X-rays can penetrate deep into the sample, but the limiting factor is the photoelectron escape depth. Only those photoelectrons which do not suffer energy loss due to collisions with other molecules can contribute to the characteristic photoelectron peaks. The probability of collision within the sample increases with increasing depth from the surface. The escape depth is the maximum depth from which photoelectrons can be ejected without suffering energy loss. The escape depth increases with increasing photoelectron kinetic energy and depends on the density of the sample surface and the mass of the particular atom. The inelastic mean free path, (λ) is the average distance in Ångstroms an electron can travel within

a sample surface without collision. The value of (λ) is a function of the kinetic energy of the photoelectron; the relationship depends on the spectrometer used. The relation derived for the instrument used in this work for kinetic energies above 50 eV is shown in equation [2.4][63].

$$\lambda = \frac{1}{2}\sqrt{E_k} \qquad [2.4]$$

$$I = I_0 \exp\left(-d / \lambda \sin\theta \right) \qquad [2.5]$$

Once the inelastic mean free path for photoelectrons of a specific kinetic energy has been obtained it is possible to calculate the intensity of photoelectrons (I) emitted as a function of depth in the sample (*d*) using the Beer-Lambert relationship [2.5]. (I_0) is original photoelectron intensity excited by the incident beam and (θ) is the photoelectron take off angle relative to the sample surface. Approximations for equation [2.5] have been calculated which can be used to estimate sampling depth in angstroms over all photoelectron kinetic energies. This is such that 65% of the photoelectron intensity will emanate from a depth of λ sinθ, 85% from a depth of 2λ sinθ, and 95% from a depth of 3λ sinθ of the surface. From equation [2.4] the photoelectrons from carbon (1s) orbitals with a kinetic energy of 969.0 eV (excited at 1253.6 eV) will have a value for λ of 15.56 A. Assuming θ to be 90°, it can therefore be calculated that 65% of the carbon signal will be from the top 15.56 A , 95 % will be from the top 46.46 A. Thus the surface sensitivity of XPS can be appreciated. From equation [2.5] it can be seen that *d* varies with sin θ . Therefore the sampling depth can be controlled by varying the angle of the sample surface with respect to the angle of the incident radiation. This is the basis of 'depth profiling'.

2.2.1.1 Quantitative Analysis

Qualitative information of the elemental composition of the surface of a material can be obtained by comparing the experimental binding energies in the spectrum to published tables of elemental binding energy assignments. Quantitative analysis is possible by measuring the intensity of photoelectron peaks. The area under the photoelectron peaks is proportional to the elemental concentration of atoms in the surface region. The measured area under a peak (I_A) is related to the atomic concentration (C_A) by equation [2.6]. C_A is an absolute value for the atomic concentration of an element in the surface. This value is only a meaningful quantity if it is expressed relative to the atomic concentration calculated from the photoelectron peak area of another element present in the same spectrum.

$$C_A = I_A / S_A \qquad [2.6]$$

In equation [2.6] the term S_A is the sensitivity factor for the particular element and its core energy level. The sensitivity factor is derived from a value called the photoionization cross-section which is the probability of photoemission for a particular photoelectron. Its value depends on a number of factors such as the element and core energy level involved, the incident frequency and the angle of the sample relative to emission. Quantitative analysis in XPS is usually carried out by referring to published sets of experimentally derived relative atomic sensitivity factors. These sensitivity factors include contributions from instrumental effects such as the analyser transmission function and detector efficiency specific to the instrument on which they were determined. Published sensitivity factors are therefore only applicable to spectrometers with similar configurations and mode of operation.

The percentage atomic concentration of an element in the surface can be calculated relative to the concentration of all the other elements present (n) using equation [2.7].

$$A\% = \frac{C_A}{\sum_1^n C_n} \times 100 \qquad [2.7]$$

2.2.1.2 Chemical Shift Information.

Siegbahn found that the binding energies of core electrons were not fixed but were variable in binding energy in the range 0.1-10 eV [61]. An increase in positive charge on the atom was found to increase the photoelectron binding energy. An increase in positive charge on the atom will increase the attraction of the core electron for the nucleus and therefore raise its binding energy. The charge on the atom depends on the environment of the atom. If there are electron withdrawing groups bound to the atom or in its immediate environment, valence electrons will be drawn away from the nucleus and so increase the net positive charge on the atom. In general terms, an increase in the electronegativity or formal oxidation state of a substituent bound to the atom of interest will cause a shift of the photoelectron peak to higher binding energy. This 'chemical shift' is particularly useful as it can provide information about the nature of molecular bonds. The precise shift in binding energy depends on the sum of the net charges of all the surrounding atoms in the molecule and can be difficult to calculate. However, the interpretation of chemical shifts is usually carried out empirically by reference to published tables and literature values of standard materials.

2.2.1.3 Energy Resolution

In order for chemical shifts to be detected it is necessary that spectral resolution is maximised. The energy resolution of the spectrum ΔE is measured by the full width at half maximum (FWHM) of the photoelectron peak, and is governed by [2.8]

$$\Delta E = (\Delta E^2_n + \Delta E^2_p + \Delta E^2_a)^{1/2} \qquad [2.8]$$

where ΔE^2_n is the natural line width of the core level involved and depends on the lifetime of the core hole following photoemission. ΔE^2_p is the line width of the X-ray source and ΔE^2_a is the analyser resolution. The X-ray line width therefore contributes to spectral resolution and unmonochromatized sources reduce resolution considerably. The absolute resolution of a photoelectron peak ΔE, defined as the full width at half maximum (FWHM) is not constant throughout the specrtrum but varies according to the kinetic energy of the core level of interest. In order for the energy resolution to be constant for every peak in the spectrum, ie independent of kinetic energy, photoelectrons are retarded so that they enter the analyser with the same constant kinetic energy, or pass energy. This mode of operation is called constant analyser energy (CAE).Alternatively they may be retarded to energies which are a constant fraction of their original kinetic energies which is known as constant retard ratio (CRR). Both modes ensure the same absolute resolution for photoelectron peaks regardless of kinetic energy.

2.2.2 XPS Instrumentation

Figure 2.4 shows a diagram of the VG ESCA 3 Mk II spectrometer used in this work. It has four main components, a source of high energy electromagnetic radiation, an analysis chamber, an electron analyser and a detector. The X-ray source is produced by bombarding a suitable anode material with a beam of high energy electrons. This causes core electrons to be ejected from the material followed by X-ray emission as the core level is filled by an electron from a higher energy orbital. The incident X-rays must have sufficient kinetic energy to excite the core level electrons of all elements, and therefore only certain anode materials are suitable as X-ray sources. The choice of anode material is also governed by the X-ray line width. The X-ray line is not monochromatic but contains a Lorenztian distribution of frequencies about the main line. The width of this distribution directly determines the resolution of the photoelectron peaks and so it is important that it is as narrow as possible if small chemical shifts are to be detected. Only two anode materials can satisfy both requirements. These are

magnesium and aluminium which produce X-rays of energy 1253.6 eV and 1486.6 eV respectively and have line widths of 0.7 eV and 0.85 eV respectively. Monochromatization of the X-ray source reduces line width and improves spectral resolution. The X-ray source is separated from the analysis chamber using a beryllium window. This window absorbs part of the high energy X-rays known as Bremsstrahlung. This is a continuous high energy background which extends up to the incident X-ray emission line which could damage the sample. The window also prevents the source from being contaminated by the sample and it emits low energy electrons which helps to reduce sample charging during analysis.

The spectrometer contains an analysis chamber, and a preparation chamber which can be separated to allow sample insertion. Before analysis both chambers must be evacuated to UHV conditions with pressures generally less than 10^{-7} torr. At low pressures, collisions of the photoelectrons with gas molecules in the chamber will be minimised. Low pressures are also required to avoid gas molecules forming a layer on the surface of the sample which alters the surface composition. UHV conditions are obtained by evacuating the chambers using two oil charged diffusion pumps cooled by liquid nitrogen cold traps. The diffusion pumps are backed by rotary pumps which extract the gas molecules. The sample is positioned under the X-ray source so that the path of the photoelectrons is aligned with the entrance slit of the analyser.

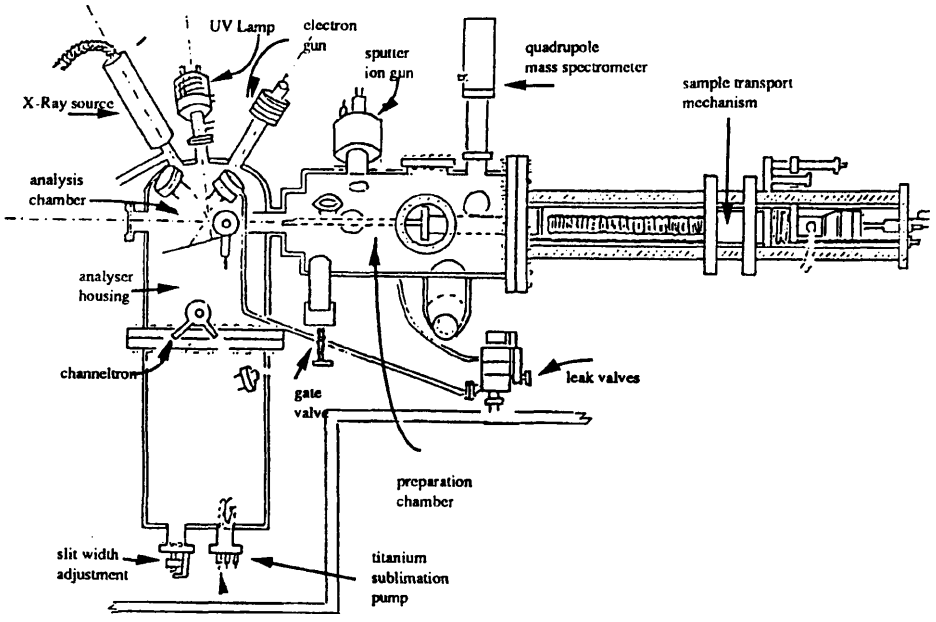

Figure 2.4 Diagram of VG ESCA 3 Mk II XPS spectrometer used in this study

2.3 Atomic Force Microscopy

2.3.1 Introduction to Atomic Force Microscopy[64 65 66]

Atomic Force Microscopy, was invented in 1986 by Binnig, Quate and Gerber[64]. With the Atomic Force Microscope (AFM) it is possible to achieve sub-nanometer scale imaging under ambient conditions. Imaging is achieved by measuring the magnitude of inter-atomic force between the sample surface and a minute tungsten probe. The probe tip is lowered to within a few nanometers of the sample surface causing a repulsive force to be generated by the overlap of electron clouds between the atom at the probe tip and the nearest atom at the sample surface. The strength of this repulsive force varies according to the distance between the probe tip and sample, it is these variations which are used to produce an image of the surface relief.

During the operation of the AFM the probe tip is actually in contact with the sample and reads the surface relief in a manner analogous to a record player stylus. The sample is moved with respect to the tip by placing it on an XYZ piezoelectric controlled stage. A raster pattern is built up of the surface relief as the specimen is moved in the X direction with a displacement of ΔY equivalent to a fraction of a nanometer. By altering the scan rate and size of the raster pattern, images can be obtained on various scales, from those visible with light microscopes, down to atomic scale features.

The probe itself has a minute tip, such as an atomically sharp shard of diamond, mounted on a soft cantilever spring. Cantilevers are microfabricated from silicon nitride and have resonant frequencies as high as 100 kHz. The higher the resonant frequency, the less sensitive the cantilever to low frequency external vibrations. The probe is flexible enough to allow response to changes in force, but rigid enough to maintain contact with the sample. As the probe scans the surface, the variations in repulsive force exerted on the tip cause tiny deflections of the cantilever spring. Measurement of the magnitude of these tiny cantilever deflections requires sub-angstrom sensitivity, Optical Beam Deflection is used which is capable of measuring cantilever deflections in the order of 0.1 angstroms. Light from a diode laser is specularly reflected from the top of the cantilever which has a mirror-like surface. Any movements in the cantilever cause a shift in the path of the reflected light beam and this is detected by a position sensitive photodiode. To avoid damage by the probe the force exerted on the specimen by the probe is kept at a minimum constant level. This is achieved by altering the height of the sample with respect to the probe as it follows the hills and valleys of the surface. A feedback

mechanism from the optical sensor responds to changes in the path of the beam reflected from the cantilever and in accordance varies the voltage applied to the Z piezo. Altering the Z piezo voltage allows the stage to be moved vertically and therefore the distance between the sample and probe to be changed. It is these changes in voltage applied to the Z piezo that are recorded and electronically translated into measurements of the height of surface features.

The specimen surface is represented by XYZ data values which are stored on computer. Using computer graphics this data is translated into a three dimensional reconstruction of the surface relief. Once the data has been collected the image can then be manipulated. For example it is possible to zoom in and out of selected areas of the image, depending on the original scanned resolution. The XYZ data can be used to provide measurements of surface details, such as distances and angles between features. An average surface roughness measurement can also be calculated.

The AFM has not been used in any previously published work to study the surface of wool fibres, however a variety of biological materials have been imaged on an atomic scale [67] [68].

High resolution imaging of the surface features of textile fibres, such as wool, has been achieved to date by the use of the Scanning Electron Microscope. The SEM relies on wave propagation for imaging and therefore resolving power is limited by the wavelength of the probing electron beam. With the AFM, resolution is limited only by the fineness of the probe tip, which if atomically sharp allows resolution on an atomic scale. Additional drawbacks of the SEM technique are firstly, the risk of sample damage by the electron beam, particularly if high resolution is required. Secondly, insulating samples must be coated with a conducting surface layer. The disadvantage of this coating is that fine surface details on fibres can be masked. With the AFM, there is no threat of electron beam damage and samples are examined without the need for coating and consequently true specimen features can be imaged.

Chapter 3

Photodegradation, Photostabilization and Spectroscopic Analysis of Wool: A Review

3.1 Photoyellowing of Wool

3.1.1 Photochemical Studies

As discussed in section 1.3.3, the triplet states of tryptophan and an unknown UV absorbing chromophore have been identified as the primary reactive species in wool [35] [39]. However, the secondary processes leading to the photoyellowing of wool, and the chromophores responsible are not known. Many studies have tried to find a correlation between the rate of photoyellowing and the degradation of the light-sensitive amino acids such as tryptophan, tyrosine, cystine and histidine. Solutions of these amino acids all yellow readily on exposure to UV light, particularly those of tryptophan[69]. Most rapid degradation of these photosensitive amino acids in solution occurs on exposure to those wavelengths which cause the most rapid yellowing, between 290-300 nm[70] [71]. Although solutions of soluble proteins containing these photo-sensitive amino acids also photoyellow, no correlation has been found between the extent of yellowing and the original concentration of any of these amino acids[69]. However, the protein clupeine, which does not contain these photosensitive amino acids, does not yellow in solution implying that these residues are involved in some way.

Although cystine is particularly susceptible to photooxidation it is not thought to be involved in the photoyellowing of wool. No relationship has been found between the rate of photoyellowing of wool and the rate of cystine oxidation[72]. Wool of low cystine content, following disulphide bond reduction, photoyellows at the same rate as untreated wool[73].

Since tryptophan is a primary reactive species in wool, many studies have tried to determine if it is also involved in reactions leading to photoyellowing. A curve relating the decrease in tryptophan content in wool to sunlight exposure time has been obtained[74]. Both photoyellowing of wool and the destruction of tryptophan rely on the presence of oxygen, and a correlation has been found between the rate of yellowing of wool and the rate of loss in tryptophan content[75]. A study of a range of 27 different keratins including wool found that on

irradiation at 310 nm there was a correlation between the initial content of tryptophan, the rate of yellowing and the rate of tryptophan degradation[76]. One study obtained direct evidence for the participation of tryptophan in wool yellowing. Tryptophan residues were radiolabelled and after irradiation, wool hydrolysates contained a yellow radioactive fraction[77] [78]. If the tryptophan content of wool is increased by the introduction of N-acetyltryptophan residues, there is a large increase in the rate of photoyellowing which is relative to the number of residues introduced[79]. In contrast, the rate of photoyellowing of tryptophan depleted wool is only slightly slower than for untreated wool[80]. This implies that the photodecomposition of other residues must also be responsible for yellowing.

Although a number of primary photoproducts have been identified on irradiation of free tryptophan in solution, many of these are not thought to be formed on irradiation of tryptophan bound in the protein chain. The yellow photoproduct N'-formylkynurenine (NFK) is thought to be formed in wool but the exact mechanisms leading this residue are not known. From solution studies, the primary reaction of tryptophan is thought to involve oxygen attack at the C-3 position of the indole ring to form a hydroperoxide group, Figure 3.1[81] [82]. Decomposition of the hydroperoxide then leads to ring opening and the formation of NFK which may then be further degraded to kynurenine[82]. This may also be the pathway for photooxidation of tryptophan in wool since kynurenine has been found in isolated yellow photoproducts from wool[78]. The importance of the indole ring in the processes leading to photoyellowing of wool has been shown in a study of indole enriched wool. After incorporation of indole-3-propionyl groups into wool the rate of photoyellowing increased twelvefold compared to untreated wool[79].

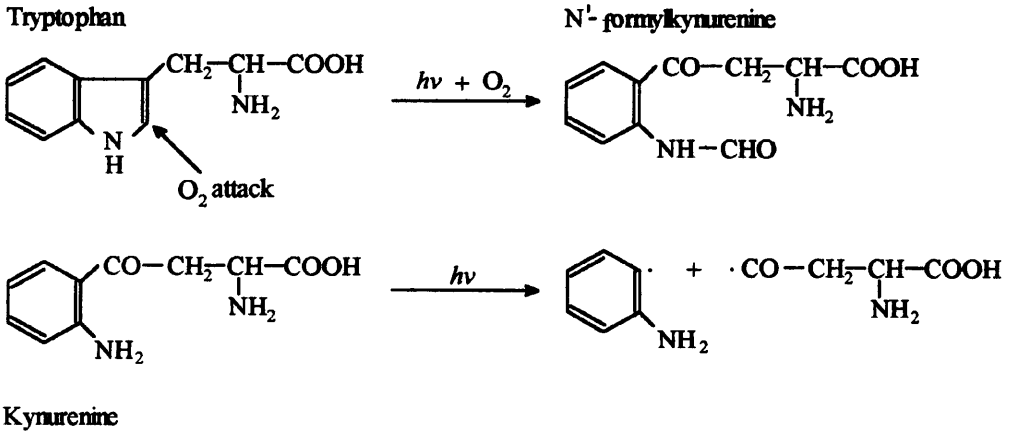

Figure 3.1 Photooxidation of tryptophan

In many studies of tryptophan in solid and solution, the concentration of detectable photoproducts is much smaller than the amount of tryptophan destroyed [82]. This is attributed to the formation of yellow polymeric material which is more difficult to isolate. Irradiation of simple model peptides containing radiolabelled tryptophan residues in solution found that the yellow material was 2-4 times higher in molecular weight than the original peptide[83]. Asquith and Rivett suggest that aromatic compounds produced on photodegradation of kynurenine may form yellow polymeric species[82] . The results of one study suggest that tryptophan, or its photoproducts may be involved in covalent crosslinking to form polymeric material[84]. Irradiation of wool and proteins in solutions which contained free radiolabelled tryptophan residues led to covalent binding of radioactive material to the protein. The amount of covalently bound material increased with an increase in concentration of tryptophan in the solution. It was suggested that covalent binding of tryptophan or its photoproducts may occur at radical sites on the protein. Covalent binding of material to proteins also occurred on irradiation in solutions of tyrosine, but the extent of binding was only 10-15% of that for tryptophan.

Although most studies have concentrated on tryptophan, the role of tyrosine and phenylalanine in photoyellowing have also been investigated[85]. Model compounds have been used to investigate the photooxidation products of these amino acids. Irradiation of free phenylalanine in solution and as the solid poly-phenylalanine produced yellow material containing the photoproducts o-tyrosine, m-tyrosine, p-tyrosine and unknown material. Yellow material was also formed on irradiation of p-tyrosine in solution and in solid form with dityrosine and dihydroxyphenylalanine (DOPA) produced. All of these phenylalanine and tyrosine photoproducts are present in small amounts in unexposed wool but increase more than threefold in concentration after Xenotest exposure. In solution these photoproducts degrade further during irradiation to give unidentified yellow products which could indicate that they are precursors to the yellowing chromophores in wool.

On exposure to light the photoexcited state of tyrosine may be involved in a photodimerization reaction to form dityrosine and polytyrosine residues. The role of these species as initiators of photochemical reactions leading to the yellowing of wool has been investigated. Although there is an increase in the concentration of dityrosine in irradiated wool, the application of dityrosine in a crosslinked form to wool fabric does not increase the rate of yellowing[86]. A number of biphenols have also been padded onto wool to represent models for dityrosine[87]. On

exposure to simulated sunlight in water, the fabrics yellowed much more rapidly than untreated wool, the yellowing rate increased with an increase in concentration of the biphenol on the fabric. Although there is evidence for the formation of dityrosine in irradiated wool, the amount detected only represents 2% of the total amount of tyrosine typical of untreated wool[85] and it is therefore unlikely that it can be solely responsible for yellowing if at all.

Photoyellowing of wool has also been attributed to an increase in carbonyl-containing groups due to the formation of α–ketoacyl groups, which absorb light around 320 nm [88 89] (see Figure 3.3). The concentration of carbonyl groups in wool has been found to increase to a maximum level of 2.5 times their original concentration after light exposure above 295 nm[90]. However, this study did not find a correlation between the rate of formation of these groups and the rate of yellowing. Other workers have attributed yellowing to an increase in conjugation in the polymer backbone leading to absorption in the blue region of the spectrum[91].

There may be a number of species responsible for absorbing wavelengths in the near UV and blue regions of the spectrum which increases the yellowness of wool. The visible fluorescence of wool is due to two species, one with an absorption maximum at 335 nm (emission at 420 nm) and the other absorbing at 380 nm (emission at 460 nm)[92]. Studies have implicated both NFK residues and dityrosine as contributors to the shorter wavelength fluorescence in wool[92] [93 94]. The species responsible for the longer wavelength fluorescence is not known but since oxidative treatments increase the emission intensity, the absorbing chromophore is thought to be an oxidation product[95]. The absorbing species responsible for this blue fluorescence is formed on exposure of wool to UV light[96] and has only been found in the weathered tips of wool fibres[95 97]. A correlation was found between the intensity of this blue fluorescence from wool and Xenotest exposure time, implying that the yellowing chromophores are responsible[98]. Bleaching of the yellow chromophores by exposure of photoyellowed wool to blue light reduced the fluorescence intensity. The increase in blue fluorescence in oxidised wool may partly be explained if the disulphide bonds, which are known to quench the UV fluorescence of tryptophan, also quench this visible fluorescence. Quenching action would be reduced after oxidation of the disulphide bonds and therefore fluorescence intensity would be increased from the unidentified chromophores.

A green/yellow fluorescence at 500 nm, due to absorption at 430 nm, has been found in the weathered tips of wool [99]. Thin layer chromatography of the wool tip digests found a number of fluorescent species, in particular β–carboline compounds. β-carboline 1,3-dicarboxylic acids are produced by the reaction of tryptophan with α-keto acids, which have been proposed to be formed in irradiated wool (see section 3.2.1).

3.1.2 Factors Influencing the Rate of Photoyellowing and Photobleaching

The most important factor which influences the rate and nature of colour change of wool is the incident wavelength distribution. Many studies have identified the waveband between 290-310 nm in sunlight or artificial exposures as causing the most yellowing of wool [70 71 100 101]. There is a decrease in yellowness index of fabrics with increasing wavelength between 270-410 nm [71]. Wool is photobleached on exposure to blue light, particularly those wavelengths between 400 -450 nm [70 101 102]. The action spectrum for wool yellowing shown in Figure 3.2 was produced from a study of wool irradiated with discrete wavebands using a xenon arc[101]. It can be seen that maximum yellowing of wool occurs with wavelengths between 266-293 nm and that light above 370 nm caused the fabric to photobleach, particularly between 400-450 nm. Between 310 nm and 380 nm the extent of yellowing decreases with wavelength.

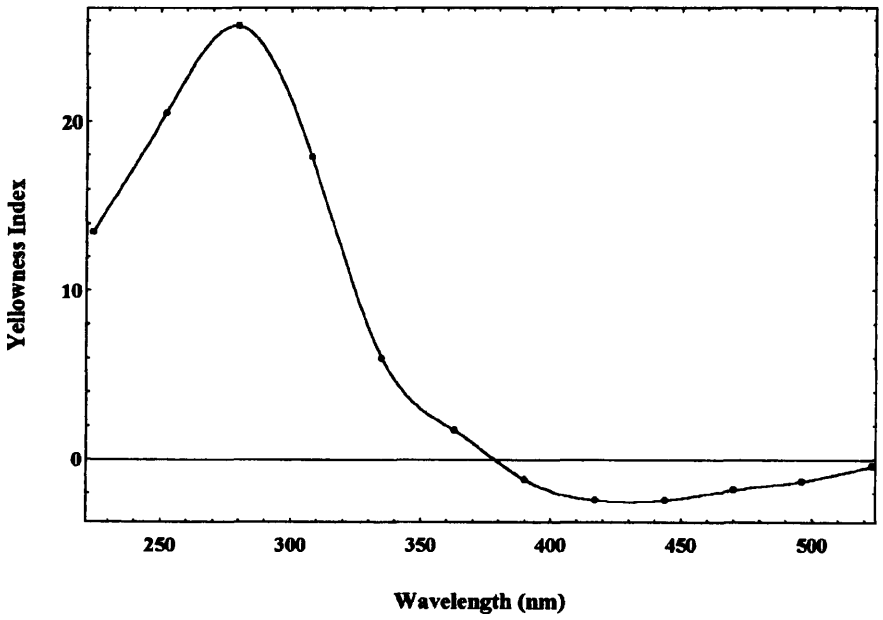

Figure 3.2 Action spectrum for wool photoyellowing[101]

Although light above 400 nm causes both naturally and artificially yellowed wools to bleach, it does not cause the destruction of photosensitive amino acids cystine, tryptophan, tyrosine and histidine, unlike UV exposure[70]. It is thought that the bleaching effect is molecularly non destructive and confined to the yellowing chromophores only. The partial reversibility of yellowing and bleaching of wool may be due to the presence of a modified amino acid residue with easily reversible oxidation/reduction forms.

The extent of photobleaching increases with the initial yellowness of wool[103] [104]. This can be explained by the increased concentration of yellow chromophores which absorb blue light. On exposure to sunlight and xenon sources, yellow wools were bleached rapidly to about 50% of their initial yellowness values[104], whereas white wools only photoyellowed. Since yellow wool only bleaches to a certain level it was suggested that two chromophores may be responsible for the inherent yellow colour of wool, only one being susceptible to bleaching.

One study suggested that the apparent photobleaching effect in wool was due to the development of a new UV absorbing chromophore which emits blue fluorescence[105]. Other workers have not found an increase in blue fluorescence of photobleached wool and contend that the bleaching effect is due entirely to destruction of the yellowing chromophores[96]. This was demonstrated by showing that the absorbance of wool in the region between 350 - 550 nm decreased after laser irradiation at 488 nm.

Since both yellowing and bleaching of wool occur simultaneously on exposure to sunlight the extent of each depends on the relative intensity and spectral distribution of the incident light. The nature and rate of colour change will depend on factors such as time of year and location.

The temperature during exposure affects the rate of photoyellowing and tendering of wool. Wool is susceptible to thermal yellowing in the absence of light and at temperatures over 90°C yellowing is particularly rapid[101]. Thermal yellowing of wool occurs on heating at 80°C, but if wool is exposed to light at an air temperature of 80°C the rate of yellowing more than doubles[86]. An increase in temperature during light exposure accelerates the rate of photochemical degradation and leads to increased photoyellowing and tendering. For example an increase in temperature from 35°C to 75°C during exposure of wool caused a threefold increase in the yellowness index[106]. It is not clear if the chromophores responsible for the thermal yellowing of wool are the same as those responsible for the photoyellowing of wool. The fluorescent species detected in photooxidised wool which absorbs at 365 nm and emits

blue fluorescence was also found to increase in concentration after thermal oxidation at 115°C for up to 5 days[98]. This suggests that a similar chromophore may be involved but oxidation processes leading to the formation of the yellowing chromophores may differ. Chemical destruction of tryptophan occurs at temperatures above 100°C and therefore an increase in temperature during exposure may accelerate reactions involving tryptophan[107].

The effect of humidity on the rate of photoyellowing of wool has not been fully established. The difficulty in assessing the role of humidity lies in the fact that heating during light exposure will cause the fabric to be drier than the surrounding atmosphere. Therefore simply measuring the humidity of the environment during the exposure will not reflect moisture conditions in the fabric. One study irradiated wool over water and over a desiccant[101]. It was found that irradiation over water reduced the yellowing of wool. This is in conflict with studies on synthetic fibres which have found that the presence of moisture increases the rate of chemical degradation[108]. In the case of synthetic fibres it is thought that water acts as a catalyst to promote the formation of hydroperoxides or it may act as a plasticiser allowing oxidising species to diffuse through the fibre.

3.2 Phototendering of Wool

3.2.1 Photochemical Studies

The photo-oxidation of cystine residues is considered to be one of the main changes responsible for the phototendering of wool. Rupture of the disulphide bonds which give the wool fibre most of its physical integrity leads to rapid losses in tensile properties. Cystine is considered to be the primary point of attack in photosensitized oxidations in biological systems. There is some evidence that singlet oxygen is the main reactive species initiating the oxidation of cystine[44]. The ultimate oxidation product of cystine is cysteic acid, but other intermediate oxidation products may also exist in photooxidised wool (see Figure 1.2). In studies of light-degraded wool the amount of cystine destroyed could not be accounted for by the amount of cysteic acid detected, suggesting the presence of intermediate species[70]. One study found that at successive periods of sunlight exposure the amount of cysteic acid detected accounted for only 20% of the total amount of cystine lost[34] .The instability of the partially oxidised products under the conditions of acid hydrolysis has meant that studies of photooxidised wool using chemical analysis have not been able to isolate them. The rate of

photo-oxidation of cystine is wavelength-dependent and it decreases with increasing wavelengths between 250 - 410 nm[71].

The strength of wool fibres is not only dependent on the extent of disulphide bonding but also relies on the integrity of bonds forming the polymer backbone. It has been proposed that the large reductions in tensile properties of light-degraded wool can not be accounted for by the oxidation of cystine alone, and that main chain cleavage is of more importance in the phototendering of wool[109]. Other studies have found that a reduction in the content of disulphide bonds in wool by 40% only decreased the breaking load of fibres by 15%[110]. In comparison, cleavage of 40% of the peptide bonds by acid hydrolysis caused a 50% decrease in breaking load[111].

Since near-UV radiation is of insufficient energy to be absorbed directly by the peptide groups in wool, protein chain scission is attributed to a free radical mechanism. Radical species generated during irradiation are thought to attack the polymer backbone mainly by hydrogen abstraction at the α-carbon atoms of particular amino acid residues[88 89]. Alternatively, energy for C-H fission at the α-carbon atoms may be supplied via transfer from the aromatic amino acids. One of the free radical species detected in wool on exposure to blue light has been attributed to the formation of α-carbon radicals[112]. The proposed mechanism for main chain cleavage is shown in Figure 3.3. The α-carbon peptide radical (ii) reacts with oxygen followed by hydrogen abstraction from an adjacent molecule to form a hydroperoxypeptide (iii). Subsequent C-N fission gives primary amide terminated (iv) and α-ketoacyl peptides (v)[88 89].

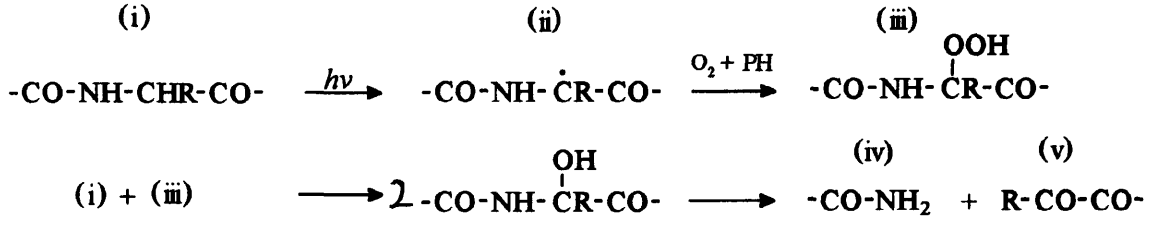

Figure 3.3 Mechanism for main chain cleavage and α-ketoacyl group formation

The detection of glyoxylic and pyruvic acids in wool led to the suggestion that peptide radicals may be formed at alanine and glycine residues leading to the formation of glyoxylyl and pyruvyl peptides[88 89]. It is possible that chain scission may occur adjacent to other amino acids,

since the α-keto acids of tyrosine, serine, threonine and glutamic acid have also been detected in irradiated wool[90].

Evidence for this reaction has been found by other workers who detected increases in the concentrations of primary amide groups and main chain carbonyl groups in exposed wool[34 109]. Both studies found that there were large increases in primary amide group content, but much smaller increases in carbonyl content. It was suggested that the α-ketoacyl groups are unstable and undergo further photo-oxidation in the fibre.

New intermolecular crosslinks may be formed in light-degraded wool which might partly offset disulphide bond and protein chain scission. Reductions in alkali solubility of irradiated wool have been attributed to the formation of new non-specific protein crosslinks[113]. The brittle nature of light-tendered wool has been attributed to protein chain scission and the formation of new crosslinks[34]. Decreases in urea bisulphite solubility in weathered wools are thought to be due to the formation of intermolecular crosslinks between protein chains[114]. Although these crosslinks initially offset the reductions in disulphide bonding, as the period of weathering increased, the extent of crosslinking became much higher than the loss of disulphide bonding. The nature of these crosslinks was not established but they were not due to lanthionine residues, often attributed to reductions in urea bisulphite solubility.

The changes which occur in the nature of crosslinking of wool in the early stages of exposure, before the fibre is appreciably weakened or discoloured, have been investigated[115]. Exposure of wool for 48 hours to simulated sunlight reduced the yield of soluble protein by 50% after alkaline reduction. This indicated the formation of intermolecular crosslinks and it was accompanied by a 26% reduction in cystine content. However, as exposure extended to 600 hours, wool was completely soluble indicating that these crosslinks were themselves photolabile. However, if wavelengths below 315 nm were filtered the crosslinks still formed after 48 hours exposure, but also remained stable to continued light exposure. This indicated that the crosslinks were destroyed by UV wavelengths. The nature of these crosslinks was not established; they were not thought to involve tryptophan, but possibly lysine or arginine residues.

3.2.2 Effect of Phototendering on Physical Properties of Wool

Phototendering of wool lowers the tensile strength and extension of fibres and consequently affects fabric properties such as tear strength, breaking load and abrasion resistance. The

surface mechanical properties of wool are also affected altering the resistance to deformation under shear, bending and compressional forces. A number of studies have looked generally at the effects of phototendering on fabric properties. Weatherall investigated the effect of sunlight exposure behind glass on the chemical and physical properties of wool fabrics in relation to phototendering[34]. Fabrics retained only 20% of their original bursting strength after 900 hours exposure to sunlight. Threads taken from fabrics exposed for up to 900 hours showed a similar rate of loss in tensile strength, but a slightly faster rate of loss in extension at break. The losses in abrasion resistance were more severe, twice the rate of the losses in bursting strength. After approximately 900 hours exposure there was a 35% reduction in cystine content, but the large decreases in tensile properties were mainly attributed to main chain cleavage since a significant increase in primary amide groups was detected after exposure.

Exposure of untreated wool to 2000 hours of a MBTF lamp gave approximately 90% reduction in breaking load of fabric[109]. Dramatic losses in abrasion resistance have been found following Xenotest 450 exposure demonstrating the tendering of the fabric surface[86]. Abrasion resistance decreased by 50 % after 48 hours exposure and by 90 % after 96 hours. This was accompanied by increases in cysteic acid indicating that strength losses are partly due to disulphide bond oxidation. The rate of cysteic acid formation was slow up to 60 hours exposure and then increased to a concentration double its unexposed value after 96 hours exposure.

The extent of phototendering is limited by the depth that light can penetrate the fabric during the exposure time. One study showed that a thick wool fabric retained 70% of its original strength compared to 45% for a lighter weight fabric after the same exposure[116]. The importance of short wavelengths, particularly those below 370 nm in the phototendering of wool was also shown in the study. Filtering of these wavelengths greatly improved the retention of tensile properties.

The rate of phototendering of wool is wavelength dependent. Wavelengths below 320 nm are particularly damaging to the tensile strength of wool, but exposure to light above 370 nm has very little detrimental effect [101]. This suggests that during the photobleaching of wool very little chemical damage occurs which leads to tendering. It was predicted that strength losses may be reduced significantly if wool was exposed behind tinted glass which filters out

wavelengths below 340 nm. Tinted glass provided 50% greater protection to tendering than ordinary window glass.

The effect of temperature during exposure directly effects the rate of tendering[106]. An increase in air temperature during irradiation from 45° C to 75°C doubled the rate of tensile strength loss for wool fabric. Loss in tear strength was 3 to 4 times faster at 75°C than at 35°C. After 200 hours exposure to an MBFU lamp strength loss was nearly five times faster at an air temperature of 95°C than at 65°C[117]. Heat alone can cause the tendering of wool, but the combination of light and heat have a much more dramatic effect[101]. Wool heated at 90°C in the absence of light for 30 days had a 30% decrease in tear strength. If the fabric was irradiated in a Xenon arc at 90°C it took only three days to achieve the same loss in tear strength.

3.2.3 Morphological Changes in Light Degraded Wool

Few studies have investigated the morphology of light degraded wool. This is of particular interest since alterations to fibre morphology will influence the nature of breakdown during wear. One study found smooth brittle fractures with no evidence of selective morphological breakdown in abraded wool fibres which had been exposed to light[34]. This smooth tensile fracture was thought to reflect the extremely brittle nature of light tendered wool with a reduced tendency to fracture with fibrillation. Another study investigated the effect of light on morphological components of the fibre[12]. It was found that the cuticle showed the first signs of damage, with disorganisation in the endocuticle and cell membrane complex between the cuticle and cortex. In some cases the cuticle had been lost completely from the fibre due to fracturing through the endocuticle. In the cortex there was a disorganisation of the microfibril / matrix structure and extended exposure caused a separation of the macrofibrils in the cortex. A study of sunlight damaged hair showed that cleavage of the cuticle occurred in the weak endocuticle layer revealing the globular surface of the endocuticle[118]. The weakening or removal of parts of the cuticle can be expected to have detrimental consequences for the physical integrity of the fibre. Studies of Martindale abraded wool fibres identified the cuticle as being the initial point of fracture[12 119] . Fibre breakdown continues with the removal of the cuticle through planes in the endocuticle or cell membrane complex. Fractures propagate into the cortex at places where initial fracture of the cuticle occurred. Fracture planes occur in the fibre at mechanically weak regions with low crosslinking density. It can be expected that light damage to the cuticle layers will accelerate the breakdown of fibres during wear.

3.3 Photostabilization of Wool

3.3.1 Photoprotective Effect of Dyestuffs

A number of studies have been carried out with the aim of identifying dyestuffs which protect wool from phototendering. Most have concentrated on premetallized dyes but no exact correlations have been found between protective effect and colour, chemical nature or dye structure. The presence of certain dyestuffs can retard the onset of tendering, but the inherent stability of the dye itself appears to determine the protective effect it can give.

A range of 40 dyestuffs of different classes were applied to wool fabrics and reductions in tensile strength were measured after sunlight and MBTF lamp exposure[116]. On short exposures some of the yellow dyes, and a few of the reds and browns gave some protection to tendering, but little protection after prolonged exposure for one year in sunlight. Chrome dyes were found to improve the strength retention presumably due to crosslinking of the mordant to the protein. One dye, Acid Yellow 17, gave increasing protection with increasing concentration and it was suggested that this dye may optically screen the near UV radiation responsible for fibre tendering.

Another study of a range of premetallized, reactive and chrome dyes found that nearly a twofold improvement in tensile strength loss was given by certain yellow, orange and brown dyes after exposure to sunlight for 1000 hours[120]. However, after exposure for 2000 hours the rate of tendering was faster for the dyed fabrics compared to the blank dyed control. An exception was Isolan Yellow which gave a threefold improvement after 2000 hours. Since not all yellow dyes had a protective effect the role of the dye as an optical screener was questioned. The blue, red and black dyes gave little protection, several appeared to accelerate the rate of tendering. The inherent stability of the dyestuff to photosensitizing action was considered to be the most important factor.

A comprehensive study of 84 high lightfastness rated 1:2 premetallized dyes was carried out which included non-sulphonated, mono-sulphonated and disulphonated dyes[121]. After 21,000 langleys sunlight exposure a number of dyes offered some protection, others offered little protection, whereas some accelerated tendering. Those which accelerated tendering were all non-sulphonated yellow, orange and red dyes. There were 25 dyes which gave a twofold improvement in tendering compared to the control and these were exposed for a further 50,000 langleys. Six dyes provided a particularly high level of protection. Of these, five were

yellow dyes and one brown, there was no distinction between the nature of sulphonation, but all had a cobalt concentration of between 2.0 - 4.4%[122] [123]. All the dyes of lower performance contained mixtures of cobalt and chromium, the majority had a higher content of chromium compared to cobalt. Even in the presence of higher amounts of cobalt, the mixture dyes did not give a high level of protection. In nylon a similar effect has been found, dyes containing only cobalt give the highest protection whereas the protective effect of chromium containing dyes is variable and appears to depend on dye structure[124]. The nature of bonding to the chromium atom may be important in controlling the stability of the complex by preventing the formation of free chromium, which catalyses the degradation of the fibre.

The presence of the metal ion in premetallized dyes is thought to reduce both dye fading and substrate tendering[125]. The excited triplet state of the dye molecule may be quenched by intramolecular energy transfer to a lower lying excited state of the metal ion. Deactivation of the triplet state dye molecule would inhibit its reaction with the substrate or with oxygen to form singlet excited oxygen.

Poor correlation has been found between protection to tendering and the lightfastness of the dyestuff on wool[121]. Although one study found that yellow premetallized and reactive dyes had the highest lightfastness performance, this apparent effect may be due to the fact that fading of a yellow dye will be compensated for by photoyellowing of the wool itself [126]. Photoyellowing of the wool will cause larger changes in hue value for blue and black dyed fabrics and may therefore partly explain the lower lightfastness performance of these dyes on wool. This study found that sulphonated 1:2 premetallized dyes had the highest lightfastness performance.

An improvement in lightfastness performance of dyed wool may be increased using dyes which have a tendency to form aggregates in the fibre[127]. On exposure to light those fabrics containing acid dyes with some degree of aggregation had a negative colour fade, ie. the chroma value appeared to increase with exposure suggesting an increase in dye concentration. This is due to the break up of dye aggregates to a more mono-molecular dispersion on exposure giving the impression of increased dye concentration. An increasing tendency for acid dyes to form aggregates in wool was achieved by increasing the hydrophobic character of the dye by introducing an additional phenylazo group to the structure.

3.3.2 UV Absorbers and Protective Treatments for Wool

There has been much research aimed at developing commercial photostabilizers for wool. Much of the work has concentrated on the application of UV absorbers, but antioxidants and reducing agents have also been applied.

Antioxidants used alone have not been successful in significantly reducing the rate of yellowing of wool[128, 144]. The reducing agent thioglycollic acid gives a limited protection to photoyellowing but has little practical use since it is not durable to washing. Thiourea dioxide (TDO) promotes the photobleaching of wool, possibly by acting as a sensitizer for the degradation of the yellowing chromophores, but it gives no protection to subsequent photoyellowing[129]. Pretreatments of wool with formaldehyde, thiourea and mixtures of the two also promote photobleaching and increase the reflectance values of wool making the fabric appear brighter[130]. However the treated fabrics were subject to accelerated heat yellowing at 75°C. Another study found that mixtures of thiourea and formaldehyde (TUF) give significant protection to photoyellowing on exposure between 290-320 nm, as well as promoting photobleaching on exposure to wavelengths between 320-390 nm[131]. The mechanism of protection is attributed to TUF acting as an excited state quencher of tryptophan. Despite the effectiveness of TUF its commercial application is limited since it is not fast to laundering.

A number of UV absorbers have been successful in retarding photoyellowing and phototendering. Three classes of absorber have been applied to wool, 2-hydroxybenzophenones (Figure 3.4 (i)), 2-hydroxyphenylbenzotriazoles (Figure 3.4 (iii), (iv)), 2-hydroxyphenyl-s-triazines (Figure 3.4(ii)). All contain a phenolic hydroxyl group which can form a hydrogen bond with an adjacent oxygen or nitrogen atom to form a 6 membered ring system. One of the first studies applied a number of sulphonated 2-hydroxybenzophenones to wool and found that there were large variations in protective effect despite similarities in UV absorbance spectra[132]. The protective effect was thought to depend on the position of substituent groups in the molecules. Certain absorbers gave wool an initial yellowness and the protective effectiveness was reduced on laundering.

Most interest has been in the hydroxyphenylbenzotriazole class absorber. One commercial product, sulphonated Tinuvin P has been studied extensively on wool. Tinuvin P is a sodium 2-(2'-hydroxy-5'-methylphenyl) benzotriazole-3'-sulphonate, Figure 3.4 (iii). Application of Tinuvin P reduces the rate of degradation of all amino acids, apart from tryptophan, after

exposure for 2000 hours to a MBTF lamp[109]. The rate of main chain cleavage was also reduced which was reflected by a 50% improvement in the rate of loss in breaking load. A 38% improvement in the rate of loss in abrasion resistance has also been found[133]. The tendering of wool irradiated at separate wavebands between 210-400 nm was reduced by over 50% at each band after treatment with Tinuvin P[101]. Tinuvin P increases the rate of photobleaching of wool on exposure to light between 400-500 nm[101]. However, the absorber is not as successful in reducing the rate of photoyellowing. It has been found to accelerate the rate of yellowing on exposure to both an MBTF lamp and to sunlight behind glass[109].

The mechanism of stabilisation of Tinuvin P has been investigated to determine if it functions additionally as an excited state quencher[134]. By examining the quantum yields of fluorescence and phosphorescence from treated wool it was found that these yields were equivalent to the values calculated assuming that the absorber functions only as an optical screener. However, at absorber concentrations above 0.5% there was some evidence to suggest that the product may also act as an excited state quencher of the singlet excited states of tryptophan and tyrosine. Although Tinuvin P did give some protection to yellowing on exposure to simulated sunlight exposure between 270-370 nm, the level of protection was much smaller than that calculated on the basis of its absorbing power in this region. It had a particularly poor performance than predicted at low concentrations. This was not due to loss of the product since the concentration reduced by only 5-10% even after severe exposure. The poor performance was attributed to disruption of the intramolecular hydrogen bonded structure due to intermolecular hydrogen bonding of the hydroxyphenyl group with the wool polymer (see Figure 1.9 (iii)). Molecules in this disrupted non-planar form are fluorescent and a new fluorescent species absorbing between 300-400 nm in wool treated with Tinuvin P was attributed to this disrupted form of the absorber. In addition, a new phosphorescent species absorbing between 380-420 nm was also present in absorber treated wool. This was assigned to the yellow phenolate anion form of the absorber produced on ionization of the hydroxyl group. The phenolate anion form is known to act as a photosensitizer in benzotriazoles promoting fibre photodegradation[135]. The non-planar form of the absorber may have similarly acted as a photosensitizer to promote photoyellowing.

The pH of application affects the protective action of Tinuvin P[136]. At pH 4 there was a slightly higher rate of tendering of the wool compared to application at pH 2, attributed to an increase in the concentration of the sensitizing phenolate anion form of the absorber.

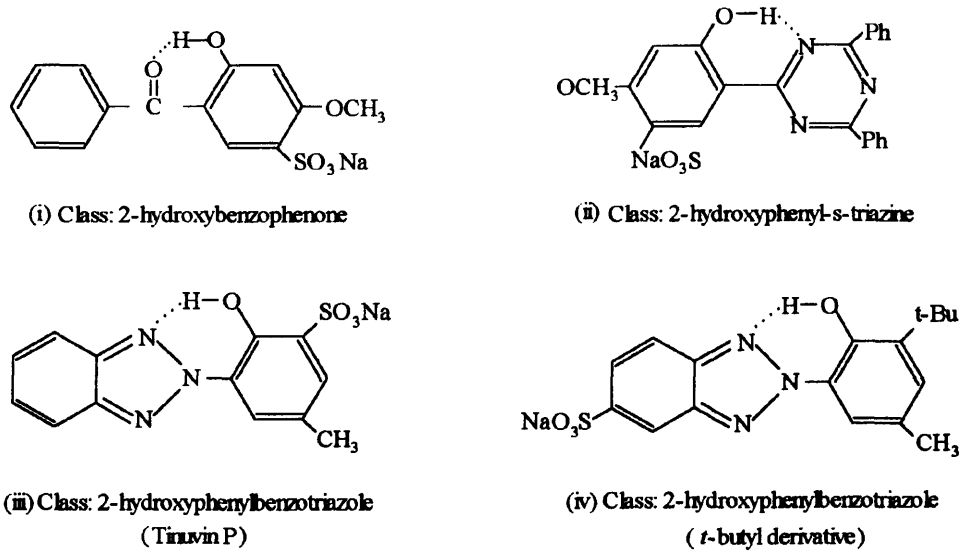

Figure 3.4 Various classes of UV absorber applied to wool

The yellow ionized form also increases the yellowness imparted to wool by the treatment.

A number of UV absorbers have been synthesized and tested based on the structure of Tinuvin P. Studies have investigated the nature and location of substituents attached to the phenolic and benzotriazole rings to try and improve the protective effect. Heller predicted that the protective effect of Tinuvin P might be increased if there was a second hydroxyl group situated on the phenolic ring ortho to the benzotriazole ring, increasing the probability of intramolecular hydrogen bond formation[52]. Such a compound was synthesized and applied to wool[137]. It gave the same protective effect as Tinuvin P to phototendering and no significant protection to photoyellowing in simulated sunlight[137 138]. This study proposed the presence of the polar sulphonate group adjacent to the hydroxyl group may reduce the likelihood of intramolecular hydrogen bond formation and account for the poor performance of Tinuvin P. A second class of absorber was synthesized in which the sulphonate group was moved para to the hydroxyl group on the phenolic ring. This compound gave better protection to tendering, but no large improvement in yellowing. Heller also suggested that the presence of hydrophobic bulky alkyl groups on the phenolic ring, situated ortho to the hydroxyl group, may shield the intramolecular hydrogen bond from disruption by polar fibre environments[52]. Absorbers synthesized with ortho groups such as *i*-propyl or *t*-butyl gave a high level of protection to tendering. The protective effect of these absorbers was improved further if the sulphonate group was moved to the benzotriazole ring. These absorbers also retarded the rate of yellowing on exposure to simulated sunlight. The most successful compound contained an

ortho *t*-butyl substituent and is illustrated in Figure 3.4 (iv). This absorber reduced the rate of yellowing and tendering on exposure to sunlight[137 138] and in simulated sunlight[139] compared to Tinuvin P. The drawback of this absorber was that it imparted a high initial yellowness to wool due to a shift in absorption maxima to slightly longer wavelengths. Wool treated with this absorber has an increase in absorption in the region 300-360 nm compared to Tinuvin P[139].

Derivatives of the 2-hydroxybenzophenone class of UV absorbers have been investigated in a number of studies, Figure 3.4 (i). A study has found that these compounds give significant protection to losses in tear strength and breaking load on exposure to both sunlight and simulated sunlight[106]. Another study has shown that hydroxybenzophenones have been able to reduce the rate of yellowing by 50% in simulated sunlight[123]. In general this class of absorber has a lower screening power between 300-380 nm compared to the 2-hydroxyphenyl-benzotriazole absorbers such as Tinuvin P[140]. They give little protection to yellowing in sunlight and certain 2-hydroxybenzophenones have accelerated the rate of yellowing on exposure to sunlight behind glass[141]. Fabrics treated with a number of these absorbers have been found to contain the yellow phenolate anion form which acts as a photosensitizer[140]. These absorbers also give a higher level of protection to tendering in sunlight if the sulphonate group is located in a side chain rather than attached to the ring[142]. The presence of a bulky ortho *t*-butyl group does not improve the performance of these absorbers indicating that steric hindrance effects may not be as important as in benzotriazole compounds[141]. The nature of substituents in 3 and 4-positions of the phenolic ring may be more important in controlling the acidity and therefore degree of ionization of the hydroxyl group.

Sulphonated 2-hydroxyphenyl-s-triazines have been applied to wool and one absorber is particularly effective in reducing the rate of both yellowing and tendering, Figure 3.4 (ii)[143 144]. On exposure to simulated sunlight for 1000 hours there was a threefold improvement in losses in fabric breaking load and abrasion resistance, nearly a fivefold improvement in tear strength loss and a reduction in photoyellowing. Significant protection is also given by this compound to the rate of photoyellowing and tendering in sunlight. Concentrations of the absorber above 2% did not improve the level of protection to yellowing but only increased the initial yellowness of wool, whereas an increase in absorber concentration up to 5% increased protection to tendering.

Many of the absorbers investigated in each class give substantial protection to tendering on exposure to both simulated sunlight and sunlight behind glass. Very few show any protection to photoyellowing, particularly on exposure to sunlight behind glass. Those compounds which show some protection generally increase the extent of photobleaching, presumably due to absorption of wavelengths responsible for yellowing and transmission of longer wavelengths which promote bleaching. These absorbers only retard the onset of yellowing, none have been found to inhibit yellowing completely. The protective action of these compounds depends on their molecular stability since altered forms of these compounds are potential photosensitizers. One study compared the most protective absorbers from each of the three classes described above[145]. On exposure to sunlight, the *t*-butyl 2-hydroxyphenylbenzotriazole gave the highest protection to yellowing, but it also imparted the highest initial yellowness to fabric. The 2-hydroxyphenyl-s-triazine absorber also gave protection to yellowing and imparted the least initial yellowness, however it was considered to be expensive to synthesize.

A synergistic effect has been found between various classes of UV absorbers and antioxidants giving significant protection to yellowing and tendering in sunlight [139] [146] . Only those antioxidants which contained a hindered phenol moiety had any synergistic effect, but had little protective effect when applied to wool alone. The synergistic effect achieved with a range of absorbers depended on the effectiveness of the particular UV absorber. A particularly successful combination was 5% *t*-butyl 2-hydroxyphenylbenzotriazole absorber with 5% Irganox 1425. On exposure to simulated sunlight there was almost complete protection to photoyellowing. The performance of the UV absorber was improved by 50% in the presence of the antioxidant. There was also a small improvement in tear strength retention compared to the absorber used alone. This synergistic effect also occurred on exposure to sunlight behind glass. The antioxidant may assist the absorber by diffusing to free radical sites in the fibre. The presence of the antioxidant improved the protection to yellowing more effectively than improving the protection to tendering implying that free radical reactions may be important in the photoyellowing of wool.

Apart from improving the photostability of undyed wool, UV absorbers also reduce the tendering of dyed wool and give some improvement in lightfastness performance. Four acid levelling dyes were applied at pH 2 to wool fabric in combination with 5% Tinuvin P[136]. Tinuvin P reduced the rate of phototendering of the dyed fabrics, but the level of protection

was the same as that given to undyed fabric. Dye fading was also reduced by the presence of the UV absorber, especially for the red dye. The *t*-butyl 2-hydroxyphenylbenzotriazole absorber also reduces the rate of tendering of wool dyed with a number of premetallized dyes[137]. Again, the level of protection to tendering was the same for absorber treated undyed and dyed wool, despite the fact that the presence of the dyestuff alone gave some protection. The UV absorber reduced the rate of dye fading by 38-50%. The protective effect of this absorber was reduced if light exposure was at 70°C rather than at 45°C. Increasing the concentration of the absorber from 1-5% increased the level of protection.

The 2-hydroxyphenyl-s-triazine was applied to wool in combination with 2:1 premetallized dyes and exposed to sunlight behind glass[143]. The dyestuffs alone gave little protection to tendering compared to undyed fabric. The UV absorber protected dyed wool from phototendering but the protection was similar or lower than that given by the absorber to undyed fabric. The reduced effectiveness of the absorber on dyed wool indicates that the dyestuff may have a photosensitizing effect. The UV absorber also reduced the rate of dye fading, but was less effective with increasing exposure time.

3.4 Studies using Spectroscopic Techniques for Analysis of Wool.

There has been growing interest in the study of the wool using non-destructive spectroscopic techniques. Since many oxidation products of wool are unstable under conditions of acid hydrolysis used for amino acid analysis, techniques such as FT-IR, XPS and more recently FT Raman spectroscopy have been applied to a number of problems in wool chemistry. The following section reviews the use of these techniques for studies on wool. Only one paper has been published which looked briefly at photo-oxidised wool using FT-IR and therefore this section aims to review the findings of studies which are important to the interpretation of results in this study.

3.4.1 Studies of Wool using Infrared Spectroscopy

Most of the early studies on wool used dispersive IR instruments and examined wool fibres after grinding with KBr and pressing into transparent discs. More recently the ATR technique (see Chapter 2.1.3) has gained much popularity for studies on wool since it is non-destructive and surface sensitive. Fabric, yarn or fibre samples can be investigated. This technique has also

been extended to microscopic use in the form of ATR microscope objectives which can be brought into contact with a selected area of a fibre surface.

Most of the previous studies have investigated the effect of various oxidising treatments on cystine residues. Bands have been assigned to the S-O stretching vibrations of cystine oxidation products between 1200 cm^{-1} and 1000 cm^{-1} (see Table 7.4)[147] [148] [149]. These assignments have made it possible to study the oxidation of cystine and the products formed both qualitatively and quantitatively. More recent workers have taken advantage of FT-IR instruments which have allowed the detection of the weak vibrations associated with the intermediate oxidation products.

An ATR study of peroxide bleached wool top detected an increase in cystine-S-monoxide, cystine-S-sulphonate and cysteic acid during bleaching under acidic conditions[30]. These species were also present under alkaline conditions even though it is generally thought that the intermediate oxidation products are unstable. The unresolved nature of these bands meant that only relatively large changes in intensity would be detected. FT-IR was used to detect increases in Bunte salt concentration after permonosulphuric acid treatments using both diffuse reflectance and KBr discs[150]. The surface of chlorinated wool has been examined using ATR[151]. The cysteic acid signal increased, but the unresolved nature of the S-O stretching band made it difficult to detect changes in intermediate products.

The overlapping nature of the S-O vibrations associated with the oxidation products of cystine in the region 1150-1000 cm^{-1} makes it difficult to distinguish between the bands associated with each of the oxidation products. Second derivative spectroscopy has been applied to resolve the overlapping absorption bands in a study of human hair fibres[152]. Flattened single fibres were examined using microspectroscopy. After hydrogen peroxide and metabisulphite bleaching, increases in cysteic acid and Bunte salt signals were detected. The change in cysteic acid concentration from the root to tip of the bleached fibre was plotted using the second derivative peak areas. In naturally weathered hair, there was also an increase in cysteic acid from root to tip direction but the level of cysteic acid at any point on the bleached fibre was higher than on the weathered fibre. There was a much greater variation between root and tip cysteic acid concentrations in the weathered hair. Bunte Salt concentration was found to be highest around the centre of the weathered fibre. This illustrates that Bunte salt is produced on photo-oxidation of the fibre, but is also susceptible to degradation at the more exposed fibre tips. Cystine monoxide levels remained constant along the hair fibre.

A direct linear correlation has been found between the second derivative band area at 1040 cm^{-1} for cysteic acid and the concentration of cysteic acid measured by amino acid analysis, after varying amounts of oxidation of wool with permonosulphuric acid[153] . Another study used second derivative ATR spectroscopy to resolve the oxidation products of cystine following dichromate treatments of wool[154]. After the treatment the only significant change was an increase in the peak area of the Bunte salt band.

Xenotest-exposed wool was examined using ATR and relative peak heights were measured in the undifferentiated absorbance spectrum[86]. After 120 hours exposure there was a twofold increase in cysteic acid concentration and a 50% increase in cystine monoxide. The cystine dioxide signal remained constant up to 72 hours then disappeared after 120 hours exposure. The rate of change in the cysteic acid signal over the period up to 120 hours exposure followed a similar curve to the change in yellowness index. No other evidence was given to link the increase in cysteic acid with yellowing.

Second derivative FTIR (ATR) is used to investigate the oxidation products of cystine after photo-oxidation and thermal oxidation[155]. The surface of wool exposed for 8 weeks in sunlight showed a more than twofold increase in cysteic acid signal. The signal continued to increase at a slower rate for the next 20 weeks at which point signal intensity had increased threefold. There was an initial increase in Bunte salt concentration up to 1 week of exposure followed by a disappearance of the signal with continued exposure up to 20 weeks. Cystine monoxide was fairly stable to photo-oxidation but had decreased in concentration slightly by 20 weeks. Cystine dioxide was rapidly degraded, presumably to cysteic acid, and its signal had disappeared after 8 weeks exposure. There was also a gradual decrease in Amide I (1652 cm^{-1}) signal up to 20 weeks exposure. No changes were detected in bands for the oxidised sulphur species after heating wool at 115°C for 6 days.

3.4.2 Studies of Wool using Raman Spectroscopy

Raman spectroscopy has had limited application in the field of wool research, mainly due to the problems encountered in obtaining good quality spectra. With the conventional dispersive technique, spectral quality was poor and since Raman scattering from wool is weak, it meant that long scan times were required at high laser powers in order to collect spectra. Visible frequency laser excitation increased the risk of sample heating and degradation, and fluorescent emission from wool gave spectra a high background intensity obscuring the weak

Raman bands. Fourier Transform Raman spectroscopy now allows highly resolved spectra to be collected for wool and in recent years there has been increased interest in the application of this technique to studies on wool. Early work by Lin and Koenig on wool, other α-keratins and proteins using dispersive instruments was particularly valuable in providing assignments for bands in wool up to 1658 cm^{-1} (see Table 7.1) [156] [157]. Lin and Koenig identified the conformationally sensitive bands in the Raman spectrum of wool. They found that with decreasing α–helical content of wool and proteins there was an increase in frequency of the Amide I band from 1658 cm^{-1} to the region of 1666 cm^{-1} . If wool is stretched to its β-sheet conformation the Amide I frequency is shifted to 1672 cm^{-1}. The Amide III band at 1245 cm^{-1} represents disordered or random coil structure and is broad and weak in wool reflecting the high α-helical content. The intensity of this band increases as the degree of disorder increases and reflects a loss in α-helical content of the fibre. The C-C skeletal stretching frequency at 935 cm^{-1} is sensitive to α–helical content and a transition to a more disordered structure or stretching to the β-sheet conformation reduces the intensity of this band.

One recent study took advantage of the improved resolution of FT-Raman instrumentation to make a number of new band assignments for wool[151]. The doublet at 1281 cm^{-1} and 1259 cm^{-1} is assigned to the Amide III vibration of the α-helix crystalline phase. The feature at 1155 cm^{-1} is assigned to C-N stretch rather than the β-skeletal stretch given by Koenig, since natural wool has a low β–keratin content. The bands at 905 cm^{-1} and 897 cm^{-1} are assigned to C-C stretch of the α-helix. A new band is assigned to tryptophan at 881 cm^{-1}. The disulphide band at 512 cm^{-1} was found to have two shoulders at 527 cm^{-1} and 546 cm^{-1} which the workers assigned to trans-gauche and trans-trans conformations respectively. No significant reductions in any band intensities could be detected after chlorination of wool.

FT-Raman analysis of hydrogen peroxide bleached wool found a decrease in the intensity of the CH_2 deformation band at 1449 cm^{-1} relative to the Amide I band[158]. The Amide I band showed a broadening around 1664 cm^{-1}. A new band appeared at 1334 cm^{-1} and bands at 1200-1280 cm^{-1} assigned to Amide III were reduced in intensity. Oxidation of cystine was shown by an increase in the band at 1042 cm^{-1} assigned to cysteic acid. The frequency of the disulphide bond vibration shifted from 507 cm^{-1} in untreated wool to 521 cm^{-1} after bleaching. This shift seemed to reflect the extent of disulphide bond oxidation since bleaching with a lower concentration of hydrogen peroxide causes a smaller shift to 514 cm^{-1} . The peak shift was attributed to changes in disulphide bond conformation: gauche-gauche (507 cm^{-1}) to

gauche-trans (514 cm^{-1}) to trans-trans (521 cm^{-1}). The changes to the Amide I and CH_2 bands were attributed to structural rearrangements of the skeletal backbone following disulphide bond fission.

The FT-Raman spectra of skin, callus, hair and nail were used to show the differences in cystine, tryptophan and tyrosine contents between these types of keratin[159]. Skin had a band at 2883 cm^{-1} assigned to the CH stretch of the CH_2 groups in the lipid matrix. Nail showed a pronounced C=O stretching band at 1727 cm^{-1} as a shoulder to the Amide I band.

A study developed a new sampling cell for wool and cotton which improved the signal to noise ratio of FT-Raman spectra[160]

The spectrum of the UV absorber Tinuvin P was investigated in water and on wool fabric using the dispersive Raman technique with laser excitation at 514.5 nm[161]. The ring structure of the UV absorber gives strong Raman bands but no assignments were made. On changing the excitation wavelength to 356.4 nm the intensity of two of these bands were resonance enhanced. These bands represent vibrational modes coupled with the electronic transition of the absorber excited at 356.4 nm.

3.4.3 Studies of Wool Using XPS

There have been no published studies using XPS to investigate the surface chemistry of photo-oxidised wool. However, there have been a number of important papers using XPS to investigate the surface chemistry of wool following a range of oxidative treatments.

The early studies of wool using XPS were carried out by Millard and workers. One paper used XPS to study the changes in concentration of organic coatings applied to wool such as fluorocarbon, silicon and phosphorus after solvent extraction and laundry tests[162]. The surface of plasma oxidised wool has also been investigated[163]. The C (1s) peak for untreated wool was peak fitted with components at 285 eV for aliphatic carbon, at 286.5 eV for carbon singly bound to oxygen and at 288.5 eV for carbonyl carbon. After oxygen plasma treatment the signal intensity of the two oxidised carbon components increased, particularly the carbonyl species. The O (1s) band for untreated wool was resolved into a main component at 532.06 eV and a smaller component at 530.04 eV with an area ratio of 9.2. The 532.06 eV line was assigned to oxygen in carbonyl, carboxylate, sulphone, sulphoxide and sulphonic acid groups. The 530.04 eV line has previously been assigned to oxides. After oxygen plasma treatment the ratio was 3.62 indicating the formation of surface oxide species. The N (1s) band was resolved

into components at 399.94 eV and 398.03 eV with an area ratio of 8.9 in untreated wool compared to 2.74 after plasma treatment. There were no clear conclusions about the species responsible for these two lines.

Most XPS studies of wool have investigated the oxidation of cystine. The S (2p) binding energy occurs at 164 eV for surface sulphur in the S (+2) oxidation state. This signal represents the disulphide sulphur of cystine residues. Millard[164] found an additional peak at 168 eV after corona treatment of wool which was subsequently assigned to the S (+6) oxidation state, or sulphur present as cysteic acid in wool[165]. The extent of surface disulphide bond oxidation can be measured by the relative intensities of the S (+2) and S (+6) signals. The effect of two chlorination treatments on surface disulphide bond oxidation was compared[165]. Treatment with hypochlorous acid gave almost complete oxidation of the surface disulphide bonds to cysteic acid, whereas after dichloroisocyanuric acid treatment only 50% of the surface sulphur was oxidised.

UV ozone treatment of the wool surface oxidises about 90 % of the surface cystine to cysteic acid[166]. Oxidised carbon species were also formed shown by a large increase in carbonyl component at 288 eV. There was no significant increase in the C-O component for hydroxyl or ether functionalities at 286 eV as found by Millard during oxygen plasma treatment.

Intermediate oxidation products of L-cystine were synthesized and analysed in powder form using XPS[167]. A shift to higher binding energy was observed with increasing oxidation on the sulphur atom with binding energies of 165.6 eV, 167.5 eV and 167.1 eV for cystine S-monoxide, cystine S,S-dioxide, and cysteine sulphinic acid respectively. Two peaks were resolved in the S(2p) spectra of cystine S-monoxide and cystine S,S-dioxide attributed to the two non-equivalent sulphur atoms. The stability of these intermediate oxidation products was investigated under mild hydrolytical conditions at pH values between 1-10 and the powdered disproportionate products of each of the intermediate oxidation products were identified by their S(2p) binding energies.

These assignments were used to identify the oxidation products of wool fibres following various chemical treatments[168]. After performic acid treatment, bands were resolved at 163.0 eV, 165.5 eV and 168.0 eV and were assigned to cystine, cystine-S-monoxide and cysteic acid respectively. There was also a peak at 167 eV which corresponded to sulphur bonded to two oxygen atoms in either cystine dioxide or cysteine sulphinic acid. After alkaline treatment of

the oxidised wool and re-analysis, the band at 167.0 eV did not change in intensity, which suggested cysteine sulphinic acid since the dioxide is not stable under alkaline conditions.
After hydrogen peroxide bleaching under alkaline conditions only cystine and cysteic acid were detected. Under acidic conditions the monoxide line also appears and there was a lower concentration of cysteic acid, but after alkali treatment the monoxide decomposed to cysteine sulphinic acid and cysteic acid. Chlorination of wool at pH 1 with sodium hypochlorite caused uneven uptake of the chlorine and led to uneven surface oxidation. Different areas of the fabric surface showed variations in the relative intensities of cystine and cysteic acid peaks. No intermediate oxidation products were formed due to the strong treatment conditions, but at pH 3 cystine monoxide was also present in some areas. At pH 5,7 and 9 only cystine and cysteic acid were present. No evidence for the presence of cystine dioxide was found. An attempt was made to investigate oxidation products present in intact wool compared to those in the cuticle and cortical components[169]. This was made difficult by the fact that the separation procedure using formic acid led to the decomposition of some of the intermediate oxidation products.

Other studies have used XPS to try and characterise the nature of the epicuticle of untreated wool, to determine its sulphur content and to find evidence for the existence of the lipid outer layer. One study considered the concentration and difference in reactivity of the polar groups in the epicuticle compared to those in the cortex[170]. The polar reactive sites in wool such as amine, hydroxyl, and primary amide groups were tagged by treating wool with hexafluoroacetone (HFA). Intact fibres and ball milled fibres were analysed to represent the epicuticle and the cortex respectively. Using amino acid analysis it was calculated that there should be a slightly higher concentration of sites which can react with HFA in the epicuticle compared to the cortex. However the fluorine to nitrogen area ratio, which provided an indication of the number of sites which had reacted with HFA, was higher in the cortex. This indicated that reactive sites in the cortex were more accessible than those in the epicuticle which are hindered in some way from reaction. The broadness of the XPS fluorine peak in the epicuticle compared to the cortex indicated a larger distribution of chemical environments in the epicuticle. The inaccessibility of reactive sites in the epicuticle may be due to steric hindrance, or hydrogen bonding or crosslinking at reactive sites within or between protein chains.

The accessibility of cystine residues in the surface compared to the bulk of the fibre has been investigated[171]. The extent of reduction of cystine residues to sulfhydryl groups after reaction with tri-n-butylphosphine was compared between the fibre bulk and the surface. The sulfhydryl groups were tagged with MeHgI and the Hg/S ratio was measured by XPS for the fibre surface and by microanalysis for the bulk. The Hg/S ratio for the whole fibre was 0.92 indicating almost complete reduction of the disulphide bonds compared to 0.82 for the surface. The lower extent of reduction in the surface was attributed to the inaccessibility of certain cystine residues, due to the highly crosslinked nature of the epicuticle and exocuticle

The hydrophobic nature of the epicuticle of wool has been attributed to the presence of an outer lipid layer known as the F-layer. Differences have been found between the chemical composition of the fibre bulk, obtained by chemical analysis, and the surface obtained by XPS[163]. The surface had half the concentration of nitrogen compared to the bulk, and this was thought to be due to a higher hydrocarbon content. The XPS studies of the surface of untreated wool reviewed in this section gave C/N ratios in the range 6.9 - 12.8. The expected C/N ratio for the whole fibre from amino acid analysis is much lower in the region of 3.6[172 174] .This high C/N ratio for the surface of the epicuticle reflects the presence of carbon rich material, possibly that constituting the fatty acid layer.

In addition, XPS studies have found that the surface S/N ratio of untreated fibres is much higher than expected for the fibre as a whole[174]. Ratios in the range 0.43 - 0.28 have been measured, compared to values for the whole fibre around 0.1. This reflects the high cystine content of the epicuticle and A-layer compared to the fibre bulk. A linear calibration curve was produced which relates the S/N ratio measured by XPS to the sulphur concentration of the surface protein. This was produced using measurements on S-carboxymethyl proteins of known sulphur content. Using this calibration plot, the epicuticle protein of untreated wool was calculated to have a 9% sulphur content by weight. This value is much higher than 3.7%, calculated by microanalysis for the whole fibre.

Treatment of wool with potassium *t*-butoxide in anhydrous *t*-butanol is reported to remove the lipid layer and release a C_{21} fatty acid. XPS analysis found no significant reduction in the C/N ratio after this treatment as might be expected if hydrocarbon material had been removed from the surface[174]. There was a decrease in S/N ratio indicating a loss in sulphur content explained by the loss of hydrogen sulphide which is formed by the action of alkali on cystine. The treatment caused a third of the surface sulphur signal to be converted to cysteic acid. The

asymmetry of the S (+6) peak at lower binding energy suggested that other intermediate oxidation products of cystine may be present. A shift in the main sulphur peak from 164 eV to 163.3 eV after the alkaline treatment was attributed to the formation of lanthionine residues.

XPS has been used to compare the epicuticle of intact wool and the surface of the cortex after clean cuticle removal[172]. The C/N ratio of the epicuticle was much higher than that calculated for the whole fibre from microanalysis. After cuticle removal the C/N ratio was lower and closer to the value expected for the whole fibre. A sulphur concentration of 8.7% was calculated for the epicuticle protein using Carr's calibration curve compared to 2.0% for the surface of cortex.

Evidence to support the existence of the F layer on the epicuticle was found using the combined techniques XPS and SSIMS[173]. The C/N ratio for untreated wool was 6.9 compared to a typical protein such as albumin of 4.3. This was due to the C (1s) peak having a larger hydrocarbon component at 285 eV. The X-ray induced Auger peaks provided information on the outermost 1 nm of the surface. The Auger C/N ratio was 19.0 reflecting the high hydrocarbon content on the outer surface of the epicuticle. An estimate for the thickness of the hydrocarbon layer was calculated from the XPS and Auger data to be approximately 0.9 nm $\pm$ 0.4 nm. The SSIMS spectra of wool identified three fatty acid components at 311, 325 and 341 a.m.u. assigned to C_{20} and C_{21} fatty acids. After treatment of wool with potassium *t*-butoxide in anhydrous *t*-butanol there was a reduction in XPS C/N ratio to 4.2 indicating removal of hydrocarbon rich material. The study did not indicate if there were relative intensity changes in the fatty acid signals, but there appeared to be reductions in the relative intensities of low atomic mass hydrocarbon peaks below 100 a.m.u. The XPS S (2p) peak contained a component for cysteic acid indicating that the treatment oxidises the underlying protein. There was a reduction in S/N ratio suggesting sulphur loss.

Chapter 4

Materials and Instrumentation

4.1 Materials

4.1.1 Automotive Fabric Development

In this study a series of 100% wool and wool blend automotive quality fabrics were produced in order to test the performance of these fabrics to current standards. All processing took place on commercial machinery at the IWS and in total 50 metres of fabric was produced. At each stage of processing the conditions were optimised in order to ensure maximum fabric performance. Three wool fibre qualities were used for fabric development in this study differing in mean fibre diameter. Table 4.1 lists the fibre characteristics of the three qualities used. Wool blend fabrics were produced using a range of staple polyester and nylon fibre qualities, the details of which are shown in Table 4.2.

Table 4.1 Physical characteristics of wool fibre qualities used

Fibre Characteristics	Wool Fibre Quality		
	60's Australian	49's Special	48's Colonial
Fibre Diameter (Projection Microscope)			
Mean (μm)	25.3	29.2	35.6
CV %	21.2	24	22.3
Mean Fibre Length (Hauter)			
Mean (mm)	82.2	82.1	118.5
CV %	46.1	55.1	40.1
95% fibres >	22.6	14.8	38.3
Yellowness Index			
Mean	19.9	21.65	22.35
CV %	3.7	4.5	4.4

Table 4.2 Characteristics of synthetic fibre qualities used.

Fibre Type	Decitex	Staple Length (mm)	Type Semidull = 0.3-0.5% TiO_2
Polyester	1.4 (11.3 μm)	65 - 100	350 Trevira Semidull / Round
Polyester	3.3 (17.4 μm)	65 - 100	Low Pill Semidull / Round
Nylon 66	2.4 (16.3 μm)	65 - 100	Type 303 Semidull / Round
Nylon 66	3.3 (19.2 μm)	75 - 125	Type 3733 Semidull / Round
Nylon 66	6.7 (27.3 μm)	65 -100	Type 3734 Semidull / Round

For maximum fabric lightfastness wool and synthetic fibres were dyed separately prior to blending. All dyeings for wool and synthetic fibres were matched to a standard Rover mid grey base shade. Grey shades are the most widely used for automotive upholstery and are also the most critical shades for lightfastness performance, particularly for wool. Recommended high lightfastness dyestuffs for each fibre type were used. Dyeing conditions recommended by WRONZ for maximum lightfastness of dyed wool were observed[185] as were those employed by automotive fabric manufacturers for dyeing polyester and nylon fibres. UV protective agents for all fibre types were co-applied in the dyebath using Ciba Geigy recommended conditions and application levels. Cibafast W, a sulphonated hydroxybenzotriazole UV absorber was applied to wool. Cibatex APS, also a sulphonated hydroxybenzotriazole derivative UV absorber was applied to polyester. Cibafast N, an organic copper complex hydroperoxide decomposer was applied to nylon fibres. All fibre dyeings were carried out in a Thies pressurised two way flow package / top dyeing machine, conditions and dye recipes are shown for each fibre type in Table 4.3.

Table 4.3 Fibre dyeing conditions

Wool Fibre Dyeing		
Dyestuffs: 2:1 Premetallised (Ciba Geigy)	Auxiliaries	Dyeing Conditions
0.46 % Irgalan Grey GL 200 % 0.11 % Irgalan Bordeaux EL 200 % 0.02 % Lanacron Yellow S-2G	2.0 % Cibafast W 0.5g/l Albegal FFA, 1.0% Albegal A 1.0% Sodium acetate	Liquor ratio 20:1, pH 5 (Acetic acid) Bath raised to 100°C at 1.5°C / minute Run 40 minutes, cool and rinse.
Nylon Fibre Dyeing		
Dyestuffs: 2:1 Premetallised (Ciba Geigy)	Auxiliaries	Dyeing Conditions
0.47 % Irgalan Grey GL 200 % 0.11 % Irgalan Bordeaux EL 200 % 0.06 % Lanacron Yellow S-2G	2.0 % Cibafast N 2.0% Albegal SW 1.0 % Ammonium sulphate	Liquor ratio 20:1, pH 6.0 - 6.5 (Acetic acid) Bath raised to 98°C at 1°C / minute Run 45 minutes, cool and rinse.
Polyester Fibre Dyeing		
Dyestuffs: Disperse (Ciba Geigy)	Auxiliaries	Dyeing Conditions
1.55 % Terasil Yellow GWL 150% 1.11 % Terasil Violet BL 0.51 % Terasil Pink 2GLA 0.47 % Terasil Blue BGE 200%	3% Cibatex APS 0.5% Univadine DP 2 g/l Sodium acetate	Liquor ratio 20:1, pH 4.5 - 5.0 (Acetic acid) Bath raised to 130°C at 1.5°C / minute Run 45 minutes, cool and rinse.

The worsted fibre processing route was followed for yarns with high orientation, strength, reduced pilling tendency and reduced surface hairiness. Fibre top was given 5 gillings during which fibre blending took place. Yarns were ring spun from 5 g/m gill sliver with the compositions shown in Table 4.4. Two fold yarns were produced for increased uniformity, tensile strength, abrasion resistance and yarn twist was optimised to reduce pilling, hairiness and increase durability. Singles yarns were spun to 62.5 tex, (16 new metric count) with an optimum Z twist level of 360 turns per metre. Doubling with S twist at 316 turns per metre gave yarns of total count 125 tex (2/16 new metric). Yarn twist was stabilised after spinning by steam setting on packages at 80°C for 10 minutes at 0.85 Bar.

Table 4.4 Worsted yarn compositions

100% Wool	65% Wool / 35% Polyester	65% Wool / 35% Nylon
25 μm	25 μm / 3.3 dtex	25 μm / 6.7 dtex
30 μm	30 μm / 3.3 dtex	30 μm / 3.3 dtex
35 μm	35 μm / 1.4 dtex	35 μm / 2.4 dtex

Fabric structure was selected to maximise cover factor and interlacing in order to give a compact and stable structure. A 2/2 twill was used for maximum durability, a flat surface profile and to avoid long yarn floats, in addition this structure is more extensible than plain weave. A nine sectioned blanket was woven using a Rapier Ruti G6100 loom after Hergeth warping. Warp and weft setts were equalised at 38 ends and picks per inch. A straight draft four end repeat with two ends per reed dent was used for the warp.

Conventional finishing routes for flat woven fabrics require alkaline scouring followed by heat setting. This may be followed by cropping for wool fabrics to remove protruding fibre ends. The recommended finishing route for Cibafast W treated fabrics specify a neutral scour using a non ionic detergent in order to avoid removal of Cibafast W. Fabrics were Dolly scoured at 35°C for 20 minutes using 'Nonidet SH30' at 0.5% on weight of wool at pH 6 and a liquor ratio of 20:1. This was followed by hydroextraction and stentering at 120°C at 5 yards / minute with 5% extension. The fabric was given a close crop and decatised at 125°C for 1.5 minutes at 1.2 Bar.

Fabrics tested to automotive standards must be in a laminated form. Fabrics were flame laminated to Rover specifications using 3.3 mm flame retardant polyester urethane foam giving a bond strength of $7N/m^2$. A warp knitted Queenscord nylon lining was laminated to the

reverse side of the foam. Laminated fabric weights were in the range 360 - 400 g/m^2 depending on composition.

4.1.2 Additional Materials

An undyed 100% wool yarn was produced to the same specification described in section 4.1.1 using the 35 μm wool quality. Small quantities of undyed plain weave fabric were produced at UMIST using a narrow width loom at 38 ends and 38 picks per inch. The fabric was alkaline scoured after weaving. Cibafast W was applied by exhaustion to the fabric at 2% oww. Fabric samples were also dyed with and without Cibafast W using the same dyestuffs and conditions described in Table 4.3.

100% Polyester fabrics were produced from 130 tex air jet textured semidull automotive quality yarn supplied by Hoechst. Fabrics were woven at UMIST with the same construction as described above for wool. Undyed fabric was treated with Cibatex APS, and dyed with and without Cibatex APS using the same conditions described in Table 4.3. In a similar manner 100% nylon fabrics were produced from 110 tex air jet textured semidull yarn supplied by Hoechst. Both undyed and dyed nylon fabrics were treated with Cibafast N.

Powdered amino acid samples, L-tryptophan, L-tyrosine, L-phenylalanine, and also powdered lysozyme (from chicken egg white) were supplied by Sigma Chemical Co. Ltd.

4.2 Light Exposure Conditions

4.2.1 Introduction to Accelerated Lightfastness Testing and Assessment[5]

Automotive manufacturers evaluate fabric photostability using accelerated test methods in which exposure conditions such as spectral distribution, temperature and humidity can be controlled in an enclosed chamber. This ensures the reproducibility of results and by defining end point criteria, lightfastness performance standards can be specified. The objective of these test procedures is to prevent in-service failure of fabric by trying to replicate the cumulative exposure conditions the average car will have to withstand during its lifetime. Much effort has been made in recent years to replicate in-service exposure conditions more accurately by correlation studies with fabrics exposed in vehicles in places such as Arizona. The accuracy with which these test methods can simulate real life exposure conditions depends mainly on the light source used. Although both Xenon Arc and Carbon Arc sources are currently used the Xenon Arc has a spectral power distribution curve which most closely resembles natural

sunlight and is therefore most widely used. The curve follows sunlight closely up to 650 nm but contains a few additional spikes in the infrared region which can be filtered. The UV spectral range permitted in exposure tests depends on the particular car manufacturers specification. Test procedures also differ in the temperatures used, in particular the difference between the chamber air temperature and the fabric surface temperature (measured by the black panel temperature). The conditions of humidity, irradiance and test duration vary between manufacturers. This inevitably leads to differences in test severity.

Most car manufacturers test methods are based on two international standards, the German DIN 75202 (FAKRA) and the American SAE J1885, both using xenon sources. The DIN specification is the basis for the tests methods of many of the European car manufacturers, for example Opel. The main feature of this test is that the light source is filtered to simulate exposure behind window glass. This ensures that UV light between 290-320 nm represents only 0.5% of the total irradiance between 290 - 800 nm and that between 290-400 nm represents 10%. Cycle duration is determined by simultaneously exposing a standard Blue Wool Scale and assessing the colour change of Blue Wool Standard 6. Exposure is ceased when Blue Wool 6 reaches a colour change equal to a rating 3 on the standard Grey Scale. This is measured colourimetrically using a spectrophotometer, with one exposure cycle specified as a colour change equal to a Δ E value of 4.3 ± 0.4 (80 ± 16 hours).

The SAE J1885 test method, used by Ford and many of the American car manufacturers, does not filter the light source and it therefore contains a significant component between 280-320 nm. This test has been argued to be unrealistic since wavelengths below 315 nm are filtered in vehicles by window glass. The test also differs from FAKRA in that the testing cycle is discontinuous, having light and dark periods to simulate daytime and night time conditions. Combined with a high relative humidity, this test aims to replicate the environmental conditions of Miami. The duration of the test is defined by the radiant exposure of the fabric, measured in kJ/m^2 at 340 nm.

Evaluation of the lightfastness of automotive fabrics is based on standards such as BS 1006/A02 or ISO 10J/B01 B02. Visual comparison is made of exposed and unexposed portions of a sample, the degree of colour change is graded according to the standard Grey Scale.* The Grey Scale runs from 5, which indicates no perceptible change from the standard, to 1. The pass level specified for most automotive fabrics is grade 4. The assessment must also specify if a change of tone has occurred during fading. Tone change is considered to be of

* NB. Blue Scale used for timing the period of light exposure. Grading of lightfastness is carried out against the Grey Scale.

equal importance as the overall level of dye fading. Although visual assessment is made by experienced judges, using D65 illumination, individual perception of colour varies, which makes this method subjective. Critical pass / fail judgements are often questionable.

4.2.2 Light Exposure Conditions Employed

In the current study, accelerated exposure methods were used since it was necessary to ensure reproducible conditions. Sunlight exposures are time consuming and expensive, they are not used routinely for fabric testing. Exposure conditions are subject to climatic and geographical variations. In this work a small amount of sunlight exposure testing was carried out in Arizona. A light exposure test method based on the FAKRA specification was considered to most realistically replicate automotive interior environmental conditions. The test method used in this work (unless otherwise indicated) is that specified by Rover Group, Table 4.5. Rover have adapted the FAKRA test by increasing air temperature and decreasing test duration to correlate with exposure studies carried out in Arizona sunlight[3].

Some testing was carried out using the test methods of Ford (SAE J1885) and General Motors (Opel, Vauxhall, DIN 75202), the conditions of which are also shown in Table 4.5 Sunlight exposures were carried out at D-SET Laboratories, New River, Arizona (latitude 25° 47' N, longitude 80° 51' W). Fabrics were exposed in Glastrac apparatus. This is an enclosed temperature and humidity controlled cabinet glazed with automotive side window glass which tracks the path of the sun for maximum solar irradiance. Fabrics were exposed to a specified level of radiant exposure equal to one cycle in the Rover test method.

Fabric samples were mounted onto white card (45 x 200 mm for Xenotest 450, 58 x 160 mm for sunlight exposures) using staples. Fabrics were half covered with white card if a visual assessment was to be made, as specified in BS 1006/A02. Three sample cards were exposed simultaneously for each fabric sample at each exposure period. For light exposure of single wool fibres, care was taken to ensure the even exposure of each fibre by mounting individual fibres side by side. Fibres were cut to 120 mm lengths and fixed to the cards at both ends using double sided tape. In the Xenotest apparatus, sample cards were mounted in holders positioned at equal distances around the central Xenon lamp. All samples were stored in brown envelopes free from contamination after exposure.

To determine the reproducibility of results from the Xenotest 450 the between testing session coefficient of variation in colour difference was obtained. Samples of each of the nine dyed

Table 4.5 Light exposure test methods used

Rover Group RES 30 CF 006 (based on FAKRA)	
Machine	Hereaus Xenotest 450 (air cooled burner)
Irradiance	85 W/m^2 at 300-400 nm
Spectral Range	295 nm -800 nm
Filters	6 IR, 1 blank
Black Panel Temperature	115°C ± 3°C
Air Temperature	70 - 75°C
Relative Humidity	10 - 30%
Exposure Cycle	Continuous
Test Duration	Blue Scale 7 to Grey Scale 4 (approx.52 hrs)

General Motors Europe (adapted from DIN 75202 FAKRA)	
Machine	Hereaus Xenotest 450 (air cooled burner)
Irradiance	not controlled
Spectral Range	310 nm -800 nm
Filters	4 IR, 3 window glass
Black Panel Temperature	115°C ± 3°C
Air Temperature	50 - 60°C
Relative Humidity	10 - 30%
Exposure Cycle	Continuous
Test Duration	ΔE of 4.3±0.4 on Blue Wool 6 (64 - 96 hrs)

Ford (SAE J1885)	
Machine	Atlas Ci65 (water cooled burner)
Irradiance	0.55 W/m^2 at 340 nm
Spectral Range	280 nm - 800 nm
Black Panel Temperature	Light Period: 89°C , Dark Period 38°C
Air Temperature	Light Period: 62 °C , Dark Period 38°C
Relative Humidity	Light Period: 50% , Dark Period 95%
Exposure Cycle	Cycled at 3.8 hours light, 1.0 hours dark
Test Duration	226.5 kJ/m^2 at 340 nm (approx. 115 hrs)

Sunlight Exposure (Arizona ASTM G7)	
Cabinet	Glastrac
Spectral Range	Terrestrial Sunlight
Filters	3mm window glass(filters light below 315nm)
Air Temperature	Day 70°C Night 38°C
Humidity	75%
Duration (28/2/92 - 4/4/92)	233 kJ/m^2 at 340 nm

wool blend fabrics were exposed for the standard exposure time of 52 hours in four separate exposure sessions. The between testing session coefficient of variation in ΔE was in the range 1.0 - 8.2 %. This variation also includes any variations associated with instrumental colour measurement.

4.3 Assessment of Lightfastness and Photoyellowing

Instrumental measurement of colour difference provides an objective method to assess lightfastness performance. This method is not currently used in the automotive industry due to the difficulty of assigning standard colour difference values to each of the Grey Scale values complicated by the variety of fabric types used. Colourimetric measurement has been used in this work since it was necessary to quantify changes in colour. In addition, the colour co-ordinates provide much valuable information regarding the nature of colour change. Measurement is made by illuminating the sample with the complete spectrum of visible light. The spectrophotometer measures the reflected light from the sample and ratios this to the incident intensity as a function of wavelength across the visible spectrum. These reflectance values from the sample are translated into the tristimulus values X,Y,Z which are transformed into the three colour co-ordinates. The colour is represented by its Hue (H), Chroma (C) and Lightness / Darkness (L) values. The colour difference values ΔL (L exposed - L unexposed) and similarly ΔC and ΔH, were calculated for each fabric to quantify the extent and nature of colour change. An overall measure of the size of the colour difference between two samples, taking the changes in ΔL, ΔC and ΔH into account, is known as ΔE. In this work ΔE was calculated using the CIE CMC 2:1 colour difference formula using a 10° Observer angle[175].

An ICS Texicon spectrophotometer was used which was coupled to an IBM computer with 'Spectraflash' software. A pulsed xenon light source was used emitting D65 illumination with a spectral range 360 nm - 750 nm. Samples were removed from the cards after exposure and positioned against the standard size spectrophotometer aperture. Readings from three pulses were averaged for each measurement and three measurements were averaged from different areas of each sample. The unexposed fabric standard was always measured prior to measurement of the exposed fabric. Undyed fabrics were assessed for changes in yellowness. The Yellowness Index (YI) was calculated from the tristimulus values X,Y,Z according to the standard formula:

$$YI = \frac{1.316\,X - 1.164\,Z}{Y} \times 100 \qquad (\text{ASTM}) \qquad [4.1]$$

4.4 Assessment of Phototendering

Assessment of the phototendering of wool fabrics has been typically carried out by other workers by measuring properties such as residual tensile strength and tear strength. These tests require a minimum amount of time and give a general measure of the extent of deterioration in fabric integrity. The rapid quality control testing employed by the automotive industry means that fabric photostability is most usually assessed by measuring the residual tensile strength of fabrics after light exposure for a specified duration. These tests are complicated by the fact that fabrics are tested in a laminated form so that the results reflect the properties of the trilaminate as a whole. These methods give no information on the rate of surface deterioration and loss of wear resistance, which is particularly important since photodegradation is mainly confined to the surface layers. In this work, abrasion testing was used to provide surface sensitive information regarding the rate of photodegradation of fabrics. The Kawabata KES-F instruments[178] were used to characterise changes in the mechanical surface properties of fabrics due to light exposure. To investigate the effect of light exposure on the fundamental tensile properties of wool, single fibre testing was carried out, which avoids the complications of fabric and yarn structure.

4.4.1 Fabric Abrasion Testing.

Abrasion testing is mainly used by car manufacturers to assess the wear resistance of unexposed fabrics. Fabrics are abraded to a specified number of cycles and at this point flat woven fabrics must contain no broken ends. Fabrics are compared to acceptable master standards for appearance retention, pilling is unacceptable. A variety of abrasion test methods are used. The Taber, Stoll and Schopper are rapid tests taking 1-2 hours for completion and use non-textile abradants. The speed of these tests means that they provide little information on short term wear properties. The Stoll test aims to replicate the action of wear across a curved surface as would be the case on a seat, but little correlation between the characteristics of in-service wear and this test has been found[176]. In addition these tests show little correlation to observed patterns of wear in service, and are generally used as a rapid means of quality control assessment. It is questionable if any accelerated abrasion test can accurately reproduce the conditions experienced during real life wear. However, the Martindale has been shown to cause fibre damage most similar to that found in actual wear of apparel fabrics compared to

the Taber and Stoll[174]. Martindale abrasion resistance has been shown to be a sensitive measure of the extent of chemical damage which may have occurred in wool fibres[177]. The Rover Group has evaluated abrasion test methods with the aim of developing a more meaningful flat abrasion resistance test, which correlates more closely with in-service wear[3]. The Martindale test was found to provide the most information and was able to reproduce the effects of short and long term wear most closely. The Rover test for aged abrasion resistance (BLS 30 AR 102) now specifies that fabrics should be exposed for 24 hours in Heraeus 'Suntest' apparatus followed by 50,000 Martindale cycles which takes approximately 18 hours. Assessment of pilling and general wear is made every 10,000 cycles against acceptable appearance standards.

The Martindale test was therefore used in this work. Its small specimen size (circular samples of 38 mm diameter) was suitable for testing the Xenotest exposed fabrics which had a width of 45 mm. Martindale testing was carried out according to BS 5690 (1988) using the standard crossbred worsted abradant material. Two adjustments were made to this test method to bring conditions in line with Rover specifications. The abradant was replaced every 25,000 cycles and the sample holders were loaded with the 21 oz weights giving a pressure on the sample of 12±0.2 kPa. Testing was carried out on the same Martindale instrument (J.H.Heal & Co.) under standard atmospheric conditions (65 ± 2% RH, 20 ± 2°C). Fabrics were conditioned in this environment for at least 24 hours prior to testing. Circular samples were cut from the standard template, four specimens were tested simultaneously for each fabric in order that mean values could be calculated.

Assessment of Abrasion Resistance.

To assess the effect of light exposure on fabric surface integrity, the rate of weight loss of each sample was measured during abrasion testing. It was considered that this would give a more sensitive measure of the rate of surface breakdown compared to the more variable measure of end point cycles. Conditioned specimens were weighed using an electronic balance sensitive to four decimal places prior to testing. Specimens were then weighed at intervals during abrasion testing. Fabrics which had not been exposed to light were weighed every 25,000 cycles. As a consequence of the successively lower end points of exposed fabrics, weight loss was measured at smaller intervals of abrasion cycles. Fabrics exposed for up to 104 hours were weighed every 10,000 cycles, those exposed for more than 104 hours were weighed after every 5,000 cycles. Fabrics were assessed for pilling and general wear at each weighing

interval. The abrasion test was continued to end point, specified by the British Standard method as the breakage of any two dissociated threads in the fabric. In certain cases, due to time limitations, fabrics testing terminated at 100,000 cycles if thread breakage had not occurred at this point.

The percentage weight loss was calculated at each interval of testing for each specimen. By plotting the percentage weight loss as a function of the number of cycles, the rate of surface breakdown for each specimen could be examined. The mean rate of weight loss for each specimen was calculated to represent an index of abrasion resistance. The residual abrasion resistance of a fabric after light exposure could then be calculated as a percentage of the original abrasion resistance by comparing the indices before and after exposure.

4.4.2 Fibre Tensile Testing

The random draw sliver sampling method (BS2545) was used to select wool fibres (35μm quality) for Xenotest exposure and subsequent tensile testing. The end of each fibre to be tested was mounted onto a small card support using epoxy resin.

The breaking load of fibres increases in proportion to the cross sectional area of the fibre. Since there would be a variability between the linear densities of wool fibres tested, to improve the accuracy of results the tex value of each fibre was calculated from diameter measurements. Fibre diameters were measured using image analysis. Three diameter measurements were averaged along the 2 cm testing length of each fibre. Equation [4.2] was used which relates fibre diameter in microns (μ) and fibre density (ρ) (1.31* for wool) to Tex. Using this calculation an assumption is made that the fibre has a circular cross section.

$$\text{Tex} = \frac{\mu^2 \times \rho}{1269} \qquad [4.2]$$

Fibre testing was carried out according to method BS3411 (1971) which states that for single wool fibres a pretension of 0.5g / tex must be applied to remove crimp from the fibre before commencing the test. Since it would be time consuming and difficult to make small alterations to the pretension weight according to the tex value of each individual fibre, a constant pretension of 0.65g was applied to all fibres, representing the average fibre diameter of 35μm. Testing was carried out on an Instron 1122 (constant rate of elongation) under standard atmospheric conditions. Each fibre was mounted in the top jaw and the pretension was applied to the free end of the fibre before closing the bottom jaw. Pretensioning was achieved using a

* WIRA

small weighted bull dog clip which was able to hang from the end of the fibre unobstructed. The inside of the jaws were lined with rubber to stop fibre slippage during testing and also to avoid the impact of the jaw closure cutting the fibre.

To compare the effect of light exposure the test conditions must remain the same for both unexposed and exposed fibres. A full scale load of 50g was used and a crosshead speed of 20 mm /min, in accordance with the recommended rate of 100% extension per minute. The Instron uses a chart recorder to plot load / elongation curves, but in this work the Instron was interfaced to a BBC computer and the breaking load, tenacity, work of rupture, specific work of rupture, extension at break and initial modulus were calculated from the loading data and test parameters. The software was adapted in this work to allow for pretensioning of single fibres. Any fibres which showed jaw breaks were rejected. The results of unexposed wool 450 fibres were tested and 120 fibres for each light exposure period. Statistical analysis was carried out using 'Systat' software.

4.4.3 Yarn Tensile Testing

Single wool yarns were taken from fabric samples before and after Xenotest exposure and tested for changes in tensile properties using the Instron 1122 under standard atmospheric conditions. Testing was carried out using a gauge length of 3 cm, full scale load 2 kg, crosshead speed 50 cm / min. Fifty yarns were tested for each exposure period.

4.4.4 Kawabata Testing

The low stress surface mechanical properties of fabrics were measured using the KES-F instruments[178] [179]. Fabric tensile, shear, bending and compressional properties are measured along with surface roughness and coefficient of friction. Standard sample size is 20 x 20 cm, but fabrics of size 4.5 x 20 cm were also tested in the case of Xenotest-exposed fabrics.

4.5 Microscopical Analysis

4.5.1 Scanning Electron Microscopy

Fabric samples were fixed to stubs using copper adhesive tape to increase the conductivity of the sample. For the analysis of single fibre tensile fractures the fibre ends of interest were sandwiched between two strips of adhesive copper tape so that the ends projected no more

than 1 mm from the edge of the tape. The tape was placed in a split stub and positioned so that the vertically projecting ends were aligned with the surface of the stub. The surface of single fibres was analysed by mounting them horizontally across an open stub. The mounted specimens were sputter coated using a gold particle discharge in argon which deposited approximately a 40 nm gold layer on the surface. Working distances were in the range 10-20 mm of the sample surface from the detector. Accelerating voltages were in the range 5-10 kV with an electron beam spot size of between 5 - 10. Magnifications up to 30,000 times were achieved.

4.5.2 Atomic Force Microscopy

Individual fibres were examined using a Digital Instruments Nanoscope II operating in Constant Force Mode (approx. 40 nN). A silicon nitride V shaped cantilever was used with a spring constant of 0.12 N/m. Single fibres were mounted onto a 10 mm diameter circular metal disc using double sided tape. The disc was placed on the XYZ piezo controlled stage and the stage was moved until the fibre was in contact with the probe tip. Sample positioning was achieved using a portable monocle.

4.6 Spectroscopic Analysis

4.6.1 FT-IR Analysis

A Nicolet Magna-IR System 750 spectrometer was used which comprised of a main analysis bench and a 'NicPlan' microscope attachment (see Figure 2.2). The main bench and microscope use the same infrared source and interferometer but have separate liquid nitrogen cooled detectors, an MCT-B (mercury cadmium telluride) for the main bench and the more sensitive MCT-A for the microscope. An Ever-Glo infrared source is used which is focused to a spot size of 7 mm for analysis in the main bench. The system uses a helium neon laser (632.8 nm, 1.0 mW) which acts as an internal calibrator since it monitors the movement and position of the moving mirror in the interferometer. All spectra are therefore collected at precise laser calibrated points with a wavenumber accuracy better than 0.01 cm^{-1}. Analysis was carried out in the mid infrared region from 400 cm^{-1} to 4000 cm^{-1} requiring a germanium coated KBr beamsplitter. The spectrometer is capable of 0.125 cm^{-1} resolution but spectra were run at 4 cm^{-1} resolution. Multiple scans (typically 200) were averaged to improve spectral signal to

noise ratio. Collection time was approximately 0.33 seconds per scan at 4 cm^{-1} resolution. In all cases the Happ-Genzel apodisation function was used in the conversion of the interferogram into a single beam spectrum.

4.6.1.1 ATR Analysis

The surface of fabrics was examined using ATR (see Figure 2.3). A vertical ATR attachment was used to examine the surface of fabrics which is positioned in the main bench sampling compartment. A synthetic KRS-5 45° crystal was mainly used, with a refractive index of 2.38 and length 30 mm, width 20 mm and thickness 5 mm and consists of about 42% thallium bromide and 58% thallium iodide. The ATR attachment had a fixed angle of incidence of 45°. Six internal reflections of the infrared beam take place as it travels the length of the crystal. The depth of penetration of the evanescent wave into the sample depends on the angle of incidence, the infrared wavelength and the refractive indices of the crystal and sample. This relationship was established by Harrick[60] and is shown in [4.3], where d_p is the effective depth of penetration in μm, λ is the infrared wavelength in microns, θ is the angle of incidence of the infrared beam, and n_1 and n_2 are the refractive indices of the crystal and sample respectively. It can be seen that if the angle of incidence, crystal and nature of the sample remain constant, the depth of penetration is directly proportional to the wavelength of the incident beam. The penetration depth was calculated as a function of incident wavelength for wool of refractive index 1.55 . Substituting $\lambda = 10^4 / x$ in equation [4.3] where x is the infrared frequency in wavenumbers (cm^{-1}), a plot of penetration depth as a function of wavenumber was calculated over the range 400 cm^{-1} - 4000 cm^{-1} and is shown in Figure 4.1.

$$d_p = \lambda / 2\pi n_1 \sqrt{\sin^2\theta - (n_2 / n_1)^2} \qquad [4.3]$$

With an increase in wavenumbers (ie decreasing wavelength) the radiation passes less deeply into the sample. An ATR spectrum therefore shows relative peak intensity differences compared to a transmission spectrum of the same material. The depth of penetration in the region for S-O vibrations of cystine between 1000 cm^{-1} - 1200 cm^{-1} is 2.43 - 2.02 μm. Greater surface sensitivity can be achieved for the same sample by using a crystal of higher refractive index as shown in Figure 4.1 for a germanium crystal with refractive index of 4.0. This crystal was used in certain cases where improved surface sensitivity was required. Since

1.55 is the approximate refractive index of most textile fibres, the depth of penetration curves shown in Figure 4.1 are also appropriate for ATR analysis of polyester and nylon fabrics.

The amount of radiation absorbed depends on the area and efficiency of contact between the sample and crystal. The sample must also extend the full length of the radiation path through the crystal otherwise part of the radiation may bypass the sample along the sides of the crystal which can cause spectral distortion. Therefore fabrics were cut to the same dimensions using a standard template of size 30 x 20 mm . Two specimens of the same fabric sample were placed in contact with the crystal ensuring that the surface of interest was in contact with the crystal. The crystal and fabrics are held in contact in a sample holder which is tightened using screw pressure. To ensure sufficient and reproducible contact from sample to sample a constant pressure of 68.9 kPa was applied to the sample holder using a calibrated torque screwdriver. Spectra were collected at 4 cm^{-1} resolution and 200 scans were averaged. The background spectrum was collected through the crystal in the absence of the fabric.

The between sample variability in signal intensity for the cystine oxidation products using ATR analysis was examined. Ten spectra were collected of unexposed untreated wool fabric and were normalised on the Amide I band. The second derivative band intensities for each of the cystine oxidation products were measured and the coefficients of variation calculated. Cysteic acid (1040 cm^{-1}) had a between sample C.V. of 10%. Cystine-S-monoxide (1078 cm^{-1}) C.V. of 13%. Cystine-S-dioxide (1126 cm^{-1}) C.V. 21%. Cysteine-S-sulphonate (1023 cm^{-1}) C.V. 50%.

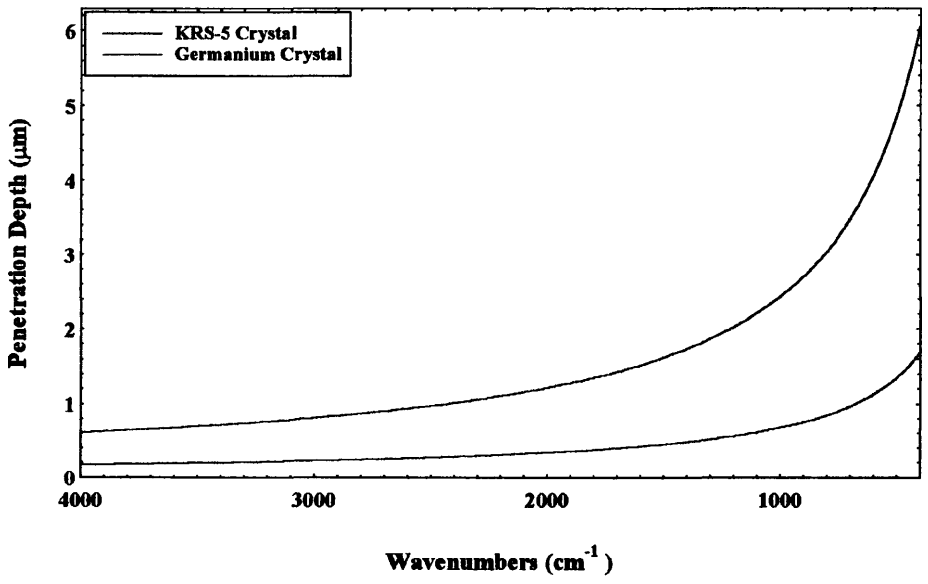

Figure 4.1 Penetration depth of infrared evanescent wave in wool using ATR crystals

4.6.1.2 Microspectroscopy for Single Fibre Analysis

The Nic-Plan infrared microscope has a 10x glass objective and 15x infrared objective. The infrared beam is focused onto the sample by an upper objective lens and is collected after transmission through the sample by a lower condenser lens. The infrared objective and condenser have Cassegrainian lenses. Spatial resolution is controlled by an adjustable aperture situated above the upper objective. Once the sample is centred and focused the area of the sample to be analysed can be selected by adjusting aperture opening using two sets of knife edges. The lower condenser lens must be focused to collect the transmitted radiation, and the lower aperture opening is adjusted to the same size as the upper aperture using knife edges. This technique using a 'redundant' lower aperture ensures that only the collimated radiation directly transmitted by the sample is collected and any radiation which may be diffracted by the sample will not pass to the detector. The 'ViewThru' microscope system allows the sample, the upper aperture and lower aperture to be viewed simultaneously allowing alignments to be made.

Single fibres were mounted across an open well of a microscope slide using tape. The fibre axis was centred on the verticalcross-hairThe upper aperture size was set to the same width as the fibre and a 100 μm along the length of the fibre. Transmission of adequate infrared energy through the sample depends on the sample thickness and absorption characteristics. It was found in this study that only wool fibres of diameter less than 20 μm would give satisfactory transmission. Single polyester and nylon fibres of linear densities between 1.4 and 3.3 dtex were suitable for analysis. Spectra were collected at 4 cm^{-1} resolution and averaged over 200 scans. The background spectrum was collected after the sample spectrum by removing the fibre from the path of the infrared beam.

In the case of wool analysis it was considered that there would be significant variations in the signal intensities of cystine oxidation products both within one fibre and between fibres. These variations were therefore examined. The root to tip variabilities within one whole fibre for cysteic acid and the partially oxidised cystine residues were investigated. An untreated unexposed fibre was sampled at approximate 10 mm intervals along the fibre length. Spectra were normalised against the Amide I band and the second derivative band intensities for each of the oxidised species measured. The cysteic acid signal remained within the limits of variability shown in Table 4.6 along the whole length of the fibre until a point 20 - 30 mm from the wool fibre tip.

Table 4.6 Variability in signal intensities of cystine oxidation products in single fibre analysis

C.V.%	Bunte Salt 1022 cm^{-1}	Cysteic acid 1040 cm^{-1}	Cystine-S-monoxide 1078 cm^{-1}	Cystine-S-dioxide 1126 cm^{-1}
Within Fibre (excluding tip)	37	9	7	19
Between Fibre	45	12	10	18

In this tip region the cysteic acid signal was 6-7 times higher than the average value for the rest of the fibre. The fibre tip had a much lower or absent Bunte salt signal. No large differences were found between the intensity of cystine monoxide and cystine dioxide signals between the fibre tip and the rest of the fibre. To avoid the more highly oxidised fibre tips, FT-IR analysis of single fibres was carried out in the middle of each fibre. The between fibre variability was examined using 20 untreated unexposed wool fibres taking measurements in the middle of each fibre. Table 4.6 shows that there is a large variation in Bunte salt signal from fibre to fibre, but much smaller variations for the other species.

4.6.1.3 Diffuse Reflectance Infrared Spectroscopy (DRIFTS)

In DRIFTS analysis the infrared beam is focused onto the surface of powdered samples and those wavelengths not absorbed are diffusely reflected and analysed. DRIFTS was used for the analysis powdered amino acids, lysozyme and UV protective agents. A Spectratech diffuse reflectance accessory was used, positioned in the sampling compartment of the main bench. To avoid complete absorbance of the infrared beam by the sample, the powders were diluted by mixing them at a concentration of between 5 to 10% with KBr powder. The KBr powder was oven dried and stored in a desiccator prior to use to avoid spectral bands due to absorbed water. Highly crystalline powders can specularly reflect the infrared beam causing absorption bands to be distorted and have first derivative-like profiles. To avoid this effect powders were finely ground. The powdered samples were placed in micro-sampling cups for analysis and the accessory was adjusted to focus the infrared beam onto the sample surface. The single beam spectrum was ratioed against a KBr powder background to give the % reflectance spectrum of the sample. This was converted into absorbance type data using the Kubelka-Munk function[180]. Spectra were collected at 4 cm^{-1} resolution and 200 scans were averaged.

4.6.1.4 Derivative Spectroscopy[181] [182]

Derivative Spectroscopy has gained much use for resolving overlapping bands in vibrational

spectroscopy. In the case of a typical infrared absorbance spectrum the differentiated spectrum is a plot of the rate of change in signal intensity as a function of wavenumber. Therefore, the first derivative is the gradient of the original spectrum at each wavenumber ($\delta Y / \delta X$). The spectrum may be repeatedly differentiated to higher orders ($\delta^n Y / \delta X^n$). Although the wavenumber resolution of the derivative spectrum remains the same as the original absorbance spectrum, differentiation decreases the bandwidth of the peak profiles and therefore allows overlapping bands to be distinguished. The even numbered derivatives are of more diagnostic use since the maximum peak amplitude of the derivative band corresponds to the maximum peak amplitude of the original band. If the even derivative order increases, ie fourth or sixth derivative, the main peak width decreases which therefore improves resolution, but this is at the expense of a decrease in peak amplitude. In addition, apart from the main peak, differentiation generates smaller satellite peaks on either side of the main band. As the even derivative order increases, more satellite peaks are generated which complicates the spectrum and may interfere with adjacent bands. For these reasons the second derivative is most widely used. Spectral noise can reduce the usefulness of derivative spectra. High frequency noise, even if it is low in intensity, gives sharp derivative peaks which increase in intensity with derivative order. The signal to noise ratio of the second derivative spectrum is decreased by a factor of four compared to the original spectrum, it decreases by a factor of sixteen for the fourth derivative. Low frequency noise however is reduced in derivative spectra.

Derivative spectroscopy discriminates in favour of sharper features in the original spectrum. It is particularly useful for resolving weaker sharper bands which are situated on broader spectral features. In the case of two overlapping Lorentzian bands of equal intensity and equal width the second derivative spectrum will show two inverted peaks of equal intensity and width separated by 50% of their original half width. If two overlapping bands are of equal intensity but one is of twice the width of the other, the amplitude of the broader peak will be one quarter that of the sharper one.

4.6.2 FT-Raman Analysis

A Nicolet FT-Raman 950 instrument was used which has a main bench and microscope attachment (see Figure 2.4). The incident source was a continuous output Nd:YAG monochromatic near infrared laser of wavelength 1064 nm. The laser is water-cooled and

unpolarised with a focused spot size at the sample of 50 μm. The instrument uses a high speed liquid nitrogen-cooled Germanium detector which spans the near infrared range from 5900 cm^{-1} to 11,000 cm^{-1} (3500 cm^{-1} Stokes to 1600 cm^{-1} anti-Stokes Raman shift). The detector is also sensitive to thermal emission from samples which can cause a high background in the spectrum. This makes it difficult to analyse many dyed samples and therefore it was not possible to investigate dyed fabrics in this work.

The intensity of Raman bands is linearly related to the concentration of the scattering species, but since the source of radiation is the sample itself, the intensity of scattering from a sample will be affected by the positioning and concentration of the sample in the laser. For quantitative purposes it is therefore difficult to make direct comparisons of absolute spectral band intensities between samples. Therefore in this work only relative peak intensities were compared.

Wool is a weak Raman scatterer and in order to investigate subtle spectral changes it was necessary to maximise signal to noise ratio. The power output of the laser is adjustable in the range 40 to 1300 milliwatts, an increase in laser power increases Raman scattering intensity. A direct linear relationship was found between laser power and the signal intensity of the CH_2 band at 2930 cm^{-1} in wool. However, caution is needed when selecting the incident laser power to avoid heat damage to sensitive samples. To determine the optimum laser power for analysis, a sample of untreated wool fabric was analysed at increasing laser powers, with 500 scans averaged for each sample. The signal to noise ratio (intensity at 2930 cm^{-1} relative to the peak to peak noise in the baseline region between 2500 - 2000 cm^{-1}) was measured as a function of laser power and is plotted in Figure 4.2. The signal to noise ratio increases rapidly up to 700 mW but there is little benefit in using laser powers above 1000 mW. Apart from the improvement in signal to noise ratio, there were no other significant changes in the Raman spectrum of wool as the laser power was increased which would indicate excessive heating, Figure 4.3. Signal to noise ratio can be improved further by increasing the number of scans. The improvement factor achieved is equal to the square root of the scan number multiplication factor. In order to obtain adequate signal to noise ratio of the spectra and avoid sample heating by using high laser powers, a moderate laser power of 500 mW was used in combination with a high number of scans. A scan number of 3,000 per sample (approx. 60 minutes collection time) was found to be suitable in terms of spectral quality and time factors. All spectra were collected at 4 cm^{-1} resolution using the Happ Genzel apodisation function. A

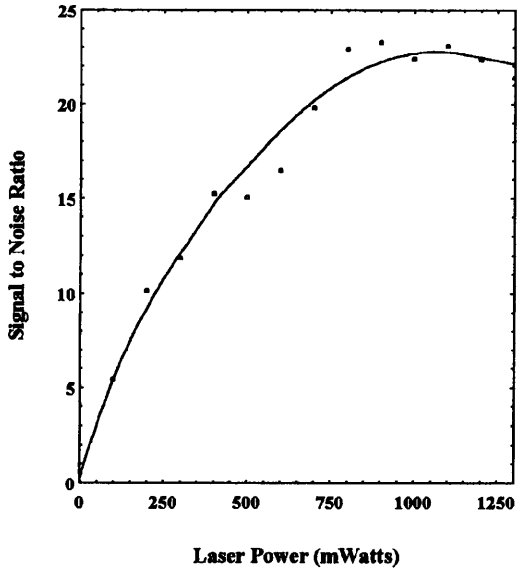

Figure 4.2 Spectral signal to noise ratio as a function of laser power

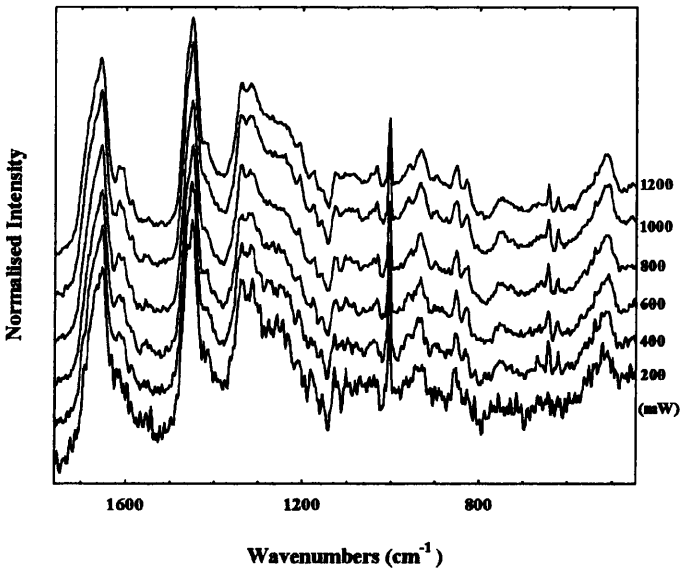

Figure 4.3 FT-Raman Spectrum of wool as a function of laser power

180° sampling geometry was used. The sample is moved laterally to the focal point of the laser using a computer-controlled sample stage Focusing is achieved when the three red dots formed on the sample from the HeNe calibration laser are collimated into one spot.

Fabric samples require no preparation and were mounted across a stainless steel frame which could be positioned in the laser path. Powdered samples, such as amino acids and photo-protective agents were analysed in 3 mm diameter NMR tubes which fit into a standard vertical sample holder supplied by Nicolet.

4.6.3 XPS Analysis

Analysis was carried out using a VG ESCA 3 MkII spectrometer with a non-monochromatised beam of Mg Kα X-rays of energy 1253.6 eV (line width 0.7 eV). A constant X-ray power of 240 W was used (12 kV accelerating voltage, 20 mA anode current). The spectrometer was evacuated using two liquid nitrogen cooled oil diffusion pumps backed by a rotary pump to residual pressures in the range 10^{-7} to 10^{-8} Torr. The instrument was operated in the Constant Analyser Energy (CAE) mode using a concentric hemispherical analyser. The detector used is a channel electron multiplier. Fabric samples of size 10 mm x 6mm were fixed to a stainless steel sample holder using double sided tape. Two

samples could be fixed to the sample holder and analysed successively. The sample holder was attached to the probe which was introduced into the spectrometer preparation chamber. Once the spectrometer had been evacuated, the samples were transferred from the preparation chamber to the analysis chamber. Using an XYZθ manipulator the sample was positioned under the X-ray source in alignment with the entrance slit of the analyser. The sample was angled at 40° to the horizontal which gave a photoelectron take off angle relative to the sample surface of 40°. The spatial resolution is governed by the spot size of the X-ray source and the collection area of the analyser (slit width). In the ESCA the X-ray spot size is 8 mm x 4 mm with a similar analyser slit width so that the majority of the sample surface was analysed.

For data acquisition VGS 1000 software on an Apple IIe computer was used. A survey scan was initially collected which provided a broad surface profile, followed by high resolution scans of each elemental core level. For each region of interest successive scans were co-added in order to improve spectral signal to noise ratio. The acquisition settings for each region were:

Survey: pass energy 50 eV, scan length 0 - 1000 eV Binding Energy, time per channel 50 ms, step size 0.5 eV, scan number 10, acquisition time 17 minutes.

Core lines: pass energy 20 eV, scan length 25 eV (12.5 eV either side of core line), step size 0.05 eV, time per channel 50 ms. For the C (1s), O (1s), N (1s) core lines 45 scans were accumulated giving an acquisition time of approximately 19 minutes. For the S (2p) Cu ($2p_{3/2}$) core lines 90 scans were co-added with an acquisition time of 38 minutes.

The data was formatted for spectral processing using M-Probe operating software on an IBM compatible PC.

4.6.3.1 Charge Referencing of Binding Energy Scale

The photoelectron process involving the loss of electrons from the sample gives rise to a positively charged surface which attracts escaping photoelectrons and reduces their kinetic energy. This causes a higher binding energy shift in the photoelectron peak positions, typically up to 3eV, by an amount equal to the charge on the surface. For non-conducting samples this surface charge cannot be removed by earthing the sample. It is therefore necessary to correct the binding energy scale to compensate for this surface charging. Charge referencing was carried by the most widely used method where the C (1s) peak is used as a binding energy reference. The C (1s) peak is adjusted to 285 eV and the shift value is applied to all other

photoelectron peaks in the spectrum. Therefore the binding energies of all photoelectron peaks are relative to the C (1s) line at 285 eV.

4.6.3.2 Quantitative Analysis (see section 2.2.1.1)

After subtraction of a linear background the photoelectron peak areas were measured using a Shirley baseline. The peak area is related to the number of scans accumulated, and therefore the photoelectron peak areas within the same spectrum were adjusted using a multiplication factor to compensate for differences in scan number. These adjusted raw peak areas were divided by the appropriate relative sensitivity factors, equation [2.6]. The Wagner[183] empirically derived atomic sensitivity factors were used which give the values: C (1s) 0.25, O (1s) 0.66, N (1s) 0.42, S (2p) 0.54, Cu ($2p_{3/2}$) 4.2. Elemental ratios and the percentage surface elemental composition could then be calculated according to equation [2.7].

The between sample repeatability for quantitative surface analysis of wool using this technique was investigated. Six samples of untreated unexposed wool were analysed using the same experimental conditions, the C (1s), O (1s), N (1s) and S (2p) regions were scanned and the elemental ratios calculated as described above. The between sample coefficients of variation for each of the elemental ratios are given in Table 4.7. The elemental ratios associated with sulphur show the largest coefficients of variation indicating a greater variability of surface sulphur concentration using XPS analysis.

Table 4.7 Between sample variability of XPS elemental ratios for untreated unexposed wool

Elemental Ratio	O/C	N/C	S/C	O/S	O/N	S/N
Mean Value	0.14	0.07	0.02	6.9	1.96	0.29
CV %	2.8	3.1	15	11.7	3.2	15.3

4.6.3.3 X-Ray Damage Study

Due to the high energy excitation source used in XPS it is important to consider if sample damage occurs during analysis, and what level of damage is caused during the analysis time. The high energy Bremsstrahlung radiation is able to penetrate the sample 'bulk' and this damage is often shown by sample discolouration. It is well known that certain polymers degrade during X-ray analysis, such as halogen-containing polymers, whereas aromatic containing polymers are little affected[184]. Most oxygen-containing polymers degrade under XPS conditions with a loss of oxygen therefore the O/C ratio decreases. With an

unmonochromated X-ray source the sample is much closer to the X-ray anode so that thermal degradation may be important. Decomposition, for example the dehydration of biological samples, may also occur due to the high vacuum conditions and reactions may take place with residual gases in the spectrometer. In addition the generation of electrons by the photoemission process may also initiate degradative reactions.

To assess the time-dependent change to untreated wool, polyester and nylon fabrics, samples were irradiated continuously with the X-ray source for a period of 8 hours. The change in O (1s) signal intensity was measured as a function of X-ray exposure time, with a reduction in this signal indicating sample degradation. Spectra were collected at the beginning of exposure and at hourly intervals thereafter with ten scans averaged. In Figure 4.4 the percentage change in O (1s) signal intensity is plotted as a function of X-ray exposure time for untreated wool, nylon and polyester fabrics. Wool shows little change in O (1s) signal up to an analysis time of 4 hours, after which sample degradation is indicated by the rapid reduction in this signal. The maximum XPS analysis time for wool samples in this work therefore did not exceed 4 hours. The O (1s) signal for nylon fabrics begins to reduce after 3 hours exposure. The maximum analysis time for nylon samples in this work did not exceed 2 hours. For polyester fabric, sample degradation does not occur until X-ray exposure for more than 5 hours. The maximum analysis time for polyester samples in this work was no more than 1 hour.

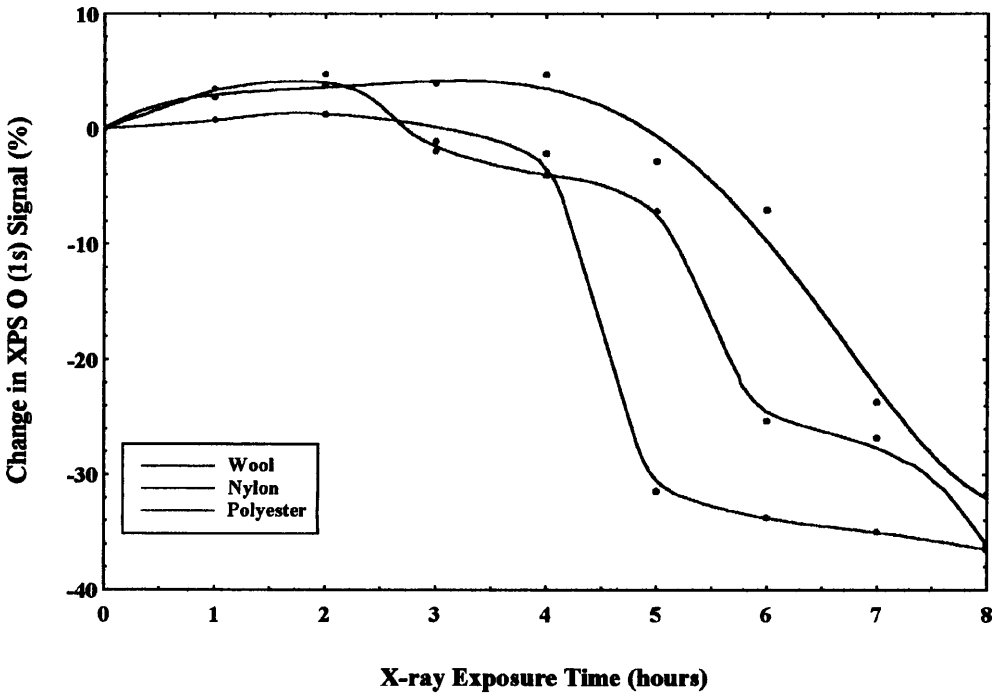

Figure 4.4 Study of X-ray damage to wool, polyester and nylon fabrics during XPS analysis

4.6.4 SSIMS Analysis

Static Secondary Ion Mass Spectrometry (SSIMS) was used for the surface analysis of the external lipid layer on the wool fibre epicuticle. Fabric samples were analysed using a VG IX23S instrument with a Poschenrieder Time of Flight analyser. A 30 keV pulsed Ga^- ion source was used with an ion current of 1.4 nA. This gives a total primary ion dose of 1×10^{11} ions/cm^{-2}. Spatial resolution is 600 μm^2. Negative secondary ion spectra were collected in the range 0- 500 atomic mass units.

Chapter 5

Lightfastness Performance of Wool

5.1 Introduction

This chapter investigates the lightfastness performance of wool on exposure to automotive interior environmental conditions. The aim is to establish if wool upholstery fabrics can meet the performance standards demanded by mass market car manufacturers. The benefit of applying a commercial UV absorber to wool was assessed in comparison to the improvement in lightfastness performance achieved by the application of photostabilizers to nylon and polyester fabrics.

Section 5.2 investigates the colour stability of wool fabrics. The sensitivity of wool to both photoyellowing and thermal yellowing is examined and the protective effect of the UV absorber, Cibafast W, is assessed. The effectiveness of Cibafast W in improving the lightfastness performance of dyed wool is examined. Similarly, the colour stability of nylon and polyester to automotive exposure conditions are investigated in sections 5.3 and 5.4 respectively, since these fibres were used as blend components with wool. An assessment is made of the protective effect of appropriate photostabilizers applied to nylon and polyester fabrics.

Section 5.5 examines the lightfastness performance of 100% wool and wool blend fabrics commercially developed to automotive specifications. The aim of this section is to establish if wool-rich fabrics can meet the lightfastness performance standards demanded by a number of car manufacturers. In this section, the influence of both wool and synthetic fibre type on fabric performance is investigated. A comparison is made between the nature of fading in sunlight and on exposure to the artificial Xenon light source. Additional factors which may affect lightfastness, such as the effect of fabric lamination and the application of softening treatments, are also considered.

5.2 Lightfastness of Wool and the Protective Effect of Cibafast W

5.2.1 Photo and Thermal Colour Stability of Undyed Wool Fabrics

In this section wool fabrics were exposed to light at intervals up to 208 hours in the Xenotest

using the test conditions specified by Rover Group, given in Table 4.5. As discussed in section 4.2, the exposure conditions specified in this test method were considered to most realistically simulate the automotive interior environment.

The rate of increase in Yellowness Index of untreated wool fabric (35 μm) as a function of exposure time is shown in Figure 5.1. Although untreated wool progressively yellows with increasing exposure time, the rate of photoyellowing decreases as the length of exposure increases. The increase in yellowness of wool was due to a decrease in reflectance mainly in the region below 480 nm. The progressive reductions in all the tristimulus reflectance values with exposure time reflects the dulling of wool after light exposure. A preliminary study using wool fibre top showed that the rate of photoyellowing increased with decreasing mean fibre diameter. After 52 hours Xenotest exposure, the Yellowness Index of 25 μm wool had increased by 46%, compared to 38% for 30 μm and 30 % for 35 μm wool. Since the initial yellowness of wool increased with mean fibre diameter, the slower rate of photoyellowing may be explained by an initial period of photobleaching of the coarser yellower wool.

The application of 2% Cibafast W increased the initial Yellowness Index of wool fabric by 9%. The reflectance spectrum of Cibafast W treated wool showed that the product mainly absorbs wavelengths below 400 nm. However absorber-treated wool had a decrease in reflectance in the region between 400 - 500 nm compared to untreated wool and this was responsible for the additional yellowness of the treated fabric.

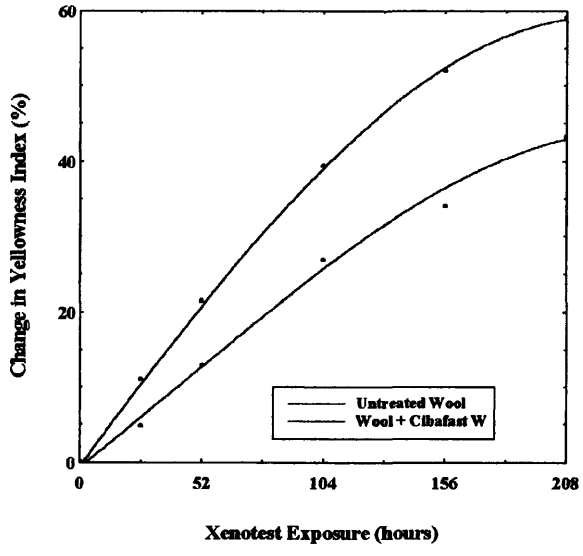

Figure 5.1 Rate of photoyellowing of undyed wool fabrics

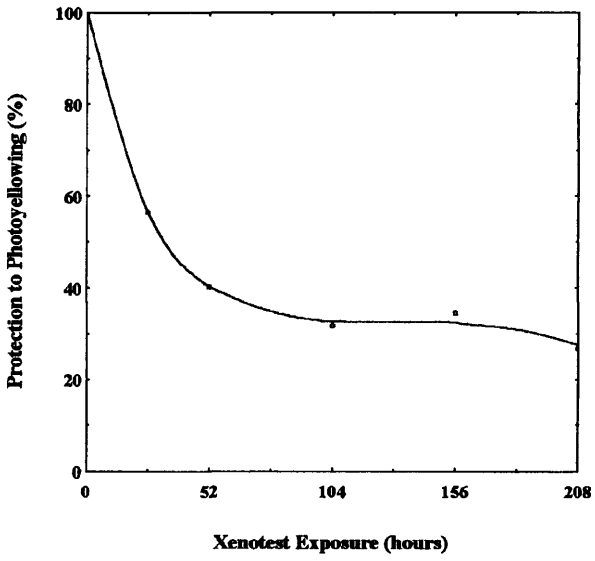

Figure 5.2 Change in effectiveness of Cibafast W with exposure time

The rate of change in Yellowness Index of Cibafast W treated wool fabric compared to untreated wool is shown in Figure 5.1. The application of Cibafast W significantly reduces the photoyellowing rate, but the similarity of the curves indicates that the absorber only reduces the rate of photochemical reactions leading to yellowing rather than eliminating them. Direct comparison of the change in yellowness of the untreated and treated fabrics at each exposure time shows that the effectiveness of the UV absorber diminishes with increasing exposure time, Figure 5.2. The protective effectiveness of the absorber at 208 hours is half that given at 26 hours. Figure 5.2 shows that this loss in effectiveness occurs over the first 52 hours of exposure after which a limiting value is reached for a minimum level of protection.

A more useful method of evaluating the effectiveness of a UV absorber is the lifetime improvement factor[106]. This is a measure of the increase in useful lifetime of a fabric resulting from application of a photostabilizer. The exposure times for untreated and treated fabrics to reach the same change in Yellowness Index are compared, the ratio of these times is the lifetime improvement factor. The curve fitted to the untreated fabric data in Figure 5.1 was used to measure the time required for untreated wool to reach the same change in Yellowness Index as the value observed for the absorber treated wool at each exposure period. This procedure can only be used if curves fitted to the data for both untreated and treated fabrics have the same general shape. Table 5.1 shows the lifetime improvement factors at each exposure time, the mean lifetime improvement factor over all exposure times is 1.7 $\pm$0.2. Therefore, the useful lifetime of wool in terms of the photoyellowing rate is increased by a factor of 1.7 after the application of Cibafast W.

Table 5.1 Lifetime improvement factors for wool photoyellowing on application of CibafastW

% Change in Yellowness Index	Exposure Time (hours)		Improvement Factor (T_C / T_U)
	Treated Fabric (T_C) (observed values)	Untreated Fabric (T_U) (read from curve)	
4.8	26	12.7	2.05
12.9	52	32.1	1.62
26.9	104	68.3	1.52
34	156	88.4	1.76
43.2	208	118	1.76

The elevated temperatures encountered in vehicles has led some manufacturers to demand high thermal colour stability of fabrics. Daimler Benz have developed a test method known as the Sahara test in which fabrics are heated in an oven at an air temperature of 115°C for six

days[239]. The sensitivity of wool to heat yellowing and the protection given by Cibafast W was assessed using this test. Wool fabrics were exposed for daily intervals, the rate of thermal yellowing up to six days exposure is shown in Figure 5.3. Thermal yellowing occurs most rapidly on initial exposure, decreasing as exposure time extends. The change in Yellowness Index after 24 hours heat exposure at an air temperature of 115°C was approximately equivalent to 120 hours Xenotest exposure at 75°C. It can therefore be appreciated that an increase in temperature during light exposure would increase the rate of photoyellowing considerably. The reflectance spectra of photoyellowed and thermally yellowed wools with similar yellowness indices differed. Photoyellowed wool had a much lower UV reflectance in the region below 440 nm compared to thermally yellowed wool. However, thermally yellowed wool had a lower reflectance above 440 nm compared to photoyellowed wool. This suggests that the nature of the chromophores responsible for the two types of yellowing differ.

Figure 5.3 shows that the rate of thermal yellowing of wool is reduced significantly by the application of Cibafast W. Since its function in this case will not be as a UV absorber, the mechanism for its protective action is unclear. This suggests that Cibafast W has other modes of stabilization apart from its function as a UV absorber. The rate of thermal yellowing of wool was investigated for fabric treated with 2% Cibafast N, the copper complex photostabilizer used for nylon, and in the presence of a combination of 2% Cibafast W and 2% Cibafast N. After 6 days exposure to the Sahara test the rate of thermal yellowing was reduced

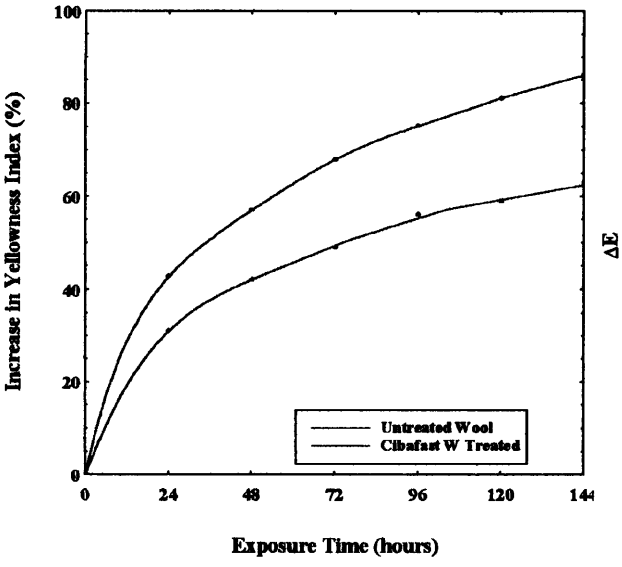

Figure 5.3 Rate of thermal yellowing of undyed wool fabrics

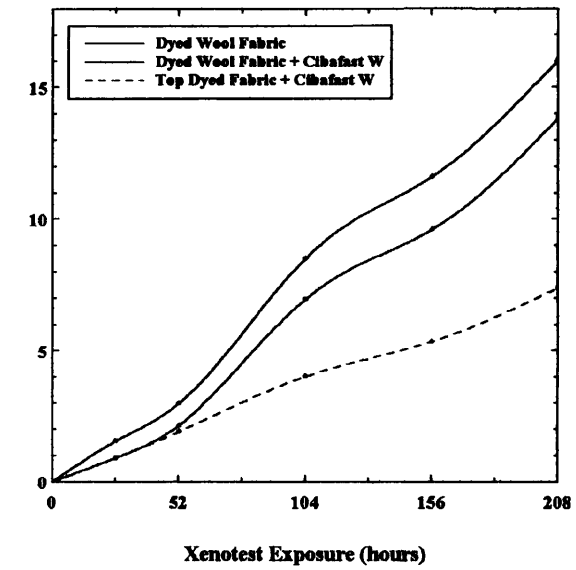

Figure 5.4 Rate of fading of dyed wool fabrics

by 27% for Cibafast W treated wool, 34% for Cibafast N treated wool and by 51% for the combined treatment. This is a considerable improvement and indicates an additive effect between the two photostabilizers. Cibafast N functions by decomposing hydroperoxide groups and since it is effective in reducing the rate of thermal yellowing it implicates the involvement of these species. Unfortunately, treatment of wool with Cibafast N did not significantly reduce the rate of photoyellowing and may even have had a slight accelerating effect. Also, the protective effect of Cibafast W to photoyellowing was reduced in the presence of Cibafast N indicating that it may act as a photosensitizer.

5.2.2 Lightfastness of Dyed Wool Fabrics

In the automotive sector, dyed fabrics must have a high lightfastness at elevated temperatures. Of equal concern along with the overall rate of fading is the degree of tone change. Fabric lightfastness depends not only on dyestuff stability, but on the inherent colour stability of the substrate and whether the substrate photosensitizes dyestuff degradation. The photoyellowing tendency of wool substantially lowers the lightfastness performance of dyed wool, particularly for grey and blue shades where the yellow tone change is more obvious. In section 5.2.1 Cibafast W was found to significantly reduce the rate of photoyellowing of wool, but its effectiveness in improving the lightfastness performance of dyed wool was also examined.

Samples of the 100% wool fabric (35 mm) were dyed in the presence and absence of 2% Cibafast W using 1:2 premetallized dyes. A standard mid grey shade was selected, the dyeing conditions are given in Table 4.3.

Figure 5.4 compares the rate of fading of untreated and treated fabrics, measured by the change in ΔE value. The application of 2% Cibafast W gives some protection to the rate of dye fading. Again, the absorber is more effective at low exposure levels and the protective benefit diminishes with increasing exposure time. Application of the absorber gives a 42% improvement in lightfastness performance after exposure for 26 hours, but an improvement of only 14% after exposure for 208 hours.

The increase in ΔE up to 52 hours exposure for both untreated and absorber treated fabrics is due mainly to a reduction in chroma value reflecting degradation of the dyestuff. There are no large changes in hue value up to this point indicating on-tone fading. However, the more rapid change in ΔE value above 52 hours exposure is due mainly to large changes in hue value as

photoyellowing of the faded fabrics becomes obvious. The chroma value also begins to increase as yellowing of the wool predominates.

The mechanism by which Cibafast W protects dyed wool is unclear. It may act by optically screening the dyestuff from absorbing near UV wavelengths. Alternatively, its protective action may be entirely due to the improvement in photostability given to the wool fibre, thereby shielding photosensitive sites which are capable of initiating dyestuff degradation. Dyed fabric was also treated with Cibafast N and a combination of Cibafast N and Cibafast W. As found for the undyed fabrics, Cibafast N alone gave no significant protection to the rate of dye fading, and its presence reduced the effectiveness of Cibafast W when the two compounds were used in combination on dyed wool.

The lightfastness performance of dyed wool fabrics can be improved considerably by dyeing wool in fibre top form and this method was used to ensure maximum performance of the automotive quality wool and wool blend fabrics developed. This is illustrated in Figure 5.4 where the photostability of piece dyed wool fabric treated with Cibafast W is compared to fabric produced from top dyed wool treated with Cibafast W. Both fabrics are dyed to the same grey shade. Although the lightfastness performance of both fabrics is the same up to 52 hours exposure, long term photostability is improved considerably by dyeing wool in fibre top form. This may be explained by improved penetration and distribution of the dyestuff in the fibre.

Despite the addition of Cibafast W, the lightfastness performance of top dyed wool fabric still remains substantially poorer than photostabilized dyed polyester and nylon fabrics. The rate of fading of wool was on average five times more rapid than polyester and three times more rapid than nylon fabrics dyed to the same shade.

5.3 Lightfastness of Nylon and the Protective Effect of Cibafast N

5.3.1 Photo and Thermal Colour Stability of Undyed Nylon Fabrics

Untreated nylon had no photoyellowing tendency, instead there was a reduction in Yellowness Index with increasing exposure time, indicating a photobleaching effect due to an increase in the reflectance spectrum between 380 - 430 nm. Photobleaching occurred most rapidly over the first 26 hours of light exposure, with little further bleaching after exposure for more than 52 hours.

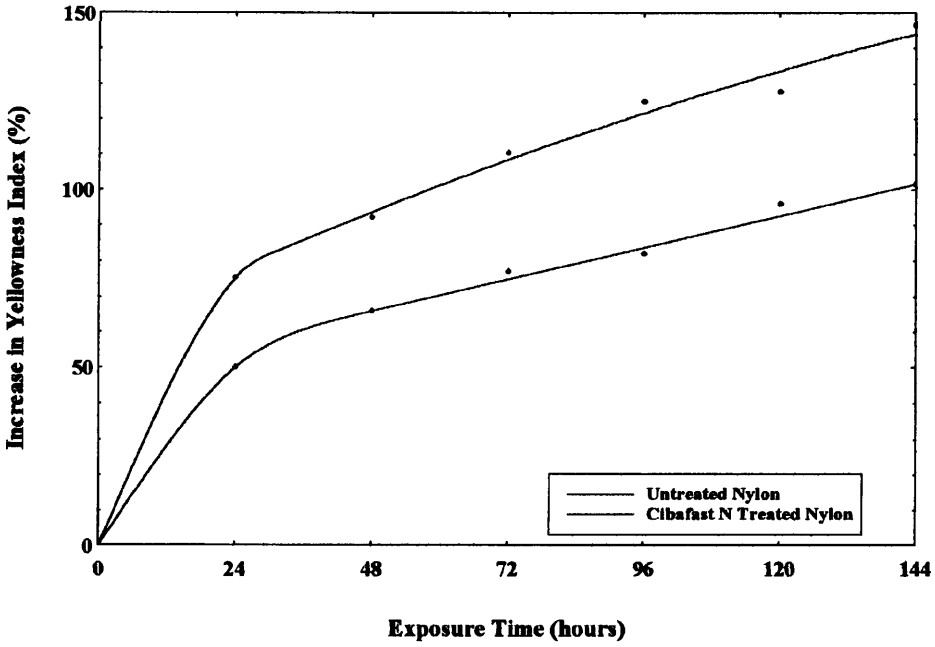

Figure 5.5 Rate of thermal yellowing of nylon fabrics

Untreated nylon is particularly susceptible to thermal yellowing and this may lower the performance of nylon fabrics during light exposure at elevated temperatures. Figure 5.5 compares the rates of increase in Yellowness Index for untreated nylon and Cibafast N treated nylon fabrics after exposure to the Sahara test. The rate of thermal yellowing of untreated nylon is similar to that for untreated wool, occurring most rapidly over the first 24 hours. The application of Cibafast N significantly reduces the rate of thermal yellowing by approximately 30 % at each exposure level. Cibafast N functions as a hydroperoxide decomposer and slows down the autooxidation process which must therefore partially initiate reactions leading to the formation of yellowing chromophores.

5.3.2 Lightfastness of Dyed Nylon Fabrics

Nylon fabric samples were dyed in the presence and absence of 2% Cibafast N using 1:2 premetallized dyestuffs under the conditions given in Table 4.3. Figure 5.6 compares the lightfastness performance of untreated and absorber treated dyed fabrics. Untreated dyed nylon shows particularly rapid fading after light exposure for more than 52 hours. The increase in ΔE was due mainly to large increases in lightness value, with only small changes in hue. Both untreated and treated fabrics have a similar lightfastness performance up to 52 hours, but the protective effect of Cibafast N becomes more apparent at higher exposure levels. After treatment with Cibafast N dye fading occurs at a more linear rate. Since Cibafast N is effective

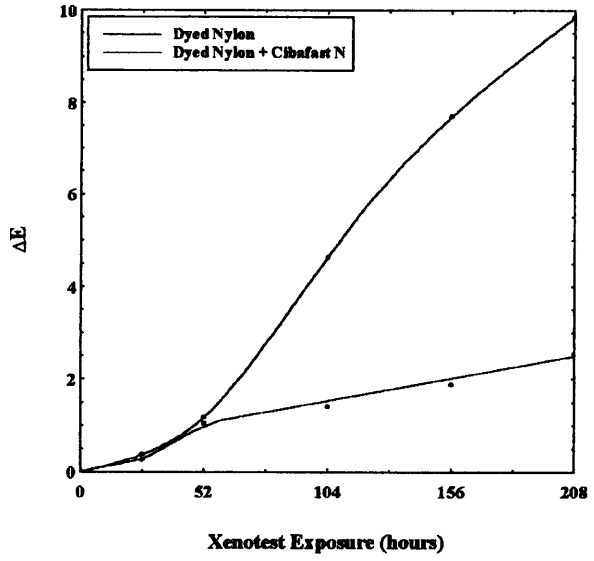

Figure 5.6 Rate of fading of dyed nylon fabrics

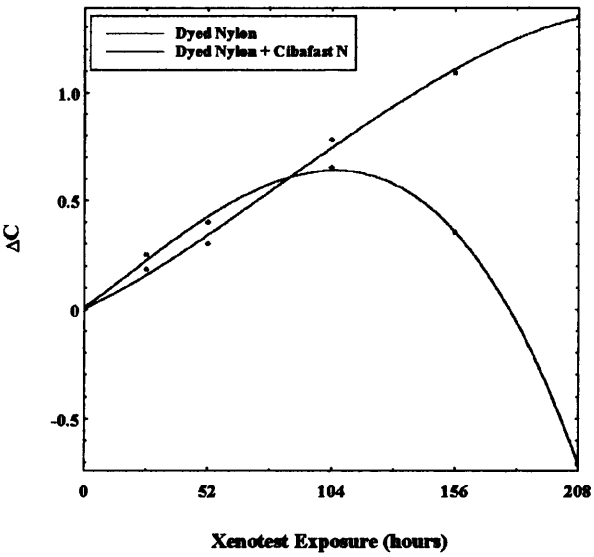

Figure 5.7 Change in ΔC value with exposure time for dyed nylon fabrics

in reducing the rapid rate of dye fading which occurs at higher exposure levels, it indicates that free radical reactions involving hydroperoxides as the oxidising species must be largely responsible for dyestuff degradation in nylon. Figure 5.7 shows the change in chroma value of both fabrics with exposure time. For the untreated fabric, the chroma value increases up to 104 hours exposure, suggesting an increase in dye concentration. This is in contrast to fading of these same dyestuffs on wool which was shown by a reduction in chroma.

This negative colour fading has previously been attributed to the break up of dye aggregates during exposure of acid dyed nylon[127]. In Figure 5.7, this effect appears to reach a maximum level at 104 hours exposure after which the chroma value begins to decrease indicating dyestuff degradation. Dyed nylon treated with Cibafast N also shows this negative colour fade and this continues with extended exposure. The protection given by Cibafast N may allow aggregate break-up to continue over a longer exposure period.

5.4 Lightfastness of Polyester and the Protective Effect of Cibatex APS

5.4.1 Photo and Thermal Colour Stability of Undyed Polyester Fabrics

Untreated polyester had no photoyellowing tendency, instead there was a reduction in Yellowness Index indicating photobleaching of the fabric. As found for untreated nylon, this photobleaching occurred rapidly over the first 26 hours with little further bleaching after exposure for more than 52 hours.

Unlike wool and nylon, untreated polyester is not particularly sensitive to thermal yellowing and only this fabric meets the stringent performance requirements demanded by the Sahara test. Although there was a 36% increase in Yellowness Index of polyester fabric after 6 days exposure to the Sahara Test, the actual Yellowness Index of polyester after this time was 5.4 compared to values of 53.4 and 24.0 for wool and nylon respectively. For untreated polyester, the Yellowness Index increased in a similar manner as found for untreated wool and nylon fabrics, with the most rapid colour change occurring over the first 24 hours of exposure. Even though polyester yellowed only slightly on heating, the application of Cibatex APS reduced the rate of yellowing by 50% after 6 days exposure.

5.4.2 Lightfastness of Dyed Polyester Fabrics

Polyester fabrics were disperse dyed in the presence and absence of 2% of the UV absorber Cibatex APS, under the conditions given in Table 4.3. Figure 5.8 compares the lightfastness performance of the untreated and absorber treated dyed fabrics. The rate of fading of untreated dyed polyester decreases with increasing exposure time. The increases in ΔE were due to increases in lightness and decreases in chroma values accompanied by a change in hue. Dyed fabric treated with Cibatex APS has a more linear fading rate. Application of the UV absorber is much more effective in improving lightfastness performance of dyed polyester than was found on application of a similar class of photostabilizer to dyed wool.

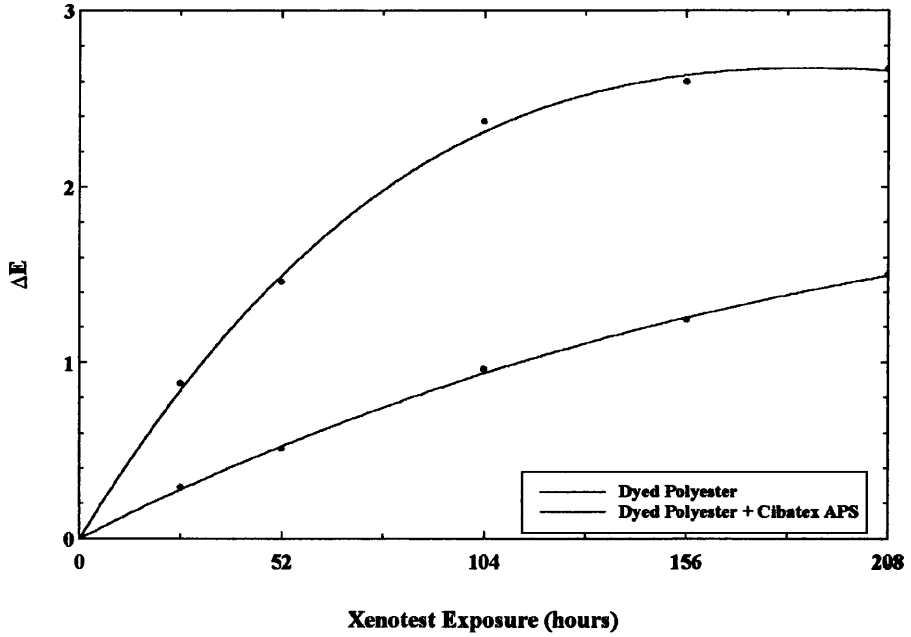

Figure 5.8 Rate of fading of dyed polyester fabrics

In a similar manner to wool, the level of protection given by Cibatex APS to dyed polyester diminishes with increasing exposure time. There is a 67% improvement in lightfastness performance of dyed polyester after 26 hours exposure, which reduces to 44% after 208 hours. In comparison, application of Cibafast W improves the lightfastness of dyed wool by 42% after 26 hours and by only 14% after 208 hours. There is a more rapid loss in effectiveness of the UV absorber applied to wool compared to that applied to polyester.

5.5 Lightfastness Testing of Wool Automotive Fabrics

The most critical test for automotive fabrics is lightfastness testing, this section aims to establish if a photostabilized wool rich automotive fabric will meet the performance specifications demanded by a number of car manufacturers. Nine flat woven fabrics were developed using commercial machinery. All material and processing specifications were carefully considered in order to ensure maximum fabric performance (see section 4.1). For maximum lightfastness performance, wool, polyester and polyamide fibres were top dyed using the recommended levels of UV protective agents. A standard mid grey shade was selected for all dyeings.

Three 100% wool fabrics were produced using different wool qualities in order to evaluate if mean fibre diameter had any significant influence on lightfastness. The improvement in performance achieved by blending each of these wool qualities with polyester and nylon fibres of different linear densities is also examined. All fabrics tested to automotive lightfastness standards are usually required to be in a laminated form. In this work all wool fabrics developed were flame laminated to a polyester urethane foam backed with nylon warp knit lining.

Representative light exposure test methods were used, namely those of Rover, General Motors and Ford, the conditions of which are detailed in Table 4.5. Lightfastness performance of fabrics was measured colourimetrically and also by visual assessment against the standard Grey Scale by experienced judges.

5.5.1 Lightfastness Performance of 100% Wool Automotive Fabrics

Three 100% wool fabrics were produced using wool qualities with mean fibre diameters of 25 μm, 30 μm and 35 μm. A comparison was made between the lightfastness performance of the

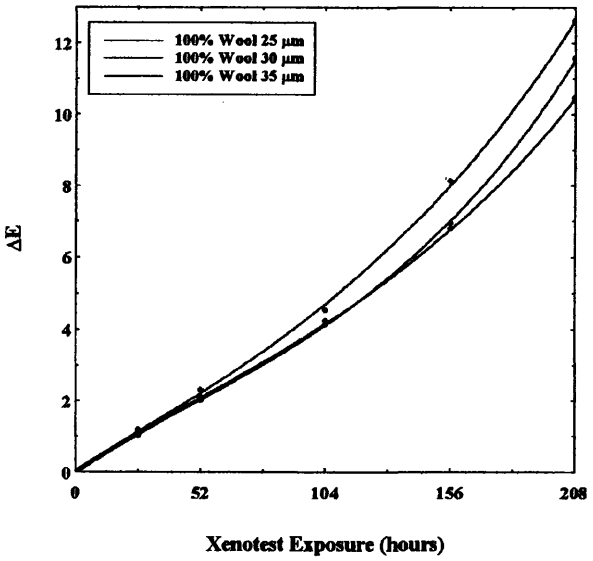

Figure 5.9 Change in ΔE value with exposure time for dyed wool fabrics

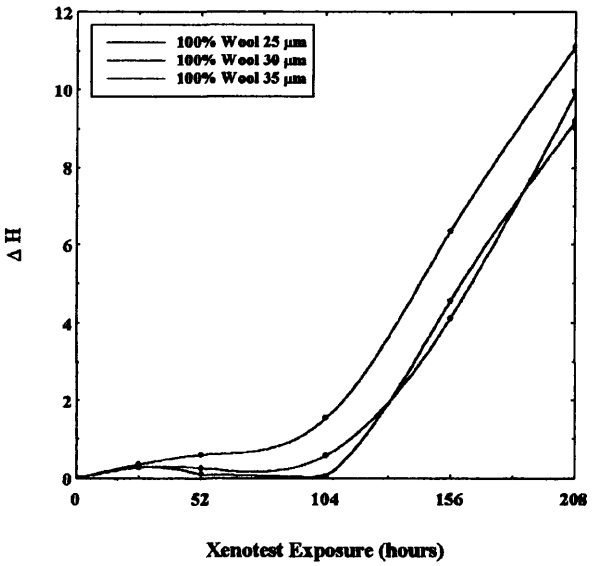

Figure 5.10 Change in ΔH value with exposure time for dyed wool fabrics

fabrics in order to determine if wool quality has any significant influence on colour stability. Figure 5.9 compares the fading rate of the three fabrics after Xenotest exposure under Rover Group conditions. For all fabrics, fading takes place at an approximately linear rate up to 156 hours exposure, but becomes more rapid with extended exposure. A slightly poorer performance of the 25 µm wool, compared to the coarser wool fabrics, becomes apparent after exposure for more than 52 hours. There is little difference between the performance of the 30 µm and 35 µm fabrics up to 156 hours, but after 208 hours exposure there is a decrease in ΔE value with increasing mean fibre diameter.

Figure 5.10 shows the change in ΔH values as a function of exposure time. The fabrics fade with only small changes in tone at low exposure levels, particularly the 35 µm wool fabric. The slightly larger ΔH values up to 104 hours for the 25 µm fabric is due to more pronounced yellowing of the fabric. The rapid increase in ΔH values between 104 and 208 hours is due to more obvious photoyellowing of the faded fabrics. The chroma value decreased at the same linear rate for each fabric up to 104 hours indicating that dye fading occurred at the same rate for each fabric. There was an increase in chroma for the 25 µm fabric between 104 and 208 hours reflecting photoyellowing, whereas this increase in chroma occurred between 156 and 208 hours for the coarser wool fabrics indicating a slower rate of yellowing. In section 5.2 the rate of photoyellowing of undyed wool was found to increase with decreasing mean fibre

diameter. This increased photoyellowing tendency of the finer wool fibre quality has lowered fabric lightfastness performance.

Lifetime improvement factors were calculated to find the improvement in lightfastness performance achieved by using 35 μm and 30 μm wool compared to 25 μm wool. In a similar manner as described in section 5.2, mean lifetime improvement factors were calculated for the 35 μm and 30 μm fabrics using the curve fitted to the ΔE values for the 25 μm fabric. A mean improvement factor of 1.10 ± 0.04 for the 30 μm fabric and 1.09± 0.05 for the 35 μm fabric were calculated relative to the 25 μm fabric. Therefore by using the coarser wool fibre qualities an improvement in the useful lifetime of wool fabric of approximately 10 % is achieved over the finer wool quality. This is a small effect but could be significant for a fabric on the borderline between a pass and fail in lightfastness testing.

5.5.2 Lightfastness Performance of Wool Blend Automotive Fabrics

The improvement in lightfastness performance of wool fabrics by blending with 35% polyester or nylon of different linear densities was investigated. Initially, the lightfastness performance of the dyed polyester and nylon fibre components used in these blends were compared in order to examine the effect of fibre type and linear density on light stability.

Figure 5.11 plots the ΔE values for each of the five fibre components as a function of exposure time. The nylon fibres generally have a similar lightfastness performance over all exposure levels regardless of fibre fineness, apart from a slightly poorer performance of the 2.4 dtex fibre below 104 hours. In addition to Cibafast N applied to the fibres by exhaustion, the 3.3 dtex nylon fibre has an antioxidant added to the polymer melt. This has not led to a significant improvement in performance of this fibre compared to the other nylon qualities. All nylon fibres showed a progressive red / blue tone change with exposure time. The 3.3 dtex polyester fibre has the highest lightfastness of all the fibres, the ΔE value is approximately 30% lower than that for the 3.3 dtex nylon fibre at each exposure level. The 1.4 dtex polyester fibre has a much poorer lightfastness compared to the 3.3 dtex polyester fibre. The rapid increases in ΔE up to 26 hours and above 156 hours exposure were due to much larger changes in hue and chroma values. Both polyester fibre types show a progressive red tone change with exposure, particularly for the finer fibre.

The lightfastness of the wool blend fabrics were compared by calculating a fading index for each fabric. Each fabric had an approximately linear rate of increase in ΔE value up to 156

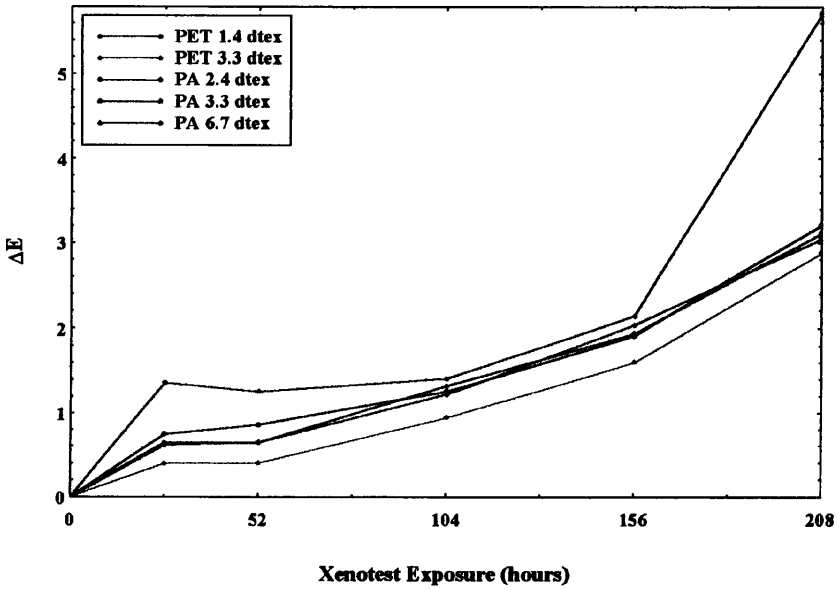

Figure 5.11 Change in ΔE value with exposure time for synthetic fibre components

hours exposure, with a more rapid rate of increase in ΔE between 156 and 208 hours. It was considered that above 156 hours exposure, where there is a departure from the more linear fading rate, fabrics could be considered to be past their useful lifetimes for lightfastness. The mean rate of increase in ΔE up to 156 hours exposure (ΔE / 10 Xenotest hours) was therefore used as the fading index for each fabric and these values are shown in Table 5.2 for the wool blend fabrics. The fading indices for the 100% wool fabrics are also shown in Table 5.2 for comparison. The percentage improvements in performance of the wool blends relative to the equivalent 100% wool fabrics are also shown.

Table 5.2 Comparison of the lightfastness performance of wool automotive fabrics

Fabric Type	Fading Index (ΔE/10 hrs)	CV %	% Improvement (wool blend / 100% wool)
25 μm Wool			
A 100% Wool	0.46	8.4	-
B Wool/Pes (3.3dtex)	0.29	8.9	37
C Wool/Pa (6.7 dtex)	0.33	4.2	28
30 μm Wool			
D 100% Wool	0.41	7.1	-
E Wool/Pes (3.3 dtex)	0.26	7.2	37
F Wool/Pa (3.3 dtex)	0.26	6.4	37
35 μm Wool			
G 100% Wool	0.42	4.6	-
H Wool/Pes (1.4 dtex)	0.28	12.3	33
J Wool/Pa (2.4 dtex)	0.28	14.3	33

The fading indices in Table 5.2 show that wool blend fabrics (B) and (C), which contain the lower performance 25 μm wool, have a poorer lightfastness than the other wool blend fabrics. The wool / nylon blend, fabric (C) has a particularly poor performance due to the lower stability of the nylon component compared to that of polyester. The lightfastness of blends (E) and (F) is slightly higher than that of fabrics (H) and (J) which can be partly attributed to the lower light stability of the finer polyester and nylon fibres used in blends (H) and (J). For the 30 μm and 35 μm wool blends, there is no significant advantage in using either polyester or nylon as components. It can be anticipated that as the percentage of synthetic fibre in the blend increases, the higher light stability of polyester compared to nylon may make differences between the two blends more apparent. Table 5.2 shows that regardless of wool quality used, blending wool with polyester or nylon gives an average improvement of 34% relative to the performance of 100% wool. This improvement is equivalent to the percentage synthetic fibre component of these blends of 35%.

Table 5.3 shows the mean rate of change in the colour difference components, ΔL, ΔC and ΔH up to 156 hours exposure for the wool blend fabrics. The wool / nylon blends, fabrics (C), (F) and (J), fade with much smaller changes in hue and slightly larger changes in chroma and lightness values compared to the wool / polyester blends. Fading with minimal changes in hue is desirable for automotive fabrics. This smaller change in hue for the nylon blends may be due to the blue fading tendency of the nylon component which offsets the yellowing tendency of wool. In contrast, the marked red fading of the dyed polyester components accentuates the yellow tone change of wool, particularly for fabric (H) which contains the fine polyester filament. If the polyester component could be dyed to give a deliberate blue tone change it may significantly improve the lightfastness performance of the wool polyester blends.

Table 5.3 Mean rate of change in colour difference components for wool blend fabrics

	ΔH/10 hrs	CV %	ΔC/10 hrs	CV %	ΔL/10 hrs	CV %
B Wool/Pes (25μm /3.3dtex)	**0.13**	22	**-0.17**	4	**0.2**	8
C Wool/Pa (25μm /6.7dtex)	**0.09**	34	**-0.22**	9	**0.22**	11
E Wool/Pes (30μm /3.3dtex)	**0.11**	27	**-0.16**	3	**0.18**	7
F Wool/Pa (30μm /3.3dtex)	**0.05**	40	**-0.17**	19	**0.2**	7
H Wool/Pes (35μm /1.4dtex)	**0.14**	28	**-0.14**	12	**0.2**	15
J Wool/Pa (35μm /2.4dtex)	**0.06**	35	**-0.18**	6	**0.21**	18

5.5.3 Performance of Wool Automotive Fabrics to Current Industry Standards

The wool automotive fabrics developed were tested according to the specifications of a number of car manufacturers. The differences in exposure conditions specified by each car manufacturer leads to considerable variations in the severity of these tests. Table 5.4 compares the differences in severity of these light exposure test methods for the same 100% wool fabric. There is a large variation in the lightfastness performance of wool according to the test method used, the Ford test being particularly severe. The differences in fabric abrasion resistance after exposure to each of these test methods illustrates the large variation in the level of photodegradation. The extent of surface photooxidation after exposure to each of these tests is shown by the increase in cysteic acid signal, measured by FT-IR (ATR) analysis of the fabric surface (see section 7.3).

Table 5.4 Comparison of severity of accelerated exposure test methods for 100% wool fabric[1]

Exposure Test Method	ΔE	Grey Scale Grade	Martindale Cycles	Cysteic Acid Signal[2]
Unexposed	0	5	128,000	1
Rover Group	2.1	3-4	85,000	1.9
General Motors	3.3	3	53,000	2.1
Ford	4.9	2	15,000	2.7

1. 35μm wool 2. FT-IR (ATR) Second derivative peak intensity at 1040 cm^{-1} (arbitrary units)

The Rover and General Motors tests use Xenotest instrument and are generally the most similar. Although the General Motors test uses a lower air temperature, the longer duration of this test means that it is more severe than that specified by Rover Group. The reason for the severity of the Ford test can be explained by the significant UV component which is permitted, with wavelengths as low as 270 nm included in the spectral distribution. In this test the light source is not filtered by window glass unlike the other two tests, therefore it can be argued that the conditions do not realistically simulate automotive interior conditions. The Ford test causes much more severe photoyellowing and tendering of wool. The test also differs from the others in that exposure is discontinuous, with alternating light and dark periods, which may have altered the rate and nature of photodegradation.

The lightfastness performance of the wool automotive fabrics on exposure to each of these test methods are shown in Table 5.5. The ΔE values shown are mean values of four specimens exposed for each fabric type in each test. The average Grey Scale grading is also given for

each fabric, assessed by three independent experienced judges. In each of these tests, the pass level is specified as Grey Scale 4. Taking all fabric samples throughout this work which were visually assessed as Grey Scale 4, the mean ΔE value for these samples was equal to 1.3 ±0.1. There are some discrepancies between the relative performance of fabrics assessed by their ΔE values compared to the visually assessed Grey Scale grades. This illustrates the subjective nature of visual assessment.

Table 5.5 Performance of wool automotive fabrics according to lightfastness test method

Fabric Type	**Rover Group**		**General Motors**		**Ford**	
25 μm Wool	ΔE	Grey Scale	ΔE	Grey Scale	ΔE	Grey Scale
A 100% Wool	2.32	3-4	4.52	3	5.72	2
B Wool/Pes (3.3 dtex)	1.5	3-4	2.65	3-4	3.7	2-3
C Wool/Pa (6.7 dtex)	1.69	3-4	2.83	3	3.98	2-3
30 μm Wool						
D 100% Wool	1.96	3-4	3.48	3	5.07	2
E Wool/Pes (3.3 dtex)	1.33	4	1.97	3-4	3.54	2-3
F Wool/Pa (3.3 dtex)	1.26	4	1.93	3	3.33	2-3/3
35 μm Wool						
G 100% Wool	2.07	3-4	3.27	3	4.91	2
H Wool/Pes (1.4 dtex)	1.4	3-4	2.04	3	4.07	2
J Wool/Pa (2.4 dtex)	1.37	4	2.31	3-4	3.18	2-3/3

Table 5.5 shows that three of the wool blend fabrics pass the Rover Group test, the wool / nylon blends (F) and (J) and the wool / polyester blend (E). On the basis of its ΔE value, the wool / polyester blend (H) would also be expected to pass this test. However, the more obvious change in tone of this fabric led to a visual bias towards a poorer Grey Scale grading. From the ΔE values, an improvement in lightfastness performance of approximately 40% would be required in order for a 100% wool fabric to reach Grey Scale 4 in this test.

None of the fabrics reach Grey Scale 4 in the General Motors test. On the basis of their ΔE values, wool / polyester blend (E) and wool / nylon blend (F) require approximately 30% improvement in performance to reach Grey Scale 4. In the case of the 100% wool fabrics, there is a clear improvement in lightfastness with increasing mean fibre diameter. A 60% improvement in performance would be required for the 35 μm fabric (G) to reach Grey Scale 4. Therefore, it is unlikely that a wool blend fabric with a wool content of more than 40% will pass this test.

Table 5.5 shows that all the fabrics perform poorly under the conditions of the Ford test. Again, there is an improvement in performance of the 100% wool fabrics with increasing mean fibre diameter. However, the 35 μm 100% wool fabric would require a 75% improvement in performance to pass this test. This indicates that wool blend fabrics with only a very small wool content, certainly no more than 20% wool, will meet the performance requirements demanded by Ford.

Comparing the between test differences in ΔE values for each fabric, the General Motors test is an average of 1.7 ± 0.2 times more severe than the Rover test, whereas the Ford test is 2.5 $\pm$ 0.2 times as severe as the Rover test.

5.5.4 Correlation Between Sunlight and Xenon Light Exposures

The main criticism of artificial lightfastness testing is that differences exist between the spectral power distribution of the light sources used and natural sunlight. This may lead to differences in the fading behaviour of fabrics in sunlight compared to artificial light. In an effort to compare the nature of fading of the wool fabrics under natural and artificial conditions, sunlight testing was carried out in Arizona. The conditions for sunlight exposure are described in section 4.2. This sunlight exposure test is a standard method adopted by the automotive industry and it is considered to replicate the conditions which exist within vehicles in sunlight conditions[2].

Figure 5.12 compares the ΔE values for each fabric after sunlight exposure with the Xenotest fading index for each fabric previously calculated in Table 5.2. There is a good correlation between the relative performance of fabrics in sunlight compared to the Xenotest. Two fabrics did show deviations from this correlation (red data points in Figure 5.12). The wool / polyester blend (35 μm / 1.4 dtex) has a better performance in sunlight compared to the Xenotest, whereas the wool / nylon blend (30 μm / 3.3 dtex) has a slightly poorer performance in sunlight than in the Xenotest. Using the Xenotest fading indices, the colour difference of each fabric after sunlight exposure was calculated to be equivalent to an average exposure time of 80 ± 2.1 hours in the Xenotest under Rover Group conditions.

Although there was a correlation between the relative lightfastness performance of fabrics in sunlight and in the Xenotest, differences were found between the nature of colour change between the two tests. If fading occurs in a similar manner under both conditions of exposure

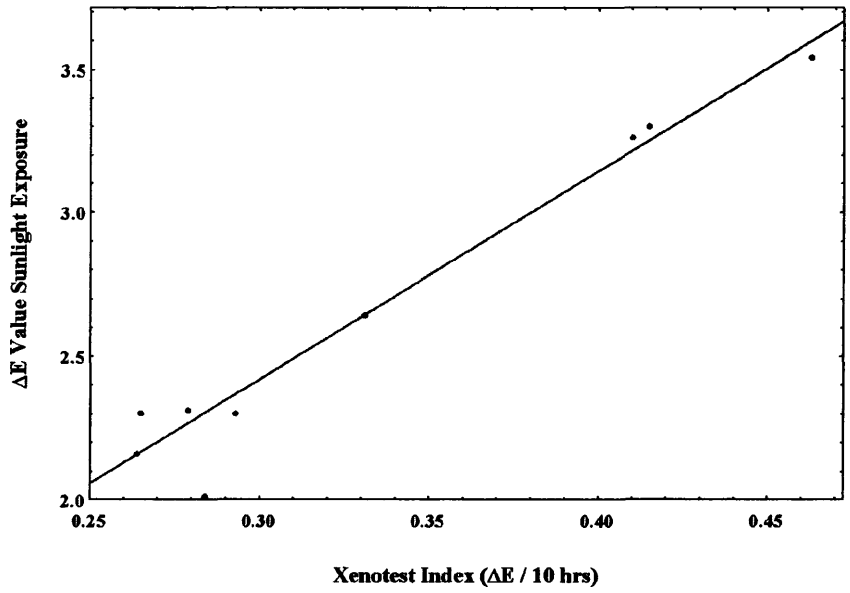

Figure 5.12 Correlation between relative performance of fabrics in sunlight and Xenotest

then the colour difference components, ΔL, ΔC and ΔH, should be in the same relative proportions for the same ΔE value. The ΔL, ΔC and ΔH values for each fabric after sunlight exposure were compared with the equivalent values for the same change in ΔE after Xenotest exposure. For all fabrics it was found that on exposure to sunlight there was a faster rate of change in ΔL value and a slower rate of change in ΔC value compared to Xenotest exposure. In addition, all the 100% wool and wool / nylon fabrics had faster rates of change in ΔH values in sunlight compared to the Xenotest. The larger changes in tone of these fabrics in sunlight was due to more rapid photoyellowing of wool most likely associated with a higher intensity short wavelength component. The rates of change in ΔH values for the wool / polyester blends were the same in sunlight as in the Xenotest indicating a smaller tone change of the polyester components in sunlight than under artificial conditions.

5.5.5 Effect of Lamination on Fabric Lightfastness Performance

The lightfastness performance of laminated automotive fabrics is generally known within the industry to be poorer than the equivalent unlaminated fabrics. An accelerated rate of dye fading and fabric degradation is mainly attributed to heat build up within the foam, which leads to an increase in fabric surface temperature. The reduction in lightfastness performance of wool blend fabrics as a result of lamination was investigated. Wool / polyester and wool / nylon fabrics unlaminated and after lamination to polyester urethane foams of thickness 3.0

mm and 6.0 mm were exposed for successive Xenotest cycles. A fading index was calculated for each fabric in a similar manner as discussed in section 5.5.2. Table 5.6 compares the rate of fading of each of the fabrics. The percentage reductions in lightfastness performance of the laminated fabrics relative to the equivalent unlaminated fabric are shown. The results show that the rate of fading increases significantly after lamination and depends on foam thickness. Lamination did not change the nature of colour change, only the rate of change in the colour difference components was accelerated. It can therefore be appreciated that to accurately assess lightfastness performance to automotive standards, fabrics must be in a laminated form.

SEM analysis of unexposed laminated fabrics showed evidence of considerable amounts of polymer type deposits on many of the surface wool fibres, often appearing to bond adjacent fibres together. These deposits can only be associated with the polyester urethane foam. After light exposure the extent of these deposits on surface fibres increased significantly due to degradation of the foam through hydrolysis. This is known to be a particular problem for polyester based urethane foams [237]. It is not clear if the presence of these surface deposits reduces the photostability or impairs the wear resistance of wool fabrics.

The application of surface treatments to fabrics may further reduce performance. To improve the handle of coarse wool fabrics softening agents are often applied to the fabric surface. The effect of a number of these treatments on the lightfastness of the wool / polyester and wool / nylon blends was briefly investigated. The application of a polysiloxane, a silicone elastomer and a cationic silicone emulsion all reduced the lightfastness performance of both fabrics by 10 - 15%, and by 25% on application of a hydrophobic urethane softener. This suggests that these treatments have a photosensitizing action, they may contain impurity chromophores capable of generating radical species which can attack the substrate and lead to accelerated dyestuff degradation.

Table 5.6 Effect of lamination on lightfastness performance of wool fabrics

Wool/Polyester 30 μm / 3.3 dtex	Fading Index (ΔE/10 hrs)	CV %	% Reduction in Lightfastness
Unlaminated Fabric	0.2	12.1	-
3.0 mm Laminate	0.26	7.2	30
6.0 mm Laminate	0.31	11.6	55
Wool/Nylon 30 μm / 3.3 dtex			
Unlaminated Fabric	0.21	6.5	-
3.0 mm Laminate	0.26	6.4	24
6.0 mm Laminate	0.32	8.7	52

5.6 Conclusions

The application of the UV absorber Cibafast W to wool significantly reduces the rate of photoyellowing, increasing the useful lifetime of wool fabric by a factor of 1.7. However, the effectiveness of the absorber diminishes with exposure time. Application of Cibafast W also significantly reduces the rate of thermal yellowing of wool. Cibafast N, which is effective in reducing the rate of thermal yellowing of nylon, is similarly effective on wool. If Cibafast W and Cibafast N are used in combination on wool they appear to act synergistically giving much greater protection to thermal yellowing. Unfortunately, Cibafast N gives no protection to photoyellowing of wool and it impairs the effectiveness Cibafast W when used in combination. Unlike wool and nylon, untreated polyester is not sensitive to thermal yellowing and therefore meets the performance requirements of the Sahara test.

The photoyellowing sensitivity of wool impairs the lightfastness performance of dyed fabrics compared to dyed polyester and nylon fabrics, whose substrates have no photoyellowing tendency. Cibafast W also improves the lightfastness performance of dyed wool, particularly at low exposure levels, after which effectiveness diminishes considerably. Application of a similar class of UV absorber to dyed polyester was much more effective in improving lightfastness performance. The application of Cibafast N is particularly effective in reducing the rapid fading of dyed nylon which occurs at higher exposure levels. This photostabilizer has no effect when used alone or in combination with Cibafast W on dyed wool. Despite the addition of Cibafast W, the lightfastness performance of dyed wool fabric still remains substantially poorer than photostabilized dyed polyester and nylon fabrics. Since the rate of wool photoyellowing decreases with mean fibre diameter, the lightfastness performance of 100% wool and wool blend automotive fabrics can be improved by using coarser wool qualities. Lightfastness testing of wool automotive fabrics showed that only wool blend fabrics will meet current industry standards. Blends produced from 30 μm and 35 μm wool qualities with 35% polyester or nylon will meet Rover Group specifications. Due to considerable differences in the severity of car manufacturers test methods, it was estimated that for a wool blend to meet General Motors requirements the wool content of the fabric must not exceed 40%. Fabrics with a wool content of more than 20% are unlikely to meet the performance standards demanded by Ford. Factors such as fabric lamination and the application of surface treatments must also be taken into consideration since these have both been shown to lower performance.

Chapter 6

Phototendering of Wool

6.1 Introduction

This chapter examines the effect of light exposure on the physical properties of wool and aims to determine the performance of wool fabrics under automotive conditions.

In section 6.2 the effect of light exposure on the fundamental tensile properties of wool fibres is investigated. The aim of this section is to characterise the nature of phototendering of the wool fibre in order to gain a greater understanding of the changes in the surface integrity of fabrics following light exposure. Section 6.3 examines changes to the surface properties of fabrics as a consequence of light exposure, both the reduction in wear resistance and alterations in the low-stress mechanical and surface properties. Section 6.4 assesses the effectiveness of Cibafast W in reducing the rate of phototendering of wool under automotive exposure conditions.

The rate of phototendering of wool automotive fabrics is discussed in section 6.5 in relation to wear performance in use. The influence of wool mean fibre diameter on unaged and aged abrasion resistance of fabrics is investigated along with the effect of synthetic fibre type and fineness on the performance of wool blend fabrics. Fabric performance is assessed to current industrial standards employed by car manufacturers. Changes in the low-stress mechanical and surface properties of these fabrics following light exposure are investigated in order to consider how the aesthetic qualities of the fabrics are altered by the automotive environment.

6.2 Tensile Properties of Wool Fibres

6.2.1 Effect of Light Exposure on Tensile Properties of Wool Fibres

The effect of light exposure on the tensile properties of wool fibres was examined, with the aim of understanding changes to the surface integrity of fabrics. The experimental protocol for single fibre tensile testing is described in section 4.4.2 with the preparation of fibres for Xenotest exposure described in section 4.2.2. All tensile fractures were retained after testing and the fracture morphology was examined using the SEM.

Table 6.1 Effect of light exposure on wool fibre tensile properties

Xenotest Exposure (hours)	Sample Size (no. fibres)	Tenacity (cN/tex)	Breaking Extension (%)	Specific Work of Rupture (cN/tex)
0	450	**12.98** ± 0.14	**38.5** ± 0.48	**3.59** ± 0.07
26	120	**12.66** ± 0.27	**37.6** ± 0.95	**3.48** ± 0.13
52	120	**11.11** ± 0.27	**35.8** ± 1.13	**3.01** ± 0.13
104	120	**9.34** ± 0.21	**27.1** ± 1.46	**2.22** ± 0.15
208	120	**7.05** ± 0.54	**5.2** ± 1.26	**0.29** ± 0.1

No previously published work could be found which has examined in any detail the tensile properties and fracture morphology of light-degraded wool fibres.

Table 6.1 shows the ultimate tenacity, breaking extension and specific work of rupture of wool fibres after successive Xenotest exposure periods. The sample mean values and the standard errors of the mean values are given. There is a reduction in mean tenacity, extensibility and specific work of rupture with increasing exposure time. Extended exposure causes a larger reduction in fibre extensibility compared to the reduction in tensile strength. After 208 hours there is an 86% reduction in extension at break compared to a 46% reduction in tenacity.

Figure 6.1 compares the percentage rates of change in tensile strength, extension at break and specific work of rupture. There is only a slight reduction in tensile properties after 26 hours exposure. The rate of loss in tenacity is more rapid between 26 - 52 hours exposure, but with further exposure tenacity is lost at a slower rate.

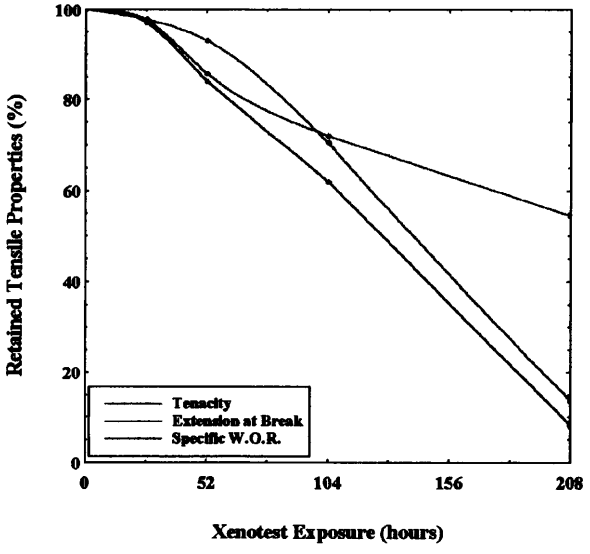

Figure 6.1 Comparison of the rate of loss in fibre tensile properties

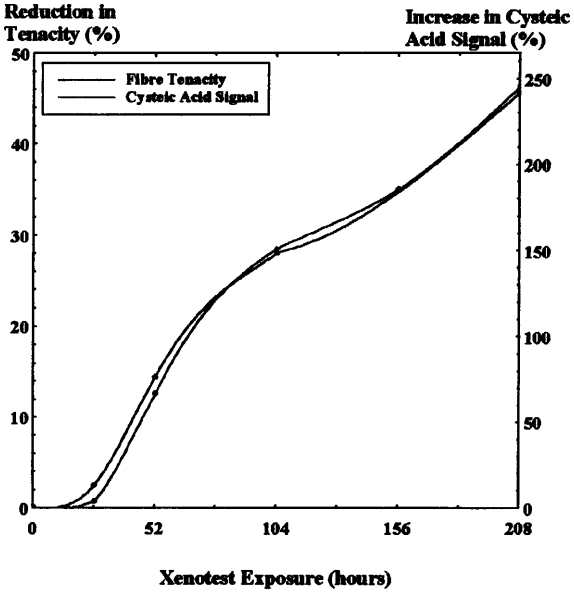

Figure 6.2 Rate of loss in tenacity and rate of cystine oxidation for wool fibres

Figure 6.2 shows that there is a close similarity between the rate of loss in fibre tenacity and the rate of cystine photooxidation, measured by the increase in cysteic acid signal from bulk FT-IR analysis of single wool fibres (see section 7.3.2). Both show an initial induction period where the rate of change in these properties is minimal. This initially slower rate of tenacity loss could be explained by only partial oxidation of cystine residues, leaving the disulphide bond intact, as found in section 7.3.2. New intermolecular crosslinks may also have formed which offset reductions in disulphide bonding at low exposure levels, but are photolabile with extended exposure[115] (see section 3.2.1). Although the loss in fibre tenacity appears to correspond with the rate of cystine photooxidation the reduction in extensibility seems to be more sensitive to the changes in structural mechanics of the fibre as a consequence of disulphide bond cleavage. Figure 6.1 shows that there is little loss in extensibility up to 52 hours but with continued exposure extensibility is lost more rapidly. At lower exposure levels, phototendering is characterised by larger reductions in fibre tenacity, but as exposure time extends a loss in fibre extensibility becomes a much more serious consequence. The specific work of rupture represents the energy required to break the fibre per unit mass, or fibre toughness, it summarises the reduction in tensile integrity of the fibre. The specific work of rupture also reflects the initial induction period during which the rate of phototendering is much slower, after which the rate of phototendering is linearly related to exposure time.

The stress strain curve for wool is characterised by three distinct regions. There is an initial linear pre-yield region up to 2% extension where stress is proportional to strain. The initial modulus is the gradient of the stress-strain curve in this region at the origin. This linear region abruptly ends at the yield point, at approximately 2-3% extension, which is followed by a yield region up to 30% extension, where the fibre extends rapidly with only small increases in stress. Finally there is a post-yield region above 30% extension where the fibre shows a greater resistance to extension than in the yield region. The post yield region continues to break point which occurs at approximately 40% extension.

The effect of light exposure on this characteristic stress-strain relationship of wool was examined. The stress-strain curve for fibres exposed for up to 52 hours remained the same as unexposed wool, but with a shortened post yield region prior to breaking point. Fibres exposed for 104 hours had similar stress-strain curves as unexposed wool up to the yield region. Breaking point occurred in the yield region or on the boundary between the yield and post yield regions. For the majority of fibres exposed for 208 hours, the stress-strain curve

was linear since breakage occurred at low extension in the pre-yield region, without reaching a yield point. Light exposure does not appear to alter the characteristic stress-strain relationship of wool. Instead, with increasing exposure time, breaking point moves to progressively lower stress-strain values along the same characteristic curve. With low levels of exposure, breaking point occurs in the post yield region, with further exposure rupture occurs in the yield region, and finally with severe exposure failure occurs at low extension in the linear pre-yield region.

The initial modulus gives a measure of the axial stiffness or resistance to extension for small extensions. The initial modulus was used to examine if light exposure altered the initial resistance to extension of the wool fibre. The influence of exposure on the yield point was also investigated. The yield point indicates the point up to which elastic recovery can take place, after this point further increases in strain cause permanent deformation. The yield point was located and measured from the stress-strain curve using the method of Meredith[186]. The mean values for the initial modulus and yield point at each exposure period are shown in Table 6.2. Light exposure does not significantly alter the value of the initial modulus, even after extended exposure for 208 hours. This indicates that the initial resistance of the fibre to extension is unaffected by light exposure. Table 6.2 also shows that there is no significant change in the yield point of the fibre after light exposure. The mean yield stress and yield strain values are similar, regardless of exposure time, with the yield point occurring at approximately 3.5% extension and at a tenacity of approximately 8.4 cN/tex. These results suggest that the structural characteristics responsible for the initial tensile response of the wool fibre are unaffected by light exposure.

Table 6.2 Effect of light exposure on tensile properties of wool fibres

Xenotest Exposure (hours)	Initial Modulus (N/tex)	Yield Stress (cN/tex)	Yield Strain (%)
0	2.63	8.53	3.65
26	2.82	8.42	3.53
52	2.86	8.13	3.42
104	2.89	8.46	3.75
208	2.88	-	-

A model proposed by Chapman and Hearle is most widely recognised as describing the structural mechanics responsible for the stress-strain curve of wet wool fibres[187] [188]. This simple two phase model is represented by crystalline microfibrils, parallel to the fibre axis, embedded in a non-crystalline, but highly crosslinked matrix. The fibrils, containing low

sulphur protein α-helical material, are crosslinked at intervals to the matrix by disulphide bonds between the high sulphur tails of the helix molecules and the high sulphur protein containing matrix. The tensile properties of wool are described by the composite response of these two phases. The linear pre-yield region is attributed to extension of the α-lattice in the microfibrils which continues until the stress reaches a critical level for transition to the extended β-structure, at the yield point. The yield region is attributed to the gradual opening out of individual fibril units to the extended form which continues at constant stress until all units have been transformed. The increased stress in the post yield region is attributed to extension of the matrix with fibre rupture occurring as the matrix reaches its limiting extension.

If this model can be used to account for the stress-strain properties of wool at normal regain the fact that light exposure does not alter the initial modulus and yield point may indicate that the initial response of the fibrillar α-helix remains unchanged with no significant photooxidation of the crystalline phases. The tensile failure which occurs in the post yield region after low and moderate exposure levels suggests a reduction in the extensibility of the matrix after exposure. This may be associated with changes in the nature of crosslinking in the amorphous phases due to photooxidation of disulphide bonds, possibly accompanied by structural changes which reduce the extensibility of the matrix such as the formation of new intermolecular crosslinks. Since the initial modulus does not alter after extended exposure it again suggests that the initial α-helical response is unchanged. However, since rupture of the fibre occurs without yielding it may indicate rapid failure through the brittle matrix at low strain.

The relationship between fibre diameter and tensile properties of wool for unexposed and exposed fibres was investigated. Table 6.3 shows the linear correlation coefficients calculated between fibre diameter and a breaking load, extension at break and specific work of rupture at each exposure level. For unexposed wool there is a good positive linear correlation between fibre diameter and breaking load as would be expected and this relationship is the same regardless of light exposure. There is no relationship between the intrinsic tenacity of wool fibres and fibre diameter for unexposed or exposed fibres. Similarly, there is no correlation between fibre diameter and extensibility for unexposed wool or after light exposure. No significant correlation was found between fibre diameter and initial modulus or yield point for either unexposed or exposed wool.

Therefore, the benefit of using coarser wool fibre lies only in the fact that the absolute breaking load increases. There are no advantages of higher extensibility and tenacity of wool fibres by increasing the fibre diameter.

Table 6.3 Level of correlation between wool fibre diameter and tensile properties

Xenotest Exposure (hours)	Linear Correlation Coefficient (ρ)[1]		
	Breaking Load / Diameter	Extensibility / Diameter	Tenacity / Diameter
0	0.74	0.1	-0.05
26	0.77	0.26	0.08
52	0.73	0.23	0.13
104	0.79	0.22	0.22
208	0.63	0.24	-0.05

6.2.2 Tensile Fracture Morphology of Light Degraded Wool Fibres

Twenty tensile fractures were examined for unexposed wool fibres and after each exposure period. Unexposed wool fibres mostly showed the typical break morphology which has previously been characterised for wool [240], Figure 6.3 (i). Fracture is caused by transverse cracks running through the fibre usually initiated from faults in the cuticle where stress becomes concentrated. As the stress increases the crack propagates through the fibre bulk giving a smooth but granular fracture, eventually followed by total rupture. The region immediately preceding the final failure point is usually characterised by a more rough surface, attributed to the stress on the unbroken part of the fibre prior to failure. This break morphology was typical for unexposed fibres regardless of fibre diameter, tenacity and extension at break. A number of fibres examined showed internal cracks, presumably due to cleavage along weak components such as the intercellular regions, Figure 6.3 (iii). Very often transverse striations were also present extending down the fibre length from the fracture point, Figure 6.3(v). These deformations, which clearly form prior to fracture of the cuticle, are thought to develop during yielding of the fibre between 2 and 30% extension[189]. Not all tensile fractures showed these striations, but no link could be found between the appearance of these striations and tensile properties of the fibres.

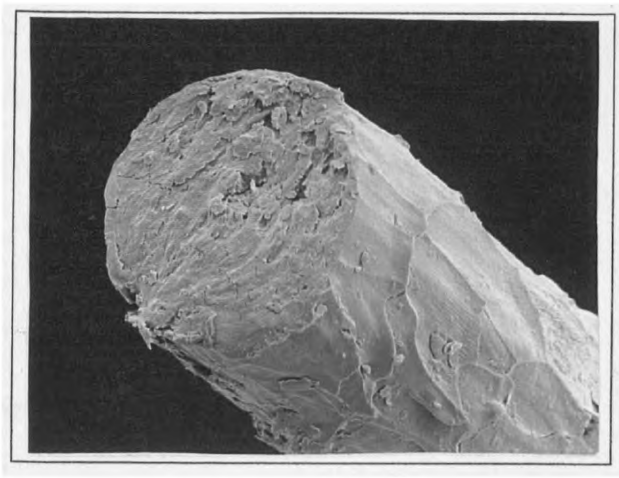

(i) Unexposed Wool
Tenacity: 14.6 cN/tex Extension: 43 %

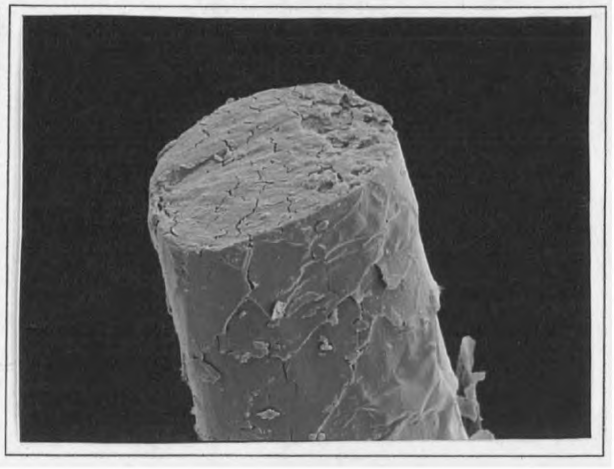

(ii) Exposed Wool (52 hours)
Tenacity: 10.6 cN/tex Extension: 34.1%

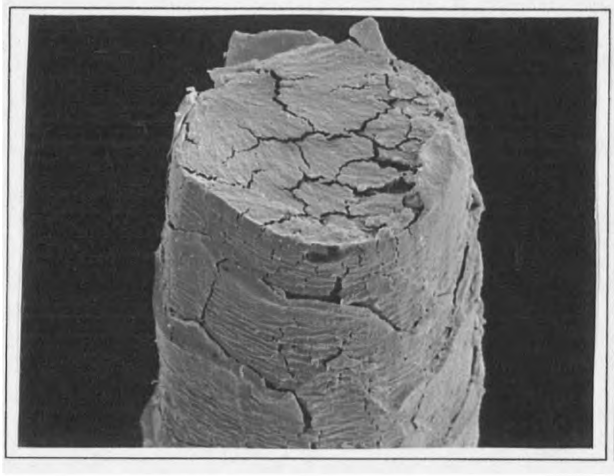

(iii) Unexposed Wool
Tenacity: 14.1 cN/tex Extension: 47.5 %

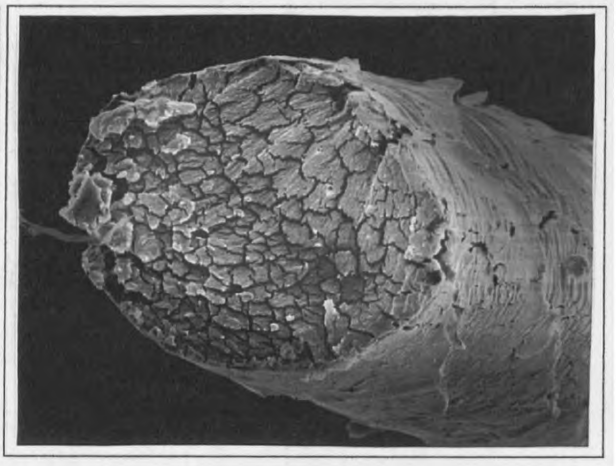

(iv) Exposed Wool (52 hours)
Tenacity: 10.1 cN/tex Extension: 21%

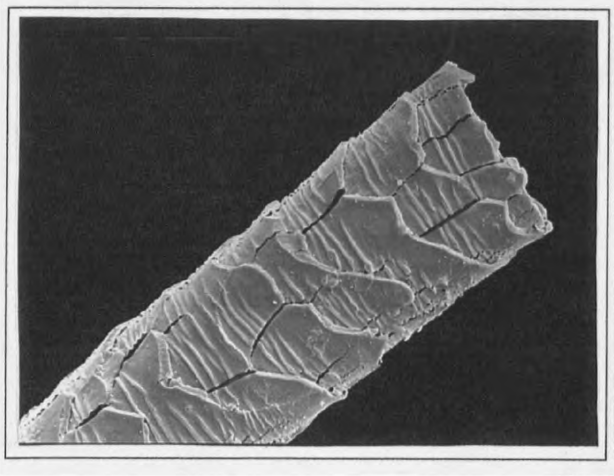

(v) Unexposed Wool
Tenacity: 14.8 cN/tex Extension: 41.6 %

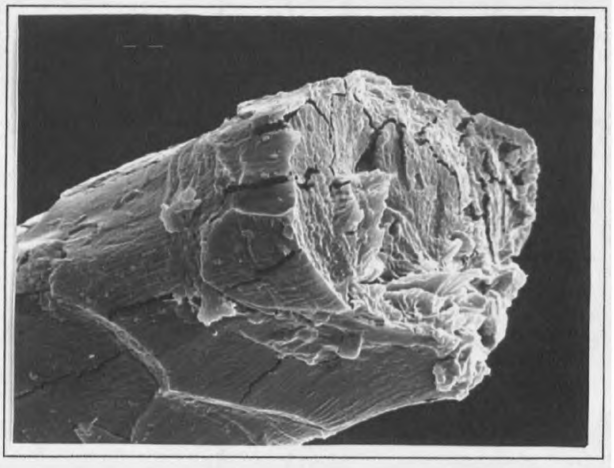

(vi) Exposed Wool (208 hours)
Tenacity: 8.7 cN/tex Extension: 8.9 %

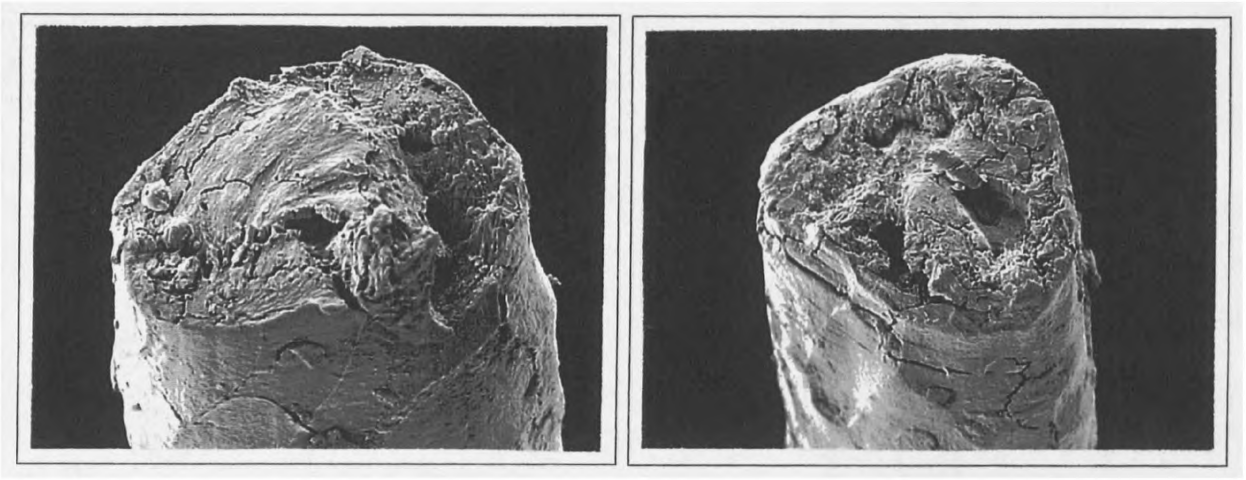

(vii) Exposed Wool (208 hours)
Tenacity: 8.3 cN/tex Extension: 4.9%

(viii) Exposed Wool (208 hours)
Tenacity: 7.6 cN/tex Extension: 3.4%

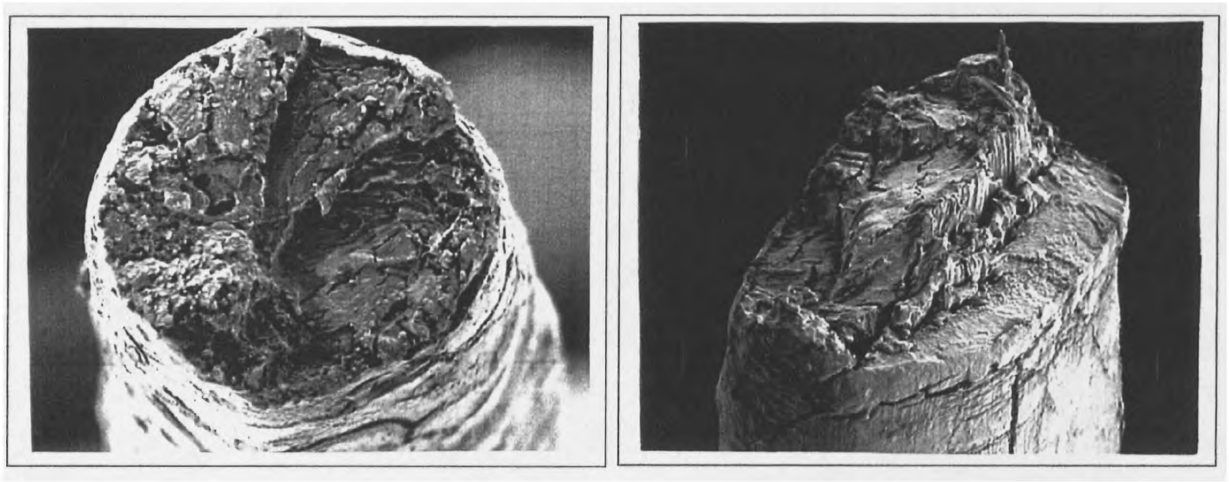

(ix) Exposed Wool (208 hours)
Tenacity: 6.7 cN/tex Extension: 4.6%

(x) Exposed Wool (208 hours)
Tenacity: 7.5 cN/tex Extension: 2.3%

Figures 6.3 (i) - (x) Tensile fractures of wool fibres

Wool fibres exposed for up to 104 hours showed similar granular transverse fractures as found for unexposed fibres, Figure 6.3 (ii). Although no significant distinctions could be found in the nature of fracture morphology before and after light exposure, it can be expected that the weakened photooxidised cuticle will be less resistant to break initiation. Where internal cracking was evident, the extent of fracturing was more severe after light exposure, Figure 6.3 (iv). This suggests that light exposure has caused internal damage leading to a greater weakening of the intercellular material. The fracture morphology of severely degraded fibres exposed for 208 hours was significantly different. Tensile failure of these fibres occurred at very low strain values reflecting the brittle nature of the fibre. The fracture morphology showed less clearly the features of transverse crack growth initiated at the cuticle. Instead, the breaks appeared much rougher with more uneven internal tearing, disturbance and internal voids, Figures 6.3 (vi) - (x). These features reflect the much more rapid failure of these fibres. They suggest that extensive photochemical damage has occurred within the cortex allowing rapid crack growth to be initiated from many of the weaker regions and voids in the fibre bulk. There was no evidence for the transverse striations which are associated with yielding of the cuticle, indicating that fracture takes place at low strain of the cuticle. No evidence was found for the smooth brittle fracture morphology previously characterised for photodegraded wool [34]. This type of very smooth fracture morphology, which had no evidence of internal disturbance, was thought to be consistent with a structure that had undergone protein chain scission and an alteration in the nature of crosslinking.

6.3 Surface Properties of Wool Fabrics

6.3.1 Effect of Light Exposure on Surface Integrity of Wool Fabric

The changes observed in the tensile properties of wool following light exposure can be expected to have serious consequences for the integrity of fibres at the surface of fabrics. Automotive upholstery must maintain a high level of wear resistance and retain its appearance and comfort properties throughout the lifetime of the vehicle. The effect of light exposure on the physical integrity of the surface of wool fabric was measured by the rate of weight loss of fabrics during Martindale abrasion testing, (see section 4.4.1). Figure 6.4 shows the effect of light exposure on the rate of surface breakdown of a 100% wool fabric (35 μm wool). Unexposed wool does not show a linear rate of surface breakdown. The fabric shows an initial higher resistance, but as the number of abrasion cycles increases above 75,000 breakdown of

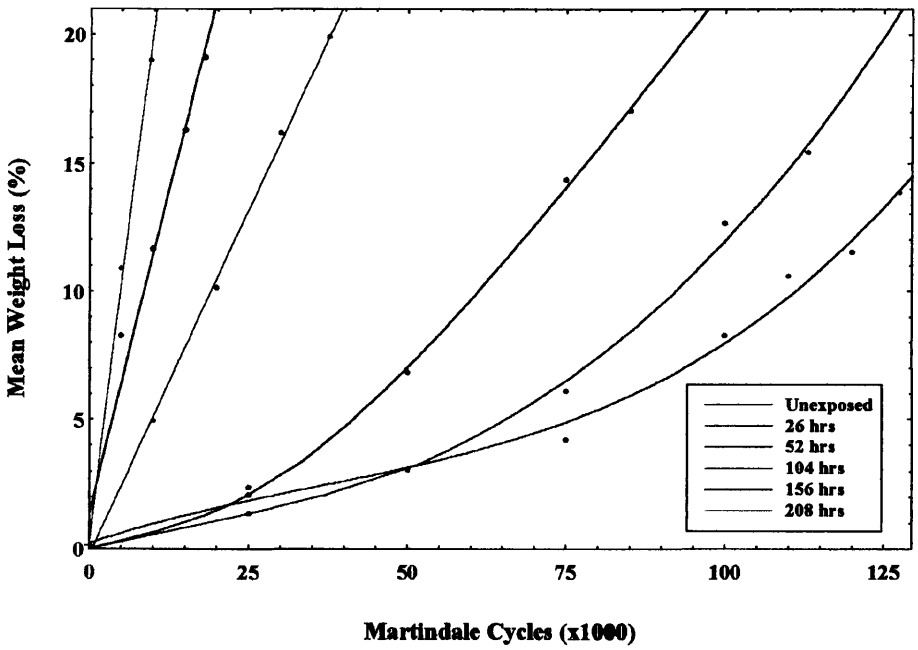

Figure 6.4 Effect of light exposure on surface integrity of wool fabrics

the surface occurs at progressively faster rate until end point is reached. Fabrics exposed for up to 52 hours show a similar pattern of wear but the rate is accelerated with exposure time. Following light exposure the point at which abrasion resistance is lost more rapidly is lowered to around 50,000 cycles after 26 hours exposure and 25,000 cycles after 52 hours. At higher exposure levels fabrics do not show a period of initial higher resistance, but instead, the rate of surface breakdown is directly proportional to the number of abrasion cycles, and it increases with exposure time. Although phototendering is confined to those fibres at the fabric surface it can be seen that it causes much larger reductions in wear resistance than might be expected. This can be explained since all fibres in the fabric will have places along their lengths where they are present on the outer surface of the yarn. Therefore phototendering is not confined to a limited number of surface fibres, but all fibres in the fabric will have weakened areas allowing abrasive breakdown to occur at an accelerated rate. The large reductions in extensibility and increasing brittleness of wool fibres after extended light exposure allows fibre fracture and removal to occur extremely rapidly with little resistance.

SEM examination of fibres in the surface of wool fabrics abraded to end point showed typical features of abrasion damage, multi axial splitting followed by fibre fracture leaving fibrillated fibre ends[236]. Continued abrasion of the fibrillated fibre ends led to scale removal and in some cases the rounding and smoothing of fibre ends. This abrasive breakdown was similar for fibres in light degraded fabrics but there was more evidence of scale removal and a greater

profusion of rounded fibre ends. This is due to phototendering of the wool fibre cuticle which is known to be the initial point of fracture during abrasive breakdown of the fibre [12 119].

6.3.2 Effect of Light Exposure on Mechanical and Surface Properties of Wool Fabrics

In addition to the deterioration in physical integrity of the fabric surface, light exposure increases the stiffness and harshness of wool fabrics, indicating considerable changes in the surface and mechanical properties. The low stress fabric mechanical and surface properties of fabrics can be measured objectively using the KES-F instruments. These tests give information on surface tensile and compressional properties, along with a measure of resistance to shear and bending deformations. The surface coefficient of friction and geometrical roughness allow changes in the handle of fabrics to be assessed quantitatively. Using these instruments, changes in the surface properties of untreated wool fabric after Xenotest exposure for 156 hours were measured, Table 6.4. Following light exposure there are significant alterations in surface tensile properties. There is an increase in tensile linearity which indicates a higher initial resistance to extension, reflecting a stiffer fabric. There is a loss in fabric extensibility which would be expected from the large reduction in wool fibre extensibility. An increase in inter-fibre friction may also increase the fabric's resistance to elongation. There is a reduction in tensile resilience indicating lower elastic recovery of the fabric from tensile deformation.

Table 6.4 Changes in mechanical and surface properties of wool fabric after light exposure

KES-F Parameter		% Change after exposure
LT	Tensile Linearity	12.36
WT	Tensile Energy	-2.92
RT	Tensile Resilience	-13.35
EMT	Extension %	-13.55
G	Shear Rigidity	32.2
2HG	Shear Hysteresis	131.03
2HG5	Shear Hysteresis	147.4
B	Bending Rigidity	11.25
2HB	Bending Hysteresis	39.3
LC	Compressional Linearity	6.91
WC	Compressional Energy	-58.73
RC	Compressional Resilience	-4.77
T0	Thickness	-29.86
MIU	Coefficient of Friction	7.56
MMD	Mean Deviation of MIU	6.74
SMD	Geometrical Roughness	4.78

There are large changes in the shear properties of wool after exposure. Shear stiffness increases by 32%, and the large increase in shear hysteresis indicates a loss of fabric elasticity in shearing. Fabric bending stiffness also increases, but by a smaller amount, and there is an increase in bending hysteresis. This further indicates an increase in fabric flexural rigidity and a reduction in elastic recovery following flexural deformation.

Wool is less resistant to compressional forces shown by the decrease in compressional energy, but with no large loss in compressional resilience. The fabric has also become thinner, or more flattened after exposure.

The coefficient of surface friction and geometric roughness of the fabric increase slightly after exposure, indicating a rougher harsher surface. There was a loss in the desirable handle properties of the fabric after exposure. The primary hand values, calculated from the KES-F parameters, describe fabric smoothness and fullness on a scale of 1-10. There was a reduction in fabric smoothness value from 2.8 (unexposed) to 0.9 after light exposure. The fabric fullness value also decreased from 6.5 (unexposed) to 3.7 after exposure. Not only does light exposure alter the physical integrity of the fabric surface, but also the aesthetic qualities of the fabric are impaired.

6.4 Protective Effect of Cibafast W to Wool Phototendering

The level of protection given to wool phototendering by the application of Cibafast W was investigated. This was assessed by tensile testing of yarns taken from untreated and absorber treated fabrics following successive Xenotest cycles. The percentage reductions in tenacity and extensibility of untreated and absorber treated yarns after light exposure are compared in Table 6.5. These values are the mean differences calculated from 50 yarns tested at each exposure level. The standard errors of the mean differences are also given.

Table 6.5 Protective effect of Cibafast W to losses in tensile properties of wool yarns

Xenotest Exposure (hours)	Mean Loss in Tenacity (%)		Mean Loss in Extension (%)	
	Untreated	Cibafast W	Untreated	Cibafast W
26	6 ± 4	(+) 1 ± 5	5 ± 3	(+) 1 ± 3
52	19 ± 5	(+) 3 ± 5	8 ± 2	(+) 3 ± 3
104	41 ± 4	14 ± 5	45 ± 2	23 ± 4
208	45 ± 5	36 ± 6	80 ± 2	66 ± 3

The rate and extent of losses in tenacity and extensibility for untreated wool yarns reflects closely the changes found in these properties from single fibre testing. The loss in tenacity of untreated yarns is most rapid up to 104 hours. There is a 46% reduction in tenacity after 208 hours exposure, similar to the reduction of 45% found for single wool fibres. Yarns treated with Cibafast W show no significant loss in tenacity after exposure for up to 52 hours but this protective effect diminishes as exposure time extends. Untreated wool yarns rapidly lose extensibility after exposure for more than 52 hours, with losses in extensibility similar to those found for single fibres. Again, the application of Cibafast W gives some protection to losses in extensibility for an induction period of 52 hours. With further exposure, protection diminishes and the loss in extensibility is at a rate similar to untreated wool. Therefore, Cibafast W gives significant protection to phototendering at low exposure levels. With extended exposure the protective effect of the absorber diminishes and phototendering occurs at a rate similar rate to untreated wool.

6.5 Rate of Phototendering of Wool Automotive Fabrics

The rates of phototendering of the flat woven wool automotive fabrics developed were investigated in order to establish wear performance under automotive conditions. Since phototendering is mainly confined to the surface layers of fabrics, abrasion testing was considered to be a much more sensitive method of measuring the rate of surface breakdown of these fabrics and assessing wear resistance. The change in abrasion resistance after light exposure was measured by the mean percentage rate of weight loss of fabrics during Martindale testing, as described in section 4.4.1.

The wool automotive fabrics were developed in order to investigate the influence of wool mean fibre diameter on unaged and aged fabric abrasion resistance. The effect on performance of blending these wool qualities with polyester and nylon of different linear densities was also examined. All fabrics were tested in laminated form.

6.5.1 Rate of Phototendering of 100% Wool Automotive Fabrics

The effect of light exposure on the abrasion resistance of the 100% wool automotive fabrics is shown in Figure 6.5. There is a rapid loss in abrasion resistance of all three fabrics after light

Table 6.6 Reduction in abrasion resistance of 100% wool fabrics with light exposure

Xenotest Exposure (hours)	25 μm Wool Fabric		30 μm Wool Fabric		35 μm Wool Fabric	
	End Cycles (x 1000)	Abrasion Index	End Cycles (x 1000)	Abrasion Index	End Cycles (x 1000)	Abrasion Index
0	71	**5.31**	107	**6.72**	128	**11.7**
26	59	**3.42**	85	**6.16**	113	**11**
52	40	**1.8**	53	**3.38**	85	**6.86**
104	16	**0.8**	27	**1.07**	38	**1.93**
156	9	**0.36**	13	**0.49**	18	**0.8**
208	6	**0.26**	8	**0.29**	10	**0.48**

exposure for more than 52 hours following which the rate of surface breakdown is linearly related to exposure time.

The reciprocal value of the mean % rate of weight loss at each exposure level was used as an index to compare the abrasion resistance of each fabric. Table 6.6 gives these abrasion resistance indices and also the end point cycles for each fabric, according to exposure time. There is a significant increase in abrasion resistance of the unexposed fabrics with increasing mean fibre diameter, and this effect is maintained at each exposure level. According to the abrasion resistance indices, there is an average improvement of factor over all exposure levels of 2.5 for the abrasion resistance of the 35 μm wool fabric relative to the 25 μm wool fabric.

The percentage retained abrasion resistance of each fabric as a function of exposure time are compared in Figure 6.6 (calculated from the abrasion resistance indices).

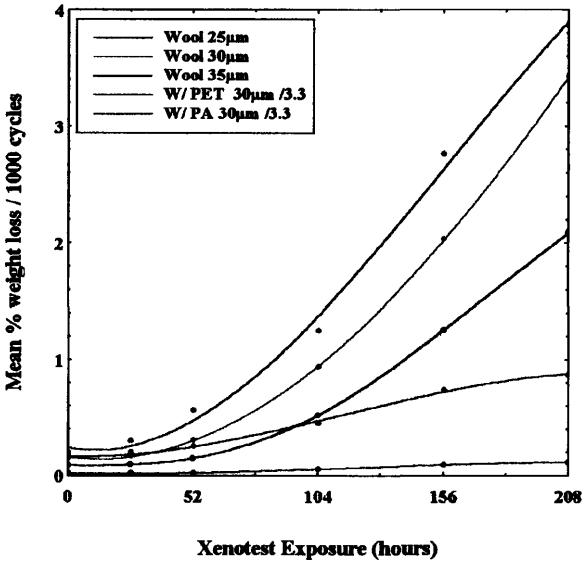

Figure 6.5 Effect of light exposure on abrasion resistance of wool fabrics

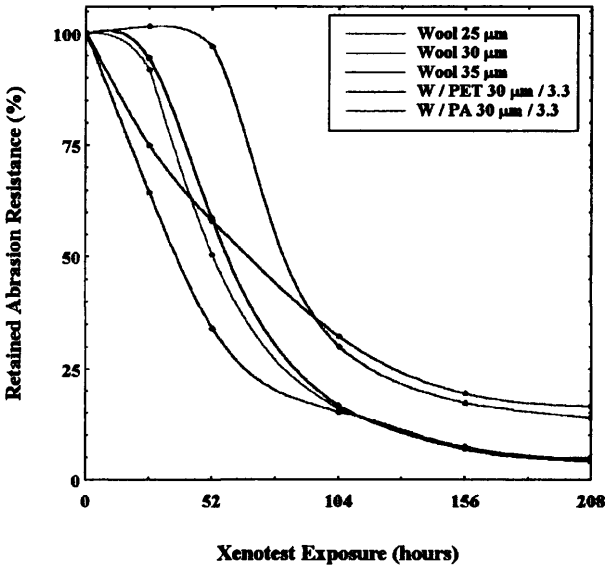

Figure 6.6 Comparison of rate of surface phototendering of wool fabrics

The 25 μm wool fabric shows a much more rapid loss in abrasion resistance over the first 26 hours exposure than the coarse wool fabrics which have an initial period of higher resistance. This initial higher resistance is subsequently lost with further exposure and the rate of phototendering is the same regardless of mean fibre diameter. In using coarser wool fibres, apart from the advantage of an increase in absolute abrasion resistance there appears to be an additional benefit of a slower rate of surface phototendering at low exposure levels. For all three fabrics, abrasion resistance is lost most rapidly up to 104 hours exposure, continued exposure reduces the fabric surface integrity only minimally. The 25 μm wool fabric had a pilling tendency, localised fibre migration into these pills led to yarn thinning and breakage. This can be attributed to easier pull out and entanglement of the weaker wool fibres. The rate of pill formation and wear off took place at an accelerated rate after light exposure. In contrast the 30 μm and 35 μm fabrics maintained good appearance during abrasion testing but the 35 μm fabric became increasingly harsh in handle. Of these three fabrics only the 35 μm wool fabric passed the Rover Group aged abrasion test. This specifies that after 52 hours Xenotest exposure followed by 50,000 Martindale cycles fabrics should maintain good appearance and there should be no thread breakages.

6.5.2 Rate of Phototendering of Wool Blend Automotive Fabrics

The rate of phototendering of wool / nylon blends compared to wool / polyester blends was investigated. Initially, the performance of two fabric blends was compared; wool / nylon (30 μm / 3.3 dtex) and wool polyester (30 μm / 3.3 dtex) since their compositions are directly comparable. Figure 6.5 shows the mean percentage rate of weight loss as a function of exposure time for both fabrics in comparison to the 100% wool fabrics. The wool / polyester blend has a similar abrasion resistance as the equivalent 30 μm 100% wool fabric up to 52 hours exposure. However, the aged abrasion resistance of the wool / polyester blend is much higher at exposure times above 52 hours, where the 100% wool fabric shows rapid losses in surface integrity. Whilst the abrasion resistance of wool up to 52 hours exposure is improved very little by blending with polyester, there is a large increase if nylon is used in the blend. The wool / nylon blend has a much higher original abrasion resistance than the other fabrics. Even after 208 hours exposure the abrasion resistance of this blend remains greater than the wool / polyester fabric. Table 6.7 compares the abrasion resistance indices and end point cycles for both wool blend fabrics at each exposure time.

Table 6.7 Reduction in abrasion resistance of wool blend fabrics with light exposure

Xenotest Exposure (hours)	**Wool / Polyester** (30 μm / 3.3 dtex)		**Wool / Nylon** (30 μm / 3.3 dtex)	
	End Cycles (x 1000)	Abrasion Index	End Cycles (x 1000)	Abrasion Index
0	103	**6.99**	200+	**66.1**
26	90	**5.24**	200+	**67.3**
52	74	**4.06**	200+	**64.2**
104	49	**2.27**	200+	**19.7**
156	35	**1.35**	200+	**11.4**
208	29	**1.15**	200+	**9.17**

At each exposure level the nylon blend was abraded to 200,000 cycles without reaching end point, even after prolonged exposure for 208 hours. There is an average improvement factor over all exposure levels of 10.5 for the abrasion resistance of the nylon blend relative to the polyester blend. Figure 6.6 shows that despite the much higher abrasion resistance of the nylon blend, phototendering takes place. However, the nylon blend retains its abrasion resistance almost entirely up to 52 hours exposure, but with further exposure the phototendering is at a similar rate to the 100% wool fabrics. This suggests that the nylon component has a protective effect over low exposure levels, capable of offsetting the reduced abrasion resistance of the phototendered wool fibres. The loss in this protective effect with further exposure suggests significant tendering of the nylon itself.

In contrast, blending wool with polyester increases the rate of loss in abrasion resistance over the first 26 hours compared to the equivalent 100% wool fabric. The polyester blend has a slower rate of phototendering between 26 and 104 hours compared to the other fabrics. The unexposed polyester blend developed a number of large pills during abrasion testing. In the initial stages of pill development free fibre ends are brushed up and pulled out by the abrasive action leading to fibre entanglements [242]. Anchor fibres are progressively drawn out and rolled up into the body of the pill. It was found that the polyester fibres, due to their high modulus, anchored the pills to the fabric surface preventing wear off. Localised fibre migration into these pills led to rapid yarn thinning and eventual breakdown of the structure. This pilling process is therefore responsible for the ultimate failure of this blend. Pilling was the cause of fabric failure at each exposure level for this blend. With increasing exposure time the rates of pill formation and wear off increased. Additionally, the pilling tendency of this fabric makes it aesthetically unacceptable for automotive end use and consequently it failed the Rover Group

aged abrasion test.

The wool / nylon blend did not have a pilling tendency, either before or after light exposure, which explains the superior performance of this blend. The fabric did not show signs of thinning and maintained a good appearance, regardless of exposure time, up to 200,000 cycles. However, as exposure time increased there was an increase in surface hairiness of the fabric after 200,000 cycles, caused by broken protruding nylon fibre ends. This wool / nylon blend passed the Rover Group aged abrasion test.

The abrasion resistance of the wool blend fabrics produced from the 25 μm and 35 μm wool qualities were examined. In Section 6.5.1 it was found that using 35 μm wool there was a considerable improvement in unaged and aged fabric abrasion resistance. A disadvantage of this wool quality is the harshness of handle, particularly after light exposure. To improve the handle of the coarse wool fabrics a finer synthetic component was used for blending. However, it was not clear how this would effect abrasion resistance. The 35 μm wool quality was blended polyester and nylon fibres of 1.4 dtex and 2.4 dtex respectively. In subjective testing of fabric handle, these blends were perceived as being less harsh than the 100% wool fabric, particularly the polyester blend. These fabrics also had an improvement in handle compared to similar blends produced using 3.3 dtex polyester and nylon fibres.

The finer 25 μm wool quality was blended with a coarse nylon fibre of 6.6 dtex with the aim of improving the abrasion resistance of the fine wool fabric. Unfortunately coarse polyester fibre was not available to produce a similar wool / polyester fabric.

The unaged abrasion resistance of all the wool blends and equivalent 100% wool fabrics are compared in Table 6.8. Apart from the polyester blend (H), there is an increase in abrasion resistance of the wool blend fabrics with increasing wool mean fibre diameter. None of the polyester blends have a significantly improved performance compared to the equivalent 100% wool fabrics. This was due in all cases to a pilling tendency of these blends which caused accelerated fabric thinning. The polyester blend produced from 25 μm wool had the most severe pilling, being enhanced by the pilling tendency of the finer wool fibre quality. The polyester blend produced from the 35 μm wool had a particularly poor abrasion resistance. This fabric readily formed very small pills on the surface. The rapid rate of formation and wear off of these pills led to extreme fabric thinning and premature failure. Microscopical examination showed the pills to be small tight balls of polyester fibres. The low tenacity and

poor cohesion of the finer polyester fibres used in this blend allowed them to be easily pulled out and entangled into small pills of low anchor tenacity. The repeating cycle of pill development and wear off removed a considerable amount of polyester fibre leaving the fabric with a wool fibre skeleton. In contrast, all the wool / nylon blends have a much higher abrasion resistance than the equivalent 100% wool and wool / polyester fabrics. The wool / nylon fabrics did not pill, retained good appearance and none of the specimens had reached end point at 200,000 cycles. The finer 2.4 dtex nylon fibre used in combination with the 35 μm wool quality did not impair the performance of this blend, although the fabric had a more hairy appearance after testing due to projecting nylon fibre ends on the surface.

Table 6.8 also shows the loss in abrasion resistance of these fabrics after sunlight exposure in Arizona. The 100% wool fabrics retain between 16 - 20% of their original abrasion resistance compared to between 30 -36 % for the wool / polyester blends. After light exposure, pilling of the wool / polyester blends occurred at a more accelerated rate. The wool / nylon blends containing 30 μm and 35 μm wool have much higher retained abrasion resistances after sunlight exposure compared to the other fabrics. The superior performance of the 30 μm wool blend may be explained by the fact that the nylon fibre used has a light stabilized polymer. More rapid phototendering of the finer nylon fibre used in the 35 μm wool blend may have reduced the performance of this fabric in comparison. The 25 μm blend has a much more rapid rate of phototendering than the other nylon blends. In section 5.5.2 this fabric was also identified as having the poorest photostability of all the wool blend fabrics.

Table 6.8 Comparison of change in abrasion resistance of wool fabrics after sunlight exposure

Fabric Type	**Unexposed**		**Sunlight Exposed**		Retained Abrasion Resistance %
25 μm Wool	End Cycles (x 1000)	Abrasion Indcx	End Cycles (x 1000)	Abrasion Indcx	
A 100% Wool	71	5.31	24	0.99	**19**
B Wool / PET(3.3 dtex)	89	5.78	48	1.72	**30**
C Wool / PA (6.7 dtex)	200+	53	200+	13.5	**26**
30 μm Wool					
D 100% Wool	107	6.72	35	1.35	**20**
E Wool / PET(3.3 dtex)	103	6.99	49	2.45	**35**
F Wool / PA (3.3 dtex)	200+	66.1	200+	50	**75**
35 μm Wool					
G 100% Wool	128	11.7	41	1.9	**16**
H Wool / PET(1.4 dtex)	79	3.75	35	1.37	**37**
J Wool / PA (2.4 dtex)	200+	81	200+	34	**42**

Of all the wool blends developed, only the wool / nylon fabrics met the performance requirements of the Rover aged abrasion test. The pilling problems associated with the wool / polyester blends meant that they were unacceptable.

6.5.3 Fabric Mechanical and Surface Properties

Light exposure has most serious consequences for the surface properties of fabrics. This is illustrated in Table 6.9 in which losses in fabric tensile properties after Xenotest exposure are relatively insignificant compared to the reductions in fabric abrasion resistance. Considerable damage has taken place at the fabric surface without appreciably altering the physical integrity of the fabric bulk. This illustrates the relative insensitivity of fabric tensile testing as indicator of the extent of photodegradation, particularly for the assessment of wear resistance.

Table 6.9 Comparison of losses in tensile properties and abrasion resistance of fabrics after Xenotest exposure for 52 hours.

Fabric Type	% Loss in Fabric Breaking Load	% Loss in Fabric Extension at Break	% Loss in Fabric Abrasion Resistance
100% Wool (25 μm)	9.6	3	66
100% Wool (30 μm)	6.5	5	50
100% Wool (35 μm)	3.4	5.2	41
Wool / PET (30 μm / 3.3)	1	5.2	42
Wool / PA (30 μm / 3.3)	6	6.7	3

Using the KES-F instruments the low-stress mechanical and surface properties of fabrics were measured to compare the surface properties of wool / nylon and wool / polyester blends and investigate the changes in these properties following light exposure. In Table 6.10 the KES-F values for unexposed wool / polyester and wool / nylon blends (unlaminated fabrics) are compared. Both fabrics are structurally identical and differ only in that one contains 35% nylon and the other 35% polyester. The nylon blend is 41 % more extensible than the polyester blend, reflected by the 43 % higher tensile energy value, but it has a slightly lower tensile resilience. The nylon blend has less flexibility in shear and bending deformations, shown by the higher shear and bending rigidity values compared to the polyester blend. The nylon blend also has poorer elastic recovery from shear and bending deformations. The nylon blend is a rougher, harsher fabric indicated by the higher coefficient of friction and geometric roughness values. The poorer surface properties of the nylon blend were confirmed from subjective handle assessment of the fabrics.

Table 6.10 Low stress mechanical and surface properties of wool blend fabrics

KES-F Parameter		**Wool / nylon** 30 μm / 3.3 dtex		**Wool / polyester** 30 μm / 3.3 dtex	
		Unexposed Value	% Change after exposure	Unexposed Value	% Change after exposure
LT	Tensile Linearity	0.762	7	0.752	-48
WT	Tensile Energy	4.24	-11	2.97	-46
RT	Tensile Resilience	53.8	-2	58	-4
EMT	Extension %	2.23	-17	1.58	4
G	Shear Rigidity	1.75	19	1.38	2
2HG	Shear Hysteresis	4.96	23	3.18	7
2HG5	Shear Hysteresis	7.65	33	5.52	6
B	Bending Rigidity	0.839	-1	0.731	-3
2HB	Bending Hysteresis	0.573	3	0.437	-3
LC	Compressional Linearity	0.389	17	0.367	23
WC	Compressional Energy	0.227	-27	0.18	3
RC	Compressional Resilience	48	4	49.1	-2
Compressibility %		26	-30	25	-17
T0	Thickness	1.222	-12	1.021	1
MIU	Coefficient of Friction	0.219	4	0.184	0.1
MMD	Mean Deviation of MIU	0.022	15	0.02	-7
SMD	Geometrical Roughness	6.33	-0.7	5.44	0.2

Table 6.10 shows the percentage change in the KES-F values of both fabrics after Xenotest exposure for 156 hours. The nylon blend shows a reduction in extensibility but no large change in tensile resilience following exposure. In contrast, the polyester blend has almost a 50% reduction in tensile linearity and tensile energy, although there is no loss in extensibility. This indicates that the fabric has a lower resistance to initial extension. The increases in shear stiffness and hysteresis for the nylon fabric after light exposure show that the fabric has become stiffer and has a loss in elastic recovery. However, these changes in shear properties are much smaller than those found for 100% wool after the same exposure time, section 6.3.2. In contrast the polyester blend has little change in shear properties after light exposure remaining a more flexible fabric. Both fabric blends show no large changes in bending properties after exposure. The nylon blend is less resistant to compressional forces after exposure, shown by the decreases in compressibility and compressional energy. The fabric also becomes thinner or more flattened compared to the polyester blend which shows no significant change in fabric thickness. The surface properties of the polyester blend are not significantly altered, whereas the nylon blend has a greater variation in coefficient of friction of the surface. The total hand values indicated that the polyester blend had become slightly smoother and fuller with exposure, whilst the nylon blend showed an opposite effect.

The effect of heat on the KES-F properties of these fabrics was also investigated after exposure to the Sahara test. The polyester blend had a 20% increase in extensibility, small reductions in shear and bending stiffness and decreases in shear and bending hysteresis. There were small increases in surface coefficient of friction and geometrical roughness. In contrast, the nylon blend had a small increase in shear hysteresis and decreases in surface roughness.

Automotive fabrics are usually in a laminated form and therefore the surface properties of the laminated fabric may differ from the face fabric. The KES-F properties of both blend fabrics were measured after lamination to a 3 mm thickness polyester urethane foam. As would be expected, lamination increases shear and bending rigidities and hysteresis. There is an increase in compressional energy and increase in compressional resilience for both fabrics after lamination. The extensibility of the nylon blend still remains much higher than the polyester blend after lamination, but the tensile resilience of both laminates is only 25% indicating a reduced recovery from stretching. Lamination also caused an increase in fabric harshness, there was a 25% increase in coefficient of surface friction for the nylon blend and a 40% increase for the polyester blend. The nylon blend also appeared to be smoother after lamination, with a 25% decrease in geometrical roughness compared to the face fabric.

After light exposure the laminated fabrics showed large decreases in bending and shear stiffness and had improved elastic recovery. There was an increase in fabric extensibility and tensile resilience increases considerably. These changes are most likely associated with a loss in foam integrity and stiffness due to degradation through hydrolysis. After light exposure the laminated fabrics show much larger increases in surface harshness and roughness than found for the face fabrics.

6.6 Conclusions

Phototendering of wool is characterised by larger reductions in fibre tenacity at low exposure levels, but as exposure extends a loss in fibre extensibility is a much more serious consequence. The loss in fibre tenacity was found to correspond with the rate of cystine photooxidation. An induction period during which the rate of phototendering of the fibre is much slower may be explained by only partial oxidation of cystine, the disulphide bonds remaining intact. The loss in extensibility seems to be a more sensitive measure of the overall change in structural mechanics of the fibre as a consequence of disulphide bond cleavage. Light exposure appears the weaken the wool fibre cuticle allowing more rapid tensile failure,

but the fracture morphology of severely degraded fibres indicated that light exposure had caused much more internal damage within the fibre bulk.

Although phototendering is confined to fibres in the fabric surface it has much more serious consequences for the physical integrity of fabrics than is apparent from measuring the tensile loss of fabrics. All the fibres in the fabric will have points along their lengths where they are uppermost in the fabric surface and suffer phototendering, causing the rate of abrasive breakdown to be accelerated. The large reductions in extensibility and increasing brittleness of wool fibres after light exposure allows easier fracture of fibres in the fabric surface and consequently increases the rate of fibre loss during abrasion testing. Light exposure also increases the flexural rigidity of wool fabrics and reduces elastic recovery following shear, bending and tensile deformations. The desirable handle properties of the fabric surface are also impaired, there is an increase in roughness and harshness and a decrease in fullness. After laminating wool fabrics there are much larger increases in surface harshness and roughness following light exposure. Cibafast W significantly reduces the rate of phototendering at low exposure levels, giving almost complete protection to losses in tensile properties up to 52 hours exposure. With extended exposure the protective effect of the absorber diminishes and tendering occurs at a similar rate as untreated wool.

The abrasion resistance of 100% wool and wool blend automotive fabrics increases considerably with increasing mean wool fibre diameter, this improvement is maintained regardless of exposure time . Additionally, coarse wool fabrics retain a higher abrasion resistance at low exposure levels, which could be explained by the increase in fibre bulk to surface ratio. The correct choice of synthetic fibre component for wool blend fabrics is imperative since it may accelerate abrasive breakdown. A very high level of abrasion resistance can be achieved by blending wool with nylon. These blends maintained an acceptable abrasion resistance even after severe light exposure and were able to meet current automotive performance standards. A nylon blend was found to retain its abrasion resistance almost entirely up to 52 hours exposure. This suggests that the nylon component has a protective effect over moderate exposure levels, in some way compensating for the loss in wear resistance of the phototendered wool. In comparison, blending wool with polyester does not significantly improve abrasion resistance. The rate of surface breakdown of polyester blends is governed by the process of pilling, with light exposure accelerating the rate of pill formation. Pilling makes these fabrics aesthetically unacceptable for automotive end use.

Chapter 7

Bulk Analysis of Photooxidised Fabrics Using Vibrational Spectroscopy

7.1 Introduction

This chapter discusses the results of work using vibrational spectroscopy for non-destructive analysis of photooxidised wool. FT-Raman spectroscopy is used to examine the nature of photochemical changes in the wool fibre bulk. The advantage of this technique for studies on wool is that bands are present for the photosensitive amino acid residues along with those sensitive to changes in structural conformation. FT-IR spectroscopy coupled to Attenuated Total Reflectance (ATR) allowed more surface sensitive analysis of photooxidised wool, in particular the rate of increase in signal intensities associated with the oxidation products of cystine was examined. Using these techniques the level of protection given by the application of Cibafast W to undyed and dyed wool fabrics was investigated. These techniques were also used to investigate the extent and nature of photochemical changes to polyester and nylon fabrics and the protection given by photostabilizers. The experimental conditions employed for FT-IR and FT-Raman analysis are detailed in sections 4.6.1 and 4.6.2 respectively.

7.2 FT-Raman Analysis of Wool

7.2.1 Analysis and Assignments for Untreated Wool

Raman spectroscopy provides similar vibrational information to infrared spectroscopy but in addition it gives strong bands for non-polar functional groups and symmetric vibrations of aromatic groups which are infrared inactive. The advantage of Raman spectroscopy for studies on wool is that it is non-destructive and it produces strong bands for non-polar functional groups and aromatic structures such as the amino acids tryptophan, tyrosine and phenylalanine. The nature of sulphur bonding can be investigated since bands have been assigned to S-S and C-S vibrations of cystine. Information on secondary structure is provided by Amide I and Amide III vibrations, and the C-C skeletal stretch which is inactive in infrared

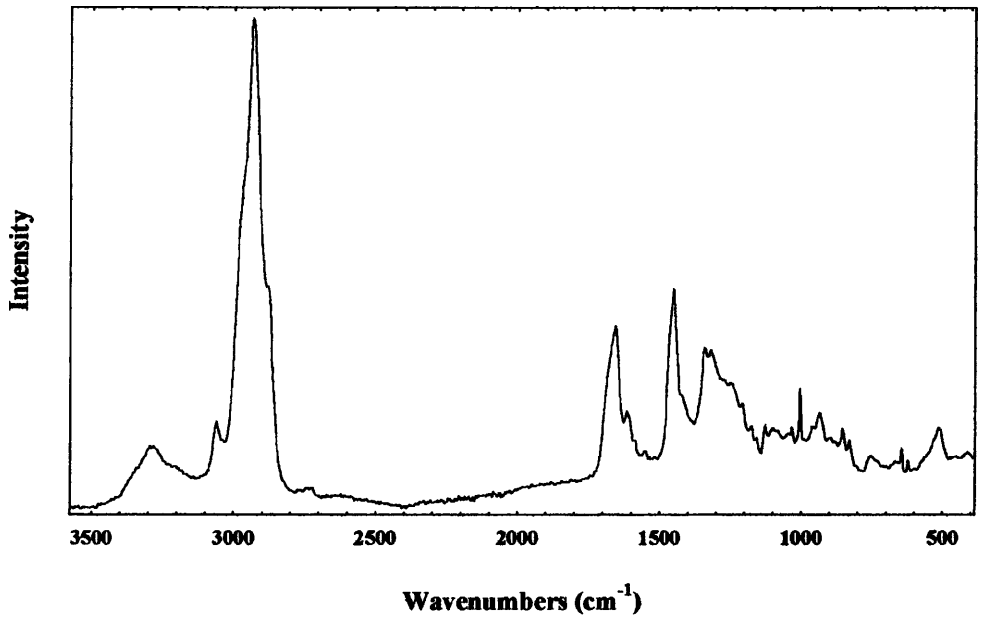

Figure 7.1 FT-Raman spectrum of untreated wool

spectroscopy. In Figure 7.1 the FT-Raman spectrum of untreated wool is shown and in Figure 7.2 the region below 1800 cm^{-1} is shown in greater detail with bands of interest annotated. Table 7.1 gives the full list of band assignments for wool according to the work of Lin and Koenig[156], with additional assignments given by Carter *et al*[151]. The secondary structure of proteins can be determined from the frequencies and intensities of the Amide I and Amide III modes which are sensitive to molecular conformation and the nature of hydrogen bonding of the peptide backbone[190].

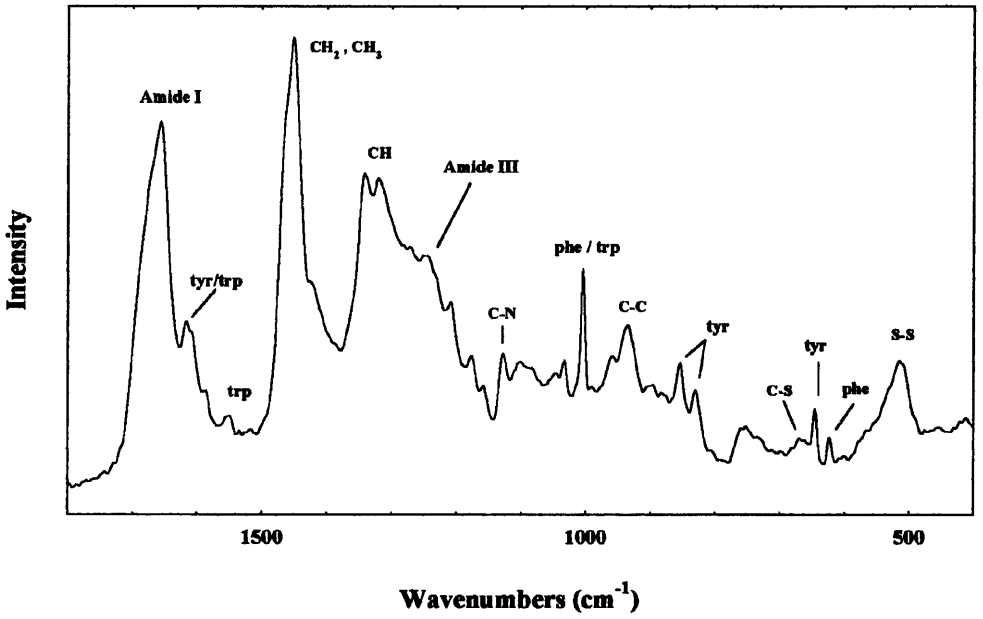

Figure 7.2 FT-Raman spectrum of untreated wool

Table 7.1 Raman spectral band assignments for wool

Raman Band Wavenumbers (cm^{-1})	Literature Value	Assignment [Lin & Koenig[156]]
514 m	512 m	Cystine S-S stretch
622 w	619 vw	Phenylalanine
645 w	644 w	Tyrosine
669 vw	665 vw	Cystine C-S stretch
752 w br	752 w br	Tryptophan
830 m	835 m	Tyrosine
853 m	852 m	Tyrosine
882 vw	881 vw	Tryptophan [151]
896 vw	897 vw	C-C skeletal stretch α-helix [151]
904 vw	905 w	C-C skeletal stretch α-helix [151]
934 m	935 m	C-C skeletal stretch, α-helix, C-C side chain
958 w	959 w	CH_2 rock
1004 s	1006 s	Phenylalanine, Tryptophan
1032 w	1034 w	Phenylalanine
1082 vw	1079 w	C-N stretch [151]
1100 vw br	1098 w br	C-N stretch
1127 w	1126 w	C-N stretch [151]
1158 vw	1155 vw sh	C-N stretch [151]
1176 w	1180 w	Tyrosine
1208 w	1209 m	Tyrosine, Phenylalanine
1245 w br	1245 m br	C-N-H bend: Amide III disordered
1271 vw	1259, 1281 w	Amide III α- helical crystalline [151]
1319 s	1316 s	Cα-H bend
1341 s	1340 s	C-H bend, Tryptophan
1450 vs	1450 vs	CH_2, CH_3 bending modes
1552 w	1558 vw	Tryptophan
1616 w	1615 m	Tyrosine, Tryptophan
1656 vs	1658 vs	C=O stretch, C-N-H bend: Amide I α–helix
2849 vw sh	2848 w sh	CH_2 symmetric stretch [151]
2880 s	2880 s	CH_3 symmetric stretch [151]
2933 vs	2931 vs	CH_2 asymmetric stretch [151]
2972 s sh	2975 s sh	CH_3 asymmetric stretch [151]
3062 m	3062 s	Amide B C-N-H bend overtone [151]
3290 m br	3302 s br	Amide A N-H stretch [151]
vs very strong s strong m medium w weak vw very weak br broad sh shoulder		

Review of Raman analysis of proteins[157]

The α-helical conformation appears between 1645 - 1656 cm^{-1}, the antiparallel β sheet and random coil conformations occur at higher wavenumbers in the region between 1665-1675 cm^{-1}. In wool the Amide I band at 1656 cm^{-1} is consistent with the high α–helical chain conformation of wool. However the broad asymmetric contour of this band also indicates the presence of other secondary structures in untreated wool. The broad and weak Amide III band at 1245 cm^{-1} is assigned to the disordered or random coil structure. It has been proposed that the absence of intensity at this band reflects a high α–helical content[191]. The Amide III vibration associated with α-helical structure has been found to have considerable variation of position for proteins in the region between 1258 cm^{-1} to 1289 cm^{-1}, but is usually very weak. In this work a weak feature is present at 1271 cm^{-1} . The intensity of the C-C skeletal stretching band at 935 cm^{-1} also reflects α–helical content, since it has been found to decrease in intensity on transition to random coil or β-sheet conformation. In untreated wool this band is present and is of medium intensity, reflecting the α–helical structure.

The S-S stretching vibrations occur over the region between 500 -550 cm^{-1}. In untreated wool the intensity of this band, with a maximum at 514 cm^{-1} , is attributed to the high disulphide bond content associated with cystine residues. The frequency of the S-S vibrations is known to be sensitive to the rotational conformation of the S-S linkage [192] [193] : gauche-gauche 510 cm^{-1}, gauche-trans 525 cm^{-1} and trans-trans 540 cm^{-1} . The broad asymmetric nature of this band in untreated wool reflects a broad distribution of disulphide bond conformations.

The Raman spectrum of wool has a band associated with the ring structures of the aromatic amino acids tryptophan, tyrosine and phenylalanine. In proteins, the frequency and intensities of those bands assigned to tryptophan and tyrosine are known to be sensitive to conformation and the local chemical environments of these residues. The doublet at 830 cm^{-1} and 854 cm^{-1} is assigned to tyrosine residues and arises due to Fermi resonance between the symmetric ring breathing vibration and the overtone of an out of plane ring bending vibration of the benzene ring. The relative intensities of both components of this doublet are sensitive to the local environment of tyrosine residues[194]. The intensity ratio of the 830 cm^{-1} and 854 cm^{-1} components is sensitive to the nature of hydrogen bonding of the phenolic hydroxyl groups. If the peak at 854 cm^{-1} is higher in intensity than the peak at 830 cm^{-1} then tyrosine residues are 'exposed' in hydrophilic regions and accessible for reaction. If this intensity ratio is reversed then the residues are 'buried' within the protein in hydrophobic regions. An intensity ratio of 2.5 (854 / 830) indicates that the hydroxyl group is the acceptor of strong hydrogen bonding

from a positive donor group. A ratio of 0.3 indicates the hydroxyl group is the donor of a strong hydrogen bond to a negative acceptor group. In accordance with this, the wool used in this investigation had exposed tyrosine residues. An intensity ratio of 1.4 (854 / 830) has been proposed for completely exposed tyrosine residues[195]. The mean relative intensity ratio found in this study was 1.3 ±0.1 calculated from measurements made on twenty spectra of untreated wool.

It was anticipated that using Raman spectroscopy the photooxidation of tryptophan could be followed using assigned bands which appear at 752 cm^{-1} , 882 cm^{-1} , 1004 cm^{-1} , 1341 cm^{-1} , 1552 cm^{-1} and 1616 cm^{-1} . In wool these bands are weak or share a joint assignment with phenylalanine or tyrosine making analysis difficult. Unfortunately, a number of these bands are sensitive to the orientation and environment of tryptophan residues. The frequency of the band near 1550 cm^{-1} is sensitive to the orientation of the indole ring relative to the α-carbon atom of the peptide backbone[196]. The intensity of the 1341 cm^{-1} band increases as the environment surrounding the indole ring becomes more hydrophobic[197]. The frequency of the band around 880 cm^{-1} decreases with an increase in the strength of hydrogen bonding to the NH group of the indole ring[197].

The strong band at 1004 cm^{-1} is assigned to the (C-C) stretching vibration of the indole ring of tryptophan and the phenyl ring of phenylalanine, however it is unclear what proportion of this signal can be attributed to tryptophan residues. Therefore, the Raman spectra of both amino

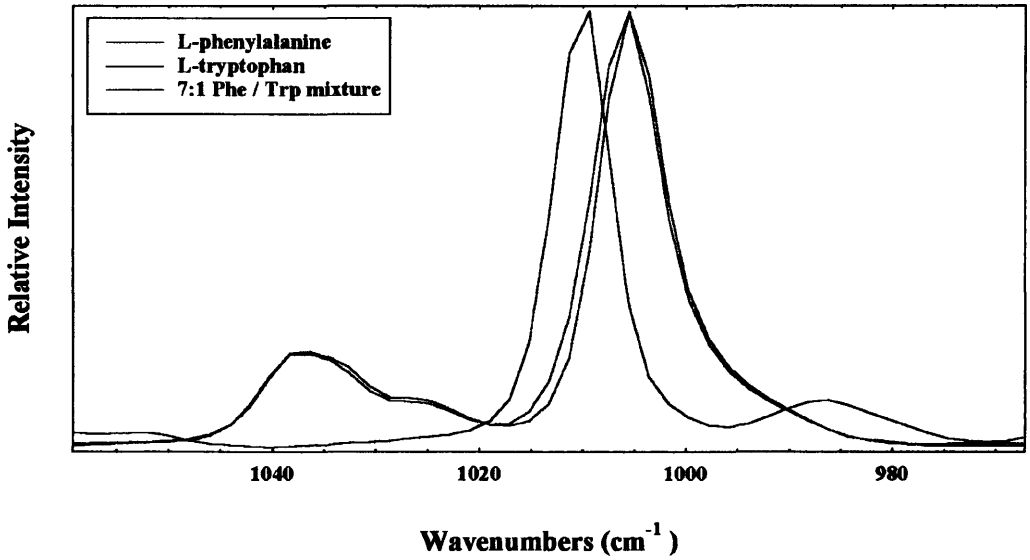

Figure 7.3 Comparison of the FT-Raman spectra of L-tryptophan, L-phenylalanine and a mixture typical of their relative concentrations in wool

acids in solid form were acquired in order to investigate the nature of this band. A mixture of L-phenylalanine / L-tryptophan was prepared using a ratio of 7:1 typical of wool. Figure 7.3 compares this mixture spectrum to the spectra of the individual amino acid components. The peak maximum for L-tryptophan occurs at 1009.6 cm^{-1} compared to 1005.6 cm^{-1} for L-phenylalanine. The mixture spectrum is nearly identical to that of L-phenylalanine, the tryptophan signal at 1009.6 cm^{-1} is too weak to be observed in comparison to the strong signal at 1005.7 cm^{-1} for phenylalanine. Therefore, due to the much higher concentration of phenylalanine relative to tryptophan in wool, this band can mainly be attributed to phenylalanine residues, it has little analytical value for tryptophan residues in wool.

Since wool contains a low concentration of tryptophan relative to the concentration of tyrosine and phenylalanine, the signal intensities of all bands assigned to tryptophan are weak. The protein lysozyme which contains a higher concentration of tryptophan has particularly strong bands as shown in Figure 7.4 in which the spectra of lysozyme and wool are compared. In the Raman spectrum of lysozyme, two bands at 1004 cm^{-1} and 1011 cm^{-1} for phenylalanine and tryptophan respectively are clearly resolved. Other strong bands for tryptophan in lysozyme appear only weakly in the wool spectrum.

The lysozyme spectrum shows other differences in comparison to wool. The Amide I frequency is shifted to 1661.5 cm^{-1} and there is an increase in intensity in the Amide III region between 1240 cm^{-1} - 1270 cm^{-1} assigned to disordered or random coil structure. The intensity

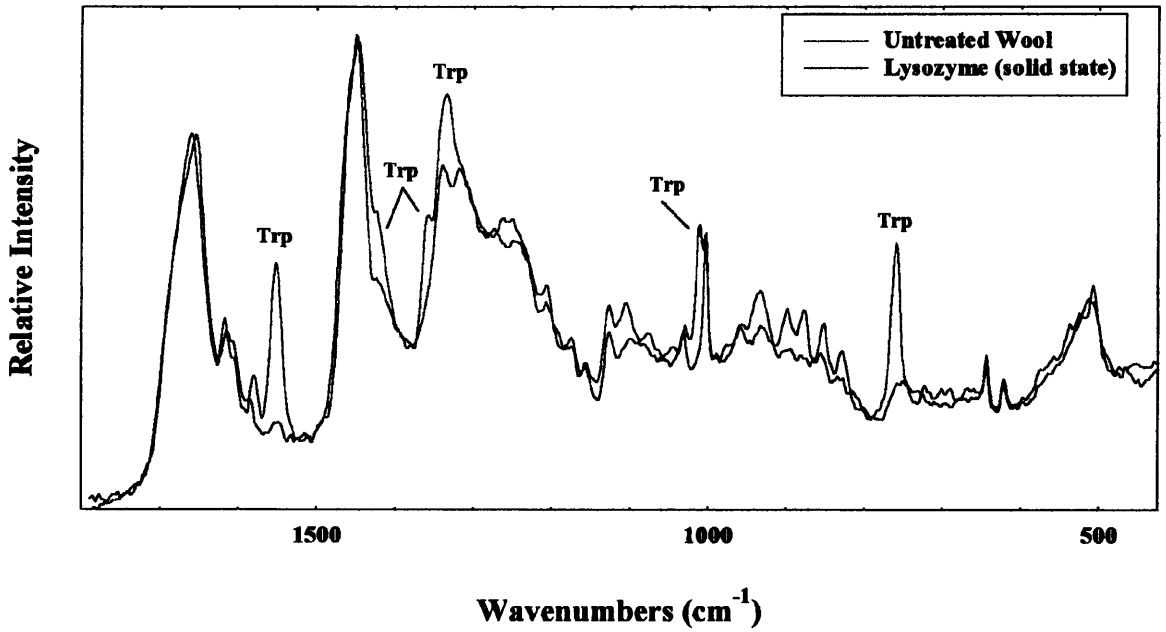

Figure 7.4 Comparison of the FT-Raman spectra of wool and lysozyme

of the band at 934 cm^{-1} is considerably lower in lysozyme. The differences in these structurally sensitive bands reflect the lower α-helical content and more random conformation of lysozyme.

7.2.2 FT-Raman Analysis of Photooxidised Wool

The FT-Raman spectra of wool fabrics after increasing Xenotest cycles were collected in order to investigate photooxidative changes to the protein structure and the photosensitive amino acid residues. In order to compare the change in band intensities after exposure all spectra were normalised against the same peak intensity of the strong CH_2 band at 2930 cm^{-1}.

Figure 7.5 compares the spectra of unexposed untreated wool to that after 208 hours Xenotest exposure. The spectra are overlaid on a common scale. The band at 514 cm^{-1}, assigned to the disulphide bond vibration of cystine, gradually decreases in intensity with increasing exposure time. A general indication of the rate of decrease in this band was obtained by measuring the change in peak intensity using spectra collected at each exposure level. Peak height measurement was carried out using a sloped linear baseline from 650 cm^{-1} to 450 cm^{-1}. The mean peak intensity at each exposure time was calculated from measurements made on ten spectra collected at each exposure time. The mean peak intensity as a function of exposure

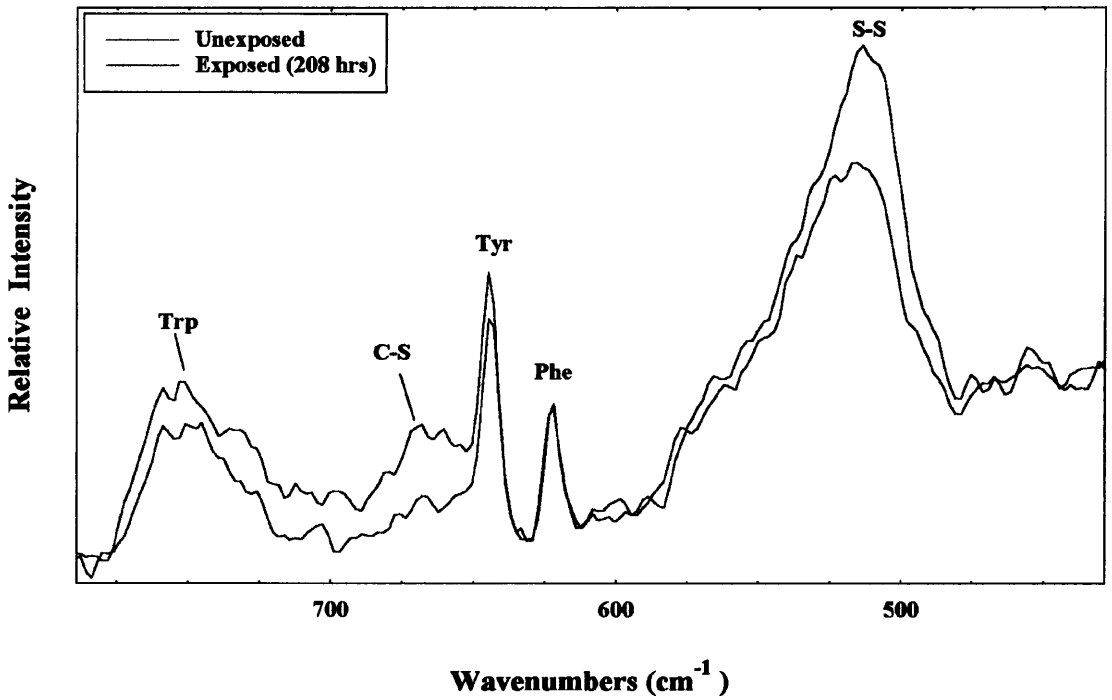

Figure 7.5 Change in FT-Raman spectrum of untreated wool following light exposure

time is shown in Table 7.2 for untreated and Cibafast W treated wool. For untreated wool the peak intensity has reduced by almost 30% after 208 hours exposure, but the most rapid reduction in signal intensity occurs after 52 hours exposure. Cibafast W treated wool shows a comparatively slower reduction in S-S signal intensity at each exposure level as shown in Table 7.2. The benefit of applying Cibafast W is shown for exposure times up to 104 hours. There is a reduction in S-S intensity of 19% for the untreated fabric compared to 6% for Cibafast W treated wool. This indicates that significant protection is given to the disulphide bonds in the bulk of the fibre by the application of the UV absorber, particularly at low exposure levels.

Table 7.2 Change in disulphide signal intensity at 514 cm^{-1} as a function of exposure time

Xenotest Exposure (hours)	Untreated Wool		Cibafast W Treated Wool	
	Signal Intensity[1] Mean	CV%	Signal Intensity[1] Mean	CV%
0	0.68	7.4	0.67	9.7
52	0.57	12.3	0.64	9
104	0.55	7.3	0.63	8.9
156	0.5	10	0.55	4
208	0.49	8.2	0.55	7.6
1. Normalised against a CH_2 (2930 cm^{-1}) peak intensity of 10.0 (arbitrary units)				

Other workers have noted a distinct shift in peak maximum of the disulphide band after hydrogen peroxide bleaching of wool attributed to a change in conformation associated with structural rearrangements as a result of some disulphide bond rupture[158]. The broad nature of this band makes it difficult to measure precisely the shift in wavenumber position of this band. Examination of all the spectra collected at each exposure period for untreated wool did show a general peak shift trend towards higher wavenumbers with increasing exposure time, to the region of 520 cm^{-1} after 208 hours.

The broad, weak band at 669 cm^{-1} is assigned to the C-S stretching vibration of cystine. Figure 7.5 shows that there is a reduction in intensity of this band after exposure. This may indicate cystine photooxidation pathways involving both S-S and C-S scission. Previous work using chemical analysis to investigate the photodegradation of model disulphides found that S-S scission occurs preferentially at the expense of C-S scission, however, prolonged irradiation caused significant C-S scission. Figure 7.6 shows other evidence for cystine photooxidation. There is an increase in signal intensity at 1040 cm^{-1} after light exposure which can be assigned

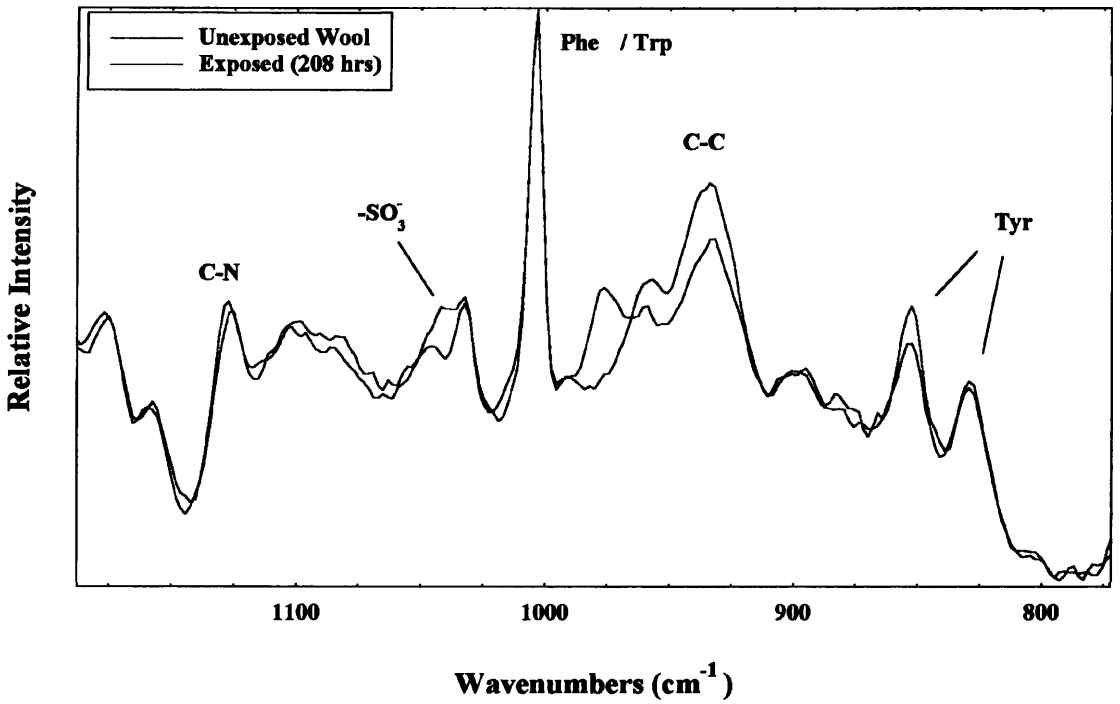

Figure 7.6 Change in FT-Raman spectrum of untreated wool following light exposure

to the S-O vibration of cysteic acid.

Figure 7.5 also shows the sharp bands at 622 cm^{-1} and 645 cm^{-1} which have been assigned by Lin and Koenig to phenylalanine and tyrosine respectively. Some workers have assigned these bands to the C-S vibration of cystine[158] [159], but from Raman spectra collected of L-phenylalanine and L-tyrosine, sharp bands associated with the ring structures of these amino acids appear at these respective wavenumbers. The band at 622 cm^{-1} for phenylalanine appears unchanged in intensity after light exposure, however there is a reduction in the band at 645 cm^{-1} assigned to tyrosine. The broad nature of the band assigned to tryptophan around 752 cm^{-1} makes it difficult to establish any reduction in intensity after exposure.

Figure 7.6 shows the overlaid spectra of unexposed and exposed fabrics between 800 cm^{-1} and 1200 cm^{-1}. The tyrosine doublet at 830 cm^{-1} and 853 cm^{-1} has a relative intensity change after light exposure, the component at 853 cm^{-1} reduces in intensity relative to that at 830 cm^{-1}. After 208 hours the 854 / 830 ratio reduces to a mean value of 1.05 ± 0.08 compared to 1.31 for unexposed wool. The reductions in signal intensity of bands associated with tyrosine residues at both 853 cm^{-1} and 645 cm^{-1}, may reflect the photodegradation of tyrosine residues. There were no significant reductions in the intensities of these bands at exposure times less than 156 hours. Previous work using amino acid analysis has detected a reduction in tyrosine

content of Xenotest exposed wool[85]. However, Raman studies of proteins have attributed intensity changes of the tyrosine bands at 853 cm^{-1} and 645 cm^{-1} relative to the band at 830 cm^{-1} to an alteration in the nature of the local chemical environment of tyrosine residues. These relative intensity changes in exposed wool suggest that there is an increase in tyrosine residues in more hydrophobic environments. This could be attributed to structural rearrangements which have caused a perturbation of tyrosine residues, or possibly a reduction in the concentration of 'exposed' tyrosine residues in regions more accessible to photooxidation.

The sharp signal at 1004 cm^{-1} found to be attributed predominantly to phenylalanine in wool shows no significant decrease in intensity as a result of light exposure. Other bands assigned phenylalanine at 622 cm^{-1} and 1032 cm^{-1} show no reduction in peak intensity with exposure.

Figure 7.6 also shows a clear reduction in signal intensity at 934 cm^{-1} after light exposure. This band is conformationally sensitive being assigned to the C-C stretching of the α–helical backbone, but is thought to contain a contribution from side chain C-C stretching[157]. A reduction in intensity of this band has previously been attributed to a reduction in α-helical content of fibres due to a transition to random coil or β-sheet conformations. Other studies have found a reduction in the helical content of weathered wool[198] which is thought to be related to the extent of disulphide bond cleavage[199].

There is also an increase in intensity at 977 cm^{-1} to give a new band not present in unexposed wool. This band appeared after 52 hours exposure and gradually increased in intensity with increasing exposure time . The infrared spectrum of exposed wool also showed the appearance of a weak band at this wavenumber (see section 7.3.2). This band has not previously been assigned for wool or related proteins and therefore the nature of the species responsible is at present unclear. It appears in the region associated with C-C stretching and CH_2 rocking vibrations, it may reflect changes in structural conformation implicated by the reductions in bands associated with disulphide bonding and C-C stretching of the α-helical backbone. The large and distinct increase in intensity of this band means that the nature of the species responsible is of particular interest, it reflects a significant change in bulk fibre chemistry of wool.

In Figure 7.7 the spectra of unexposed and exposed wool are compared in the region containing bands associated with the Amide group. As discussed in section 3.2.1, it is thought

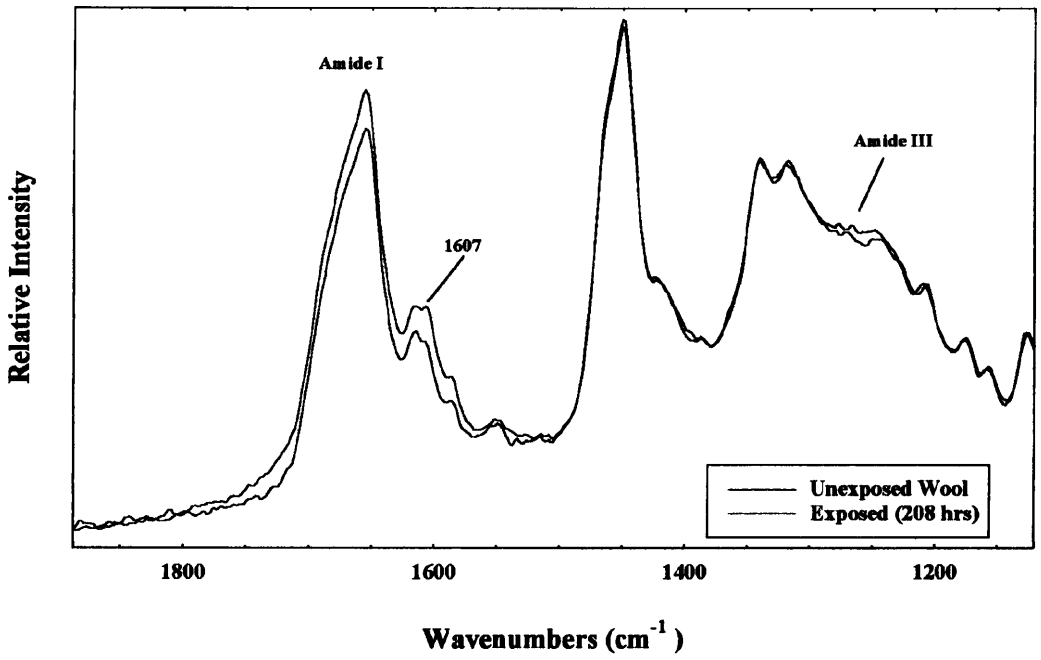

Figure 7.7 Change in FT-Raman spectrum of untreated wool following light exposure

that main chain cleavage must accompany the reductions in disulphide bonding on exposure of wool to light in order to account for the large decreases in tensile properties. Peptide bond scission is not thought to occur, accordingly there was no significant reduction in the Amide I band at 1658 cm^{-1} . Protein chain scission is thought to take place at C-N bonds to give primary amide terminated and α ketoacyl peptides. The Amide I band showed an increase in intensity in the C=O functional region between 1700 cm^{-1} and 1800 cm^{-1} which may reflect an increase in main chain carbonyl group content. The C-N bond vibrations in the Raman spectrum of wool have been assigned to a number of bands around 1100 cm^{-1} (see Table 7.1). After light exposure no significant changes in intensity of these bands was found, Figure 7.6. Figure 7.7 shows a small increase in intensity in the Amide III region around 1240-1250 cm^{-1}. This may reflect an increase in disordered protein chain conformation, implicated by the reduction in signal intensity at 934 cm^{-1} associated with C-C stretching of the α- helix.

One other notable change in the FT-Raman spectrum of exposed wool is an increase in signal intensity at 1607 cm^{-1} adjacent to the tyrosine band at 1616 cm^{-1} . This band progressively increased in intensity with increasing exposure time but no previous assignment could be found for wool or related proteins. This band may also be associated with tyrosine residues, however a band at this wavenumber was found only in the spectrum of L-phenylalanine.

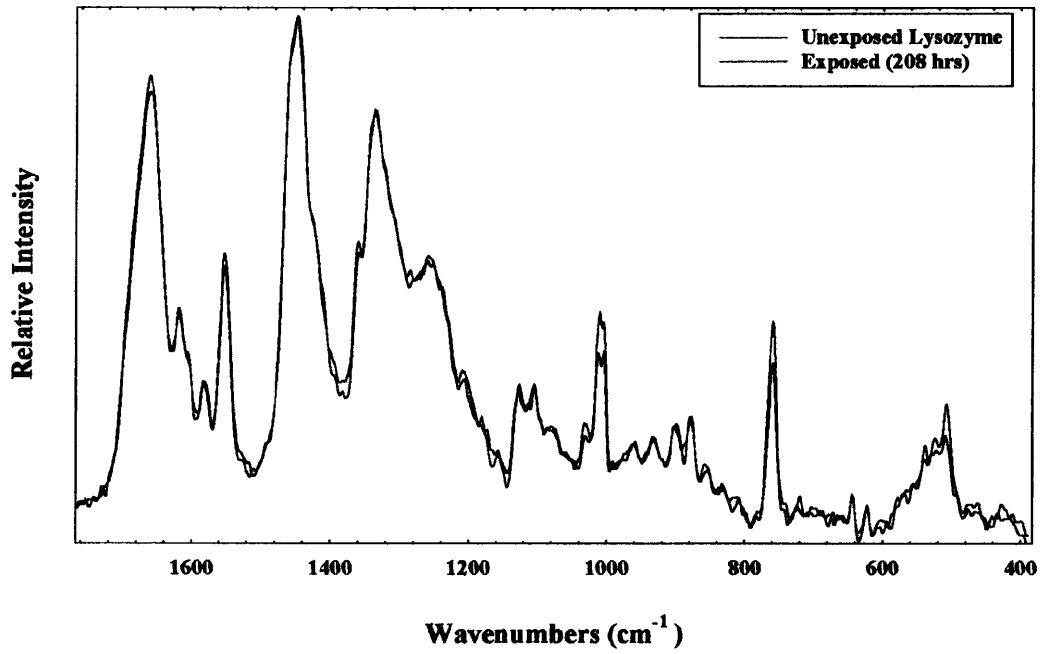

Figure 7.8 Effect of light exposure on FT-Raman Spectrum of lysozyme

To investigate the effect of light exposure on Raman bands assigned to tryptophan the spectrum of lysozyme was collected after 208 hours exposure (normalised against 2930 cm^{-1}). Figure 7.8 compares the spectra of unexposed and exposed lysozyme. Photodegradation was indicated by the yellowing of lysozyme after exposure and the reduction in the intensity of the disulphide band at 509 cm-1. There are reductions in intensity of the tryptophan bands at 1011 and 760 cm^{-1} compared to the band at 1554 cm^{-1}. L-tryptophan was also exposed for 208 hours in the Xenotest and similar changes in relative band intensities were found. There were reductions in intensity of the strong bands at 1011 and 760 cm^{-1} relative to those at 1557 cm^{-1}, 1424 cm^{-1} and 1358 cm^{-1}. These bands may therefore be diagnostic of changes to the structure of tryptophan as a result of light exposure, in particular indole ring photooxidation.

7. 3 FT-IR Analysis of Wool

7.3.1 Analysis and Assignments for Untreated Wool

The alterations to the surface chemistry of wool after light exposure have been investigated using FT-IR spectroscopy. The technique is particularly useful for the analysis of the oxidation products of cystine. Attenuated Total Reflectance (ATR) spectroscopy was used for the surface analysis of wool using fabric samples. Microspectroscopy was used to collect transmission spectra of whole wool fibres providing information on the rate of bulk chemical

changes. The protective effect of Cibafast W in retarding the rate of cystine photooxidation was assessed both in the wool surface and fibre bulk. A number of other notable changes in the FT-IR spectra of photooxidised wool were observed some of which may be associated with main chain cleavage and conformational changes.

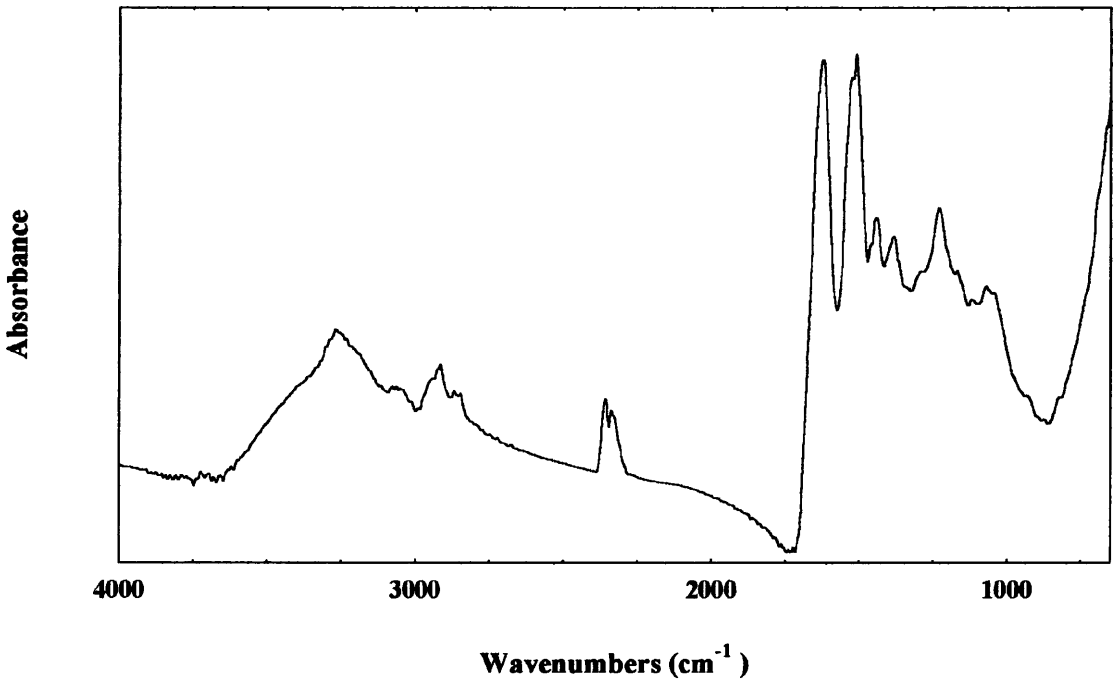

Figure 7.9 FT-IR (ATR) spectrum of unexposed untreated wool

Table 7.3 Infrared band assignments for wool[200]

Frequency cm^{-1}	Assignment
3300	N-H (s) secondary amides O-H (s) hydrogen bonded (broad)
3080	Amide II overtone
2964	CH_3 (as)
2935	CH_2 (as)
2877	CH_3 (ss)
2853	CH_2 (ss)
1627	Amide I C=O (s), C-N (s), C-C-N (d)
1520	Amide II N-H (ib), C-N (s), C-C (s)
1446	C-H (d) CH_2 CH_3
1387	CH_3 symm def.
1233	Amide III N-H (ib), C-N (s)
(s) stretch (as) asymmetric stretch (ss) symmetric stretch (d) deformation (ib) in phase bend	

Table 7.4 Infrared band assignments for the oxidation products of cystine in wool[147 - 149, 152, 153]

Species		Frequency (cm^{-1})
Cysteine-S-sulphonate (Bunte salt)	$R—S—SO_3^-$	1022 ss 1190 as
Cysteic acid	$R—SO_3^-$	1040 ss 1175 as
Cystine-S-monoxide	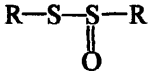	1060 ss + 1075 ss -
Cystine-S-dioxide	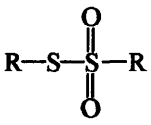	1120 ss

The ATR absorbance spectrum of untreated unexposed wool is shown in Figure 7.10. The main band assignments are given in Table 7.3. The features of the infrared spectrum of interest in studying the photodegradation of wool are the bands assigned to the S-O stretching vibrations in the region 1200 -1000 cm^{-1}. Table 7.4 lists those cystine oxidation products for which the infrared assignments are known. Figure 7.10 shows the ATR absorbance spectrum of untreated unexposed wool in the S-O stretching region. The broad nature of the spectrum makes it difficult to assess intensity changes in bands associated with oxidised cystine species.

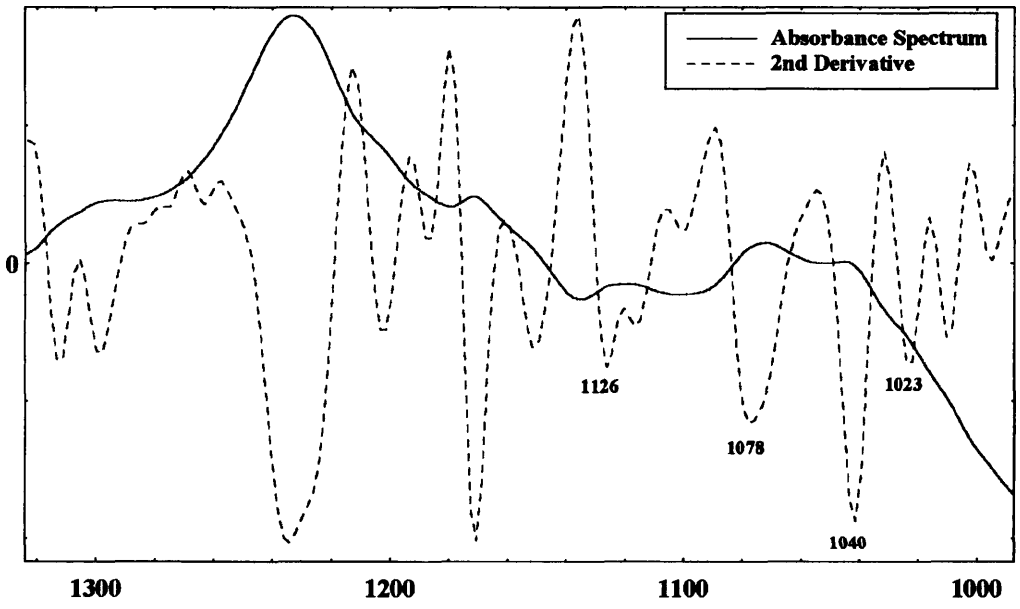

Figure 7.11 FT-IR absorbance and second derivative spectra of unexposed untreated wool

However, as discussed in section 4.6.1.4, second derivative spectroscopy allows bands associated with the oxidation products of cystine to be resolved. In Figure 7.10 the second derivative absorbance spectrum is superimposed on the original absorbance spectrum of wool. The inverted second derivative peaks correspond to the shoulders present in the original absorbance spectrum. Using this technique it is therefore possible to resolve the overlapping bands which represent absorptions due to cysteic acid, cystine-S-monoxide, cystine-S-dioxide and Bunte salt.

7.3.2 Rate of Cystine Photooxidation in Untreated Wool

Untreated wool fabric samples were exposed for successive Xenotest cycles and the exposed surface was analysed using the ATR attachment as described in section 4.6.1. This allows surface analysis of wool to a depth of 2.5 - 2.0 μm in the S-O stretching region between 1000 cm^{-1} - 1200 cm^{-1} . Three samples were analysed for each period of exposure. In order to compare band intensities spectral normalisation was necessary. All absorbance spectra were normalised against the strong Amide I band intensity before taking the second derivative. The between sample coefficients of variation for the second derivative band intensities of the oxidised cystine species using this method are given in section 4.6.1.1.

For bulk analysis, single wool fibres were analysed in transmission mode using Microspectroscopy as described in section 4.6.1.2. Analysis was carried out in the central portion of each fibre in order to avoid the more highly oxidised fibre tips, as discussed in section 4.6.1.2. Three fibres were analysed for each exposure period. Spectral normalisation was carried out using the Amide I band intensity. Section 4.6.1.2 also gives the between fibre coefficients of variation for the second derivative band intensities of the oxidised cystine species.

Figure 7.12 compares the ATR absorbance spectra for untreated wool before and after exposure. After 208 hours Xenotest exposure, the wool surface shows a broad increase in absorbance over the entire S-O stretching region between 1200 -1000 cm^{-1} due to increases in cystine oxidation products. The most prominent change is a sharp increase in absorbance at 1039 cm^{-1} attributed to the formation of cysteic acid. In Figure 7.13 the second derivative absorbance spectrum for unexposed wool is compared to that after 208 hours exposure. The second derivative spectrum gives a sharp and intense band for cysteic acid at 1039 cm^{-1} . The intensity of this band increased with increasing exposure time making it a useful index of the

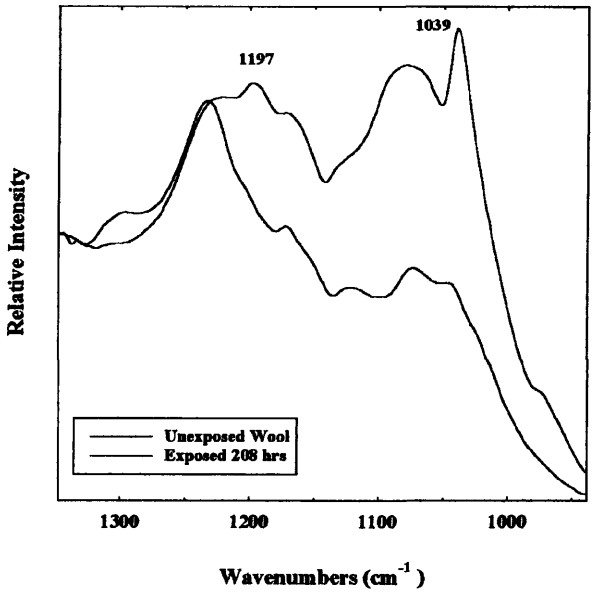

Figure 7.12 Change in FT-IR (ATR) absorbance spectrum of untreated wool after light exposure

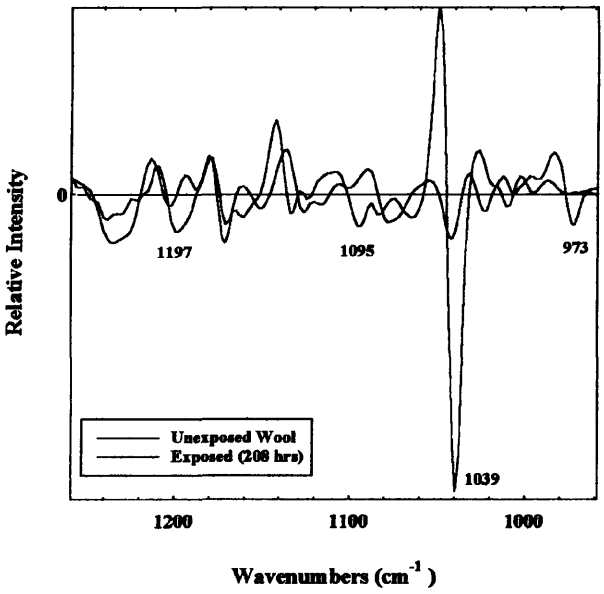

Figure 7.13 FT-IR (ATR) second derivative spectra of untreated wool

rate of cystine photooxidation. The peak height at 1039 cm^{-1} from the zero baseline was measured at each exposure level from the ATR spectra. The increase in second derivative band intensity as a function of exposure time for the wool surface is shown in Figure 7.14. The rate of increase in cysteic acid is particularly rapid between 26 and 156 hours exposure, with a near linear increase in signal intensity. The rate of increase in cysteic acid is slower after exposure for more than 156 hours which may indicate that the fabric surface reaches a

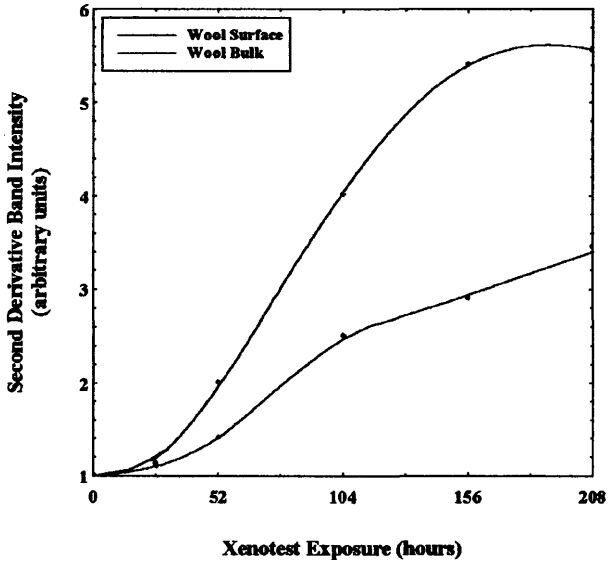

Figure 7.14 Rate of change in cysteic acid signal intensity for wool surface and fibre bulk

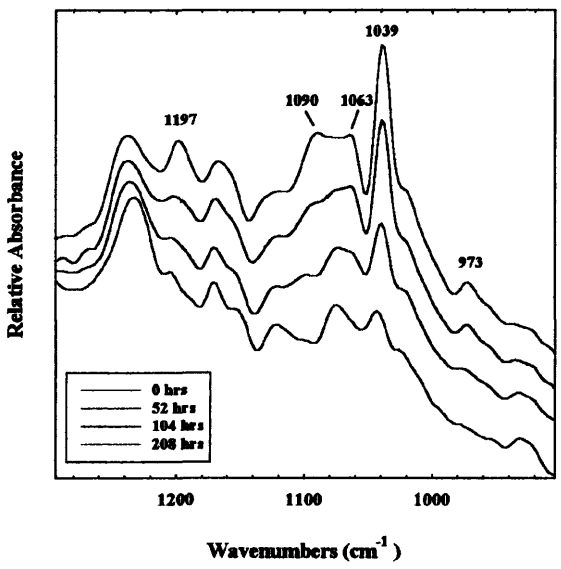

Figure 7.15 Fourier Self Deconvoluted absorbance spectra of untreated wool

maximum level of oxidation. Further oxidation may be restricted by limiting factors such as the accessibility of cystine residues in the wool cuticle.

Single wool fibres were analysed in order to investigate the rate of cystine oxidation throughout the whole fibre bulk. It is not possible to compare absolute peak intensities between the transmission spectra of the whole fibre and the ATR spectra of the wool fabric surface. However, the rate of change in second derivative peak intensity for cysteic acid was compared for the bulk and surface, shown in Figure 7.15. The rate of increase in cysteic acid signal with exposure in the surface of wool (up to a depth of approximately 2.5 μm) is approximately twice the rate for the fibre as a whole.

Figure 7.12 shows that apart from the increase in cysteic acid signal, there are other notable changes in the surface ATR spectrum of untreated wool after exposure. The increase in S-O absorbance in this region can be attributed to the presence of intermediate cystine oxidation products. There is a broad increase in intensity between 1100 cm^{-1} - 1070 cm^{-1} and a sharp increase in intensity at 1197 cm^{-1}. There was an increase in intensity of a shoulder around 973 cm^{-1}, similar to the pronounced FT-Raman band found in photooxidised wool. These spectral changes increased progressively with successive exposure periods up to 208 hours.

The second derivative spectrum, Figure 7.13, resolves these features but does not reflect the large increase in intensity of these signals relative to the cysteic acid signal. As discussed in Section 4.6.1.4, a limitation of derivative spectroscopy is that the amplitude of the peaks in the derivative spectrum is a function of the widths of the original peaks. This leads to a strong bias in favour of sharp features present in the peak envelope, for example the sharp and intense band for cysteic acid at 1039 cm^{-1} shown in Figure 7.13. However, the derivative spectrum does not reflect the broader increases in intensity in the region around 1090 cm^{-1}. For this reason the technique of Fourier Self Deconvolution is gaining increasing popularity over derivative spectroscopy for the separation of overlapping infrared bands[201] [202]. Fourier Self Deconvolution mathematically enhances spectral resolution by reprocessing the interferogram using a resolution enhancement factor. Figure 7.15 shows the Fourier Self Deconvoluted ATR spectra for untreated wool after successive Xenotest cycles. Constant deconvolution parameters were used for each spectrum, a resolution enhancement factor of 1.5 and bandwidth of 18.

The deconvoluted spectra resolve a number of bands in the S-O stretching region, some of which can be assigned by their frequencies in Table 7.4 to intermediate oxidation products or

cystine. The main changes in this region after exposure, apart from the increase in cysteic acid, are the progressive increases in signals at 1063 cm^{-1} , 1090 cm^{-1} and 1197 cm^{-1}. In unexposed wool the cystine-S-monoxide signal is clearly resolved at 1075 cm^{-1} but it is obscured in exposed wool by signals at 1063 cm^{-1} and 1090 cm^{-1} . An increase in signal intensity at 1090 cm^{-1} has previously been found in weathered wool, this was assigned to cysteine sulphinic acid ($-SO_2H$) [148] . The same workers assigned the absorbance around 1060 cm^{-1} to cysteine sulphenic acid (-SOH). However, most studies now assign the band at 1060 cm^{-1} to the α-isomer of cystine-S-monoxide, with the β-isomer at 1078 cm^{-1} [153], according to the work of Savige *et al* [149]. No assignment could be found for the increase in absorbance at 1197 cm^{-1} in exposed wool. However in the study of weathered wool, the band at 1175 cm^{-1} (assigned to S-O asymmetric stretching of cysteic acid) had split into two features at 1161 cm^{-1} and 1089 cm^{-1} after weathering. No interpretation was given. This may be similar to the increase in intensities at 1197 cm^{-1} and around 1160 cm^{-1} after 208 hours Xenotest exposure. Figure 7.15 also shows a decrease in intensity of the cystine-S-dioxide signal at 1126 cm^{-1}. The increase in intensity of the band at 973 cm^{-1} is also clearly shown.

Other studies of oxidised wool have used second derivative analysis to investigate the rate of change in the intermediate oxidation products cystine-S-monoxide, cystine-S-dioxide and Bunte Salt. Table 7.5 shows the rate of change in second derivative peak heights for these species. The signal at 1023.3 cm^{-1} assigned to Bunte salt reduces in intensity after exposure for more than 26 hours. The peak maximum shifts to 1018.5 cm^{-1} after 52 hours and to 1016.7 cm^{-1} after 208 hours. The signal at 1126.4 cm^{-1} for cystine -S-dioxide decreases with exposure time and the peak maximum gradually shifts to 1122.7 cm^{-1} after 208 hours. The cystine -S-monoxide signal at 1078 cm^{-1} decreases after exposure for more than 26 hours. This is accompanied by a progressive increase in the other cystine -S-monoxide isomer signal at 1063.8 cm^{-1}. This may suggest differences between the photostability of the stereoisomeric forms of cystine-S-monoxide.

In the spectra of single unexposed wool fibres, the absorbance intensities of the partially oxidised species were much higher relative to the cysteic acid intensity than found for the ATR spectra of the surface. This indicates lower concentrations of partially oxidised cystine residues, relative to the concentration of cysteic acid, in the fibre surface compared to whole fibre. For the fibre bulk, the second derivative band intensities for these partially oxidised species reduced with increasing exposure time , as found for the fibre surface.

Table 7.5 Effect of light exposure on signal intensities of partially oxidised cystine species from ATR analysis of untreated wool fabric surface

Xenotest Exposure (hours)	Second Derivative Band Intensities (arbitrary units)[1]			
	Bunte Salt 1023.3 cm^{-1}	Cystine-S-monoxide 1078.3 cm^{-1}	1063.8 cm^{-1}	Cystine-S-dioxide 1126.4 cm^{-1}
0	0.41	0.6	0	0.44
26	0.44	0.63	0.17	0.37
52	0.29	0.5	0.25	0.29
104	0.16	0.31	0.46	0.3
156	0.25	0.21	0.53	0.31
208	0.13	0	0.53	0.05
1. Values relative to a second derivative peak intensity of 1 for cysteic acid in unexposed wool.				

7.3.3 Protective Effect of Cibafast W on Rate of Cystine Photooxidation

Undyed fabric treated with Cibafast W, dyed fabric and dyed fabric treated with Cibafast W were also examined after successive Xenotest cycles using FT-IR (ATR). The rate of increase in second derivative band intensity for cysteic acid was measured for each of these fabrics. This allowed an investigation of the level of protection given by the UV absorber to surface photooxidation. Figure 7.16 compares the rate of increase in cysteic acid signal for untreated wool, Cibafast W treated wool, dyed wool and dyed wool treated with Cibafast W. The addition of Cibafast W to undyed wool significantly reduces the rate of increase in cysteic acid signal. This rate is reduced by approximately 50% above 52 hours exposure. Dyed wool shows a slower rate of increase in cysteic acid signal compared to undyed wool. The application of Cibafast W further reduces the rate of increase in cysteic acid but only to the same level as the undyed absorber treated fabric. Cibafast W gives protection to cystine oxidation in both undyed and dyed wool. These results reflect other work investigating the protective effect of various classes of UV absorber on the rate of phototendering of wool[203 204]. It was found in these studies that dyed wool fabric showed a comparably slower rate of phototendering than undyed wool. The addition of UV absorbers reduced the rate of tendering of dyed wool further but the protective effect was no greater than given to absorber treated undyed wool. There does not appear to be an additive effect between the protection given by the dyestuff and by the absorber.

The protective effect of Cibafast W also extended throughout the wool fibre bulk. Transmission analysis of single wool fibres showed that the rate of increase in cysteic acid

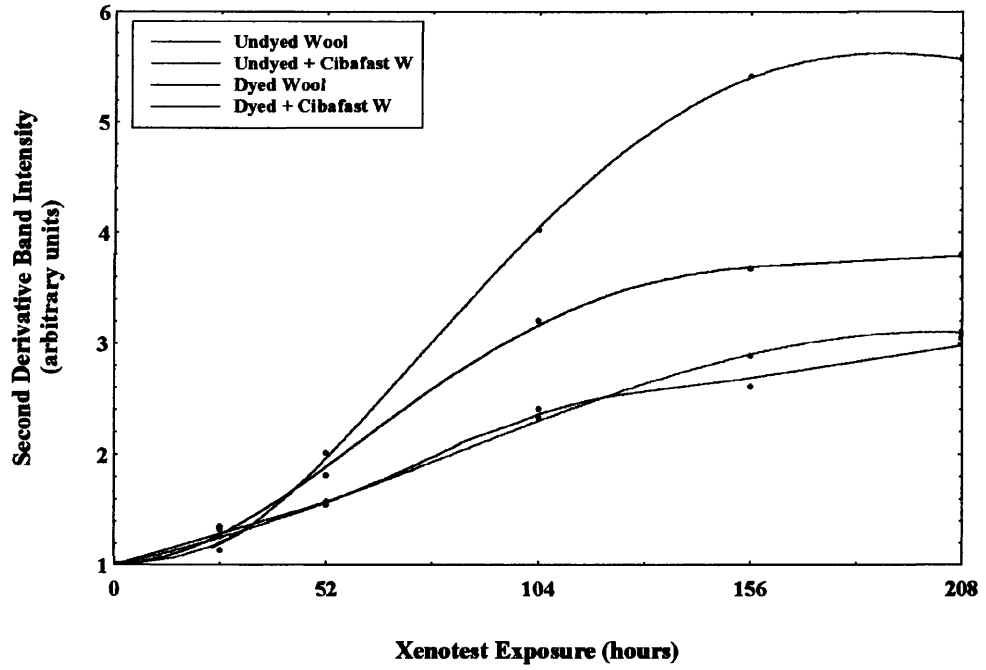

Figure 7.16 Comparison of the rates of increase in cysteic acid signal in the surface of undyed and dyed wool fabrics and the protective effect given by Cibafast W ($1039 cm^{-1}$)

signal was reduced in both undyed and dyed fibres treated with Cibafast W. Infrared bands associated with the UV absorber were too weak to be detected in either the ATR or transmission spectra of wool. This is unfortunate since ATR spectroscopy would have provided a method to investigate if surface migration of this product occurs during exposure.

7.3.4 Other Spectral Changes in Photooxidised Wool

Apart from the spectral changes in the region 1200-1000 cm^{-1} associated with increases in S-O absorbance, there were a number of other notable changes in the spectra of all wool fabrics after exposure. The spectral changes discussed below altered consistently with increasing exposure time, and were more pronounced for dyed wool fabrics compared to undyed wool. In Figure 7.17 the ATR spectrum of unexposed untreated wool is compared to that after 208 hours exposure. The spectra are overlaid on a common scale. It can be seen that there is a relative intensity change between the Amide I and Amide II bands after exposure. There is a shift in the Amide I band to higher frequency of at least 4 cm^{-1} . The band also broadens slightly with exposure. The FWHM increased by 6% after 208 hours exposure. However this broadening was much greater for dyed wool with a 26% increase in FWHM after 208 hours exposure and 15% for dyed fabric treated with Cibafast W. The Amide I band is known to be

conformationally sensitive and the frequency of this band has been correlated with chain conformation in polypeptides and proteins[205]. The broadening and shift in intensity of this band may reflect alterations in protein chain conformations following light exposure and scission of the stabilising disulphide crosslinks.

There is a considerable increase in intensity at the base of the Amide I band in the C=O functional region between 1700 - 1780 cm^{-1} associated with the formation of carbonyl containing groups. This may be due to photooxidation of the side chains, but it may also represent main chain cleavage. It is thought that main chain cleavage takes place at C-N bonds to form primary amide and α-ketoacyl groups[88] [89] (see section 3.2.1). The increase in C=O absorbance may be associated with an increase in main chain carbonyl group content following C-N cleavage. The equivalent increase in primary amide groups on C-N scission may explain the relative intensity change of the Amide I and Amide II bands. The Amide II vibration is present for secondary amide groups only, whereas primary amides only have an Amide I band. C-N cleavage involving the formation of primary amide groups would therefore reduce secondary amide group content relative to primary amide group content. An increase in absorbance of a shoulder at 3190 cm^{-1} on the secondary amide N-H stretching band at 3268 cm^{-1} was found after light exposure. This may also be attributed to the increase in primary amide groups which have a symmetric stretching frequency near 3180 cm^{-1}.

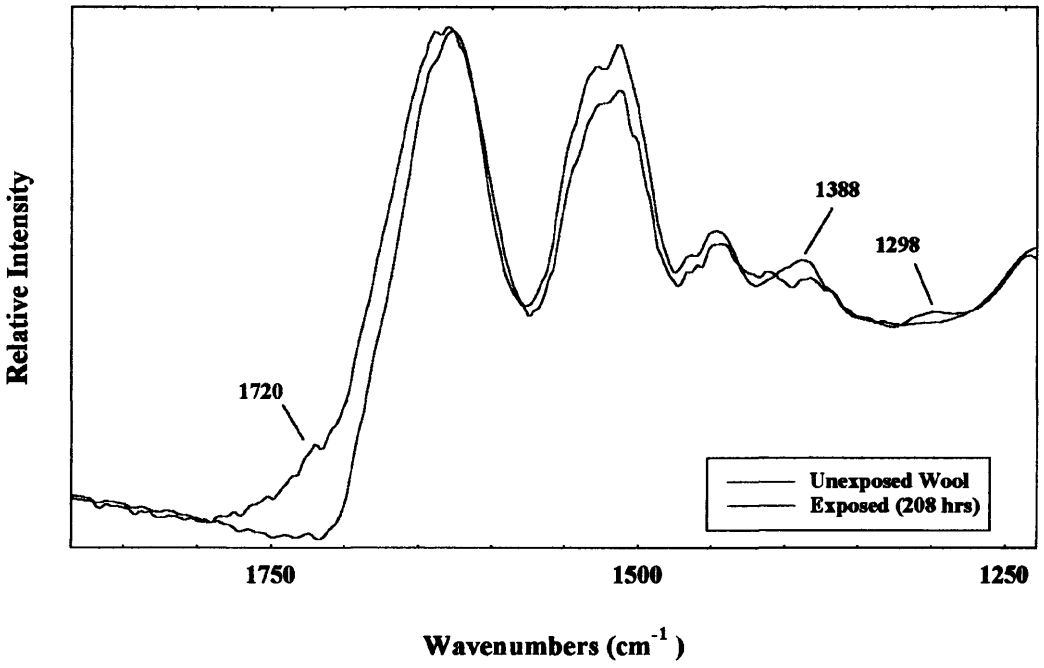

Figure 7.17 Change in FT-IR (ATR) spectrum of untreated wool after light exposure

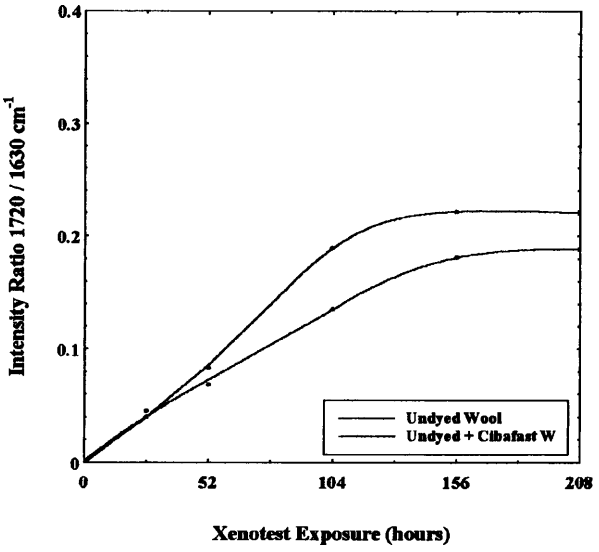

Figure 7.18 Rate of Increase in C=O absorbance in surface of undyed wool

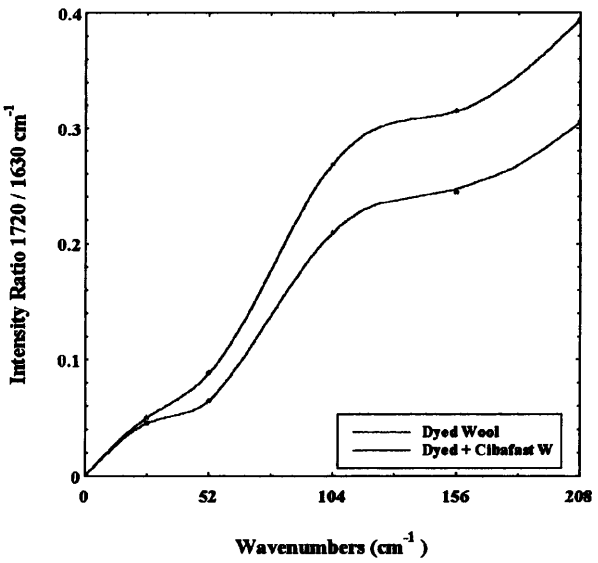

Figure 7.19 Rate of Increase in C=O absorbance in surface of dyed wool

The increase in C=O absorbance in FT-IR spectra of polymers is often used as an index of the rate of photooxidation[206]. The rate of increase in C=O absorbance as a function of exposure time was measured for wool. The absorbance intensity at 1720 cm^{-1} was measured relative to the intensity of the Amide I band at 1627 cm^{-1} using a linear baseline from the base of the Amide I band to 850 cm^{-1}. The rate of increase in C=O absorbance relative to the Amide I band is plotted in Figure 7.18 for undyed untreated wool and Cibafast W treated wool fabrics. It can be seen that for untreated wool there is a linear increase in absorbance at 1720 cm^{-1} up to 104 hours followed by a slower rate. Cibafast W treated fabric follows a similar trend but with a slower rate of increase up to 104 hours exposure. There is a faster rate of increase in absorbance at 1720 cm^{-1} for dyed wool compared to undyed wool, Figure 7.19. The rate of increase in C=O absorbance for dyed wool is reduced by the application of Cibafast W.

Figure 7.17 shows that after exposure there is a significant reduction in intensity of the broad band at 1388 cm^{-1} accompanied by a gradual increase in intensity at 1415 cm^{-1} . There is also a reduction in intensity at 1297 cm^{-1}. This region contains bands associated with CH_2 and CH_3 deformation modes and CH_2 wag modes, the frequencies of which depend on the substituents attached to these groups. It is difficult to interpret these spectral changes but they may reflect photodegradation of a number of amino acid side chains.

7.4 Analysis of Photooxidised Polyester Fabrics using Vibrational Spectroscopy

Although FT-Raman spectrum of polyester shows sharp intense bands which are mainly assigned to the benzene ring, C=O vibrations[207] [208] no large changes could be detected in the spectra of photooxidised polyester fabrics. Since Raman spectroscopy is a bulk analysis technique it will be relatively insensitive to photochemical changes which are restricted to the surface of polyester fabrics.

FT-IR (ATR) spectroscopy was used for more surface sensitive analysis of photooxidised polyester fabrics. No significant changes were found in the spectra of untreated polyester fabrics exposed for up to 208 hours using a KRS-5 crystal. Previous studies using ATR analysis to examine light degraded poly(ethylene terephthalate) have found increases in signal intensity assigned to carboxylic acid end groups in the region of 3290 cm^{-1} [209] [210]. An increase in concentration of these end groups after light exposure reflects polymer chain scission (see section 1.3.5). One study also found an increase in the concentration of hydroxyl end groups in photooxidised polyester which absorb at 3540 cm^{-1} [210]. A broad increase in absorbance was found at 3290 cm^{-1} in light exposed dyed polyester reflecting some increase in carboxylic acid end group content.

It was considered that the exposure conditions used in this work had caused relatively little damage to polyester and that even greater surface sensitivity would be required to detect photochemical changes. FT-IR analysis was also carried out using a germanium crystal which gives an analysis depth of 1.7 - 0.17 μm in the region between 400 - 4000 cm^{-1} .

After 208 hours exposure small but significant changes in the spectrum of untreated polyester were found. Using the germanium crystal, the signal intensity in the region above 3200 cm^{-1} was too weak to allow an investigation of the change in end group concentration. However, there were other changes in the spectrum of photooxidised polyester associated with conformationally sensitive bands. The infrared spectrum of poly(ethylene terephthalate) has been characterised in a number of studies[211] [212] [213]. Conformationally sensitive bands associated with the crystalline and amorphous phases of the polymer are related to the rotational configurations of the oxygen atoms about the C-C bond of the flexible ethylene glycol unit (-O-CH_2-CH_2-O-). Bands found in crystalline PET are due to the *trans* form of this group, whereas those characteristic of amorphous PET are due to the *gauche* form of this group.

However, the *trans* and *gauche* forms are not exclusive to crystalline and amorphous regions respectively, for example, ordered *trans* structures may be found in amorphous regions.

Figure 7.20 compares the ATR spectra of untreated unexposed polyester to that after 208 hours exposure. Reductions in the intensity of bands associated with the *gauche* form were found. There were reductions in the intensities of bands at 1100 cm^{-1} and 1042 cm^{-1} assigned to the *gauche* C-O stretching vibration of the ethylene glycol unit[214]. In addition there were reductions in intensity of the bands at 900 cm^{-1} and 1175 cm^{-1} which have previously been associated with perturbations of the amorphous phases of PET[213]. There were no significant changes in bands associated with the *trans* form at 1470 cm^{-1} 1340 cm^{-1} 1120 cm^{-1} 975 cm^{-1} 845 cm^{-1} . Since the *gauche* bands are mainly associated with the amorphous regions these changes therefore indicate disruption within the amorphous phases of the fibre after light exposure. The reductions in the *gauche* C-O bands possibly indicate polymer chain cleavage at these bonds in the ethylene glycol unit. Chain cleavage at these bonds is consistent with the proposed photodegradative mechanisms leading to the formation of carboxylic acid end groups (see Figure 1.8). As mentioned, the spectral intensity in the region above 3200 cm^{-1} associated with absorption of these end groups was too weak to confirm polymer chain scission. Similar changes were found in the case of polyester fabrics treated with the UV absorber Cibatex APS and exposed for 208 hours. Since these changes were not detected in transmission analysis of single polyester fibres, or during surface analysis of fabrics at a greater

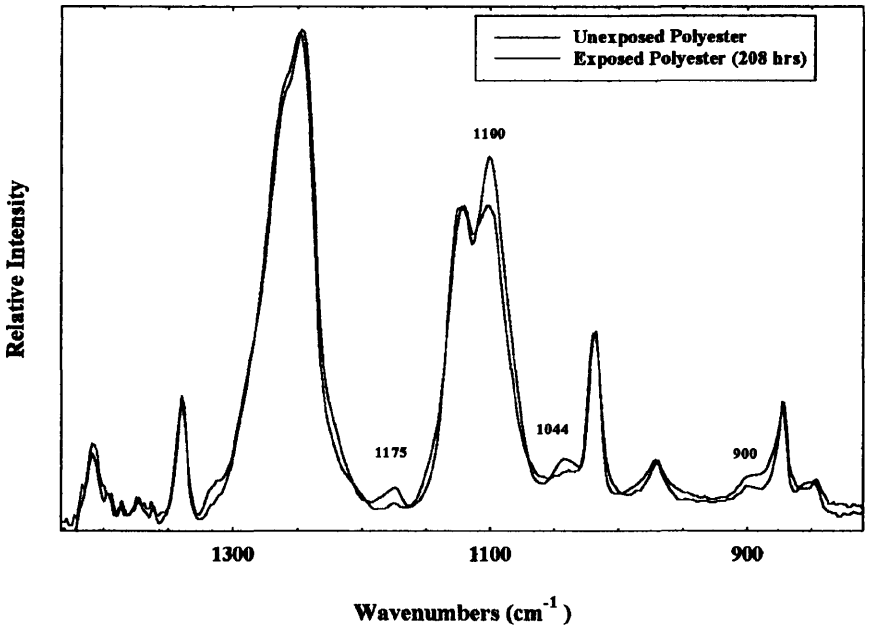

Figure 7.20 Change in FT-IR(ATR) absorbance spectrum of untreated polyester fabric after light exposure

analysis depth, these changes must be confined to amorphous regions at a depth of less than 1 μm into the fibre surface.

Similar reductions in the *gauche* C-O bands and other associated amorphous bands were found for dyed polyester fabrics after light exposure. These changes were apparent after only 52 hours exposure and there was a progressive reduction in intensity with exposure time. However for dyed polyester the decreases in intensity of these bands was accompanied by increases in bands associated with the *trans* form of the ethylene glycol unit at 1123 cm^{-1} , 975 cm^{-1} and 850 cm^{-1}. The reductions in *gauche* bands accompanied by an increase in *trans* bands may therefore reflect an increase in *trans* isomer due to transformation from the *gauche* form. This is most likely associated with conformational changes of the polymer chains in amorphous regions due to disruption of these regions as a result of light exposure. The same spectral changes were found for the surface of dyed polyester fabrics treated with Cibatex APS after light exposure.

7.5 Analysis of Photooxidised Nylon Fabrics using Vibrational Spectroscopy

No previously published work could be found which used infrared or Raman spectroscopy to investigate photodegradation of polyamides. Previous studies in which infrared spectroscopy has been applied to investigate chemical modification of polyamides have mainly been concerned with the effect of temperature on the strength of hydrogen bonding[215] and thermal ageing [216]. Earlier studies have been valuable in characterising infrared bands sensitive to crystalline and amorphous content [217], and correlating spectral bands with crystal structures of a number of polyamide types[218].

Although the FT-Raman spectrum of nylon has sharp bands assigned to Amide I, CH_2 , and C-C skeletal stretching modes no significant changes were found in the spectrum of untreated nylon after 208 hours exposure. This indicates that there are no large changes in bulk chemistry under the exposure conditions used. This is in contrast to changes in the FT-Raman spectrum of thermally oxidised nylon fabric after exposure to the Sahara test. There were small reductions in intensity of the CH_2 and C-C modes relative to the Amide I band. The reductions in these signals can be attributed to C-H and C-C bond cleavage associated with the autooxidation process responsible for the thermal oxidation of polyamides.

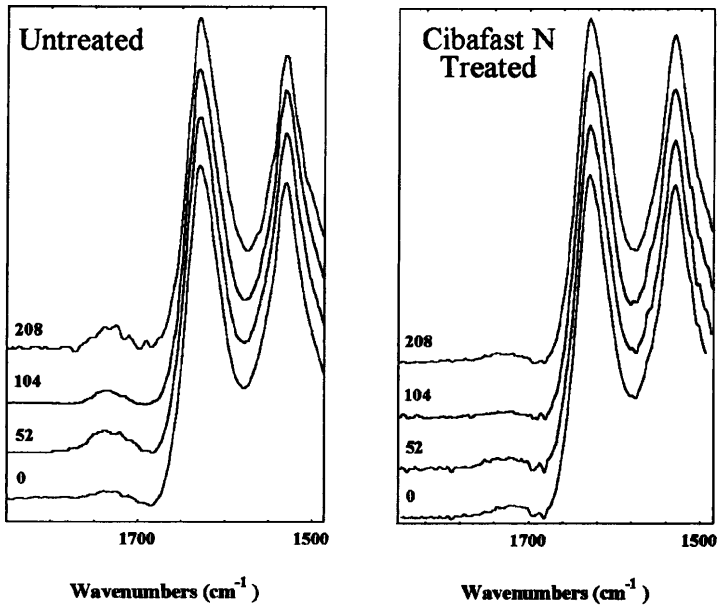

Figure 7.21 Increase in C=O absorbance in FT-IR (ATR) spectra of dyed wool fabrics

FT-IR (ATR) spectroscopy was used for more surface sensitive analysis of photooxidised nylon fabrics. Using a KRS-5 crystal no large changes in the spectrum of untreated nylon could be detected after light exposure for up to 208 hours, apart from small reductions in the CH_2 stretching bands relative to the Amide I and Amide II signals. However, evidence for photooxidation of the surface of dyed nylon was found from ATR analysis. There is an increase in carbonyl absorbance at 1735 cm^{-1} relative to the Amide I band after light exposure. In Figure 7.21 the increase in absorbance in this region for dyed nylon in the presence and absence of Cibafast N is compared. The photostabilizing effect of Cibafast N is shown by the less pronounced increase in carbonyl signal after light exposure.

Using a germanium crystal, greater surface sensitivity was achieved and a number of spectral changes were apparent for untreated nylon after light exposure associated with bands sensitive to the degree of crystallinity. Previous studies have made extensive use of the bands at 935 cm^{-1} and 1145 cm^{-1} in nylon 66, which have been found to be sensitive to the crystalline and amorphous content of the polymer respectively [219]. There is a direct positive correlation between the 936 cm^{-1} / 1146 cm^{-1} peak intensity ratio and fibre density and hence crystallinity. With increasing exposure time, the crystalline band at 935 cm^{-1} became progressively sharper and more intense relative to the amorphous band at 1145 cm^{-1}. The ratio 936 cm^{-1} / 1146 cm^{-1} therefore increased with exposure time suggesting that photooxidation leads to an increase in fibre density or crystallinity. An increase in the crystalline band at 935 cm^{-1} relative to the amorphous band at 1145 cm^{-1} was also found from transmission analysis of single wool fibres

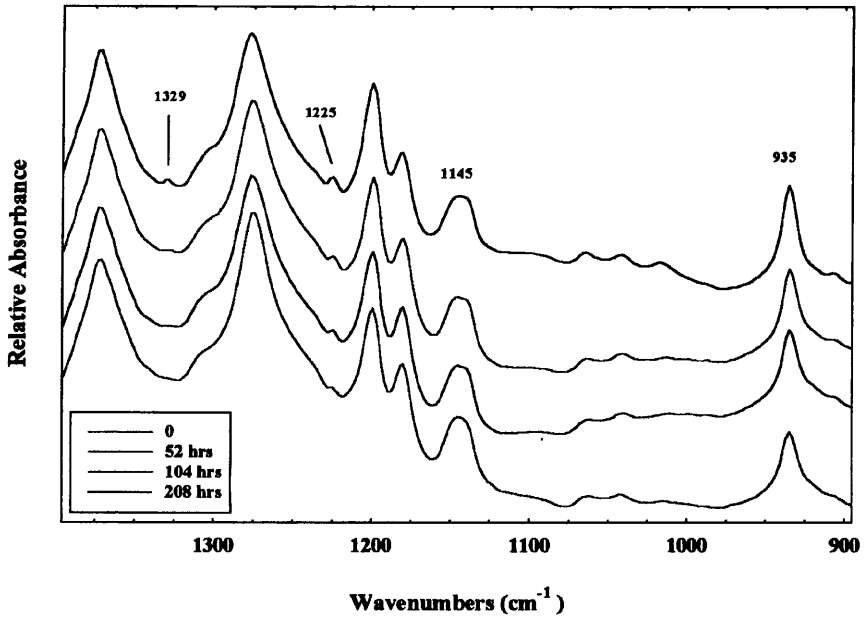

Figure 7.22 Changes in FT-IR spectra of nylon fibres after light exposure

after light exposure, Figure 7.22. There were also increases in weak bands at 1225 cm^{-1} and 1329 cm^{-1} with increasing exposure time which have been assigned to the folded chain structures in nylon 66[220]. These spectral changes may reflect reordering of polymer chains in the amorphous regions following photooxidative chain cleavage. An increase in this ratio for thermally oxidised nylon 66 was attributed to the greater sensitivity of the amorphous regions to oxidation than the more stable crystalline regions[221]. The increase in 935 cm^{-1} / 1145 cm^{-1} ratio as a function of exposure time is shown in Table 7.6 for both untreated nylon fibres and after treatment with Cibafast N. The values given are the mean of five fibres measured at each exposure period, the coefficient of variation between samples was approximately 10%. After treatment with Cibafast N, the rate of increase in this ratio reduced up to 156 hours. By using this index as a measure of the extent of photodegradation, Cibafast N appears to have a protective effect at moderate exposure levels.

Table 7.6 Increase in crystalline / amorphous ratio for nylon fibres after light exposure

FT-IR Absorption Intensity Ratio 935 cm^{-1} / 1145cm^{-1}		
Xenotest Exposure (hours)	Untreated	Cibafast N Treated
0	1.4	1.3
52	1.7	1.3
104	1.8	1.4
156	1.8	1.4
208	2.2	2.1

7.6 Conclusions

The combined techniques of FT-Raman and FT-IR spectroscopy have given complementary information with regard to the photochemical changes occurring in wool. Photooxidation of cystine residues was detected using Raman spectroscopy by reductions in signal intensity of the disulphide band, accompanied by an increase in cysteic acid signal. A reduction in cystine C-S bond vibration after extended exposure indicates that photooxidation also proceeds via C-S bond scission. After treatment of wool with the UV absorber Cibafast W, there was a slower rate of reduction in disulphide bond signal, particularly at low exposure levels. This indicates that the absorber is effective in reducing the rate of cystine photooxidation. Using FT-IR spectroscopy the photooxidation products of cystine were investigated in more detail. ATR analysis allowed the surface of wool to a depth of 2.5 - 2.0 μm in the S-O stretching region to be examined. The rate of surface photooxidation was measured by the increase in cysteic acid signal. It was found that photooxidation in the surface regions took place at approximately twice the rate found for the fibre as a whole. The surface cysteic acid signal does not increase linearly with exposure time, there is an induction period with little increase in signal intensity. This can be explained by only partial oxidation of cystine residues, since over this initial exposure period there were increases in bands associated with the intermediate oxidation products Bunte salt and cystine-S-monoxide. As exposure time increases, these intermediate products are further oxidised to cysteic acid, shown by reductions in their signal intensities accompanied by much more rapid increases in cysteic acid signal. However, there were distinct increases in other band intensities in the S-O stretching region with increasing exposure time, apart from those associated with cysteic acid. One of these bands has previously been assigned to cysteine sulphinic acid, indicating that it may be a more stable intermediate oxidation product under these exposure conditions.

The protective effect of Cibafast W was further confirmed from FT-IR spectroscopy. In both surface and bulk analysis of wool, Cibafast W was found to be effective in reducing the rate of increase in cysteic acid signal when applied to both undyed and dyed wool.

As a consequence of cleavage of the stabilising disulphide bonds structural rearrangements may have taken place within the fibre leading to disordering in the crystalline microfibrillar components. Raman spectra of light exposed wool showed significant reductions in the band assigned to the C-C skeletal stretch of the α-helix. Studies of other proteins have interpreted

this as a loss in α-helical content in favour of more random chain conformations. Changes in the Amide III region of wool after light exposure also indicated an increase in disordered protein chain conformations. Additionally an intense band appears at 977 cm^{-1} which increases in intensity with exposure time. This band has not previously been noted or assigned for wool or proteins but the large increase in intensity of this band suggests a significant alteration in the bulk chemistry of wool. Since this band appears in the C-C skeletal stretching region it may reflect conformational changes in the fibre.

Both Raman and FT-IR spectroscopy detected increases in intensity in the C=O functional region after exposure. This may represent an increase in concentration of a number of carbonyl containing species as a result of side chain photooxidation. It could also reflect the formation of α-ketoacyl groups following main chain cleavage. The rate of increase in this signal intensity was reduced in the presence of Cibafast W for both undyed and dyed wool.

Using Raman spectroscopy, changes in the bands assigned to tyrosine were found after light exposure. These changes were attributed to alterations in the local chemical environment of these residues due to structural rearrangements following disulphide bond cleavage. It has not been possible to investigate photooxidation of tryptophan residues using Raman spectroscopy since the low concentration of this amino acid in wool means that assigned bands are relatively weak in intensity. However, analysis of the protein lysozyme, which has much stronger tryptophan bands, showed reductions in intensity of particular tryptophan bands after light exposure.

In contrast to the considerable photochemical changes which were found from bulk analysis of untreated wool fabrics using Raman spectroscopy, no significant changes in the chemistry of untreated polyester and nylon were detected after light exposure using Raman spectroscopy. Using FT-IR (ATR) spectroscopy, much higher surface sensitivity was required to detect any significant spectral changes, indicating that unlike wool photooxidation is limited to regions much closer to the surface. Following light exposure, both polyester and nylon had changes in conformationally sensitive bands, indicating apparent increases in crystallinity. These spectral changes are most likely associated with reordering of the polymer chains in the amorphous regions close to the surface following photooxidative chain cleavage. It was found that the application of Cibafast N to nylon reduced this rate of photooxidative crystallisation. Cibafast N was also found to be effective in reducing the rate of carbonyl group formation in the surface of dyed nylon.

Chapter 8

Surface Analysis of Photooxidised Fabrics

8.1 Introduction

In this chapter a number of surface sensitive analytical techniques have been used to investigate the effect of light exposure on the outermost surface of fabrics. X-ray Photoelectron Spectroscopy (XPS) is the main technique used and section 8.2 briefly discusses chemical shift assignments for wool and synthetic polymers. Section 8.3 discusses the results of work using XPS to obtain quantitative information of the changes in elemental composition of the outermost surface of the wool fibre and the nature of the oxidised species present. The level of protection given to surface photooxidation for both undyed and dyed wool by the application of Cibafast W is also assessed. In this section, changes found in the surface chemistry of wool are compared to those found from XPS analysis of undyed and dyed nylon and polyester fabrics. The level of protection given by photostabilizers applied to these fabrics is considered. Static Secondary Ion Mass Spectroscopy allows even greater surface sensitivity than XPS, in section 8.4 it was used to study the effect of light exposure on the outermost lipid layer, which functions as a protective hydrophobic barrier. In section 8.5 a combination of Scanning Electron Microscopy and Atomic Force Microscopy are used to examine damage to the surface morphology of light degraded wool. Finally, section 8.6 considers the photostability of UV stabilizers and provides evidence for the surface migration of stabilizers in light exposed fabrics.

8.2 XPS Chemical Shift Assignments for Wool and Synthetic Polymers

Using XPS the surface chemistry of fabrics to a depth of approximately 3 nm was investigated. The surface sensitivity of this technique means that analysis is confined to the wool fibre epicuticle, which being the outermost surface of the fibre can be expected to be most susceptible to photooxidation. The experimental conditions used for XPS analysis are detailed in section 4.6.3, with a general introduction to the technique given in section 2.2.

The elemental core level peaks present in an XPS spectrum of untreated wool are carbon (1s), oxygen (1s), nitrogen (1s) and sulphur (2p). These have binding energies of 285 eV, 532 eV, 400 eV and 164 eV respectively. Shifts in these binding energies may occur depending on the nature of the substituent attached to these atoms. XPS can therefore provide information on the functional groups present in the sample surface.

The C (1s) binding energy is particularly sensitive to substituent effects with distinct binding energy shifts observed. Carbon attached to an oxygen atom induces a shift to higher binding energy relative to the C-C / C-H line at 285.0 eV. In general, the C (1s) peak is shifted to higher binding energy by 1.5 ±0.2 eV per C-O bond. In Table 8.1 the C (1s) binding energy shifts are listed with the corresponding functional group assignments given in experimental studies on synthetic polymers[222 - 226]. Also listed are the binding energy assignments given for wool from previous experimental studies [163, 166]. All binding energy shifts given are relative to the saturated hydrocarbon signal at 285.0 eV.

The binding energy shifts of the O (1s) and N (1s) core levels are smaller and less informative. The O (1s) binding energies fall in a narrower range of approximately 2 eV around 533 eV.

Table 8.1 Experimentally observed XPS core level binding energy shifts

Functional Group Assignment	Binding Energy (eV)	
	Assignments from Polymer Studies[222 - 226]	Assignments from Wool Studies[163, 166]
C (1s) Binding Energies		
C-C C-H polymer backbone	285	285
C-O C-OH C-OOH C-O-C C-O-C=O alcohol, hydroperoxide, ether, ester	286.4 - 286.6	286.4 - 286.6
C=O O-C-O ketone, aldehyde	287.8 - 288.0	288.4 - 288.5
O-C=O carboxylic acid or ester	289.0 - 289.4	-
O-(C=O)-O carbonates	290.4 - 290.6	-
C-N amide, amine	286.0 - 286.3	285.3
N-C=O amides	288	-
Aromatic C-H	284.7	-
Aromatic ring shake-up satellite	291.6	-
O (1s) Binding Energies		
O-C=O ester, carboxylic acid	532.8 - 532.9	-
C=O C-O-C C-OH ketone, ether, alcohol	533.6 - 533.7	-
C-O-O-R C-O-O-H peroxide, hydroperoxide	534	-
O-C=O ester, carboxylic acid	534.3	-

The most distinctive shift in the O (1s) spectrum is due to the ester oxygen in carboxyl groups which shifts to higher binding energy of around 1.5 eV, shown in Table 8.1.
N (1s) binding energies for many functionalities occur in a narrow range between 399-401 eV ie. -CONH- -$CONH_2$ -CN. This makes it difficult to observe distinct chemical shifts.

The S (2p) binding energy is sensitive to the oxidation state of the sulphur atom. In wool the (+2) oxidation state for disulphide sulphur has a binding energy of 164 eV [164]. A shift to higher binding energy of between 4.0 - 4.5 eV is observed for sulphur in the (+6) oxidation state. A photoelectron peak at 168 eV in wool is assigned to cysteic acid residues [165]. Sulphur in the (+4) oxidation state is reported to show a binding energy shift of 1.0 - 1.5 eV [167].
The ability to resolve the closely spaced spectral features associated with these binding energy shifts relies on the energy resolution of the spectrum (section 2.2.1.3). The two instrumental factors which affect resolution are the X-ray line width and analyser resolving power. The instrument used in this work has an unmonochromatized X-ray source which reduced the resolution that could be achieved. Although some improvement in analyser resolving power can be achieved by lowering the analyser pass energy, this is at the expense of signal intensity. The improvement was still not sufficient to resolve the features of the C (1s) envelope. In addition, instrumental broadening of the peaks further reduced spectral resolution, and so the chemical shift information which could be obtained using this instrument was limited.

8.3 XPS Analysis of Photooxidised Wool Fabrics

8.3.1 Changes in Surface Elemental Composition

Wool fabrics were analysed after successive Xenotest cycles. The change in the surface elemental ratios as a function of exposure time for undyed and dyed fabrics are shown in Tables 8.2 - 8.5. In comparison to untreated wool the surface of unexposed dyed wool has a much higher oxygen concentration, the O/C, O/S and O/N ratios are approximately twice the value for untreated wool. It also has a lower S/N ratio than untreated wool. These differences are most likely attributable to hydrothermal damage during the dyeing process.

Table 8.2 shows that there is a progressive increase in O/C ratio with increasing exposure time for untreated wool. This can mainly be attributed to an increase in surface oxidised species. The O/C ratio is used as a measure of the rate of surface photooxidation of polymers[222-226].

Table 8.2 XPS surface elemental ratios for untreated wool

Xenotest Exposure (hours)	C	O	N	S	O/S	O/N	S/N
0	100	14	7.1	2	6.9	2	0.29
26	100	18.9	6.4	1.7	11.2	3	0.27
52	100	21.2	8	2.1	10.1	2.7	0.26
104	100	22.8	9.7	2.3	9.9	2.4	0.24
156	100	23.7	9.1	2.2	10.7	2.6	0.25
208	100	24.8	9.1	2.3	11	2.7	0.25
Sahara Test	100	14.5	7.3	1.9	7.5	2	0.26

Table 8.3 XPS surface elemental ratios for Cibafast W treated wool

Xenotest Exposure (hours)	C	O	N	S	O/S	O/N	S/N
0	100	18.2	7.1	2.1	8.9	2.6	0.29
26	100	25.1	10.5	2.7	9.3	2.4	0.26
52	100	22.7	7.8	2.1	11	2.9	0.27
104	100	26.2	9.8	2.4	11	2.7	0.24
156	100	24	8.4	2.2	11.1	2.9	0.26
208	100	28.3	10.9	2.3	12.5	2.6	0.21

Table 8.4 XPS surface elemental ratios for dyed wool

Xenotest Exposure (hours)	C	O	N	S	O/S	O/N	S/N
0	100	24.4	7.3	1.7	14	3.4	0.24
26	100	34.6	9.7	2.6	13.2	3.6	0.27
52	100	38	9.1	3	12.6	4.2	0.33
104	100	48.4	16.8	3.1	15.5	2.9	0.19
156	100	48	15.4	2.7	17.7	3.1	0.18
208	100	40.2	9.9	2.1	18.8	4.1	0.22

Table 8.5 XPS surface elemental ratios for Cibafast W treated dyed wool

Xenotest Exposure (hours)	C	O	N	S	O/S	O/N	S/N
0	100	21	6.3	1.8	11.8	3.4	0.28
26	100	27.7	9.2	2.5	11	3	0.28
52	100	28.7	9.7	2.4	12	3	0.25
104	100	37.6	12.9	2.8	13.4	2.9	0.22
156	100	43.3	14.9	3	14.6	2.9	0.2
208	100	40.3	17	2.8	14.3	2.4	0.17

In Figure 8.1 the percentage increase in O/C ratio with exposure time is shown for untreated wool. For comparison, the rates of increase in O/C ratio for 100% polyester and 100% nylon fabrics are shown to illustrate the more rapid surface oxidation of wool. For wool, surface oxidation occurs most rapidly at low exposure levels, the rate slowing down considerably after exposure for more than 52 hours. After only 26 hours there is a 35% increase in O/C ratio compared to a total increase in O/C ratio of 77% after 208 hours. Oxygen is rapidly incorporated into the surface of wool on initial exposure, but after prolonged exposure the rate of oxidation may be limited by the accessibility of reactive sites in the surface. The slower rate of increase in O/C ratio above 52 hours could also be explained by a loss of volatile oxidised species from the surface, such as CO_2, which is evolved from the surface of wool irradiated with near UV light [241]. A reduction in surface crosslinking with increasing exposure time may also lead to easier migration of oxidised species into the fibre bulk.

Figure 8.1 shows that the rate of increase in O/C ratio for untreated polyester is most rapid up to 52 hours. The O/C ratio levels off after exposure for more than 104 hours. This is a typical curve for the rate of oxygen uptake of many polymers during photooxidation[222 - 226]. The curve is characterised by an initial rapid rate of oxygen incorporation into the surface after which a limiting stoichiometry is reached due to the low access of oxygen to regions below the surface. After 208 hours there is only a 40% increase in O/C ratio for untreated polyester, indicating a

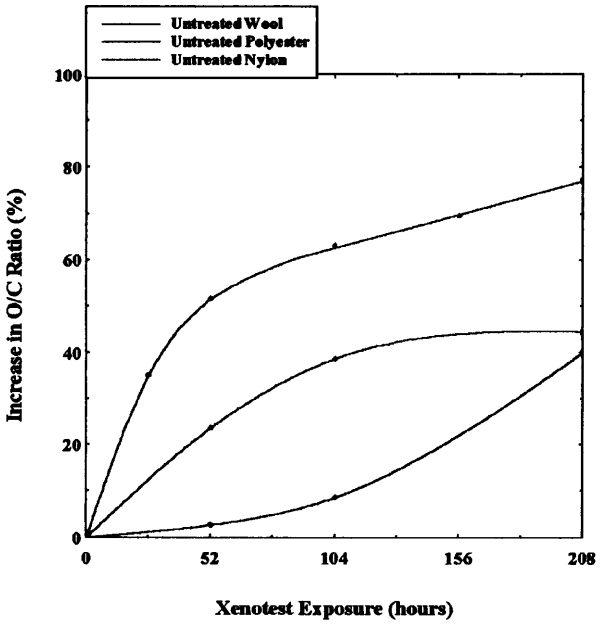

Figure 8.1 Increase in XPS O/C ratio for untreated wool, polyester and nylon

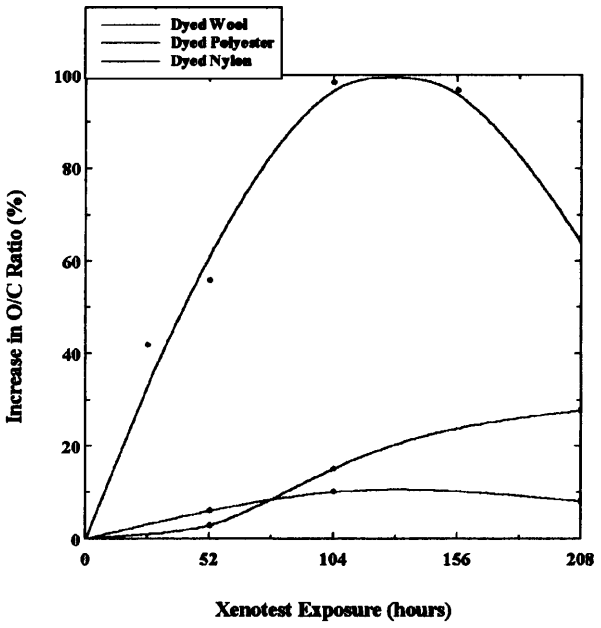

Figure 8.2 Increase in XPS O/C ratio for dyed wool, polyester and nylon

much smaller amount of surface oxidation compared to wool.

Untreated nylon shows an opposite effect to wool and polyester, the rate of surface oxidation increasing gradually as a function of exposure time. Other XPS studies have found that those polymers containing aromatic rings have a much more rapid rate of surface photooxidation, due to light absorption and energy transfer by these groups [222 - 226]. This may partly explain the initially slower rate of surface photooxidation of nylon compared to polyester. However, since the level of surface oxidation increases with exposure time it suggests that there is a gradual build up of reactive sites. This may reflect the free radical initiated autooxidation process thought to be mainly responsible for photooxidation of polyamides (section 1.3.4). After 208 hours there is a 40% increase in O/C ratio for untreated nylon, similar to the level for polyester.

The surface elemental ratios for thermally oxidised untreated wool, on exposure to the Sahara test, are shown at the bottom of Table 8.2. After 6 days exposure at 115°C there is very little increase in the O/C ratio indicating that the surface of wool is not significantly oxidised due to exposure to heat alone. There was no significant increase in O/C ratio for untreated polyester after exposure to the Sahara test, but untreated nylon had a 16% increase in O/C ratio indicating thermal oxidation of the fabric surface had occurred, presumably due to the autooxidation process.

The rate of increase in O/C ratio for wool treated with Cibafast W is shown in Table 8.3. Although the ratio has an overall increasing trend with exposure time, it does not change in the progressive manner as found for untreated wool. The application of Cibafast W does not reduce the rapid rate of surface oxidation of wool which occurs up to 26 hours, the O/C ratio increases by 38% similar to the level of 35% for untreated wool. However, the absorber may have some effect at higher exposure levels. For absorber treated wool there is a 44% increase in O/C ratio after 104 hours compared to 63% for untreated wool, and an increase of 55% after 208 hours compared to 77% for untreated wool.

The application of the photostabilizer Cibafast N to untreated nylon did not reduce the rate of surface photooxidation, the increase O/C ratio was at the same rate for both untreated and treated fabrics. This is despite the fact that an increase in concentration of the stabilizer in the fabric surface was found after light exposure (see section 8.6).

The application of the UV absorber Cibatex APS to untreated polyester increased the initial rate of surface photooxidation. There was a 36% increase in O/C ratio for the absorber treated fabric after 52 hours exposure compared to 24% for untreated fabric. With further exposure there was a decrease in the O/C ratio for the absorber treated fabric. Again, this is despite the fact that there is an increase in surface concentration of the absorber after exposure (see section 8.6). It is not clear why the rate of surface photooxidation is apparently enhanced by the presence of the UV absorber, but a similar effect has been found in a previous XPS study of polystyrene treated with the same class of UV absorber [238]. The higher concentration of oxidised species at the surface may be due to the absorber in some way reducing the rate at which these species are lost from the surface, for example restricting the ease of migration from the fibre surface to the bulk.

Figure 8.2 shows the rate of increase in O/C ratio for dyed wool. The change in O/C ratios for dyed nylon and polyester fabrics are also shown as a means of comparison. Dyed wool has a more rapid increase in O/C ratio compared to undyed wool. Although the O/C ratio increases at approximately the same rate for both undyed and dyed wool up to 26 hours, the ratio for dyed wool continues to increase rapidly up to 104 hours exposure. There is a 98% increase in O/C ratio for dyed wool after 104 hours exposure compared to 63% for undyed wool. The percentage surface elemental composition after 104 hours exposure for dyed wool is $C_{59.4}$ $O_{28.8}$ N_{10} $S_{1.8}$ compared to the composition for undyed wool of $C_{74.2}$ $O_{16.9}$ $N_{7.2}$ $S_{1.7}$, reflecting a much higher surface oxygen concentration. The dyestuff may have acted as a photosensitizer to accelerate the rate of surface oxidation, or the dyestuff itself may be oxidised at the surface. As exposure time continues, the O/C ratio for dyed wool appears to reach a maximum level and then begins to reduce, which may be associated with a loss of volatile oxidised species from the surface.

The rate of increase in O/C ratio for dyed nylon and polyester fabrics is much smaller. In contrast to wool, the application of dyestuffs to polyester reduces the rate of surface oxidation compared to undyed polyester. Undyed and dyed nylon fabrics show a similar rate of increase in O/C ratio up to 52 hours, but dyed nylon has a faster increase in O/C ratio between 52 - 104 hours exposure. This could be associated with photooxidation of the dyestuff at the surface.

Table 8.5 shows that application of Cibafast W to dyed wool reduces the rate of increase in O/C ratio by 20-30% at exposure times up to 104 hours. However, the O/C ratio for the

absorber treated fabric continues to increase up to 156 hours before levelling off, compared to untreated dyed wool which reaches a maximum value after 104 hours. Although both dyed fabrics follow the same trend, the presence of the absorber may have slightly retarded the rate of surface oxidation.

The rate of increase in O/C ratio for dyed nylon is not reduced on application of Cibafast N and may even by slightly increased. Dyed polyester treated with Cibatex APS showed an opposite effect to untreated dyed polyester, there was a progressive decrease in O/C ratio with light exposure suggesting an increase in surface carbon concentration.

Table 8.2 shows that there are significant changes in some of the other surface elemental ratios for untreated wool. The surface of unexposed untreated wool has a C/N ratio of 14.0. This value is much higher than that which would be expected for wool protein. The bulk C/N ratio of wool based on microanalysis of a whole merino wool fibre is 3.57 [227]. Other XPS studies have found that the surface of untreated wool is characterised by a similarly high C/N ratio, in comparison with the value which would be expected for the whole fibre protein [163 172 - 174]. The high C/N ratio is attributed to the carbon rich lipid layer present on the outer surface of the epicuticle[174]. After light exposure there is a reduction in the C/N ratio of untreated wool. This may be associated with photooxidation of the lipid layer involving a loss of carbon rich material from the fibre surface. Complete removal of the lipid layer by treating wool with potassium *t*-butoxide in anhydrous *t*-butanol reduces the XPS C/N ratio to 4.2, a value similar to that expected for wool protein[173]. The C/N ratio of untreated wool exposed for 208 hours in this study is 11.0, which is still much higher than the value found for complete removal of the bound lipid layer. This suggests that photooxidation causes only partial damage to the lipid layer. In section 8.4, Static Secondary Ion Mass Spectrometry is used to investigate further the effect of light exposure on the outer surface lipids of the epicuticle.

The S/N ratio for unexposed untreated wool is 0.29 compared to a value of 0.10 from microanalysis of the whole fibre[227]. This high S/N ratio is consistent with other XPS studies and is attributed to the high cystine content of the epicuticle proteins [172 - 174]. A calibration curve has been calculated in a previous study which relates XPS S/N ratio to the sulphur content of the epicuticle proteins[174]. Using this calibration curve the sulphur content of the epicuticle proteins in unexposed untreated wool in this study is approximately 7-8% by weight. There is a reduction in S/N ratio after light exposure indicating a reduction in surface

sulphur content. This is most likely associated with photooxidation and loss of high sulphur protein containing material.

The N/C ratio and S/C ratio show a similar trend with an initial decrease after 26 hours followed by increases with continued exposure. The epicuticle of wool is known to be rich in the nitrogen containing amino acid lysine as well as its high cystine content[15]. The initial decrease in these ratios may indicate a reduction in sulphur and nitrogen concentration due to photooxidation of these residues. The increase in N/C and S/C ratios with continued exposure may represent a more rapid loss of surface carbon containing material possibly associated with photooxidation of the lipid layer.

It is difficult to interpret some of the changes in the elemental ratios for dyed wool fabric. However, compared to untreated wool there are much larger changes in the elemental ratios associated with nitrogen. The N/C ratio increases up to 52 hours exposure, similar to undyed wool, but after 104 hours there is a much larger increase in N/C ratio for dyed wool. The N/S and N/O ratios also show large increases between 52 and 104 hours. This indicates a substantial increase in surface nitrogen concentration, most likely associated with surface migration of the dyestuff. The Cobalt ($2p_{3/2}$) region at 781 eV was scanned at each exposure level as a marker for the premetallized dyestuff in the surface. Although no signal was detected in the surface of unexposed wool, a very weak signal was present in the spectra of fabrics exposed for 104 and 156 hours, but it was too weak for quantification purposes. The presence of the dyestuff at the surface may therefore explain why there are much larger increases in surface oxygen concentration for dyed wool compared to untreated wool. After extended exposure for 208 hours the N/C, N/S and N/O ratios for dyed wool all decrease, which may indicate photodegradation of the dyestuff at the surface.

For dyed wool treated with Cibafast W, the N/C, N/S and N/O ratios still increase progressively, but the rapid rate of increase in these ratios between 52 and 104 hours is reduced on application of the absorber. These ratios continue to increase steadily up to 208 hours. If the large increases in the nitrogen ratios represent surface migration of the dyestuff, there may be a similar migration of the UV absorber which would also lead to an increase in the surface nitrogen concentration. Since there is no distinctive elemental tag for the UV absorber, it was not possible to investigate if surface migration of the product had taken place. However, photo-induced surface migration of a UV absorber applied to polyester fabric has

been found in this work which suggests that a similar effect may take place in wool (see section 8.6).

8.3.2 Chemical Shift Analysis of Surface Oxidised Species

Analysis of the individual core level peak profiles, particularly those of carbon and sulphur provides further information on the nature of the surface oxidised species present.

Carbon Chemistry

For untreated wool the C (1s) peak showed a broadening and an increase in asymmetry at high binding energy with increasing exposure time. The full width at half maximum (FWHM) increased progressively from 4.1 eV for unexposed wool to 4.42 eV after 208 hours. Similar changes in the C (1s) peak profile were found for Cibafast W treated wool. The increase in signal intensity at high binding energy is due to an increase in the concentration of oxidised carbon species at the surface. The C(1s) spectrum of dyed wool showed much larger increases in signal associated with oxidised carbon species after exposure. The FWHM of the C(1s) peak increased from 3.84 eV for unexposed fabric to 4.87 eV after 156 hours exposure with a corresponding increase in peak asymmetry at high binding energy from 14% to 24%. The change in the C (1s) peak profile for dyed wool after light exposure can be seen clearly by comparing Figures 8.3 and 8.4. Dyed fabric treated with Cibafast W had similar changes in the C(1s) spectrum associated with an increase in oxidised carbon species.

The C (1s) spectra for undyed and dyed nylon fabrics, and to a greater extent, polyester fabrics also showed increases in signal intensity associated with an increase in concentration of oxidised carbon species after light exposure.

The limited energy resolution of the XPS instrument meant that C (1s) band was too broad to clearly resolve peak shifted components associated with oxidised carbon functionalities. A general indication of the of the change in the C (1s) band after exposure was obtained using spectral subtraction. The C (1s) peak maxima at 285 eV at each exposure level were normalised to a signal intensity of 10,000 counts. The exposed spectra were then subtracted from the C (1s) spectrum of unexposed wool. Figures 8.5 and 8.6 show the spectral subtractions at each exposure level for undyed and dyed wool fabrics respectively. The region above 285 eV, associated with oxidised carbon species, is shown. For undyed wool there is

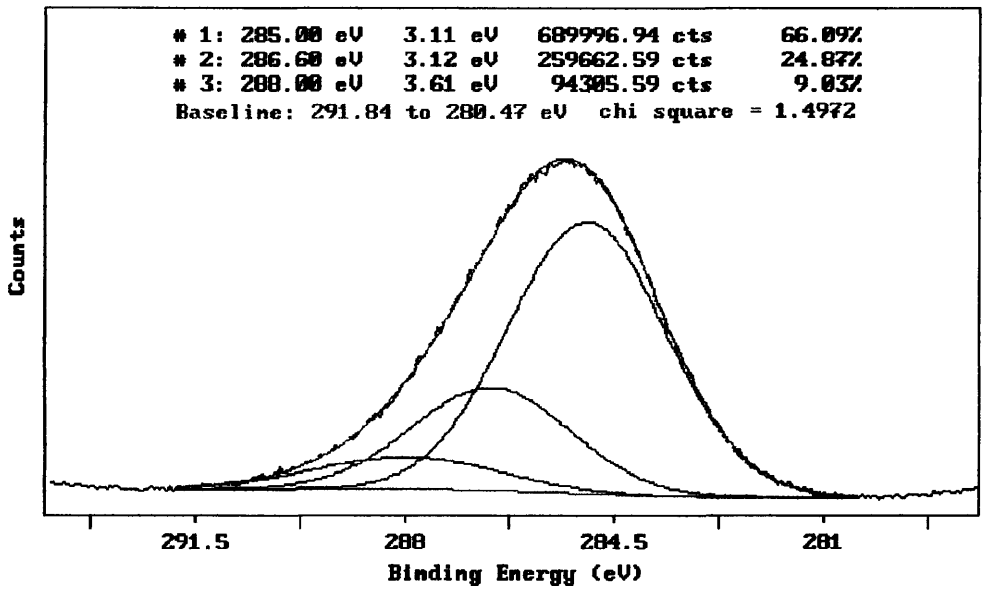

Figure 8.3 XPS C (1s) spectrum of unexposed dyed wool fabric

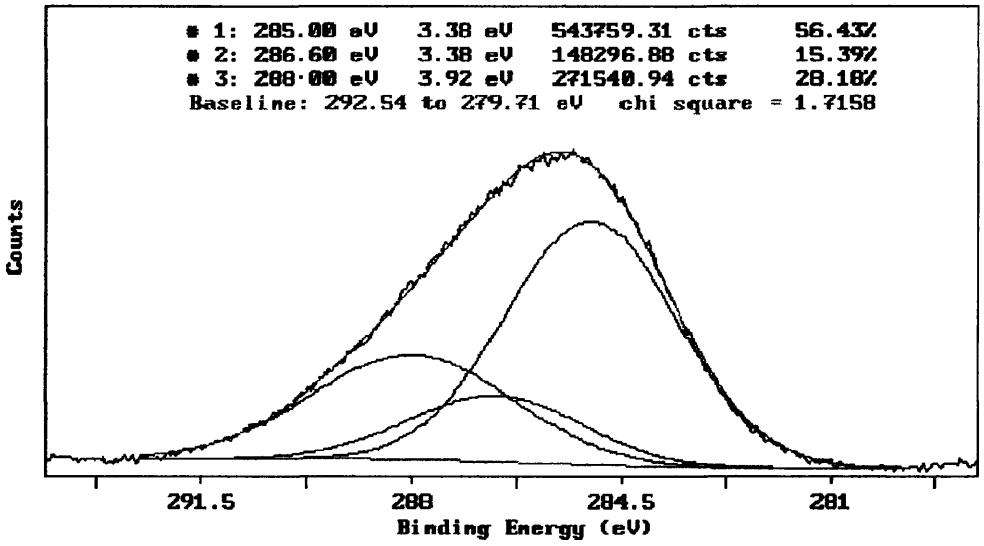

Figure 8.4 XPS C (1s) spectrum of dyed wool fabric exposed for 156 hours

little increase in signal intensity in this region up to 52 hours exposure. After 104 hours there is a broad increase in intensity between 286 - 291 eV, but particularly at 288 eV assigned to C=O or O-C-O functionalities. The signal at 288 eV can be assigned to both amide and carbonyl carbon, but the increase in intensity with exposure reflects surface carbon oxidation and the formation of carbonyl containing species. The signal intensity at 288 eV continues to increase with increasing exposure time and it is accompanied by an increase in intensity around 289 - 290 eV. This suggests that more highly oxidised species may be present such as carboxylic acids and esters.

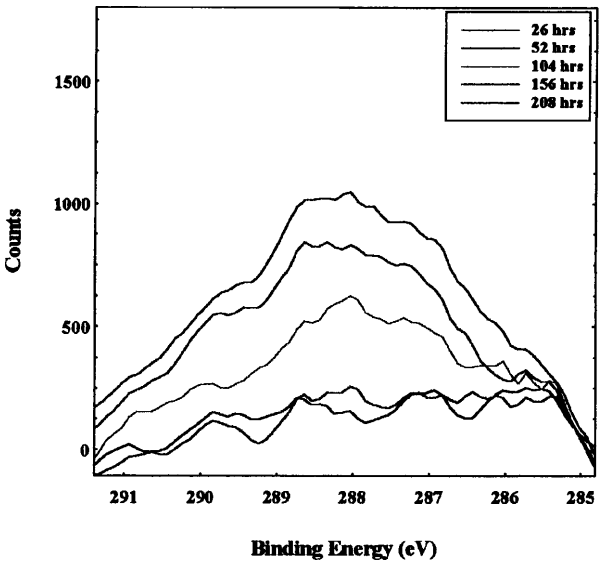

Figure 8.5 XPS subtraction spectra of C (1s) peak for untreated wool

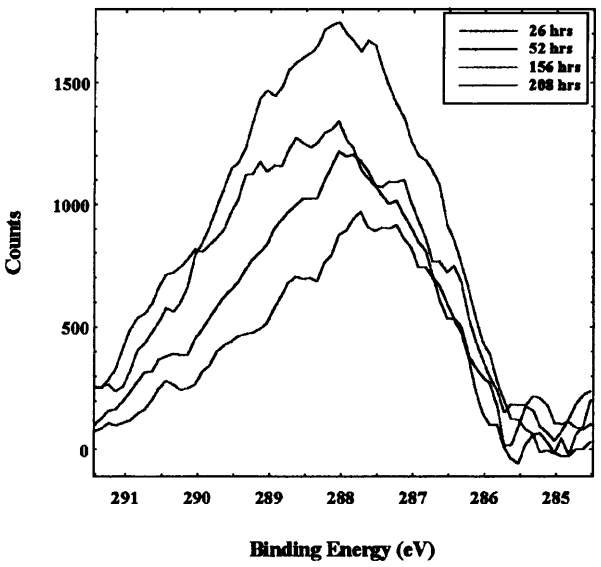

Figure 8.6 XPS subtraction spectra of C (1s) peak for dyed wool

In the case of dyed wool, there are much larger increases in signal intensity in the region between 286 eV- 291 eV, particularly after only 26 hours. After 156 hours the carbonyl signal at 288 eV is approximately twice the intensity of undyed wool exposed for the same time. The subtraction spectra show a broadening and increase in intensity in the region above 289 eV with increasing exposure time. There is also a gradual shift in the maximum of the subtraction spectrum from 288 eV to 288.5 eV with increasing exposure time. This indicates that as exposure time increases there is an increase in concentration of more highly oxidised carbon species at the surface, such as carboxylic acids.

If improved resolution had been possible, the component bands of the C (1s) spectrum could have been resolved with greater confidence using peak fitting methods. An attempt was made to peak fit the C (1s) envelope in order to illustrate the increase in oxidised carbon species after light exposure. A three component model was fitted to the C (1s) spectrum of unexposed dyed wool using a least squares peak fitting program with gaussian peak profiles, Figure 8.3. These components were fixed at binding energies of 285 eV for C-C / C-H, at 286.6 for C-O and at 288 eV C=O according to the assignments in Table 8.1 for wool. Figure 8.4 shows clearly the increase in the C=O component of this model after 156 hours exposure.

Oxygen Chemistry

Unexposed untreated wool had a symmetric O (1s) peak profile with a maximum at 532.0 eV

(relative to C (1s) at 285.0 eV). There was no significant shift in peak maximum or change in peak profile after exposure. This was also the case for Cibafast W treated wool. For dyed wool the O (1s) peak maximum gradually shifted to lower binding energy with exposure times up to 156 hours, where its value was 531.6 eV. After 208 hours the peak maximum shifted back to 532.0 eV. This shift was also found for dyed wool treated with Cibafast W, but the shift was still present after 208 hours. The shift must therefore reflect the presence of oxygen functionalities associated with the highly oxidised fabric surface.

Nitrogen Chemistry

There were no significant changes in the N (1s) peak profile with exposure for untreated wool or dyed wool. The peak maximum remained constant at 400.0 eV and there was no significant broadening or change in the symmetry of this peak with light exposure.

Sulphur Chemistry

The S (2p) spectrum of untreated wool shows one main component at 164 eV for disulphide sulphur of cystine residues, Figure 8.7. This band shows some degree of asymmetry to higher binding energy, a gaussian profile could be fitted to the band with 14% asymmetry. The asymmetry indicates the presence of a small amount of oxidised sulphur in the form of cysteic acid and intermediate oxidation products of cystine. Peaks at binding energies of 165.5 eV and 167 eV have been assigned to sulphur bonded to one or two oxygen atoms respectively[167]. The broad nature of the S (2p) envelope makes it difficult to resolve components associated with these oxidised species.

After light exposure the cysteic acid component at 168.4 eV can be clearly resolved from the disulphide band. This component increases in intensity, at the expense of the disulphide band, with increasing exposure time. Figures 8.8 and 8.9 show the S (2p) spectrum after exposure for 104 and 208 hours respectively. Other intermediate oxidation products such as cystine-S-monoxide and cystine-S-dioxide may also be present but are not resolved.

The rate of increase in cysteic acid signal relative to disulphide signal was determined using a peak fitting model to measure the relative areas of the components at 164 eV and 168.4 eV. Gaussian profiles were used with a fixed FWHM of 4.0 eV for both components, the peak maxima binding energies were not fixed.

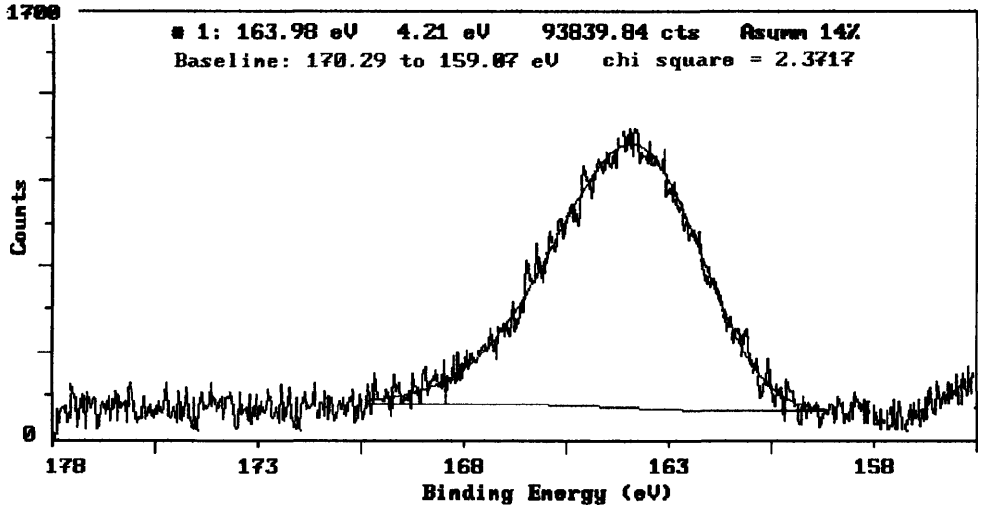

Figure 8.7 XPS S(2p) spectrum of unexposed untreated wool

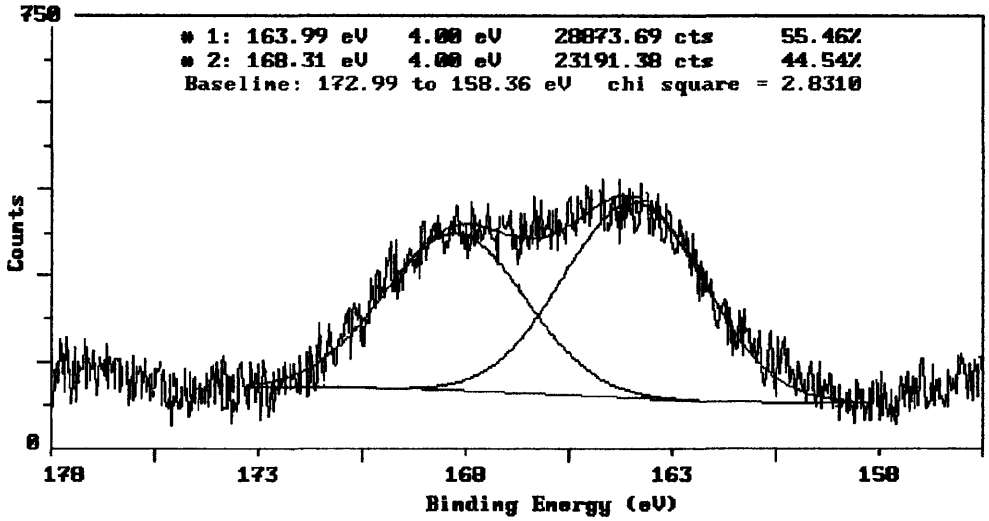

Figure 8.8 XPS S(2p) spectrum of untreated wool exposed for 104 hours

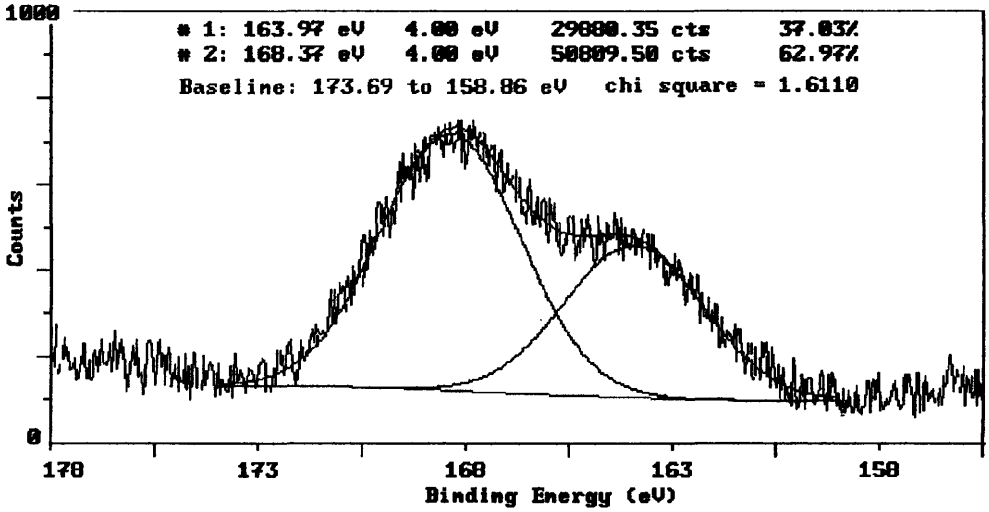

Figure 8.9 XPS S(2p) spectrum of untreated wool exposed for 208 hours

The binding energies of the two components did not shift significantly from 164 eV and 168.4 eV after exposure (relative to the C (1s) binding energy of 285 eV). The same relative sensitivity factor was assumed for both sulphur states. The peak fitted spectra are shown in Figures 8.8 and 8.9 compared to unexposed wool in Figure 8.7.

Using this model, the rate of photooxidation of disulphide sulphur to cysteic acid could be measured. Figure 8.10 plots percentage sulphur signal present as S (+6) as a function of exposure time. The rate of disulphide oxidation is compared for untreated and Cibafast W treated wool. For untreated wool, after only 26 hours exposure, approximately 30% of the disulphide sulphur has been oxidised to cysteic acid. With continued exposure the rate of increase in cysteic acid is reduced, after 208 hours 60% of the surface disulphide bonds have been oxidised to cysteic acid. The surface cystine residues are most rapidly oxidised at low level of exposure. Of the total disulphide oxidation which had occurred after 208 hours, half of this had taken place during the first 26 hours of exposure. This is in agreement with the overall rate of surface oxidation measured by the change in O/C ratio, where it was found that the surface was most rapidly oxidised during the first 26 hours with the rate slowing down and following a similar curve as that for cysteic acid with extended exposure. Figure 8.10 shows that the application of Cibafast W to wool gives no significant protection to disulphide bond photooxidation in the epicuticle. This may be explained by a low concentration of the product in the epicuticle.

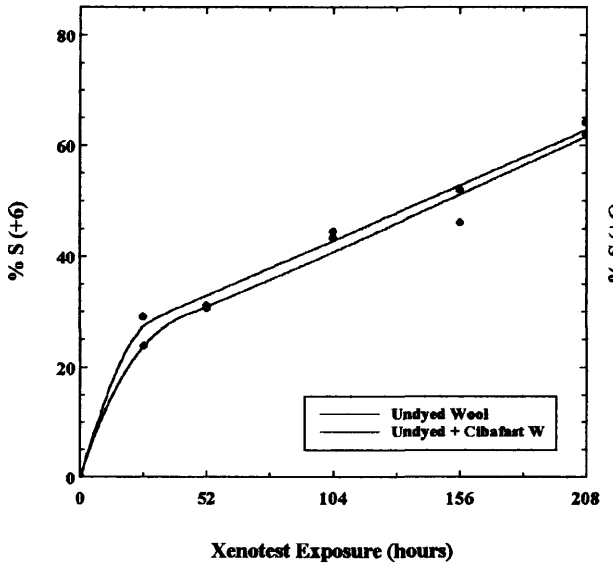

Figure 8.10 Increase in cysteic acid signal with exposure time for undyed wool fabrics

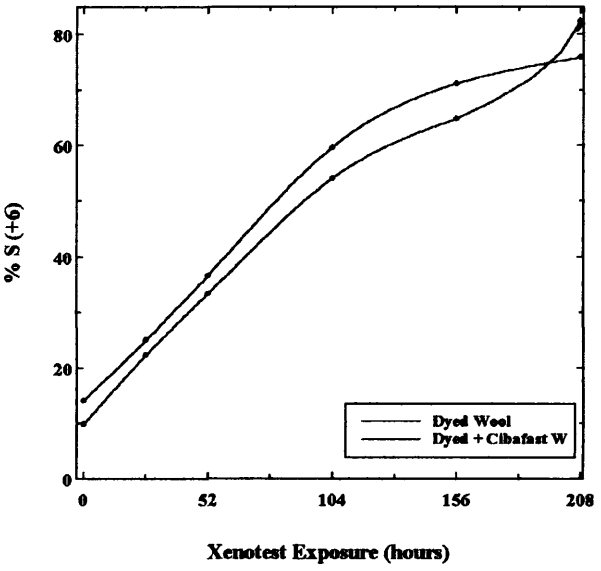

Figure 8.11 Increase in cysteic acid signal with exposure time for dyed wool fabrics

The absorber may be less effective at the immediate surface where photooxidation is most rapid and where it may be susceptible to degradation itself. It may be anticipated that if the UV absorber is migrating to the fabric surface with exposure, there will be an increase in the surface sulphonate concentration which would cause an apparent increase the cysteic acid signal intensity at 168 eV. However, any increase is likely to be relatively small and therefore would not be expected to significantly alter the signal associated with an increase in cysteic acid.

It is interesting that even after severe exposure surface cystine oxidation is incomplete, since 30-40% of the surface disulphide signal remains after 208 hours. This may be explained by the accessibility of cystine residues in the epicuticle. After an initial rapid oxidation of accessible sites, further oxidation may be limited by the location of these residues. A previous XPS study found differences between the reactivity of cystine residues with reagents in the surface of wool compared to the fibre bulk[171]. This was attributed to the reduced accessibility of these groups in the highly cross linked epicuticle compared to the fibre bulk.

The S (2p) spectrum for thermally oxidised untreated wool was also investigated as a comparison to photooxidised wool. After 6 days exposure at 115°C there was a small amount of cystine oxidation, 12% of the surface sulphur signal was present as cysteic acid. This small level of surface oxidation is consistent with the minimal increase in O/C ratio. Referring again to Table 8.2 it can be seen that after heating there are some small changes in the atomic ratios associated with sulphur. The O/S ratio increases, the S/N and S/C ratios decrease which all suggest a reduction in surface sulphur concentration and that surface cystine residues are sensitive to thermal degradation.

Using the same peak fitting procedure and constants as described for the analysis of untreated wool, the S (2p) spectrum for dyed wool was resolved into the components for disulphide and cysteic acid. Figure 8.11 plots the percentage S (+6) signal as a function of exposure time for dyed wool. The rate of increase in cysteic acid signal is also shown for dyed wool treated with Cibafast W. The unexposed dyed fabrics have a significant cysteic acid signal of approximately 15% reflecting an initially more oxidised surface compared to untreated wool. For both dyed fabrics, there is a rapid, closely linear rate of increase in cysteic acid signal up to 104 hours exposure. At this point 50-60% of the surface disulphide bonds have been oxidised to cysteic acid. With further exposure the cysteic acid signal increases at a slower rate, after 208 hours

approximately 75-85% of the surface sulphur signal is present in the oxidised form. At low exposure levels the rate of increase in cysteic acid is more rapid for undyed wool compared to the dyed wool. However, after exposure for more than 26 hours, disulphide bond oxidation occurs more rapidly and is more extensive for dyed wool. The application of Cibafast W to dyed wool does not significantly reduce the rate of surface disulphide bond oxidation.

A brief comparison was made between the extent of surface disulphide bond oxidation for 100% wool, wool / nylon and wool / polyester blend fabrics. XPS analysis was carried out on the dyed photostabilized automotive fabrics (unlaminated) which had been exposed simultaneously for 52 hours. Whilst the 100 % wool (30 μm) and wool / nylon fabrics (30 μm / 3.3 dtex) had the same cysteic acid signal intensity, the wool / polyester blend (30 μm / 3.3 dtex) had a significantly higher level of surface oxidation, Figure 8.12. Due to time limitations it was not possible to collect spectra at successive exposure levels to establish if the wool / polyester blend had a consistently higher cysteic acid signal compared to the other fabrics. If the presence of polyester does have a detrimental effect on the rate of surface photooxidation of wool it may partly explain the more rapid rate of phototendering of this blend found during abrasion testing.

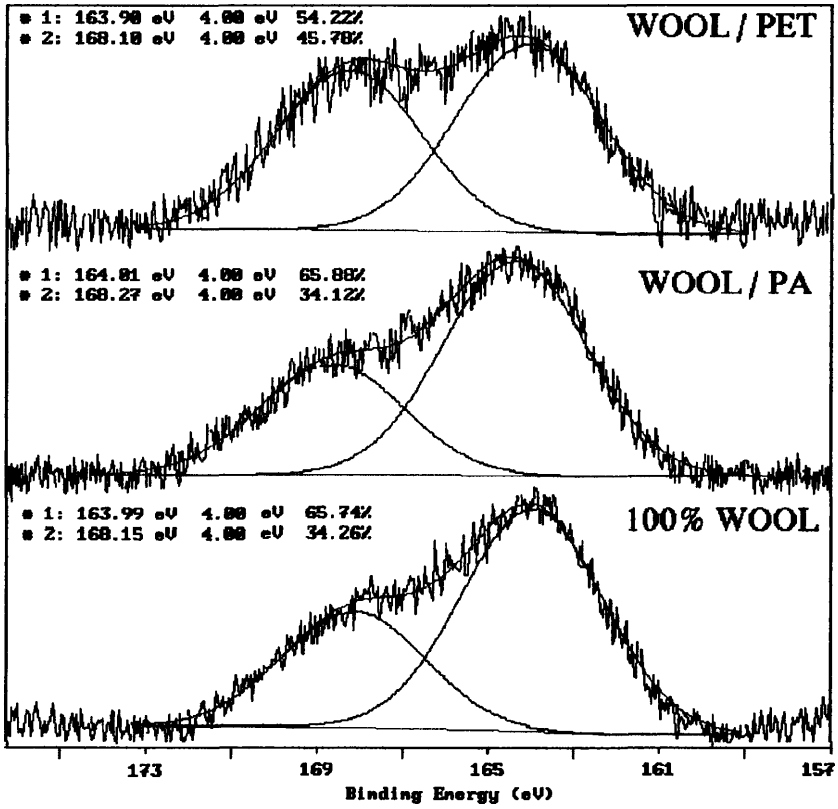

Figure 8.12 Comparison of XPS S (2p) spectra of wool fabrics after 52 hours light exposure

8.4 Static Secondary Ion Mass Spectrometry (SSIMS) Analysis of Wool

8.4.1 Introduction to SSIMS Analysis

Although XPS provides valuable surface sensitive information, it is limited in studying the nature of specific chemical species, in particular surface lipids. In SSIMS analysis, the surface of a sample is bombarded by a primary ion beam and the sputtered secondary ion fragments emitted from the surface are analysed for mass. By using a low primary ion flux density (typically 10^{-8} - 10^{-11} A / cm^{-2} at 0.1 - 10 keV) and a relatively large sampling area, the surface integrity is maintained without damage. A mass spectrum can therefore be collected which is a fingerprint of the chemical structure of the sample surface. This technique provides molecular as well as elemental information since both cluster and elemental ions are emitted. SSIMS is more surface sensitive than XPS, secondary ions are only emitted from within a depth of 1 nm of the sample surface. In contrast to XPS, SSIMS can only provide qualitative information with regard to the nature of surface species, it cannot be used for quantification.

8.4.2 SSIMS Analysis of Photooxidised Wool

Since SSIMS is particularly useful for characterising hydrocarbon material, it was used to investigate photooxidation of the lipid layer on the surface of the epicuticle. This lipid layer is known to consist of fatty acids covalently bound to the surface epicuticle protein. Chemical analysis has revealed that the main component is a C_{21} fatty acid, 18-methyleicosanoic acid (18-MEA), which represents approximately 70% of this layer by weight[228, 229]. This fatty acid is thought to be bound to the epicuticle mainly by thioester linkages to cysteine residues[230]. A proposed model of the epicuticle suggests that the surface protein is studded with fatty acid chains orientated away from the fibre[231]. It is suggested that the epicuticle protein may have a folded configuration which would give an abundance of cysteine residues at the surface for fatty acid attachment. In addition to 18-MEA, other fatty acids have been detected in smaller amounts by chemical analysis, such as eicosanoic acid, stearic acid, oleic acid and palmitic acid[18, 229]. This outer fatty acid layer is thought to function as a protective barrier which is responsible for the hydrophobic nature of the epicuticle.

A significant change in the hydrophobic nature of the wool fibre epicuticle following light exposure is shown by a considerable increase in the wettability of fabrics. Figure 8.13 plots the average wetting time for droplets of water from a pipette to be absorbed into the surface of

untreated wool fabrics exposed for successive Xenotest periods. The rate of increase in fabric wettability for untreated wool correlates closely with the rate of surface photooxidation of the epicuticle measured by the XPS O/C ratio (Figure 8.1). This increase in wettability indicates photodegradation of the lipid layer.

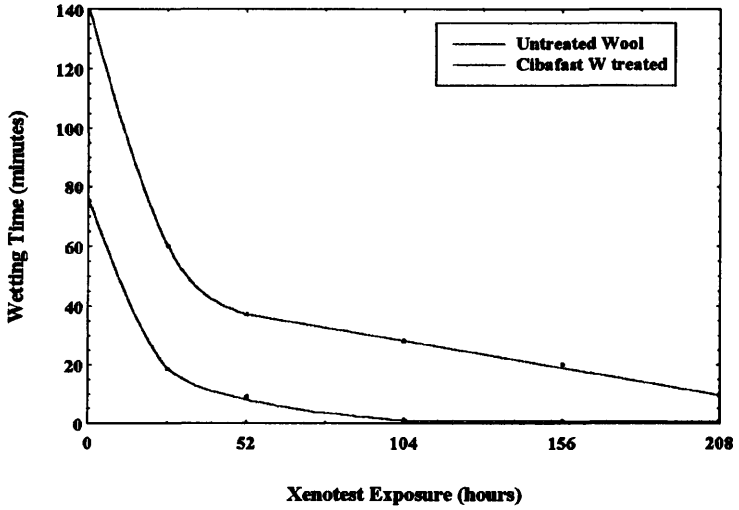

Figure 8.13 Increase in wettability of wool fabrics with light exposure

Only one study has previously used SSIMS to characterise the surface of untreated wool[173]. Three peaks were detected and assigned by their atomic mass to fatty acid species. The lowest intensity peak at 311 atomic mass units (a.m.u.) was assigned a C_{20} fatty acid, eicosanoic acid ($C_{19}H_{39}COO^-$). A peak at 325 a.m.u. was assigned to the C_{21} fatty acid, 18-MEA, ($C_{20}H_{41}COO^-$). The highest intensity peak at 341 a.m.u. was assigned to hydroxylated 18-MEA ($C_{20}H_{40}OHCOO^-$). These assignments assume an oxygen ester attachment rather than a thioester. The 341 a.m.u. assignment for the hydroxylated species was subsequently questioned by other workers on the grounds that no covalently bound hydroxylated fatty acids had been isolated from chemical analysis of the wool epicuticle [232]. Since 18-MEA is known to be mainly bound by thioesters, the peak at 341 a.m.u was assigned to the thiolate ion of 18-MEA ($C_{20}H_{41}COS^-$).

The SSIMS spectrum of scoured untreated wool is shown in Figures 8.14 (a-c). Apart from the distinct peaks at 341, 325 and 311 a.m.u, there were other high atomic mass peaks which have not previously been assigned for wool. These occurred at 326, 299, 297, 283, 281, 271 and 255 a.m.u. Assignments are given for these peaks in Table 8.6 based on the atomic masses of the fatty acid species, palmitic, stearic and oleic acids, which have been detected by

chemical analysis of this layer. Each of the fatty acids shown in Table 8.6 has a signal assigned to both -COS^- and -COO^- ions, implying both thioester and oxygen ester attachments.

The intensity of each of the SSIMS peaks was measured, from which the relative percentages of each of the fatty acid species was calculated for both unexposed wool and after 208 hours exposure. In Table 8.6 the relative percentages for each of the ion species is shown, along with the total percentage for each fatty acid species. The total relative percentages of the fatty acids calculated from the SSIMS spectra for unexposed wool, are in agreement with the relative percentages established from chemical analysis of this layer for merino wool [231].

The SSIMS spectrum after light exposure is shown in Figure 8.14 (d-f). Table 8.6 shows that the total relative percentages of each of the fatty acids remain in similar proportions to those for unexposed wool. However, there is a reduction in the total 18-MEA concentration relative to the other species and an increase in the total eicosanoic acid signal. There is a distinct change in the relative intensities of the two 18-MEA species after exposure. There is a decrease in the -COS^- signal at 341 a.m.u. and an increase in the -COO^- signal at 325 a.m.u. The large reduction in the 341 a.m.u signal relative to that at 325 a.m.u is shown clearly by comparing Figures 8.14 (a) and (d). The considerable reduction in this strong signal indicates clearly that 18-MEA is susceptible to photooxidation. A reduction in the concentration of 18-MEA has previously been found in weathered wool [231].

Table 8.6 SSIMS relative spectral intensities of surface lipids on untreated wool

Fatty Acid Species		SSIMS Peak (a.m.u.)	Relative Percentages			
			Unexposed Wool		Exposed (208 hrs)	
18-MEA	$C_{20}H_{41}COS^-$	341	55.8	**63.4**	37.8	**58.5**
	$C_{20}H_{41}COO^-$	325	7.6		20.7	
Eicosanoic acid	$C_{19}H_{39}COS^-$	326	3.8	**9.9**	5.9	**14.2**
	$C_{19}H_{39}COO^-$	311	6.1		8.3	
Stearic acid	$C_{17}H_{35}COS^-$	299	2.3	**8.9**	4.8	**9.1**
	$C_{17}H_{35}COO^-$	283	6.6		4.3	
Oleic acid	$C_{17}H_{33}COS^-$	297	2	**5.6**	3.9	**6.8**
	$C_{17}H_{33}COO^-$	281	3.6		2.9	
Palmitic acid	$C_{15}H_{31}COS^-$	271	3.6	**12.2**	3.1	**11.4**
	$C_{15}H_{31}COO^-$	255	8.6		8.3	

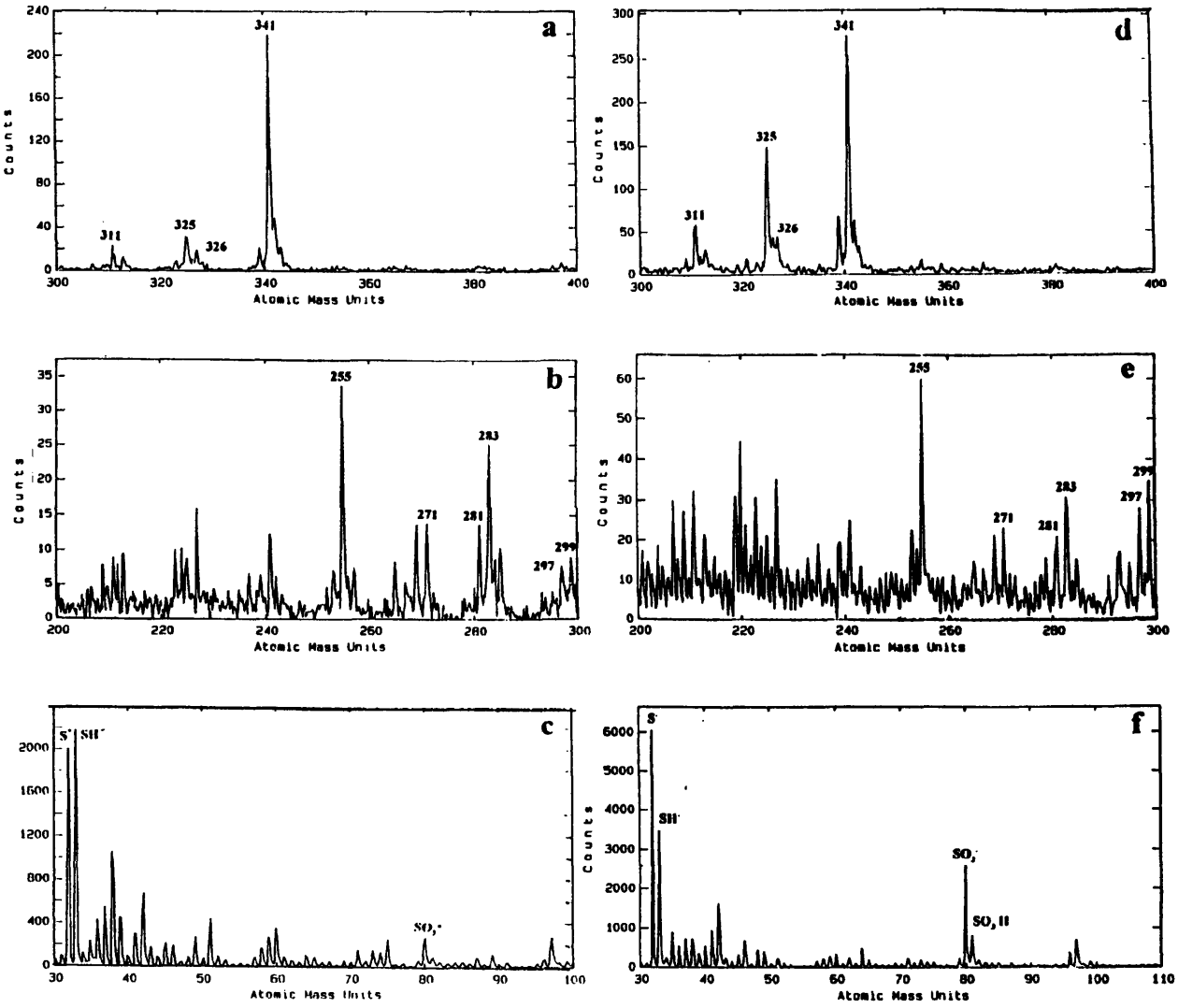

Unexposed Wool Exposed Wool (208 hrs)

Figure 8.14 Negative ion SSIMS spectra of untreated wool fabrics

SSIMS analysis of chlorinated and plasma treated wool also show similar, but much larger reductions in the signal at 341 a.m.u. relative to the other fatty acid signals[233]. It is known from chemical analysis that chlorination reduces the concentration of bound 18-MEA on the wool epicuticle [230].

This implies that there is a significant reduction in the concentration of 18-MEA after light exposure. In section 8.3.1, the XPS C/N ratio was found to decrease after exposure, further indicating a loss of carbon rich material. Unfortunately, the SSIMS technique does not allow absolute band intensities to be compared between spectra, so it is not possible to quantify the extent of lipid loss after light exposure. Although these results indicate photodegradation of

the lipid layer, signals for the fatty acid species are still present in the SSIMS spectra after quite severe light exposure indicating that it is not completely degraded. In addition, after 208 hours exposure, the XPS C/N ratio still remained much higher than would be expected for complete removal of the lipid layer. Although these results indicate that the lipid layer is only partially degraded the large increase in fabric wettability suggests uneven removal or perforation of this layer after light exposure.

The SSIMS spectrum of unexposed wool shows a strong sulphur signal at 32 a.m.u. compared to the intensity of the fatty acid signals, indicating large concentrations of cystine in the outer 1 nm of the wool fibre, Figure 8.14 (c). Smaller signals are present at 80 and 81 a.m.u. for cysteic acid (SO_3^- and SO_3H). After light exposure there are significant increases in these signals assigned to cysteic acid relative to the unoxidised sulphur signal at 32 a.m.u (compare Figures 8.14 (c) and (f)). The intensity ratio SO_3^- / S^- (80 / 32 a.m.u) was 0.13 for unexposed wool increasing to 0.43 after exposure. This confirms photooxidation of surface cystine residues as found from XPS analysis. As a means of comparison, the SO_3^- / S^- intensity ratio for chlorinated hercosett treated wool was much larger at 1.9.

8.5 Microscopical Surface Analysis of Wool

Changes in the surface morphology of photooxidised wool fibres were examined using Scanning Electron Microscopy (SEM) and Atomic Force Microscopy (AFM). Although SEM is the conventional technique used for the analysis of textile samples, the advantages of AFM in terms of resolution, the ability to rapidly measure surface features and the fact that samples do not require coating, means that the technique can provide much valuable complementary information. The principle of the AFM technique is described in section 2.3, whilst the experimental conditions for both SEM and AFM analysis are described in section 4.5.

8.5.1 SEM Analysis of Photooxidised Wool

Single untreated wool fibres (35 μm crossbred) were exposed for 208 Xenotest hours and examined using the SEM. Some examples of the surfaces of these photooxidised fibres are shown in Figures 8.15 (ii) - (v) with Figure 8.15 (i) showing an unexposed fibre for comparison. None of the fibres were subject to any tensile or abrasive forces following

Figures 8.15 (i) - (vii) SEM Images of Wool Fibres

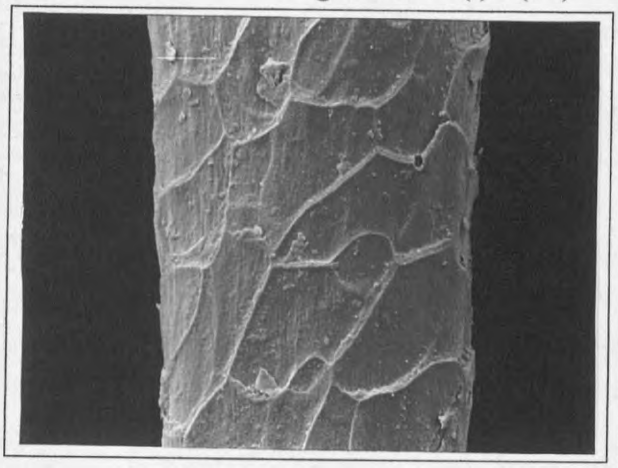

(i) Unexposed Wool Fibre: 1260 x

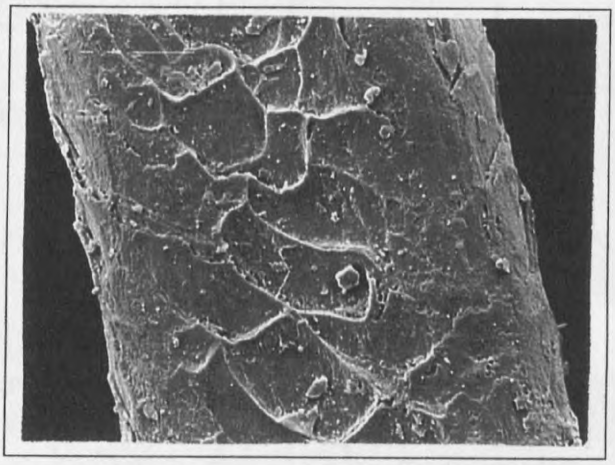

(ii) Light Degraded Wool Fibre: 1250 x

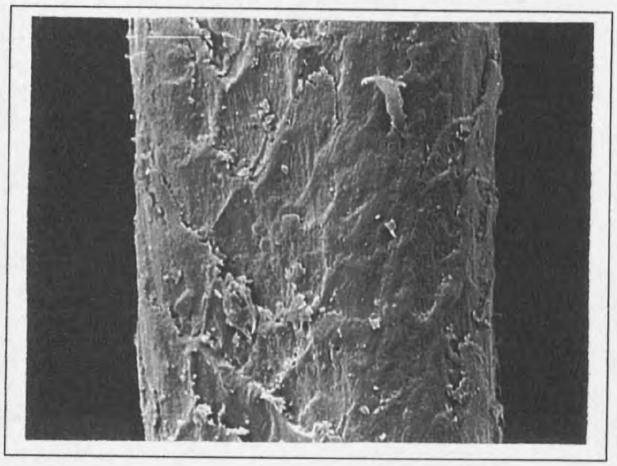

(iii) Light Degraded Wool Fibre: 1260 x

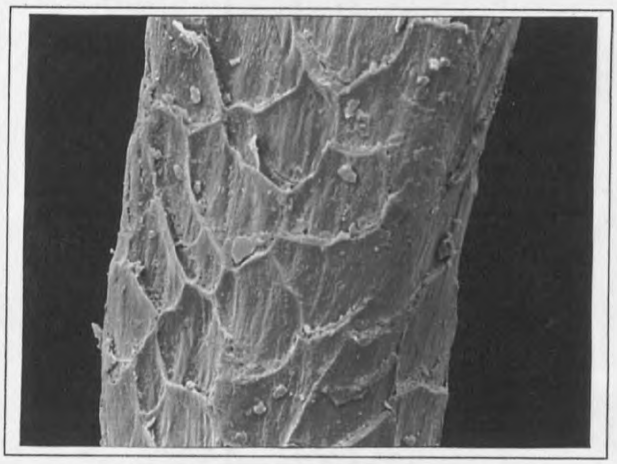

(iv) Light Degraded Wool Fibre: 1250 x

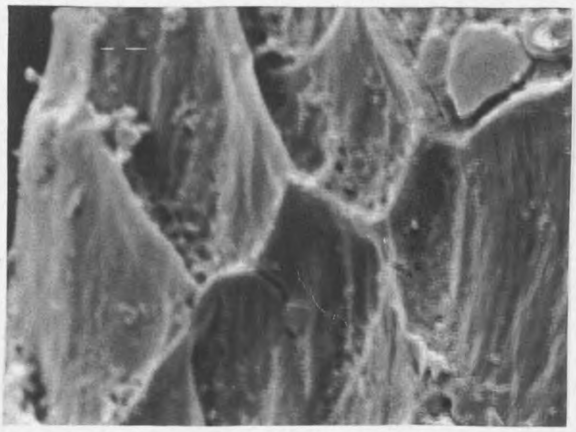

(v) Light Degraded Wool Fibre: 4500 x

(vi) Surface of Unexposed Wool: 20,000 x

(vii) Surface of Exposed Wool: 20,000 x

exposure, so the damage shown is attributed to light exposure only. The smooth, almost waxy appearance of the scale surface in unexposed wool is lost after exposure, and the fibre appears to have a more dry and granular surface. The light degraded fibres show areas where scale edge definition is no longer present, Figure 8.15 (iii). The cuticle material forming the scale edge structure has been removed or eroded to leave an uneven, raised surface which has a globular appearance. The more brittle nature of the cuticle after exposure makes the scales more easily damaged and fractured, which is shown by the debris of scale fragments present on the fibres. Fracture lines were also common across the scale surface. In other areas the scale edge structure was still present, but its definition seemed to be enhanced by a more protruding and ridged appearance suggesting erosion of the underlying cuticular material, Figure 8.15 (iv). In these areas the scale surface is no longer smooth, but has a sunken appearance with pronounced longitudinal striations. Also in these areas, the inner face of the scale edge had large perforations shown in the magnified view, Figure 8.15 (v). These perforations were not found in the scale edge structure of unexposed fibres. It suggests that damage is not confined only to the upper surface of the scale, but there is also internal damage within the cuticle layers. In Figure 8.15 (vi) and (vii) a direct comparison of the surfaces of unexposed and exposed wool both at 20,000 times magnification is shown. After light exposure the fibre surface appears clearly porous and uneven with many indentations compared to the smoother featureless surface of the unexposed fibre.

8.5.2 AFM Analysis of Photooxidised Wool

Single untreated wool fibres (35 μm crossbred) were exposed for 208 Xenotest hours and examined using the AFM. Figure 8.16 shows an AFM image of the surface of an unexposed untreated wool fibre. The image clearly shows the scale edge and detail of the upper surface of the scale which has a smooth, waxy appearance with fine surface irregularities similar in appearance to orange peel. Since the AFM constructs an image from XYZ co-ordinate points, it is possible to take two dimensional sections through images and measure specific surface details. Also shown in Figure 8.16 is a transverse sectional plot of this image with the a profile of the scale edge. The table of measurements shows that the scale height is 0.76 μm. This value is consistent with mean scale height values for crossbred wool in the range 0.7 - 0.9 μm [234]. The upper surface detail of the unexposed wool scale is shown at higher resolution in Figure 8.17. The surface has many fine undulations and small crevices. The transverse

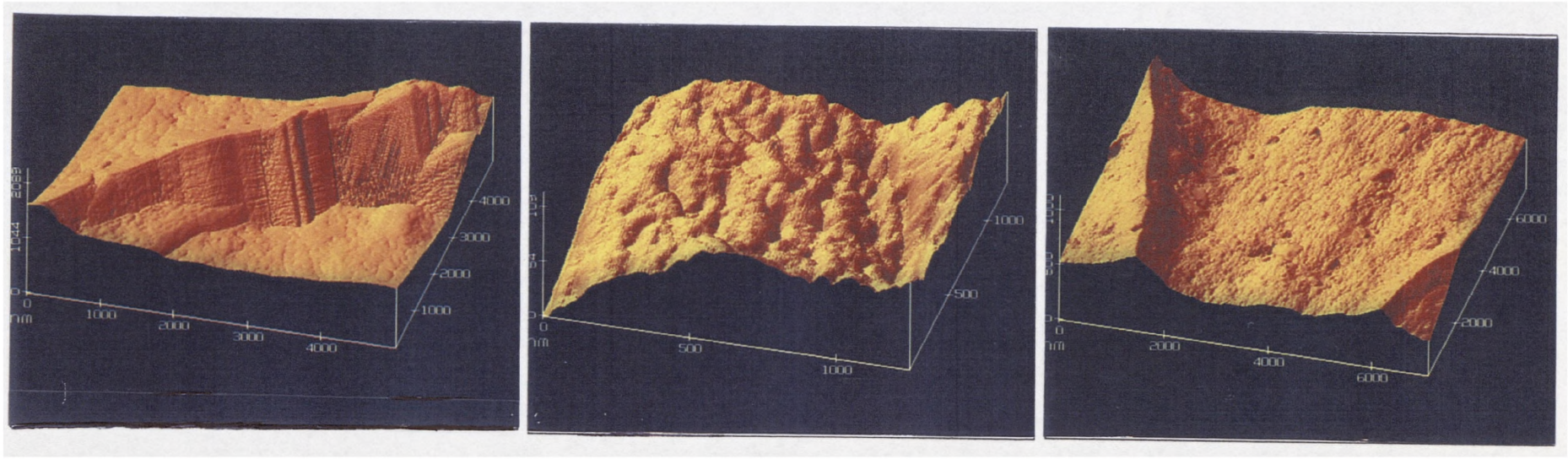

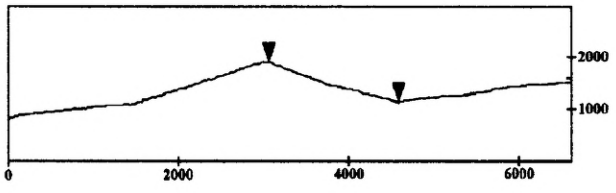

Horizontal distance [nm]	1,520
Vertical distance [nm]	758
Angle [degrees]	26.5

Figure 8.16 AFM image of unexposed wool

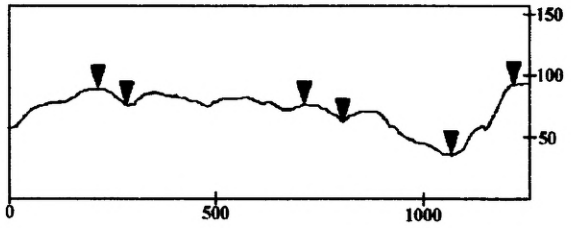

Horizontal distance [nm]	68.7	80.2	134
Vertical distance [nm]	13.5	13.3	61.5
Angle [degrees]	11.1	9.4	24.7

Figure 8.17 AFM image of unexposed wool

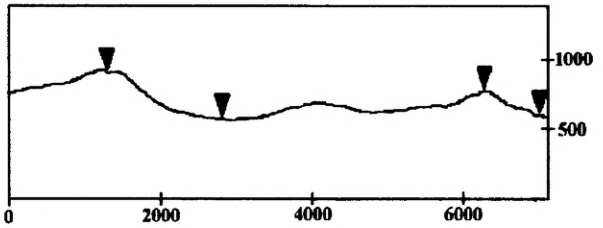

Horizontal distance [nm]	1,522	778
Vertical distance [nm]	343	183
Angle [degrees]	12.7	13.2

Figure 8.18 AFM image of light exposed wool

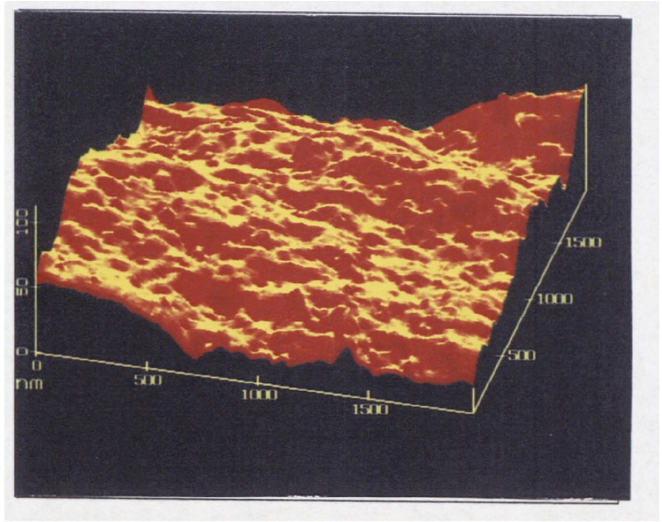

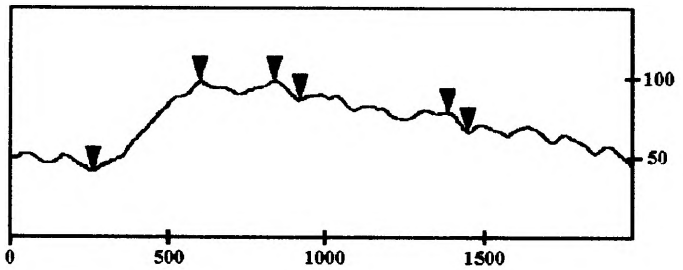

Horizontal distance [nm]	340	80	60.8
Vertical distance [nm]	52.9	11.3	11.5
Angle [degrees]	8.8	8	10.8

Figure 8.19 AFM image of light exposed wool

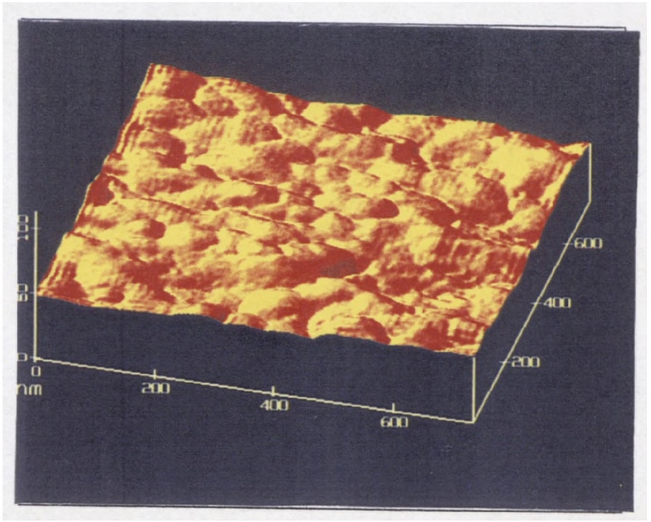

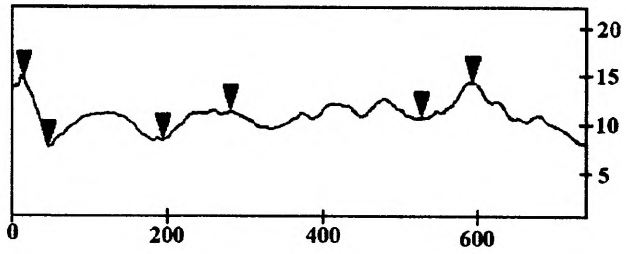

Horizontal distance [nm]	32.9	87.8	62.8
Vertical distance [nm]	7	2.9	3.2
Angle [degrees]	12	1.9	2.9

Figure 8.20 AFM image of light exposed wool

sectional plot shows that these fine surface irregularities have a depth in the cuticle surface of approximately 15 nm.

Figure 8.18 shows the surface of a wool fibre after Xenotest exposure for 208 hours. The scale edge at the left of the image has a height of 0.34 μm less than half the height of the unexposed fibre. This value lies significantly below the lower limit of variation expected for wool fibres of 0.5 μm [234]. This indicates a large loss of material from the cuticle of photooxidised wool which causes the reduction in scale height and definition as shown in the SEM images. The scale surface shown in Figure 8.18 has an eroded and granular appearance in comparison to the smoother undulating and waxy appearance of the unexposed fibre. This grained and porous appearance is similar to the surface shown in the high resolution SEM image in Figure 8.15 (vii). Figure 8.19 shows the nature of this surface at higher resolution. After light exposure the surface has lost the smooth undulations, it appears flatter but has many small ridges, asperites and evidence of pitting. Figure 8.20 shows a higher resolution image of the globular nature of this light degraded surface with features of a depth of a few nanometers.

These images show that after light exposure the surface topography of the wool alters from the waxy appearance with smooth irregular features to a flatter featureless surface which has a grained and porous appearance, with particles and pitting. At higher resolution this surface is characterised by a globular appearance. The reduction in scale height and definition after light exposure indicates a loss of surface material most likely due to fracture through the weakened cuticle. Previous studies using Transmission Electron Microscopy to examine light degraded wool [12] and hair [118] found that damage first occurred in the weak endocuticle. This was often followed by cleavage and removal of the cuticle through this layer to leave the exposed surface of the endocuticle which was globular in appearance.

8.6 Photostability of Light Stabilizers [235]

The effectiveness of a photostabilizer depends on its stability and permanence in the polymer. Reductions in the concentration of a stabiliser in a polymer may be due to photochemical degradation or physical loss. Physical loss of stabilisers from polymers is mainly due to surface

volatilization which occurs if the stabiliser has a high enough vapour pressure. This is a thermally activated process and the rate of volatilization increases with decreasing fibre thickness and increasing surface area. The extent of physical loss is governed by the rate at which the stabilizer diffuses to the surface layers of the fibre. The loss of stabiliser from the surface may itself create a concentration gradient which causes bulk to surface diffusion. The rate of diffusion depends on the properties of both the stabiliser and polymer and the compatibility of the two. The diffusion rate increases if the stabilizer has a low solubility in a particular polymer, it also increases with decreasing molecular weight, or more specifically molecular volume of the stabilizer. The greater the polarity of both the stabiliser and the polymer, the lower the rate of diffusion due to forces of attraction between the two. The introduction of long alkyl groups into stabiliser molecules also restricts the ease of diffusion. Diffusion is also governed by the free volume and hence crystallinity of the polymer. Photostabilizers are concentrated in the amorphous phases which are most susceptible to degradation, diffusion only proceeds in these more mobile amorphous regions. In these regions greater segmental mobility of polymer chains is possible which creates free space for diffusion of the stabiliser molecules. Diffusion may be restricted by the presence of crosslinking in amorphous regions which restricts chain mobility, and also by the presence of polar groups in the polymer which increase cohesive forces.

Providing that surface volatilisation is not favoured, an increase in concentration of the stabiliser in the surface layers would be beneficial giving greater protection to those regions most susceptible to photodegradation. However, it is possible that the stabiliser may be removed from the surface by other means such as abrasive wear.

Evidence for light-induced migration of a UV absorber to the surface of polyester fabrics was found using XPS analysis. The N (1s) and S (2p) regions were scanned as elemental tags for the sulphonated 2- hydroxyphenylbenzotriazole UV absorber, Cibatex APS, at the surface of both undyed and dyed polyester. For undyed polyester treated with the absorber, the N (1s) and S (2p) signals were not initially present in the unexposed fabric surface. However, after 52 hours a weak signal was present which increased in intensity with exposure time. After 208 hours the N (1s) signal at 400.2 eV and the sulphonate signal at 168 eV increased substantially indicating a significant concentration of the UV absorber at the fabric surface. The N/S ratio was 3.3 which is approximately the expected value based on the elemental composition of the

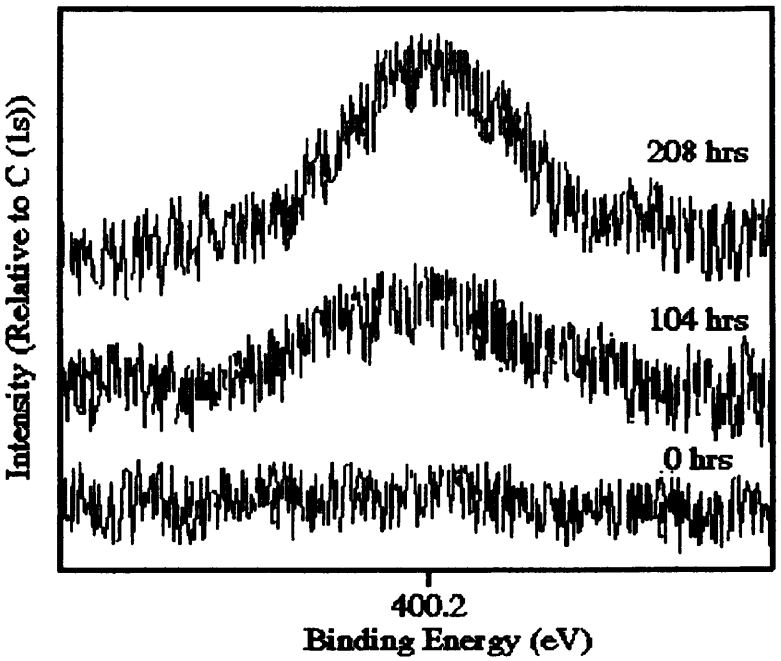

Figure 8.21 Increase in XPS N (1s) signal associated with surface migration of UV absorber in undyed polyester fabric

absorber. After 208 hours the N (1s) signal represented 0.66 % of the XPS surface elemental composition. The increase in the N (1s) signal intensity with exposure time for undyed polyester is shown in Figure 8.21 (signal intensity at each exposure time normalised against C (1s) peak intensity). For dyed polyester this effect was more difficult to determine since both untreated and treated dyed fabrics had initial nitrogen signals presumably associated with the dyestuff. Although the surface N (1s) signals for both untreated and treated fabrics increased with exposure time, there were much larger increases in signal intensity for the treated dyed fabric. This suggests that surface migration of Cibatex APS also occurs in dyed polyester.

Further evidence for diffusion of the UV absorber in light exposed polyester fabrics was obtained using FT-IR (ATR) analysis. The infrared spectrum of the UV absorber was first collected using DRIFTS analysis in order to identify characteristic bands. These UV absorber bands were too weak to be detected in the ATR spectrum of undyed unexposed polyester, or after Xenotest exposure for up to 52 hours. However, after exposure for 104 hours or more, additional bands were present at 1496 cm^{-1}, 1455 cm^{-1}, 1050 cm^{-1} and 826 cm^{-1} which could be assigned to the UV absorber on the basis of the DRIFTS spectrum. Untreated polyester exposed for the same time did not show these bands confirming that they are associated with the absorber. In Figure 8.22 the increases in intensity of the FT-IR (ATR) spectra at 1496 cm^{-1}

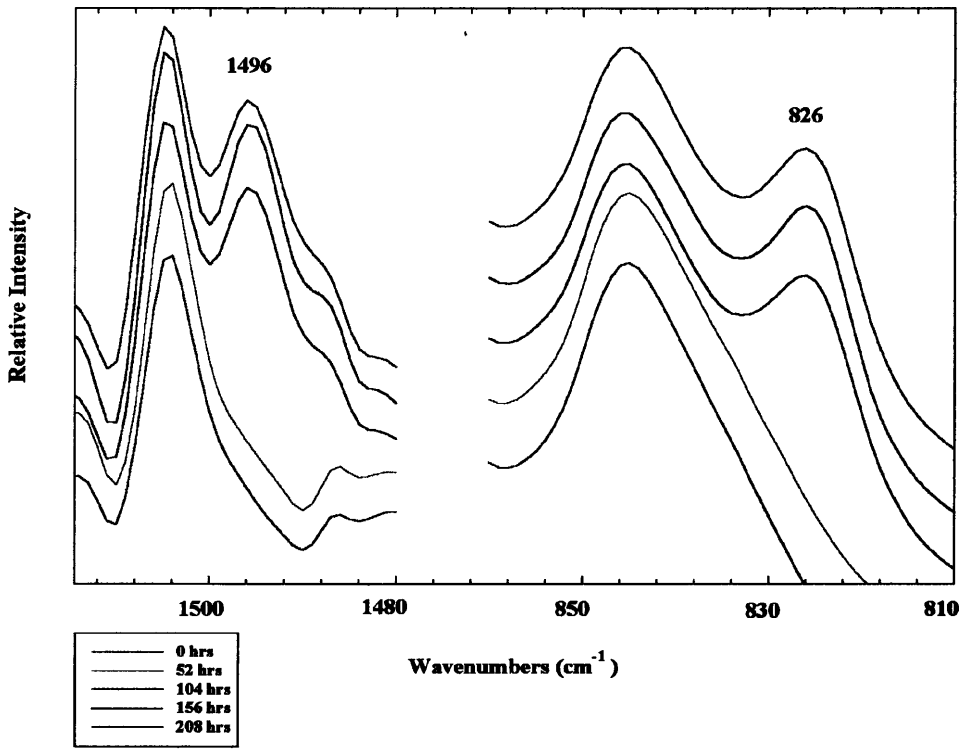

Figure 8.22 FT-IR (ATR) spectra of untreated polyester fabric showing increase in signals associated with UV absorber

and 826 cm^{-1} after exposure for more than 104 hours are shown (spectra normalised on the strong polyester C=O stretch at 1720 cm^{-1}). Analysis was carried out using a KRS-5 crystal giving an analysis depth for polyester of 3.0 - 1.5 μm in the region between 800 cm^{-1} - 1500 cm^{-1} . These results suggest that there is a significant increase in the concentration of the UV absorber in the regions closer to the surface of the fibre, presumably due to diffusion of the stabiliser from further within the bulk. This diffusion process appears to be governed by exposure time, being particularly rapid after extended exposure. Although no infrared signals were detected below 104 hours this does not imply that migration of the absorber does not take place, but that the concentration remains below the limits of detection.

In the case of dyed polyester treated with Cibatex APS, the bands for the UV absorber were initially present in the FT-IR (ATR) spectrum of the unexposed fabric. These bands were approximately 50 % of the intensity of those shown in Figure 8.22 for the undyed treated fabrics. These bands also increased in intensity with exposure time indicating that a similar surface diffusion takes place in dyed polyester.

XPS also provided evidence for diffusion of the organic copper complex stabiliser, Cibafast N, to the surface of nylon fabrics during light exposure. To examine the surface migratory effect the Cu ($2p_{3/2}$) region at 932.8 eV was scanned as an elemental tag for the stabilizer in the surface. For undyed nylon treated with the stabiliser, there was no initial signal present in the surface of the unexposed material, or after exposure for up to 104 hours. However, after extended exposure for 208 hours a copper signal was present in the XPS spectrum and quantitative analysis showed that it represented 0.07 % of the XPS surface elemental composition. This surface migratory effect was also found for dyed nylon treated with the stabiliser. Again, no copper signal was detected on the surface of the unexposed dyed fabric, but after 52 hours exposure a signal was present at 0.03 % of the elemental composition. This signal increased in intensity after 104 hours to 0.08 %, but reduced slightly with further exposure to 0.06 % after 208 hours suggesting volatilization of the product from the surface. This is shown in Figure 8.23, where the Cu ($2p_{3/2}$) signal intensity is normalised against the C (1s) peak intensity. The stabilizer has a faster rate of diffusion in the surface of dyed nylon compared to undyed nylon. This may be attributed to greater photochemical disturbance of the surface layers of dyed nylon allowing easier migration of the stabilizer.

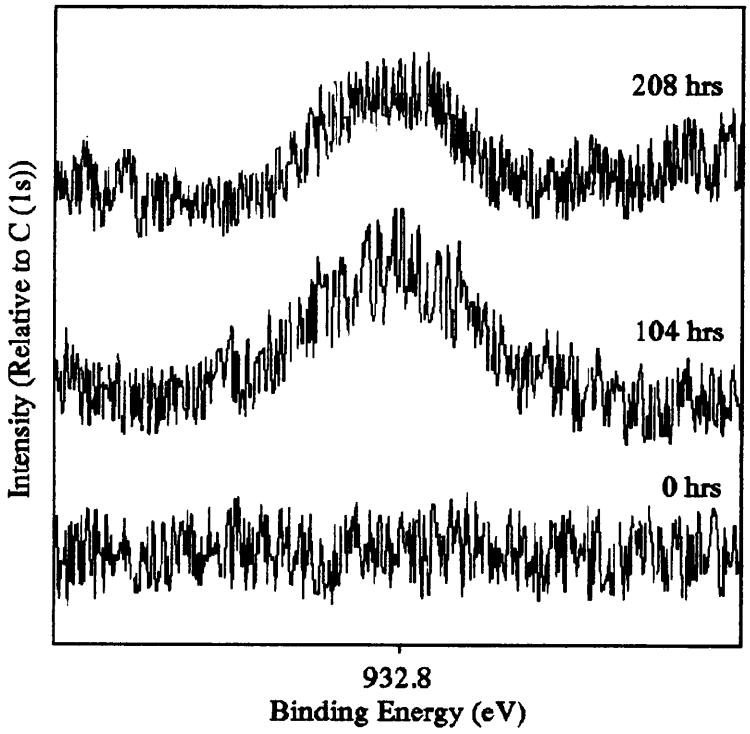

Figure 8.23 Increase in XPS Cu ($2p_{3/2}$) signal associated with surface migration of photostabilizer in dyed nylon fabric

Alternatively, ring dyeing of nylon may be responsible for a larger concentration of the stabilizer in the surface bulk.

Surface migration of Cibafast N did not occur as a result of thermal oxidation of treated nylon after exposure to the Sahara test (6 days at 115°C). Although the diffusion of stabilisers is known to be a thermally activated process, it seems that in nylon the process must rely on surface structural alterations caused by photooxidation to allow migration to take place. FT-IR bands for Cibafast N were too weak in the spectrum of treated nylon to allow an investigation of diffusion further within the nylon fibre bulk.

As mentioned in section 8.3.1, there is no distinguishing elemental tag which could allow surface migration of Cibafast W in wool to be investigated using XPS. Table 8.3 shows that in contrast to untreated wool, Cibafast W treated wool shows quite large increases in those ratios associated with nitrogen after 26 hours. This could represent an increase in Cibafast W at the surface of wool after light exposure but this cannot be confirmed. To investigate this effect further, XPS analysis of Cibafast W treated silk fabric is suggested. Since the concentration of cystine in silk is much smaller than in wool, the surface sulphur signal will be only negligible in silk. Therefore, migration of the UV absorber can be detected by increases in surface sulphonate signal.

In Figure 8.13 it was shown that Cibafast W treated wool has a much slower rate of wetting than untreated wool, indicating considerable differences in the surface properties of the two fabrics. This may implicate the presence of the UV absorber at the surface of wool which restricts the rate of diffusion of water. FT-IR (ATR) analysis proved to be of no value for examining this effect since the bands associated with the absorber were too weak to be resolved from the broad infrared absorbance of wool. Since migration of a similar UV absorber has been found in the more crystalline and less photosensitive polyester fibre, it may be anticipated that a similar process occurs in wool fibres. However, the more polar environment of the wool fibre may inhibit diffusion of Cibafast W due to forces of attraction between the wool polymer and the absorber. For example, intermolecular hydrogen bond formation between the hydroxyphenyl group of the absorber and the fibre would reduce mobility and additionally reduce the protective effect of the absorber (see sections 1.4 and 3.3.2). Cibafast W also contains a bulky *t*-butyl side group which is likely to further reduce the ease of diffusion of this product. Although photooxidation of the disulphide crosslinks in the

wool cuticle may allow less restriction for migration of the absorber, the possible formation of new intermolecular crosslinks as a result of light exposure may have an inhibiting effect.

HPLC analysis was used to investigate if there was a reduction in concentration of the UV absorber on wool after light exposure due to surface volatilization. Samples of Cibafast W treated dyed wool fabrics were analysed after Xenotest exposure for 52 hours. No significant reductions in the concentration of Cibafast W on 100% wool or wool blend fabrics were found.

FT-Raman bands associated with the ring structures of Cibafast W are particularly sharp and intense making them readily detectable in the Raman spectrum of treated wool, even at an absorber concentration of 2%. Although this technique is not surface sensitive it was used to investigate the nature of the absorber in the wool fibre and the effect of light exposure on signal intensity. In Figure 8.24 the subtraction spectrum of Cibafast W treated wool minus untreated wool is shown, leaving only those bands associated with the UV absorber. This spectrum of the absorber on wool fabric was qualitatively the same as that collected for the UV absorber in powder form and also in solution in water.

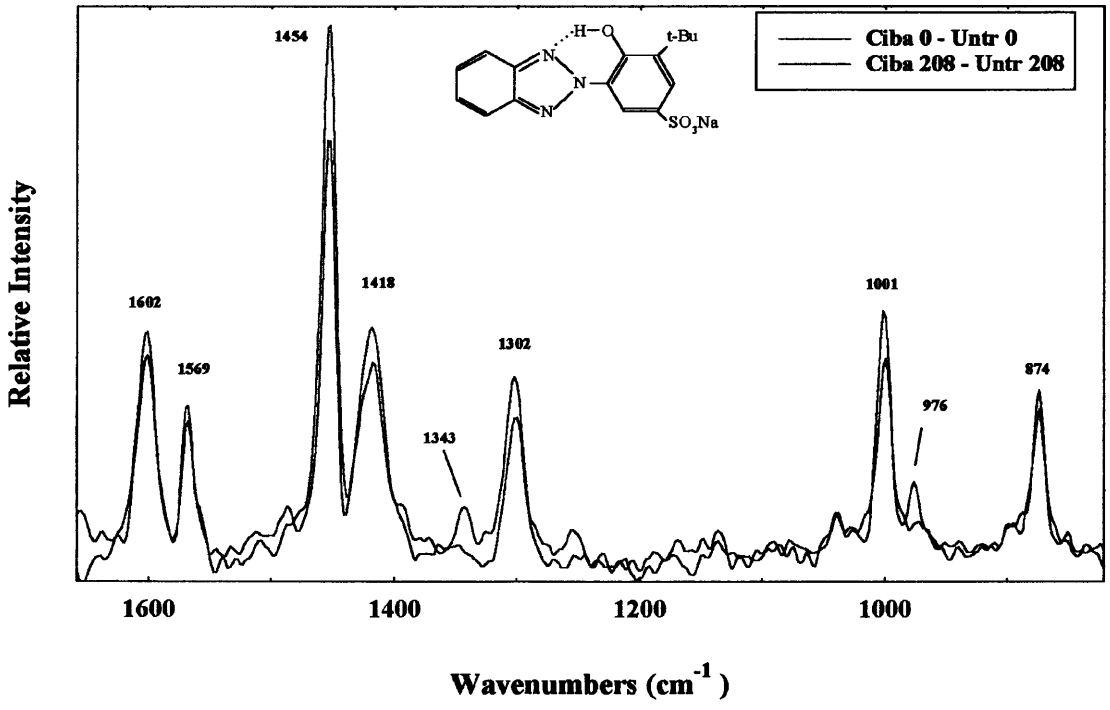

Figure 8.24 FT-Raman subtraction spectra showing UV absorber bands

The subtraction spectrum of the UV absorber in wool fabric was investigated after light exposure. For each exposure period, the spectrum of UV absorber treated wool was

subtracted from the spectrum of untreated wool exposed for the same time, therefore leaving only those bands associated with the absorber. The subtraction spectra for fabrics exposed for up to 104 hours showed no significant changes in the intensity or frequency of the UV absorber bands. However, with further exposure there were significant reductions in the intensity of a number of the UV absorber bands relative to other bands, particularly those at 1454 cm^{-1} and 1001 cm^{-1}, Figure 8.24. This may indicate an alteration in the structure of the absorber after extended light exposure. Additionally, two weak bands associated with the absorber at 1343 cm^{-1} and 976 cm^{-1} were no longer present in the spectrum after 208 hours exposure but they did appear in the subtraction spectra of fabrics exposed for up to 104 hours. Although these bands are relatively weak their absence in the spectrum of exposed wool may be of particular significance. A research note by Leaver *et al.* investigated the Raman spectrum of a sulphonated 2-(2'-hydroxy-5'methylphenyl) benzotriazole UV absorber [161]. Its spectrum was qualitatively similar to Cibafast W. The study also collected a resonance enhanced Raman spectrum of the absorber by using a UV (356.4 nm) incident laser frequency for analysis. Since the incident line coincides with electronic absorption band of the compound, those molecular vibrations coupled to the electronic transition of the UV absorber give enhanced signals in the Raman spectrum. Two bands were enhanced at 979 cm^{-1} and 1343 cm^{-1} which indicates that these bands are sensitive to the electronic transition of the UV absorber. It is therefore interesting that these two bands are absent in the subtraction spectrum of Cibafast W after extended light exposure. Although further work would be required to clarify this point, the loss of these signals may indicate a disruption of the molecular structure, altering the UV absorption characteristics of the product.

8.7 Conclusions

XPS analysis allowed photochemical changes in the wool fibre cuticle to a depth of 3 nm to be examined. From the change in O/C ratio it was found that the surface of untreated wool is most rapidly photooxidised on initial exposure to light. As exposure time increases there is a slower increase in O/C ratio suggesting that the rate of photooxidation may be limited by the accessibility of reactive sites in the surface. It could also reflect a loss of volatile oxidised species from the fibre surface. Untreated polyester shows a similar but much slower rate of surface photooxidation compared to wool, whereas surface photooxidation of untreated nylon

only becomes significant after extended exposure. Heating alone has little effect on the surface chemistry of untreated wool and polyester although a small amount of surface thermal oxidation is apparent for untreated nylon after exposure to the Sahara test.

XPS analysis of wool shows that there is an increase in oxidised carbon and sulphur species after light exposure. For untreated wool there is a progressive increase in signal intensity associated with carbonyl containing groups, such as ketones and aldehydes, with increasing exposure time. After extended exposure there is evidence for the presence of more highly oxidised carbon species at the fibre surface. Dyed wool shows a more rapid rate of surface photooxidation compared to undyed wool, with larger increases in O/C ratio and much greater increases in signal intensity associated with oxidised carbon species. The dyestuff may therefore have a photosensitizing effect at the fibre surface. This is in contrast to polyester fabrics where the presence of the dyestuff appears to reduce the rate of surface photooxidation.

Progressive photooxidation of the surface disulphide sulphur to sulphonic acid groups S (+6) was found for untreated wool with increasing exposure time. Other intermediate cystine oxidation products may also be present but could not be resolved. For untreated wool the increase in S (+6) signal is most rapid on initial exposure up to 26 hours with the rate slowing down considerably as exposure time continues. However, even after severe exposure 30 - 40 % of the surface disulphide signal still remains. This suggests that there may be differences in the accessibility of cystine residues in the surface, hindering complete oxidation. Again, more rapid photooxidation of the surface of dyed wool compared to undyed wool is reflected by much larger S (+6) signals at each exposure period.

Application of Cibafast W did not significantly reduce the rate of surface cystine photooxidation for either undyed or dyed wool. This is in contrast to the protective effect of this product at a greater surface depth which was found from FT-IR (ATR) analysis, and from Raman and FT-IR analysis of the fibre bulk. Similarly, it was found from XPS analysis of undyed nylon fabrics that application of the photostabilizer Cibafast N, did not reduce the rate of surface photooxidation. Additionally, treatment of undyed polyester with the UV absorber Cibatex APS, appeared to accelerate the rate of surface oxidation. This may indicate that the photochemical mechanisms taking place in the bulk of fibres differ from those at the surface so that compounds which have been found to be effective in the fibre bulk may not be effective at the immediate surface.

XPS analysis of photostabilized nylon and polyester fabrics found that light exposure caused these stabilizers to migrate to the fabric surface, increasing their concentration in these regions. It was not possible to establish if migration of Cibafast W similarly occurs in wool, although further work is suggested to examine this effect in silk fabric. FT-Raman analysis of Cibafast W treated wool found that there were changes in the intensity of bands associated with the UV absorber after extended light exposure. These changes could indicate an alteration in the molecular structure of the compound leading to a loss in effectiveness of the absorber.

A reduction in XPS C/N ratio was found for untreated wool after light exposure suggesting a loss in carbon-rich material from the fibre surface. SSIMS analysis allowed photooxidation of the outer lipid layer of the epicuticle to be investigated. Spectral assignments were made for the fatty acid components of this layer. The relative percentages of these species calculated from SSIMS analysis of untreated wool were in agreement with those calculated previously from chemical analysis. After extended light exposure a reduction in signal intensity assigned to the main fatty acid component, 18-methyleicosanoic acid, relative to the other signals implicated photooxidation of this species. Despite large increases in the wettability of wool fabrics after exposure, XPS and SSIMS analysis suggests that a significant lipid component is still present on the epicuticle surface. This may indicate that the lipid layer is only partially degraded or perforated during light exposure.

The combined microscopic techniques of SEM and AFM allowed changes in the surface morphology of wool fibres to be investigated. After light exposure there was a considerable loss in material from the cuticle causing a reduction in scale height and definition. At higher magnification the surface lost its smooth waxy undulating appearance and was granular with small indentations. This eroded more porous looking surface may explain the dramatic increase in wettability of fabric after light exposure and the harsher handle of fabrics.

Chapter 9

Conclusions

9.1 Summary and Conclusions

The aim of this study was to investigate the photostability of wool, relative to its performance in automotive upholstery. This involved an investigation of the effect of automotive interior environmental conditions on the physicochemical properties of wool, along with the development and performance testing of wool fabrics for this end use.
The following section summarises the main finding of this work.

On initial exposure of wool to light, phototendering is mainly characterised by reductions in fibre tenacity. The rate of loss in fibre tenacity corresponded with the rate of increase in cysteic acid signal measured from FT-IR analysis. On initial exposure of wool to light there seems to be an induction period where the rate of phototendering is much slower. This corresponds with a slower increase in cysteic acid signal, accompanied by increases in bands associated with the intermediate oxidation products of cystine. This induction period could be explained by partial oxidation of cystine residues, the disulphide bonds remaining intact. As exposure time extends, a loss in fibre extensibility is a much more serious consequence of phototendering. The loss in extensibility may therefore be a more sensitive measure of the gross changes in structural mechanics of the fibre as a consequence of disulphide bond cleavage.
FT-IR analysis showed that the rate of increase in cysteic acid signal in the surface regions, to a depth of around 2.5 μm, takes place at approximately twice the rate found for the fibre as a whole. A significant reduction in the tensile integrity of the cuticle can therefore be expected, allowing this outer surface to be fractured and damaged more easily. SEM and AFM analysis showed that after light exposure there was a considerable loss in material from the cuticle, causing a reduction in scale height and definition and leaving the surface with an eroded appearance. The tensile fracture morphology of severely degraded fibres suggested that light exposure had caused greater internal damage throughout the fibre bulk. FT-Raman spectroscopy indicated that there may have been some structural disordering in the fibre as a

consequence of cleavage of the stabilising disulphide bonds. Changes in bands sensitive to the molecular conformation of the protein chain, suggested a reduction in α-helical content in favour of more random chain conformations. Since α-helical proteins are mainly found in the microfibrils, this suggests that photooxidation may have caused a disturbance of the crystalline material in the fibre. Structural rearrangements may also explain the change in local chemical environment of tyrosine residues found from FT-Raman analysis. High tyrosine proteins are thought to occur in the matrix of the orthocortical cells and therefore this indicates some alteration in bulk fibre structure. FT-Raman and FT-IR spectroscopy detected increases in intensity in the carbonyl functional region after exposure which may be associated with main chain cleavage and the formation of α-ketoacyl groups.

Using XPS analysis, photochemical changes in the wool fibre epicuticle were examined. Oxygen is rapidly incorporated into the outermost surface of the fibre on initial exposure to light. This is reflected by increases in oxidised carbon and sulphur species. There is an increase in signal intensity associated with carbonyl containing groups, such as ketones and aldehydes. After extended exposure there is evidence for the presence of more highly oxidised carbon species such as carboxylic acids and esters. With increasing exposure time there was a gradual photooxidation of the surface disulphide sulphur to sulphonic acid groups S (+6). For untreated wool the increase in S (+6) signal is most rapid on initial exposure to light, the rate slowing down considerably as exposure time continues. However, even after severe exposure 30 - 40 % of the surface disulphide signal still remains. This suggests that complete oxidation is hindered by differences in the accessibility of cystine residues in the epicuticle. Dyed wool shows a more rapid rate of surface photooxidation compared to undyed wool, with larger increases in signal intensity associated with oxidised carbon and sulphur species. The dyestuff may therefore have a photosensitizing effect at the fibre surface.

After light exposure untreated wool had a reduction in XPS C/N ratio suggesting a loss of carbon rich material from the epicuticle. Using SSIMS analysis the effect of light exposure on the fatty acid components of the outer lipid layer of the epicuticle was investigated. There was a reduction in signal intensity assigned to the main fatty acid component, 18-methyleicosanoic acid, relative to the other signals, implicating photooxidation of this species. Despite large increases in the wettability of wool fabrics after exposure, XPS and SSIMS analysis suggest that a significant lipid component is still present. This may indicate that the lipid layer is only partially degraded or perforated during light exposure. AFM and SEM analysis showed that

the surface of the wool fibre lost its smooth waxy appearance after exposure, becoming granular with small indentations. This eroded more porous looking surface may explain the dramatic increase in wettability of light degraded wool fabrics.

In contrast to the considerable photochemical changes which were found from FT-Raman and FT-IR analysis of untreated wool, much higher surface sensitivity was required to detect any significant spectral changes in nylon and polyester fabrics. This indicates that photooxidation is limited to regions much closer to the surface. Following light exposure, both polyester and nylon had changes in conformationally sensitive bands, indicating apparent increases in crystallinity. These spectral changes are most likely associated with reordering of the polymer chains in the amorphous regions close to the surface following photooxidative chain cleavage. This oxidative crystallisation may alter the surface properties of fibres making them more brittle and susceptible to mechanical damage. Additionally, XPS analysis showed that the photooxidation of the outermost surfaces of nylon and polyester fabrics occurred at a much slower rate than wool.

Application of the UV absorber Cibafast W to wool significantly reduces the rate of photoyellowing under automotive environmental conditions. The absorber gives the greatest protective effect over short term exposure periods, where the rate of photoyellowing is most rapid. However, its effectiveness also diminishes most rapidly over this period. This suggests that the absorber may itself be susceptible to photochemical degradation. Cibafast W also significantly reduces the rate of thermal yellowing of wool, but the stabilizing mechanism is unclear. The stabiliser Cibafast N, known to be an effective hydroperoxide decomposer for polyamides, gave a similar level of protection to thermal yellowing of wool as it did to nylon. In addition, when Cibafast W and Cibafast N were used in combination on wool they appear to act synergistically giving much greater protection to thermal yellowing. However, Cibafast N gives no protection to photoyellowing of wool, highlighting that the mechanisms involved in these two yellowing processes differ.

Cibafast W also improves the short term lightfastness performance of dyed wool, but there is a rapid loss in effectiveness with exposure time. Application of a similar class of UV absorber to dyed polyester had a larger protective effect and there was a slower loss in effectiveness. This suggests that effectiveness of these compounds is influenced by the photostability of the substrate to which they are applied.

The short term effectiveness of Cibafast W is also shown by its protection to phototendering of wool. At low exposure levels it gives almost complete protection to losses in yarn tensile properties, but as exposure time extends the protective effect of the absorber diminishes and tendering occurs at a similar rate as untreated wool. This protective effect can be explained by the fact that the absorber reduces the rate of cystine photooxidation. FT-IR analysis of the wool surface and bulk found that Cibafast W was effective in reducing the rate of increase in cysteic acid signal when applied to both undyed and dyed wool. This protective effect through the fibre bulk was further confirmed from Raman spectroscopy. There was a slower rate of reduction in disulphide bond signal, particularly at low exposure levels. FT-IR analysis also showed that Cibafast W treated wool had a slower rate of increase in carbonyl absorbance suggesting that it protects other photosensitive sites in wool.

Despite the protective effect of Cibafast W in the bulk and surface bulk, XPS analysis showed that it seems to have little effectiveness on outer surface of the fibre. Application of Cibafast W did not significantly reduce the rate of surface cystine photooxidation for either undyed or dyed wool. Similarly, XPS analysis of undyed nylon found that application of the photostabilizer Cibafast N, did not reduce the rate of surface photooxidation. Treatment of undyed polyester with the UV absorber Cibatex APS, appeared to accelerate the rate of surface photooxidation. This may indicate differences between surface and bulk photochemistry so that compounds which have been found to be effective in the fibre bulk may not be effective at the immediate surface. Photostabilizers may themselves be susceptible to degradation at the surface, and therefore have a photosensitizing effect on the substrate. XPS analysis of photostabilized nylon and polyester fabrics found that light exposure caused these stabilizers to migrate to the fabric surface, increasing their concentration in these regions. It was not possible to establish if this migration occurs in Cibafast W treated wool, although in section 9.2 further work is suggested to examine this effect in silk fabric. FT-Raman analysis of Cibafast W treated wool found that there were relative intensity changes in the bands associated with the UV absorber after extended light exposure. These changes could indicate an alteration in the molecular structure or chemical environment of the absorber, leading to a loss in effectiveness. However, further work would be required to interpret the nature of these changes.

Due to the rapid rate of photoyellowing which occurs when wool is first exposed to light, the short term colour stability of dyed wool fabrics is seriously reduced compared to polyester and

nylon fabrics whose undyed substrates have no photoyellowing tendency. Since the rate of wool photoyellowing decreases with mean fibre diameter, the lightfastness performance wool fabrics can be improved by using coarser wool qualities. Similarly, the lightfastness performance of polyester and nylon reduces with fibre fineness. Despite the improvement given by the addition of Cibafast W, the lightfastness performance of dyed wool still remains substantially poorer than photostabilized dyed polyester and nylon fabrics, which are currently used in automotive upholstery. None of the 100% wool fabrics which were developed passed even the most lenient industry standards for lightfastness performance. Therefore wool can only enter this market place if it is used in a synthetic fibre blend. Blends produced from 30 μm and 35 μm wool qualities with 35% polyester or nylon content will meet Rover Group specifications. Since considerable differences exist between the severity lightfastness test methods used by car manufacturers, the percentage synthetic fibre component required in the blend would need to be altered accordingly. It was estimated that for a wool blend fabric to meet General Motors requirements the wool content of the fabric must not exceed 40%. The severity of the Ford test means that fabrics with a wool content of more than 20% are unlikely to meet the required standard.

Lightfastness performance of wool automotive fabrics is reduced after lamination. There was a 25% reduction in performance after the fabrics were laminated to a 3 mm polyester urethane foam and a 50% reduction for a foam thickness of 6 mm. This can be mainly attributed to heat build up within the foam, which leads to an increase in fabric surface temperature. Often, two different foam thicknesses can be used on the same seat which may lead to differences in fabric lightfastness depending on seat area. It is not clear if photostability is influenced by the presence of foam deposits found on the surface fibres. The application of surface treatments such as softening agents to improve the handle of coarse wool fabrics must also be carefully considered since a number of these treatments have been found to accelerate fabric fading.

Although phototendering is confined to fibres in the fabric surface it has much more serious consequences for the physical integrity of fabrics than is apparent from measuring the tensile loss of fabrics. All the fibres in the fabric will have points along their lengths where they uppermost in the fabric surface and suffer phototendering, causing the rate of abrasive breakdown to be accelerated. The large reductions in extensibility and increasing brittleness of wool fibres with light exposure allows fibre fracture and removal to occur extremely rapidly

with little resistance. Therefore, there is a considerable advantage in using stronger wool fibres. The abrasion resistance of 100% wool and wool blend automotive fabrics increases substantially with increasing mean wool fibre diameter, this improvement is maintained regardless of exposure time . For coarse wool fabrics, phototendering is less apparent at low exposure levels, retaining a higher proportion of their original abrasion resistance. The correct choice of synthetic fibre component for wool blend fabrics is imperative since it may accelerate abrasive breakdown. A very high level of abrasion resistance can be achieved by blending wool with nylon. These blends maintained an acceptable abrasion resistance even after severe light exposure and were able to meet current automotive performance standards. A nylon blend was found to retain its abrasion resistance almost entirely up to 52 hours exposure. This suggests that the nylon component has a protective effect over moderate exposure levels able to compensate for the loss in wear resistance of the phototendered wool. In comparison, blending wool with polyester does not significantly improve abrasion resistance. The rate of surface breakdown of polyester blends is governed by the process of pilling, with light exposure accelerating the rate of pill formation. Pilling makes these fabrics aesthetically unacceptable for automotive end use.

Light exposure also increases the flexural rigidity of wool fabrics and reduces elastic recovery following shear, bending and tensile deformations. The desirable handle properties of the fabric surface are also impaired, there is an increase in roughness and harshness and a decrease in fullness. After the fabric is laminated these changes in handle as a result of light exposure are more noticeable.

The aesthetic qualities of wool and advantages of comfort and flame retardancy will ensure that there will always be an interest in using wool in the automotive industry. In this study, wool blend fabrics were found to meet one car manufacturer's performance specifications for lightfastness and wear resistance. Additionally, a seat wear trial which was conducted as part of this research found that these wool blend fabrics do perform in service. Unfortunately, the lightfastness performance standards currently demanded by many car manufacturers generally prohibits the entry of wool rich fabrics into mass market sectors. In order for wool rich fabrics to be accepted, considerable improvement in lightfastness performance of dyed wool is required. Although Cibafast W has been shown to improve the photostability of wool, a product which gives a greater and longer term effectiveness is required. Research over the last 20 years has examined a large range of photostabilizers for wool and this has led ultimately to

the development of Cibafast W. It is unlikely that in the near future a more effective photostabilizer will be developed which is capable of improving the lightfastness performance of dyed wool to the level demanded by the automotive industry.

9.2 Suggestions for Further Work

Since FT-Raman spectroscopy is still a relatively new technique for chemical analysis of wool, more work is needed in order to interpret spectral changes. In particular, further work is required to establish the nature of the species responsible for the new Raman band at 977 cm^{-1} which appears to be sensitive to photochemical changes in the wool fibre. It is suspected that this band may be sensitive to structural rearrangements in the fibre, possibly reflecting changes in protein chain conformation. FT-Raman analysis of wool fabrics after various chemical treatments may help to characterise this band.

Tryptophan residues are most widely considered to be involved in wool photoyellowing. Although Raman spectroscopy provides a means of non-destructive analysis of these residues, the low concentration of tryptophan in wool means that assigned bands are too weak to investigate photooxidation of tryptophan. However, by employing the resonance Raman technique, it may be possible to investigate the nature of the chromophores responsible for the photoyellowing of wool, along with those responsible for the initial yellowness and thermal yellowing of wool. By using an excitation wavelength which falls in the electronic absorption band of these chromophores, a resonance enhanced spectrum of bands associated with the particular chromophore can be produced, giving a spectral fingerprint of the nature of the species responsible.

Since Raman spectroscopy gives particularly strong bands for UV absorbers on wool and other natural fibre substrates, a more detailed investigation of the effect of light exposure on these compounds could be made in order to examine the loss in effectiveness. The effect on the Raman spectrum of a change in the chemical environment of the absorber could be investigated by collecting spectra of the absorber in polar and non polar solvents.

Further work could be carried out using XPS to establish if light induced surface migration of Cibafast W occurs in protein substrates using silk fabric. Since the concentration of cystine in silk is much smaller than in wool, the surface sulphur signal will be only negligible in silk. Therefore, migration of the UV absorber can be detected by increases in surface sulphonate

signal. Additionally, analysis of Cibafast N treated wool before and after light exposure would give some indication if migration of photostabilizers in wool can take place. The copper content of Cibafast N means that it has a distinctive elemental tag which would allow XPS analysis.

If access to XPS equipment with higher resolving power is possible, more detailed analysis of the nature of oxidised carbon species formed on the surface of wool during light exposure would be of interest.

It may be possible to improve the effectiveness of Cibafast W on wool by applying it in combination with other classes of photostabilizer such as antioxidants. Further work is needed to investigate combination treatments which act synergistically to improve the short term lightfastness performance of dyed wool.

Further work is suggested to examine the effect of surface softening treatments on the photostability of wool and their influence on lightfastness performance and wear resistance of fabrics. The rate of surface photooxidation of wool after treatment with a range of these softeners could be examined using FT-IR (ATR) spectroscopy. The incorporation of hindered amine groups into silicone based softeners has recently been found to reduce the oxidative yellowing of softeners which occurs on many fabrics during use [243]. These new softeners could be evaluated for use on wool, with particular interest in any photoprotective effect they may give at the surface. It would also be interesting to investigate if softening treatments could be modified with antioxidants to improve the photostability of wool.

Further work is needed to evaluate the influence of the foam laminate on the lightfastness performance of wool fabrics. Factors such as foam type, density and thickness could be examined. Alternative backing products to the traditional foams, such as uncut polyester double needle bar raschel fabrics, could be evaluated. This study found that foam degradation occurred as a result of light exposure of fabrics, leaving foam deposits on the surface fibres. Work is required to establish if these deposits have any detrimental effect on photostability and wear resistance of wool fabrics.

Since little published work was found using vibrational spectroscopy to characterise changes in the chemistry of nylon and polyester fibres after light exposure, an FT-IR (ATR) polarisation study is suggested to examine surface conformational changes in more detail.

References

1 R.W.Singleton, P.A.C.Cook, *Text. Res. J.*, **39**, 43, (1969)
2 Technical Information, Pilkington Automotive Glazing Products Ltd, UK.
3 M.A.Parsons, Rover Group, 'Fabric Requirements for Automotive Use' Autotech Conf., Birmingham NEC., Paper No. C427/9/079, (1991)
4 R.G.Merrill, C.W.Roberts, *J. Appl. Polm. Sci.*, **21**, 2745, (1977)
5 A.Wootton, *JSDC*, **108**, 239, (1992)
6 H. Baumann, 'Applied Aspects of Keratin Chemistry', in 'Fibrous Proteins: Scientific, Industrial and Medical Aspects', Ed. D.A.D.Parry, L.K.Creamer, Academic Press, **1**, 299, (1979)
7 I.J.O'Donnell, E.F.Woods, *J.Polym. Sci.*, **21**, 397, (1956)
8 J.M.Gillespie, 'Cellular and Molecular Biology of Intermediate Filaments', Ed. R.D.Goldman, P.M.Steinert, Plenum Press, New York (1990)
9 J.M.Gillespie, 'Biology of the skin and hair growth' Ed. A.G.Lyne, B.F.Short, Angus & Robertson, Sydney, 377, (1965)
10 J.M.Gillespie, R.L.Darskus, *Aust. J. Biol. Sci.*, **24**, 1189, (1971)
11 H.Zahn, M.Biela, *Eur. J. Biochem.*, **5**, 567, (1968)
12 D.F.G.Orwin, R.W.Thomson, *Proc. 5th Int. Wool Text. Res. Conf.* Aachen, **II**, 173, (1975)
13 J.H.Bradbury, N.L.R.King, *Aust. J. Chem.*, **20**, 2803, (1967)
14 J.H.Bradbury, G.V.Chapman, N.L.R.King, *Aust. J. Biol. Sci.*, **18**, 353, (1965)
15 N.L.R.King, J.H.Bradbury, *Aust. J. Biol. Sci.*, **21**, 375, (1968)
16 J.D.Leeder, J.H.Bradbury, *Nature*, **218**, 694, (1968)
17 J.D.Leeder, J.A.Rippon, *JSDC*, **101**, 11, (1985)
18 D.J.Evans, J.D.Leeder, J.A.Rippon, D.E.Rivett, *Proc. 7th Int. Wool Text. Res.Conf.*, Tokyo, **I**, 135, (1985)
19 J.H.Bradbury, K.F.Ley, *Aust. J. Biol. Sci.*, **25**, 1235, (1972)
20 J.D.Leeder, R.C.Marshall, *Text. Res. J.*, **52**, 145, (1982)
21 J.H.Bradbury, *Adv. Protein Chem.*, **27**, 111, (1973)
22 R.D.B.Fraser, G.E.Rogers, *Aust. J. Biol. Sci.*, **8**, 288 (1955)
23 W.G.Crewther, *Proc. Int. Wool Text. Res. Conf.* Aachen, **I**, 1, (1975)
24 J.H.Bradbury, V.G.Kulkarni, *Text. Res. J.*, **45**, 79, (1975)
25 J.M.Gillespie, M.J.Frenkel, *Proc.5th Int.Wool Text. Res. Conf.* Aachen, **II**, 265 (1975)
26 M.S.C.Birbeck, E.H.Mercer, *J. Biophys. Biochem. Cytol.*, **3**, 203, (1957)
27 V.G.Kulkarni, R.M.Robson, A.Robson, *Appl. Polym. Symp.*, **18**, 127, (1971)
28 M.J.Frenkel, J.M.Gillespie, P.J.Reis, *Aust. J. Biol. Sci.*, **27**, 31, (1974)
29 W.E.Savige, J.A.Maclaren, 'The Chemistry of Organic Sulphur Compounds', Ed. N.Kharasch, C.Y.Meyers, Pergamon Press, Oxford, **2**, 367, (1966)
30 U.Schumacher-Hamedat, J.Fohles, H.Zahn, *Proc. 7th Int. Wool Text. Res. Conf.*, Tokyo, **IV**, 120, (1985)
31 H.Baumann, L.D.Setiawan, D.Gribbin, *Surface and Interface Anal.*, **8**, 219, (1986)
32 A.Gilbert, J.Baggott, 'Essentials of Molecular Photochemistry', Blackwell Scientific Publications, Oxford, (1991)
33 B.Ranby, J.F.Rabek, 'Singlet Oxygen: Reactions with Organic Compounds and Polymers', Wiley, (1978)

34 I.L.Weatherall, *Proc. 5th Int. Wool Text. Res. Conf.* Aachen, **II**, 580, (1975)
35 C.H.Nicholls, M.T.Pailthorpe, *J. Text. Inst.*, **11**, 397, (1976)
36 T.Shiga, L.H.Piette, *Photochem. Photobiol.*, **3**, 223, (1964)
37 K.P.Ghiggino, C.H.Nicholls, M.T.Pailthorpe, *J. Photochem.*, **4**, 155, (1975)
38 I.H.Leaver, *Photochem. Photobiol.*, **21**, 197, (1975)
39 K.P.Ghiggino, C.H.Nicholls, M.T.Pailthorpe, *Photochem. Photobiol.*, **22**, 169, (1975)
40 P.Walrant, R.Santus, L.I.Grossweiner, *Photochem. Photobiol.*, **22**, 63, (1975)
41 G.J.Smith, *J. Photochem. Photobiol.*, **12**, 173, (1992)
42 R.Nilsson, P.B.Merkel. D.R.Kearns, *Photochem. Photobiol.*, **16**, 117, (1972)
43 I.B.C.Matheson, J.Lee, *Photochem. Photobiol*, **29**, 879, (1979)
44 R.W.Murray, S.L.Jindal, *Photochem. Photobiol.*, **16**, 147, (1972)
45 N.S.Allen, J.F.McKellar, *J. Polym. Sci. Macromol. Rev.*, **13**, 241, (1978)
46 N.S.Allen, J.F.McKellar, G.O.Phillips, *J. Polym. Sci. Polym. Chem.*, **13**, 2857, (1975)
47 H.A.Taylor, W.C.Tincher, W.F.Hamner, *J. Appl. Polym. Sci.*, **14**, 141, (1970)
48 B.Marek, E.Lerch, *JSDC*, **81**, 481, (1965)
49 M.Day, D.M.Wiles, *J. Appl. Polym. Sci.*, **16**, 203, (1972)
50 D.M.Wiles, *Polym. Eng. Sci.*, **13**, 74, (1973)
51 G.A.Horsfall, *Text. Res. J.*, **52**, 197, (1982)
52 H.J.Heller, *Eur. Poly. J. Suppl.*,105, (1969)
53 G.S.Egerton, A.G.Morgan, *JSDC*, **86**, 79 & 242, (1970)
54 P.Bentley, J.F.McKellar, G.O.Phillips, *Rev. Prog. Color.* **5**, 33, (1974)
55 C.H.Bamford, J.S.Dewar, *JSDC*, **65**, 674, (1949)
56 G.S.Egerton, A.G.Morgan, *JSDC*, **87**, 268, (1971)
57 N.B.Colthup, L.H.Daly, S.E.Wiberley, 'Introduction to Infrared and Raman Spectroscopy' Academic Press, New York (1975)
58 L.J.Bellamy, 'Infrared Spectra of Complex Molecules', Chapman & Hall, London, **1** (1975)
59 C.V.Raman, *Nature* (London), **121**, 501 & 619, (1928)
60 N.J.Harrick, 'Internal Reflection Spectroscopy', Interscience, New York, (1967)
61 K.Siegbahn, C.Nordling, A.Fahlman, R.Nordberg, K.Hamrin, J.Hedman, G.Johannson, T.Bergmark, S.E.Karlsson, I.Lindgren, B.Lindberg, 'ESCA: Atomic Molecular and Solid State Structure Studied by means of Electron Spectroscopy', Almquist & Wiksells, Uppsala, Sweden, (1967)
62 B.P.Straughan, S.Walker, 'Spectroscopy', Chapman and Hall, London, **3**, 240, (1976)
63 M.P.Seah, W.A.Dench, *Surface and Interface Anal.*, **1**, 2, (1979)
64 G.Binnig, C.F.Quate, C.H.Gerber, *Physical Rev. Lett.*, **56**, 930, (1986)
65 P.K.Hansma, V.B.Elings, O.Marti, C.Bracker, *Science*, **242**, 4876, (1988)
66 D.Rugar, P.Hansma, *Physics Today*, **43**, 23, (1990)
67 H.G.Hansma, J.Vesenka, C.Siegerist, G.Kelderman, H.Morrett, R.L.Sinsheimer, V.Elings, C.Bustamante, P.K.Hansma, *Science*, **256**, 1180, (1992)
68 B.Drake, C.B.Prater, A.L.Weisenham, S.A.C.Gould, T.R.Albrecht, C.F.Quate, D.S.Cannell, H.G.Hansma, P.K.Hansma, *Science*, **243**, 1586, (1989)
69 R.S.Asquith, L.Hirst, D.E.Rivett, *Text. Res. J.*, **3**, 285, (1970)
70 F.G.Lennox, A.S.Inglis, L.A.Holt, *Text. Res. J.*, **36**, 837, (1966)
71 A.S.Inglis, F.G.Lennox, *Text. Res. J.*, **35**, 104, (1965)
72 J.A.Maclaren, *Text. Res. J.*, **33**, 773, (1963)
73 A.Kirkpatrick, J.A.Maclaren, *Text. Res. J.*, **34**, 1082, (1964)

74 D.Hildebrand, *Zeitschift fur die gesamte Textilindustrie*, **61**, 180, (1959)
75 I.H.Leaver, G.C.Ramsay, *Photochem. Photobiol.*, **9**, 531, (1969)
76 F.G.Lennox, R.J.Rowlands, *Photochem. Photobiol.*, **9**, 359, (1969)
77 L.A.Holt, B.Milligan, D.E.Rivett, *Biochemistry*, **10**, 3559, (1971)
78 L.A.Holt, B.Milligan, *Aust. J. Biol. Sci.*, **26**, 871, (1973)
79 L.A.Holt, B.Milligan, *J. Text. Inst.*, **67**, 269, (1976)
80 L.A.Holt, B.Milligan, W.E.Savige, *J. Text. Inst.*, **68**, 124, (1977)
81 E.Leete, *J. Am. Chem. Soc.*, **83**, 3645, (1961)
82 R.S.Asquith, D.E.Rivett, *Biochim. Biophys. Acta*, **252**, 111, (1971)
83 L.A.Holt, B.Milligan, D.E.Rivett, H.C.Frederick, *Biochimica et Biophysica Acta.*, **499**, 131, (1977)
84 L.A.Holt, B.Milligan, D.E.Rivett, *Proc. Int. wool Text. Res. Conf.*, Aachen, **II**, 559, (1975)
85 D.Goddinger, K.Schafer, H.Hocker, *Wool Tech. Sheep Breeding*, **42**, 83, (1994)
86 K.Roper, E.Finnimore, *Proc. 7th Int. Wool Text. Res. Conf.*, Tokyo, **IV**, 21, (1985)
87 R.S.Davidson, G.M.Ismail, D.M.Lewis, *JSDC*, **103**, 308, (1987)
88 A.Meybeck, J.Meybeck, *Photochem. Photobiol.*, **6**, 355, (1967)
89 A.Meybeck, J.Meybeck, *Proc. 3rd Int. Wool Text. Res. Conf.*, Paris, **II**, 525, (1965)
90 L.A.Holt, B.Milligan, *Text. Res. J.*, **47**, 620, (1977)
91 J.L.Hoare, *J.Text. Inst.*, **65**, 503, (1974)
92 W.H.Melhuish, G.J.Smith, *JSDC*, **109**, 163, (1993)
93 G.J.Smith, W.H.Melhuish, *Text. Res. J.*, **55**, 304, (1985)
94 S.S Lehrer, G.D.Fasman, *Biochemistry*, **6**, 757, (1967)
95 S.Collins, S.Davidson, P.H.Greaves, M.Healey, D.M.Lewis, *JSDC*, **104**, 348, (1988)
96 S.Collins, R.S.Davidson, *JSDC*, **109**, 202, (1993)
97 S.Collins, R.S.Davidson, M.E.C.Hilchenbach, *Dyes and Pigments*, **24**, 151, (1994)
98 K.Schafer, *JSDC*, **107**, 206, (1991)
99 G.J.Smith, K.R.Markham, W.H.Melhuish, *Photochem. Photobiol.*, **60**, 196, (1994)
100 H.K.Launer, *Text. Res. J.*, **35**, 395, (1965)
101 L.A Holt, P.J.Waters, *Proc. 7th Int. Wool Text. Res. Conf.*, Tokyo, **IV**, 1, (1985)
102 M.G.King, *J.Text. Inst.* **62**, 251 (1971)
103 F.G.Lennox, M.G.King, *Text. Res. J.*, **38**, 754, (1968)
104 P.E.Ingham, J.M.Till, *J. Text. Inst.*, **80**, 605, (1989)
105 W.S.Simpson, *J.Text. Inst.*, **6**, 430, (1987)
106 L.A.Holt, B.Milligan, *Text. Res. J.*, **54**, 521, (1984)
107 S.V.Konev, 'Fluorescence and Phosphorescence of Proteins and Nucleic acids', Plenum Press, New York, 1967
108 C.D.Shah, R.Srinivasan, *J. Text. Inst.*, **69**, 151, (1978)
109 P.J.Waters, N.A.Evans, L.A.Holt, B.Milligan, *Proc. Int. Wool Text. Res. Conf.*, Pretoria, **V**, 195, (1980)
110 M.Friedman, S.Tillin, *Text. Res. J.*, **44**, 578, (1974)
111 E.Elod, H.Nowotny, H.Zahn, *Melliand Textilber*, **23**, 577, (1942)
112 R.F.C.Claridge, A.Shatkay, I.L.Weatherall, *J. Text. Inst.*, **7**, 316, (1979)
113 F.G.Lennox, M.G.King, I.H.Leaver, G.C.Ramsay, W.E.Savige, *Appl. Polym. Symp.* **18**, 353, (1971)
114 I.L.Weatherall, L.A.Dunn, *Photochem. Photobiol.*, **55** 305, (1992)
115 I.H.Leaver, R.C.Marshall, D.E.Rivett, *Proc. 7th Int. Wool Text. Res. Conf.*, Tokyo, **IV**, 11, (1985)

116 W.S.Simpson, C.T.Page, *Proc. Int. Wool Text. Res. Conf.*, Pretoria, **V**, 183, (1980)
117 R.Hamilton, J.Matthews, G.Walters, 'Drive on a wool rich seat' in 'Objective Evaluation of Apparel Fabrics' (conference proceedings), 499, (1983)
118 L.D.Hunter, M.L.Garcia, W.N.Cohen, G.L.Cohen, *Text. Res. J.*, **44**, 136, (1974)
119 D.Tester, *Text. Res. J.*, **54**, 75, (1984)
120 W.S.Simpson, *Wronz. Communication*, **C77**, (1982)
121 J.W.A.Matthews, Project TD6, Aust. Wool Corp. March (1983)
122 L.Benisek, G.K.Edmondson, J.W.A.Matthews, *Text. Res. J.*, **55**, 256, (1985)
123 L.Benisek, G.K.Edmondson, P.C.Myers, *Proc. 7th Int. Wool Text. Res. Conf.*, Tokyo **IV**, 79, (1985)
124 E.Promper, V.Rossbach, *Schriftenr. Dtsch. Forschungsinst.*, Aachen, **91**, 164, (1982)
125 H.M.Greaves, L.G.Johnson, *Photochem. Photobiol.*, 183, (1988)
126 M.M.Dodds, C.T.Page, *Wronz. Report*, **R144**, (1990)
127 I.H.Weatherall, H.L.Needles, *Text. Chem. & Col.*, **24**, 7, (1992)
128 L.A.Holt, B.Milligan, L.J.Wolfram, *Text. Res. J.*, **44**, 846, (1974)
129 R.S.Davidson, G.M.Ismail, D.M.Lewis, *JSDC*, **103**, 9, 308, (1987)
130 W.S.Simpson, *Proc. 7th Int. Wool Text. Res. Conf.*, Tokyo, **IV**, 70, (1985)
131 I.H.Leaver, *Text. Res. J.*, **10**, 610, (1978)
132 W.G.Rose, M.K.Walden, J.E.Moore, *Text. Res. J.*, **31**, 495, (1961)
133 P.J.Waters, N.A.Evans, *J.Text. Inst.*, **2**, 99, (1983)
134 I.H.Leaver, *J.Polym. Sci. Polym. Chem.*, **20**, 2417,& 2429, (1982)
135 I.H.Leaver, P.J.Waters, N.A.Evans, *J. Polym. Sci. Polym. Chem Ed.*,**17**, 1531, (1979)
136 N.A.Evans, P.J.Waters, J.F.K.Wilshire, *Text. Res. J.*, **56**, 203, (1986)
137 N.A.Evans, J.Rosevear, P.J.Waters, J.F.K.Wilshire, *Polym. Deg. Stab.*, **14**, 263, (1986)
138 N.A.Evans, J.Rosevear, P.J.Waters, J.F.K.Wilshire, *Proc. 7th Int. Wool Text. Res. Conf.*, Tokyo, **IV**, 41, (1985)
139 C.M.Carr, I.H.Leaver, J.F.K.Wilshire, *Proc. 7th Int. Wool Text. Res. Conf.*, Tokyo, **IV**, 50, (1985)
140 I.H.Leaver, *J.Appl. Polym. Sci.*, **33**, 2795, (1987)
141 B.Milligan, L.A.Holt, *Polym. Deg. Stab.*, **10**, 335, (1985)
142 L.A.Holt, I.H.Leaver, B.Milligan, P.J.Waters, J.F.K.Wilshire, *Proc. 7th Int. Wool Text. Res. Conf.*, Tokyo, **IV**, 31, (1985)
143 P.J.Waters, N.A.Evans, B.Milligan, *Proc. 7th Int. Wool Text. Res. Conf.*, Tokyo, **IV**, 60, (1985)
144 P.J.Waters, B.Milligan, *Polym. Deg. Stab.*, **16**, 187, (1986)
145 L.A.Holt, I.H.Leaver, B.Milligan, P.J.Waters, J.F.K.Wilshire, *Proc. 7th Int. Wool Text. Res. Conf.*, Tokyo, **IV**, 31, (1985)
146 C.M.Carr, I.H.Leaver, J. Appl. Polym. Sci., **33**, 2087, (1987)
147 C.Robbins, *Text. Res. J.*, **37**, 811, (1967)
148 A.Strasheim, K.Buijs, *Biochim. Biophys. Acta*, **47**, 538, (1961)
149 W.E.Savige, J.Eager, J.A.Maclaren, C.M.Roxburgh, *Tetrahedron Lett.*, **44**, 3289, (1964)
150 L. Coderch, R.Pons, P.Erra, *JSDC*, **107**, 410, (1991)
151 E.A.Carter, P.M.Fredericks, J.S.Church, R.J.Denning, *Spectrochimica Acta*, **50A**, 1927, (1994)
152 M.Joy, D.M.Lewis, *Int. J. Cosmetic Sci.*, **13**, 249, (1991)

153 F.J.Douthwaite, D.M.Lewis, U.Schumacher-Hamedat, *Text. Res. J.*, **63**, 177, (1993)
154 D.M.Lewis, G.Yan, *JSDC*, **109**, 193, (1993)
155 C.M.Carr, D.M.Lewis, *JSDC*, **109**, 21, (1993)
156 B.G.Frushour, J.L.Koenig, 'Advances in Infrared and Raman Spectroscopy', Ed. R.J.H. Clark abd R.E.Hester, Heyden, London, **1**, 35, (1975)
157 H.Fabian, P.Anzenbacher, Vibrational Spectroscopy, Ed. J.R.Durig, Vol.4, 125, Elsevier Science, Amsterdam, (1993)
158 L.J.Hogg, H.G.M.Edwards, D.W.Farwell, A.T.Peters, *JSDC*, **110**, 196, (1994)
159 A.C.Williams, H.G.M.Edwards, B.W.Barry, *J. Raman Spect.*, **25**, 95, (1994)
160 J.S.Church, A.S.Davie, D.W.James, W.H.Leong, D.J.Tucker, *Appl. Spect.*, **48**, 813, (1994)
161 I.H.Leaver, R.E.Hester, R.B.Girling, *Text. Res. J.*, **58**, 182, (1988)
162 M.M.Millard, A.E.Pavlath, *Text. Res. J.*, **42**, 460, (1972)
163 M.M.Millard, *Proc. Int. Wool Text. Res. Conf.*, Aachen, **II**, 44, (1975)
164 M.M.Millard, *Anal. Chem.*, **44**, 828, (1972)
165 C.M.Carr, S.F.Ho, D.M.Lewis, E.D.Owen, M.W.Roberts, *J. Text. Inst.*, **6**, 419(1985)
166 R.H.Bradbury, I.L.Clackson, D.E.Sykes, *Appl. Surface Sci.*, **72**, 143, (1993)
167 L.D.Setiawan, H.Baumann, D.Gribbin, *Surface & Interface Anal.*, **7**, 188, (1985)
168 H.Baumann, L.D.Setiawan, D.Gribbin, *Surface & Interface Anal.*, **8**, 219, (1986)
169 H.Baumann, L.Setiawan, *Proc. 7th Int. Wool Text. Res. Conf.*, Tokyo, **IV**, 108, (1985)
170 S.J.Tillin, A.E.Pavlath, S.H.Zeronian, A.G.Pittman, *Text. Res. J.*, **50**, 724, (1980)
171 C.M.Carr, I.H.Leaver, A.E.Hughes, *Text. Res. J.*, **56**, 216, (1986)
172 L.M.Dowling, L.N.Jones, I.H.Leaver, *Text Res. J.*, **58**, 640, (1988)
173 R.J.Ward, H.A.Willis, G.A.George, G.B.Guise, R.J.Denning, D.J.Evans, R.D.Short, *Text. Res. J.*, **63**, 362, (1993)
174 C.M.Carr, I.H.Leaver, A.E.Hughes, *Text. Res. J.*, **56**, 457, (1986)
175 B.Rigg, F.J.J.Clarke, R.McDonald, *JSDC*, **100**, 128, (1984)
176 C.A.Anderson, *J.Text. Inst.*, **62**, 281, (1971)
177 W.Schefer, *Melliand Text.*, **63**, 368, (1982)
178 S.Kawabata, 'The Standardisation and Analysis of Hand Evaluation' 2nd ed., TMSJ, Osaka, (1980)
179 T.J.Mahar, R.C.Dhingra, R.Postle, *Text. Res. J.*, **57**, 357, (1987)
180 P.Kubelka, *J. Opt. Soc. Amer.*, **38**, 448, (1948)
181 T.P.Bridge, A.F.Fell, R.H.Wardman, *JSDC*, **103**, 17, (1987)
182 W.F.Maddams, W.L.Mead, *Spectrochimica Acta*, **38A**, 437, 445 & 459, (1982)
183 C.D.Wagner, L.E.Davis, M.V.Zeller, J.A.Taylor, R.M.Raymond, L.H.Gale, *Surf. Interface Anal.*, **3**, 211, (1981)
184 R.Chaney, G.Barth, *Fres. Z. Anal. Chem.* **329**, 143 (1987)
185 P.E.Ingham, R.J.Smith, *WRONZ Report*, **R129**, (1986)
186 B.M.Chapman, *Text. Res. J.* **39**, 1102, (1969)
187 J.W.S.Hearle, B.M.Chapman, G.S.Senior, *Appl. Polym. Symp.* **18**, 1775, (1971)
188 R.Meredith, *J.Text. Inst.*, **36**, T107, (1945)
189 A.R.Haly, *Text. Res. J.* **40**, 965, (1970)
190 A.T.Tu, 'Spectroscopy of Biological Systems' in 'Advances in Spectrosopy' Ed. R.J.H.Clark, R.E.Hester, Wiley, Chichester, **13**, 47, (1986)
191 J.L.Lippet, D.Tyminski, P.J.Desmeules, *J. Am. Chem. Soc.*, **98**, 7075, (1976)
192 H.Sugeta, A.Go, T.Miyazawa, *Chem. Lett.*, 83 (1972)

193 R.L.Remmele, P.McMillan, A.Bieber, *J.Protein Chem.*, **9**, 475, (1990)
194 M.N.Siamwiza. R.C.Lord, M.C.Chen, T.Takamatsu, I.Harada, H.Matsuura, T.Shimanouchi, *Biochemistry*, **14**, 4870, (1975)
195 M.L.Raymond, A.T.Tu, Biochim. Biophys. Acta, **285**, 498, (1972)
196 T.Miura, H.Takeuchi, I.Harada, *J.Raman Spect.*, **20**, 667, (1989)
197 T.Miura, H.Takeuchi, I.Harada, *Biochemistry*, **27**, 88, (1988)
198 M.Spei, R.Holzem, *Melliand Textil.*, **70**, 786 (E338), (1989)
199 H.Zahn, G.Blankenburg, *Text. Res. J.* **32**, 986 (1962)
200 *Wool Science Review*, **35**, 35 (1960)
201 J.K.Kauppinen, D.J.Moffatt, H.H.Mantsch, D.G.Cameron, *Anal. Chem.*, **53**, 1454, (1981)
202 D.I.James, W.F.Maddams, P.B.Tooke, *Appl. Spectroscopy*, **41**, 1362, (1987)
203 N.A.Evans, J.Rosevear, P.J.Waters, J.F.K.Wilshire, *Polym. Deg. Stab.*, **14**, 263 (1986)
204 P.J.Waters, B.Milligan, *Polym. Deg. Stab.*, **16**, 187, (1986)
205 S.Krimm, *Biopolymers*, **22**, 217, (1983)
206 S.Sack, S.Schar, E.Steger, *Polym. Deg. Stab.* **7**, 193, (1984)
207 I.M.Ward, M.A.Wilding, *Polymer*, **18**, 327, (1977)
208 J.Stokr, B.Schneider, D.Doskocilova, J.Lovy, *Polymer*, **23**, 714, (1982)
209 P.Blais, M.Day, D.M.Wiles, *J. Appl. Polym. Sci.*, **17**, 1895, (1973)
210 M.S.Kuligina, L.P.Kolov, A.F.Tumanova, *Tech. Text. Ind. USSR*, **6**, 87, (1970)
211 I.M.Ward, *Chem. and Ind. (London)*, 1102 (1957)
212 W.W.Daniels, R.E.Kitson, *J. Polym. Sci.*, **33**, 161, (1958)
213 L.D'Esposito, J.L.Koenig, *J.Polym. Sci. Polym. Phys. Edn.*, **14**, 1731, (1976)
214 A.Miyake, *J. Polymer Sci.*, **38**, 479, (1959)
215 D.J.Skrovanek, S.E.Howe, P.C.Painter, M.M.Coleman, *Macromolecules*, **18**, 1676, (1985)
216 C.H.Do, E.M.Pearce, B.J.Bulkin, *J. Polym. Sci. Polym. Chem.*, **25**, 2409, (1987)
217 R.S.Hallos, J.H.Keighley, *J. Appl. Polym. Sci*, **19**, 2309, (1975)
218 A.Miyake, *J.Polym.Sci*, **44**, 223, (1960)
219 H.W.Starkweather, R.E Moynihan, *J.Polym. Sci.*, **22**, 363, (1956)
220 J.L.Koenig, M.C.Agboatwalla, *J.Macromol. Sci. Phys.* **B2**, 391, (1968)
221 C.H.Do, E.M.Pearce, B.J.Bulkin, *J. Polym. Sci. Polym. Chem.* **25**, 2409, (1987)
222 A.Dilks, D.T.Clark, *J. Polym. Sci. Polym. Chem.*, **19**, 2847, (1981)
223 D.T.Clark, A.Dilks, H.R.Thomas, 'Developments in Polymer Degradation' Ed. N.Grassie, Applied Science Publishers, London, **1**, 87, (1977)
224 A.Dilks, *Polym. Deg. Stab.*, **1**, 600 (1983)
225 A.Dilks, *J.Poly. Sci. Polym. Chem.*, **19**, 2847, (1981)
226 J.Peeling, D.T.Clark, *J. Appl. Polym. Sci.*, **26**, 3761, (1981)
227 R.D.B.Fraser, T.P.MacRae, G.E.Rogers, 'Keratins, Their Composition, Structure and Biosynthesis' Charles C. Thomas, Springfield, **III**, 39 & 56-82, (1972)
228 A.P.Negri, H.J.Cornell, D.E.Rivett, *Aust. J. Agric. Res.*, **42**, 1285, (1991)
229 D.J.Peet, R.E.H.Wettenhall, D.E.Rivett, A.K.Allen, *Comp. Biochem. Physiol.*, **102B**, 363, (1992)
230 A.P.Negri, H.J.Cornell, D.E.Rivett, *Text. Res. J.*, **62**, 381, (1992)
231 A.P.Negri, H.J.Cornell, D.E.Rivett, *Text. Res. J.*, **63**, 109, (1993)
232 D.J.Peet, R.E.H.Wettenhall, D.E.Rivett, *Text. Res.J*, **65**, 58, (1995)

233 D.C.Jones, C.M.Carr, to be published
234 F.J.Wortmann, G.Wortmann, 'Scanning Electron Microscopy as a Tool for the Analysis of Wool / Speciality Fibre Blends' D.W.I., (1991)
235 J.Luston, 'Physical loss of stabilisers from polymers', Developments in Polymer Stabilisation, Ed. G. Scott, Appl. Science Publishers, London, **Vol.2**, 5, 185, (1980)
236 C.A.Anderson, *J. Text. Inst.* **62**, 281, (1971)
237 M.Kowalski, 'Automotive Textile Presentation' Autotech Conf., Birmingham NEC., Paper No. C427/9/078, (1991)
238 H.S.Munro, *Polym. Mater. Sci. Engng.*, **58**, 344, (1988)
239 Daimler-Benz, Draft Standard DBL 5824/5306, Test Method 66, Determination of fastness to heat.
240 Fibre Fracture and Wear of Materials; An Atlas of Fracture, Fatigue and Durability, J.W.S.Hearle, W.D.Cooke, Pub. Ellis Harwood, (1989)
241 H.F.Launer, D.Black, *Appl. Polym. Symp.* **18**, 347, (1971)
242 W.D.Cooke, *Text. Res. J.* **55**, 409, (1985)
243 A.Van Der Spuy, *Int. Dyer*, **180**, (10), 11, (1995)

Appendix

THE PHOTODEGRADATION OF WOOL AND WOOL BLEND FABRICS IN RELATION TO THEIR USE IN AUTOMOTIVE UPHOLSTERY.

D.C. Jones, C.M. Carr, W.D.Cooke, R. Mitchell, J.C.Vickerman

Proceedings of the 9th International Wool Textile Research Conference, Biella, 1995

SYNOPSIS

The performance of wool and wool blend automotive fabrics under commercial manufacturers test conditions has been investigated. In general, wool blend fabrics have a superior performance to 100% wool fabrics both in terms of lightfastness and wear resistance. Dye fading and strength losses are reduced by the application of photostabilisers to wool, nylon and polyester. The analytical techniques FT-IR, FT-Raman and XPS have been used to probe the nature of surface and bulk photodegradation mechanisms. SSIMS was used for analysis of the bound fatty acid components of the outer lipid layer of the wool fibre epicuticle.

INTRODUCTION

Automotive upholstery faces a particularly severe work environment, being subject to a combination of both light exposure and wear. Exposure to near UV light reduces the useful lifetime of fabrics, causing rapid dye fading, resistance to abrasion and lowering tensile integrity [1]. Photodegradation is catalysed by the high temperatures often found in enclosed vehicles. Automotive manufacturers therefore demand stringent performance and quality standards for upholstery fabrics. The appearance, handle and physical integrity of fabrics must remain unchanged for the greater part of the life-span of the vehicle. A large number of specialised tests have been developed to evaluate fabric in-service performance, with each manufacturer specifying their own individual test procedures and performance criteria. Lightfastness is of primary importance along with an assessment of physical integrity such as abrasion resistance or tensile strength. Photostability is evaluated using accelerated test methods which aim to replicate the cumulative light exposure conditions the average car will have to withstand during its actual lifetime. Control over spectral distribution, temperature and humidity allows test reproducibility and provides a method of specifying performance levels.

New textile products must be engineered to meet specific performance levels. Critical control of material specifications such as fibre type, dyestuff, photostabiliser, fabric structure and processing conditions is necessary. Wool currently occupies niche markets, for example in luxury vehicles, which are often not subject to the rigorous performance requirements of mass market sectors. The inherent photoyellowing and phototendering tendency of wool has restricted its use despite its aesthetic qualities and advantages of comfort, handle and flame retardancy [2,3]. The development of commercial photostabilisers for wool [4] along with the trend for greater comfort and luxury of interior styling has generated greater interest amongst certain mass market manufacturers. There is much caution however since the performance of wool to current automotive standards is uncertain, also the inherent variability of the physical and chemical properties of wool poses some difficulty to the product engineering approach.

The aim of this research was to investigate the rate of photodegradation of wool under automotive interior conditions. A number of complimentary analytical techniques have been used to investigate surface and bulk chemistry in order to examine the photochemical changes which lead to a reduction in fabric performance. The level of protection given to wool by the application of a commercial UV absorber, Cibafast W was evaluated. In addition the performance of wool and wool blend fabrics to automotive test specifications is assessed.

EXPERIMENTAL

Materials

Worsted fabric (2x2 twill 300 g/m^2) was produced from crossbred 35 μm wool. A mid grey automotive base shade was chosen for all dyeings using recommended high lightfastness 2:1 premetallised dyestuffs. Cibafast W (Ciba Geigy) was applied by exhaustion at 2% oww. to the undyed fabric and co-applied to fabric during dyeing by the recommended procedure [5].
Automotive standard fabrics were produced using 25, 30, 35 μm wool qualities. Wool was top dyed with 2% Cibafast W. Nylon fibres (3.3 dtex semidull) were top dyed using the same dyestuffs applied to wool and with 2% Cibafast N. Polyester fibres (3.3 dtex semidull) were top dyed using automotive standard high lightfastness disperse dyes with 3% Cibatex APS. Wool was blended with a 35% synthetic fibre component during gilling. The 100% wool and wool blend worsted fabrics produced (2x2 twill flat woven 395 g/m^2) were given a commercial aqueous scour and flame laminated to a 3.3 mm polyester urethane F.R. foam with a warp knit nylon backing. All processing was carried out at the IWS and lamination at Guilford Automotive, Derbyshire.

Exposure Conditions

The test specification of Rover Group (RES 30 CF 006) was used. This is based on DIN 75.202 but conditions have been adjusted by Rover after considerable research to correlate results with real time testing in endurance vehicles in Arizona [6]. The test conditions were therefore considered to most realistically reproduce in-service exposure conditions. An air cooled Heraeus Xenotest 450 is used with an air temperature of 70-75°C, Black Standard Temperature of 115°C ± 3°C and relative humidity 10-30%. Light below 300 nm is filtered to simulate exposure behind window glass. Total UV irradiance is 85 W/m^2 between 300-400 nm and exposure is continuous with end point specified by a change equal to grey scale 4 on blue wool standard 7 (approximately 52 hours). Fabrics were exposed for successive test cycles based on 52 hours, three samples of each fabric were tested for each cycle.

Instrumentation

Martindale testing was carried in accordance with BS 5690 1988. Four specimens were tested for each fabric sample and weight loss was measured at 25,000 cycle intervals for exposures up to 52 hours, and at 10,000 cycle intervals for higher exposure levels.
Colour measurement was carried out using an ICS Texicon 'Spectraflash' spectrophotometer using D65 illumination and 10° Observer averaging three readings on each sample. The ΔE (CMC 2:1) values for each sample were averaged to give a mean value at each exposure level. The Yellowness Index of undyed fabrics was measured according to ASTM D1925.

FT-Raman analysis used a Nicolet 950 Raman Spectrometer with a liquid nitrogen cooled germanium detector and a Neodymium-YAG laser source (1064 nm) emitting 500 mW of optical power focused at the sample. Fabric samples of size 10 mm^2 were mounted on a small stainless steel frame and positioned vertically in the path of the laser. Spectra of lysozyme were collected using NMR tubes. A sampling geometry of 180° was used, and spectra were collected at 4 cm^{-1} resolution maintaining the same instrument alignment conditions. Due to its heterogeneous nature, wool is an inherently weak Raman scatterer. To obtain spectra with adequate signal to noise ratio to allow peak intensity comparisons, 3000 scans were averaged with a collection time of 62 minutes. To allow comparison of band intensities between samples, spectral normalisation was necessary against the peak intensity of the strong CH_2 stretch at 2930 cm^{-1}.

FT-IR analysis used a Nicolet 750 FTIR spectrometer with a liquid nitrogen cooled MCT/B detector. For surface analysis of fabric samples a vertical Attenuated Total Reflectance (ATR) attachment was used with a KRS-5, 45° crystal. Spectral reproducibility was achieved by maintaining constant contact pressure of between the crystal faces and fabric. A calibrated torque screwdriver was used to apply a pressure of 68.9 kPa to the crystal holder. Spectra were collected at 4 cm^{-1} resolution and accumulated over 200 scans. Quantitative analysis was carried out by measuring peak intensities in the second derivative absorbance spectrum.

X-ray Photoelectron Spectroscopy (XPS) analysis was carried out using a VG ESCA 3 Mk II spectrometer using a non-monochromatic MgKα X-ray source of energy 1253.6 eV at a power of 240 W under a residual pressure of 10^{-8} Torr. Fabric samples were attached to the probe using double sided tape. Measurements were made at constant analyser energy with a pass energy of 20 eV and were the average of 45 - 90 scans. Spectra were charge referenced against the C-C/C-H (1s) peak at 285 eV. Quantitative analysis was carried out using the photoelectron peak areas with a Shirley baseline correction, and applying the appropriate atomic sensitivity factors [7].

Static Secondary Ion Mass Spectrometry (SSIMS) analysis used a VG IX23S instrument with a Poschenrieder time of flight analyser and a pulsed liquid metal ion source (Ga^+, 30 keV) and a total primary ion dose of 1 x 10^{11} ions cm^{-2}. Negative secondary ion spectra were recorded from a sample area of 600 x 600 μm.

RESULTS AND DISCUSSION

Photostability of Wool Automotive Fabrics

Polyester and nylon are mainly used in automotive upholstery. The initial part of this study was to compare the photostabilisation of 100% wool, 100% polyester and 100% nylon fabrics. The application of Cibafast W to wool, Table I, reduces photoyellowing, phototendering and dye fading, the level of retardation of dye fading diminishing with increasing exposure time. In comparison, Cibatex APS gives a greater level of protection to polyester than the comparable photoprotected dyed wool, however extended exposure again produces a reduction in photo-protective effect. In contrast, the benefit of Cibafast N is much more obvious at higher exposure levels where much greater retardation of dye fading is observed. Overall the lightfastness performance of Cibafast W treated dyed wool is inferior to stabilised polyester

Table I Photoprotection of wool by Cibafast W[1]

Xenotest Exposure (hours)	Reduction in rate of yellowing[2] %	Reduction in dye fading %	Retained Tensile Properties[3] %				Cibatex APS % reduction in fading dyed PET[4]	Cibafast N % reduction in fading of dyed PA[4]
			Untreated		Cibafast W			
			Ten.	Ext.	Ten.	Ext.		
26	56	42	95	96	100	100	67	30
52	40	28	80	92	100	100	65	20
104	32	18	55	54	86	77	60	70
156	35	17	-	-	-	-	52	76
208	27	14	53	21	63	34	44	74

1. All values measured relative to unexposed controls 2. Undyed wool
3. Calculated from mean of 50 yarns taken from exposed fabrics 4. 100% composition

and nylon fabrics. Despite wool's relatively poorer photochemical behaviour the obvious comfort benefits of wool have resulted in this subsequent evaluation of wool blend fabrics.

All Xenotest exposures in this work were carried out under the conditions specified by Rover Group since they were considered to most closely reproduce in-service conditions [6]. The standard test time of 52 hours correlates to exposure for 6 summer months in Arizona and as shown in Table II the 100% wool fabric does not reach the lightfastness performance requirement of Grey Scale 4. Table II also shows the performance of this fabric under the exposure conditions specified by other manufacturers. Each test uses a Xenon light source, but the variation in performance is due to differences in air temperature, spectral distribution, and test duration. Thus the extent of photodegradation of wool is affected and is reflected by the loss of abrasion resistance and increased surface oxidation. This illustrates the difficulty of producing a fabric which will perform under the conditions specified by each individual manufacturer. The Ford test is particularly severe for wool. This test does not allow for the filtering effect of wavelengths below 315 nm by window glass, and therefore includes a significant UV component, permitting wavelengths as low as 270 nm. The effect of the short wavelength component on wool is shown by the poor lightfastness and rapid phototendering.

The rate of fading of 100% wool as a function of exposure time is shown in Figure 1. It was found that the 30 and 35 μm fabrics had the same lightfastness at all exposure levels, but the 25 μm fabric had a consistently poorer performance, having an average of 10-15% higher ΔE value at all exposure levels. An obvious improvement in lightfastness of wool is achieved by blending with 35% polyester or nylon Figure 1, this beneficial effect increasing with the percentage of synthetic fibre component. The improvement was sufficient to reach Grey Scale 4 after 52 hours, but further improvement is required to meet the General Motors and Ford tests.

Table II Variation in performance of wool fabric according to accelerated exposure test method

Exposure Test Method	ΔE	Grey Scale Grading	Increase in Cysteic Acid[2]	Martindale Cycles
Control[1]	0	5	1	128,000
Rover Group 52 hrs	2.1	3-4	1.9	85,000
General Motors Europe (DIN 75202) [3]	3.3	3	2.1	53,000
Ford (SAE J1885) [4]	4.9	2	2.7	15,000

1. 100% Wool 35μm Dyed + 2% Cibafast W 3mm laminate
2. FT-IR (ATR) Second derivative peak intensity at 1040 cm^{-1} (arbitrary units)
3. BST. 115°C, R.H. 20± 10 % spectral range > 310 nm, exposure to ΔE 4.3 on Blue Scale 6 (approx.110 hrs.)
4. BST. 89° C, R.H. 50± 10% spectral range > 270 nm, exposure 226.5 KJ/m^2 at 340 nm (approx. 115 hrs)

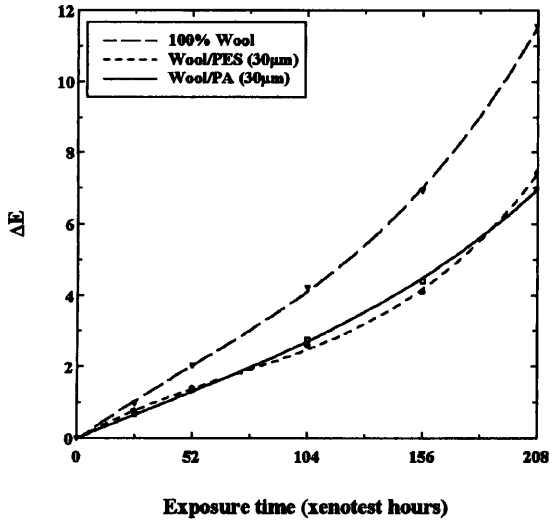

Figure 1 Lightfastness performance of wool fabrics (3mm laminates)

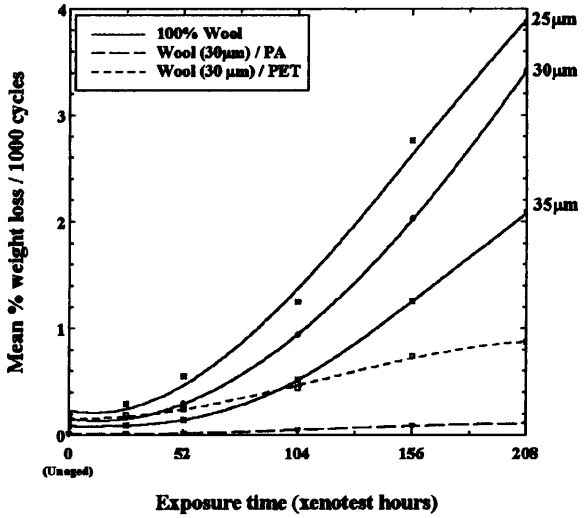

Figure 2 Effect of light exposure on fabric abrasion resistance (3mm laminates)

All fabrics tested to automotive standards are required to be in a laminated form. In Table III the effect of lamination on fabric lightfastness is illustrated. There is a greater level of dye fading as lamination thickness increases. This can be attributed to heat build within the foam backing leading to an increased surface temperature which has accelerated the rate of dye fading. It can therefore be appreciated that fabric lightfastness performance to automotive standards cannot be assessed accurately using face fabrics.

Table III Effect of fabric lamination on lightfastness performance

ΔE	52 hours			156 hours		
	Face Fabric	3 mm Lam	6 mm lam	Face Fabric	3 mm Lam	6 mm lam
100% Wool 30µm	1.8	2.1	-	6.1	6.9	-
Wool/PET 30µm	1.1	1.4	1.7	3.4	4.1	5.3
Wool/PA 30µm	1.1	1.35	1.8	3.5	4.3	5.4

In Figure 2 the rate of breakdown of the fabric surface as a function of exposure time was measured by the mean rate of weight loss of fabric during Martindale abrasion testing. The abrasion resistance of wool increased significantly with increasing mean fibre diameter. The unaged 35 µm wool fabric reached over twice the end point cycles of the 25 µm fabric and this improvement was maintained at each subsequent exposure level. Figure 2 also shows that the abrasion resistance of wool is improved considerably on blending with nylon, with a much slower breakdown of the fabric. Even after 208 hours exposure, the abrasion resistance is still higher than the equivalent unexposed 100% wool fabric. The 100% wool (35 µm) and wool / nylon blend both passed the Rover aged abrasion test specified by 52 hours Xenotest exposure followed by 50,000 Martindale cycles. The wool / polyester blend also exhibited improved abrasion resistance but failed this test due to considerable pilling which impaired appearance and therefore reduced useful lifetime. Pilling tendency increased with decreasing wool mean fibre diameter used in the blend. A wool / polyester 'microfibre' blend was developed to have improved tactile properties, however, this lower tenacity fibre readily formed small pills which were easily removed from the fabric and this caused rapid thinning and premature failure.

Physicochemical Changes in Photo-oxidised Wool

Fabric properties can be influenced by the nature of both the bulk and surface properties of the fibre. Changes in tensile properties affect the wear resistance of fabrics and an alteration in surface properties affects dyeability and handle. To understand and monitor the chemical changes associated with light exposure a range of complimentary techniques have been utilised.

Vibrational Spectroscopic Analysis of Photo-oxidised Wool

FTIR spectroscopy coupled to Attenuated Total Reflectance (ATR) is now established as a non-destructive technique for providing qualitative and semi-quantitative information about the oxidation products of cystine in wool [8-10] . Using a KRS-5 crystal an analytical depth of 2.5 -2.0 μm can be probed in the S-O stretching region 1000 - 1200 cm^{-1}. The rate of cysteic acid formation as a function of exposure time was measured by the increase in the second derivative band intensity at 1040 cm^{-1} .For untreated wool there was an increase in cysteic acid signal with increasing exposure time, particularly up to 156 hours exposure. The rate of increase of this cysteic acid signal is reduced approximately 50% by the application of 2% Cibafast W. Dyed wool shows a slower rate of increase in cysteic acid signal compared to undyed wool and the addition of Cibafast W to the dyed fabric again reduces the rate of increase in signal intensity further, but only to the same level as undyed UV absorber treated fabric.The overall behaviour of untreated wool with regard to the formation and disappearance of cystine intermediate oxidation products is similar to that reported previously [8].

FT-Raman spectroscopy provides complimentary information to FT-IR, probing the same molecular vibrational energy levels, but is a bulk analysis technique. The advantage of Raman spectroscopy for studies on wool is that it is non-destructive and it produces strong bands for non-polar functional groups, and aromatic structures such as the amino acids tryptophan, tyrosine and phenylalanine and the S-S and C-S vibrations of cystine, which are difficult to detect in the FT-IR spectrum. In Figure 3 the spectra of unexposed wool fabric and after 208 hours exposure are overlaid on a common scale with assignments given[11]. The band at 513 cm^{-1}, assigned to the S-S vibration of cystine, gradually decreased with exposure time with a

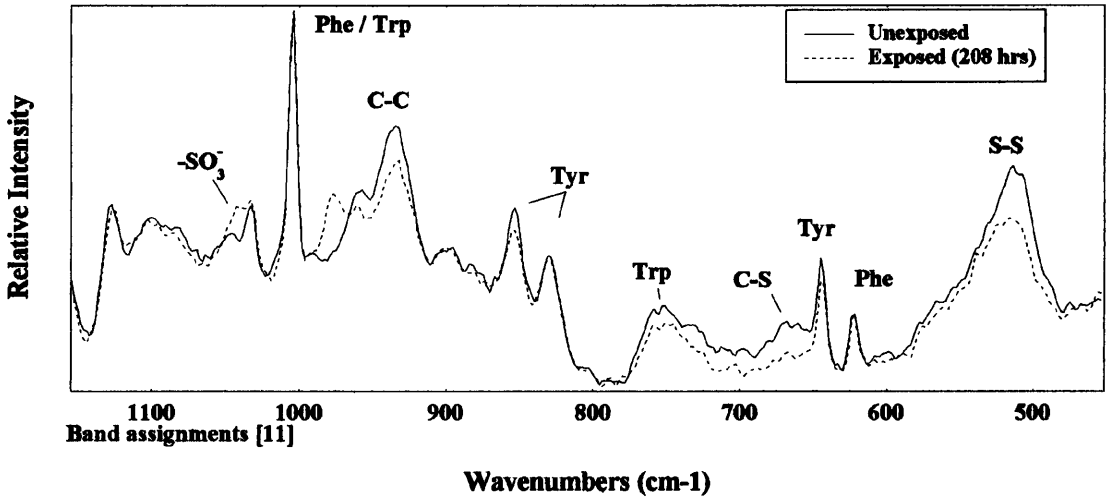

Figure 3 Effect of light exposure on FT-Raman spectrum of untreated wool

reduction in signal intensity of between 25-30% after 208 hours. The fabric treated with Cibafast W showed a comparably slower reduction in intensity at each exposure level with a reduction of 10 -15% after 208 hours. There is a decrease in intensity at 665 cm^{-1} assigned to cystine C-S stretch. This indicates cystine photo-oxidation pathways involving both S-S and C-S fission. Further evidence for cystine photo-oxidation is provided by the increase in signal intensity at 1040 cm^{-1} attributed to the S-O vibration of cysteic acid. Bands assigned to ring breathing modes of tyrosine appear at 643 cm^{-1} , and the Fermi doublet at 830 cm^{-1} and 854 cm^{-1}. After exposure there is a reduction in the bands at 643 cm^{-1} and 854 cm^{-1} relative to 830 cm^{-1}. This may reflect photodegradation of tyrosine residues, but other Raman studies of proteins have attributed these relative intensity changes to an alteration in the nature of the local chemical environment of tyrosine residues due to conformational changes [12] . Light exposed wool shows a reduction in signal intensity at 935 cm^{-1} , assigned to the C-C stretching of both the α-helical backbone and sidechains. A reduction in this band has previously been attributed to a loss in α-helical content of fibres to a disordered chain conformation[11]. There is also a new band in the photo-oxidised wool at 977 cm^{-1} which appeared after 52 hours exposure and gradually increased in intensity with exposure time . This band has no previous assignment for wool or related proteins and therefore the nature of the species responsible is at present unclear, however it may be related to the band at 935 cm^{-1} and represent changes in main chain conformation and structural rearrangements as a result of disulphide bond oxidation. No significant reduction in the Amide I band intensity was found in either the Raman or FT-IR spectra after exposure but both techniques showed an increase in intensity of this band in the C=O functional region between 1700 cm^{-1} and 1750 cm^{-1}.

The sharp signal at 1004 cm^{-1} is assigned to the C-C stretching vibration of the ring structures of tryptophan and phenylalanine. It was anticipated that this band would allow the photo-oxidation of tryptophan to be followed but there was no significant change in intensity after exposure. Spectra collected of L-tryptophan and L-phenylalanine showed peak maxima at 1009 cm^{-1} and 1005 cm^{-1} respectively. The low concentration of tryptophan in wool relative to phenylalanine means that the band at 1004 cm^{-1} can mainly be attributed to phenylalanine. In lysozyme, which has a higher relative concentration of tryptophan, the two components of this band are clearly resolved as shown in Figure 4. In addition, other intense bands are present for tryptophan at 760.7 cm^{-1} and 1553.5 cm^{-1} (not shown) which are too weak to be of any analytical value in the wool spectrum. Figure 4 also shows the spectrum of lysozyme after 208 Xenotest hours and only a small reduction in signals associated with tryptophan was observed.

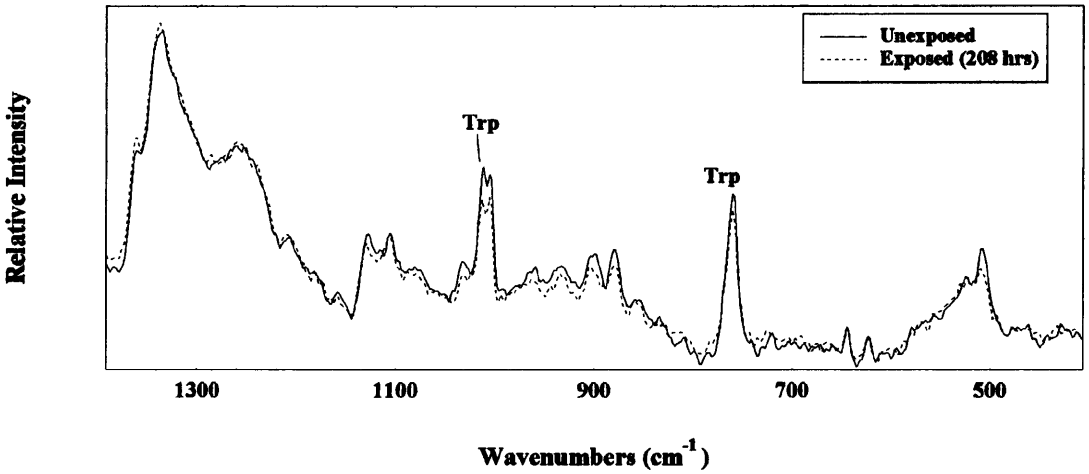

Figure 4 FT-Raman spectra of Lysozyme

Surface studies of photo-oxidised wool using XPS and SSIMS.

The photochemical breakdown of the surface of wool, polyester and nylon fabrics was studied using X-ray photoelectron spectroscopy (XPS) and static secondary ion mass spectrometry (SSIMS). These techniques have an analysis depth of 2-4 nm and 1 nm respectively, providing epicuticle specific information. XPS can provide qualitative and quantitative information of the surface elemental composition of wool but is limited in studying the nature of specific chemical species which may only be analysed by SSIMS.

The change in the O/C ratio is used to provide an index of the rate of surface oxidation of polymers [13]. Untreated wool has an increase of 70% in the O/C ratio after 208 hours exposure. This can be compared to untreated polyester and nylon which have a 40% increase in O/C ratio. Surface photo-oxidation of wool occurs rapidly, after 26 hours there is a 35% increase in O/C ratio suggesting rapid saturation of accessible reactive sites. The increase in FWHM of the C1s peak and increasing asymmetry at high binding energy indicate oxidised carbon species such as carbonyls and carboxylic acids. This initially rapid rate of surface oxidation is also reflected by the increase in oxidised sulphur signal. The S (2p) peak at 164 eV is attributable to sulphur present in the disulphide bonds of cystine (+2) and after exposure there was an additional distinct peak at 168 eV assigned to sulphur in the (+6) oxidation state of cysteic acid [14]. After 26 hours exposure 30% of the total surface sulphur signal was present as cysteic acid, increasing more slowly to 60% after 208 hours exposure as shown in Figure 5. In Figure 5 the rate of increase in cysteic acid is compared for untreated wool fabric and fabric treated with 2% Cibafast W. Cibafast W gives no significant protection to the 'outer' surface of undyed or dyed wool suggesting that it may be absent from the surface. This behaviour is in contrast to FT-IR analysis results which indicate that Cibafast W significantly reduces the increase in cysteic acid at 1040 cm^{-1} in the 'inner' surface.

XPS analysis of light exposed polyester and nylon fabrics provided evidence of stabiliser migration to the fabric surface. Copper was detected on the surface of dyed and undyed nylon fabrics treated with the copper complex stabiliser, Cibafast N, after light exposure, Figure 6. The signal was not present on the unexposed fabrics but increased in intensity between 52 and

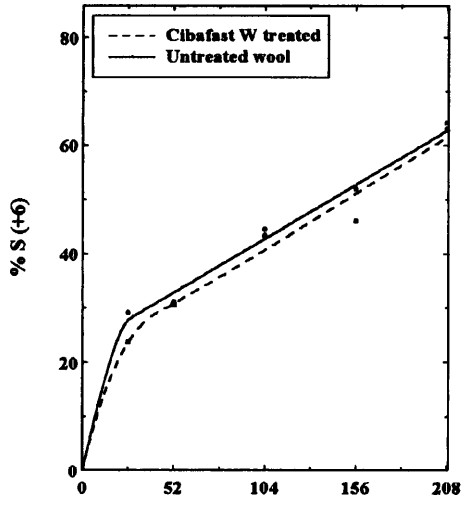

Figure 5
Increase in S (+6) intensity relative to S (+2) intensity of XPS S (2p) peak

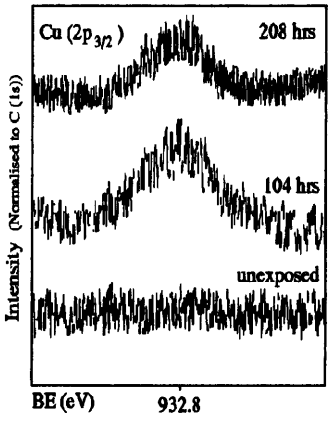

Figure 6
XPS spectra of $Cu(2p_{3/2})$ on nylon fabric

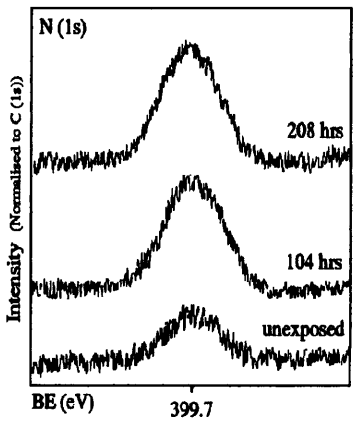

Figure 7
XPS spectra of N (1s) on polyester fabric

208 hours exposure. In addition undyed and dyed polyester fabrics treated with the hydroxybenzotriazole UV absorber, Cibatex APS, similarly showed an increase in surface nitrogen concentration with increasing exposure time, with over twice the original relative surface atomic concentration after 208 hours, Figure 7. This suggests light induced surface migration of this product. It was not possible to investigate migration of Cibafast W on wool as there is no specific elemental tag to distinguish it from the wool signals.

The epicuticle is reported to be composed of fatty acids covalently bound to the outer surface protein by thioester linkages, with a C_{21} fatty acid, 18-methyleicosanoic acid (18-MEA), representing 70% of this layer [15,16]. Using SSIMS analysis, the effect of light exposure on the fatty acid components of this lipid layer was investigated. The relative spectral intensities and assignments of surface species for scoured untreated crossbred wool are given in Table IV. The peaks at 311, 325, and 341 a.m.u. have been assigned in previous reports [17,18], but we include assignments for palmitic, stearic and oleic acids. There is a relative intensity change of the C_{21} fatty acid signals (341 and 325) after exposure, shown clearly in Figure 8. This suggests photo-oxidation and loss of 18-MEA after light exposure. SSIMS does not allow absolute band intensities to be compared between spectra so it is not possible to quantify total lipid loss. However, the increased fabric wettability and reduction in XPS C/N ratio of exposed wool indicates a reduction in lipid material. Signals at 80/81 a.m.u. assigned to cysteic acid increased significantly relative to other signals after exposure. Current studies of shrink resist chlorinated wool also show a similar, but much larger decrease in the 18-MEA signal at 341 a.m.u. accompanied by increases the SO_3^- / SO_3H signals [19].

Table IV SSIMS Relative Spectral Intensities of Surface Lipids on Untreated Wool

Species i -COS^- ii -COO^-	**Assignment** (a.m.u.)	**Relative %** Unexposed		**Relative %** (Exposed 208 hrs)	
C_{21} 18-methyleicosanoic acid	i 341	55.8	**63.4**	37.8	**58.5**
	ii 325	7.6		20.7	
C_{20} Eicosanoic acid	i 326	3.8	**9.9**	5.9	**14.2**
	ii 311	6.1		8.3	
C_{18} Stearic acid	i 299	2.3	**8.9**	4.8	**9.1**
	ii 283	6.6		4.3	
C_{18} Oleic acid	i 297	2	**5.6**	3.9	**6.8**
	ii 281	3.6		2.9	
C_{16} Palmitic acid	i 271	3.6	**12.2**	3.1	**11.4**
	ii 255	8.6		8.3	

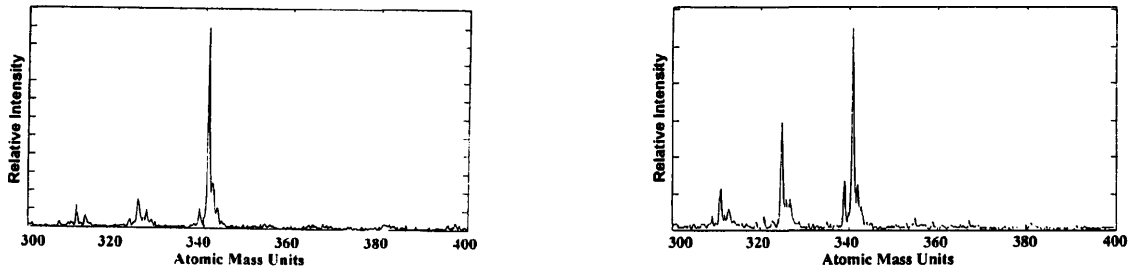

Unexposed **Exposed (208 hours)**

Figure 8 Negative ion SSIMS spectra of untreated scoured wool

CONCLUSIONS

Photostabilised wool blend fabrics will meet car manufacturers lightfastness standards depending on the blend percentage used. Both lightfastness and abrasion resistance of wool fabrics improves with increasing mean fibre diameter. Wool polyester blends have a pilling tendency making them unacceptable for automotive use, whereas wool nylon blends have a very high aged abrasion resistance. Fabric lamination increases the rate of photodegradation. Vibrational spectroscopy indicates surface and bulk disulphide bond photo-oxidation which is retarded by Cibafast W. Raman analysis also indicates changes in protein chain conformation. XPS shows photo-oxidation of the disulphide bonds occurs readily at the wool surface (outer 3 nm) at low exposure levels but remains incomplete even after extended exposure. No protection is given to the epicuticle by Cibafast W. SSIMS implicates a loss of C_{21} fatty acid from the epicuticle of wool after light exposure. XPS shows surface migration of photo-stabilisers in polyester and nylon, but in wool this migratory behaviour is still unproven.

ACKNOWLEDGEMENTS

The authors would like to thank Guilford Automotive, Nicolet Instruments, Ciba Geigy and Coates Viyella for financial support.

REFERENCES

1. B.Milligan, Rev. Prog. Col. 1986, 16, 1
2. C.H.Nicholls, 'Developments in Polymer Photochemistry' Vol.1 (Barking, Applied Science Publishers Ltd.) 1980, 125
3. I.L.Weatherall, Proc. 5th Int. Wool Text. Res Conf. Aachen, (1975), Vol.II, 580
4. W.Mosimann, L.Benisek, K.Burdeska, I.H.Leaver, P.C.Myers, G.Reinert, J.F.K.Wilshire, Proc. 8th Int. Wool Text. Res. Conf. Christchurch, 1990, Vol. IV, 239
5. Cibafast W: Technical Information Bulleton, Ciba Geigy
6. M.A.Parsons (Rover Group Ltd.), 'Fabric Performance Requirements for Automotive Use', Autotech Conf. Birmingham NEC, 1991 (C427/9/079)
7. C.D.Wagner, L.E.Davis, M.V.Zeller, J.A.Taylor, R.M.Raymond, L.H.Gale, Surf. Interface Anal. 1981, 3, 211
8. C.M.Carr, D.M.Lewis, JSDC, 1993 109, 21
9. F.J.Douthwaite, D.M.Lewis, U.Schumacher-Hamedat, Text. Res. J. 1993, 63, 177
10. U.Schumacher-Hamedat, C.Laurini, V.Schmider Proc. 8th Int. Wool Text. Res. Conf. Christchurch (1990), Vol. IV, 451
11. B.G.Frushour, J.L.Koenig, Advances in Infrared & Raman Spect.(Ed. R.J.H.Clark & R.E.Hester) Vol.1, 35, Heyden, London 1975
12. N.T.Yu, B.H.Jo, C.S.Liu, J. Amer. Chem. Soc. 1972, 94, 7572
13. J.Peeling, D.T.Clark, J. Appl. Polym. Sci. 1981, 26, 3761
14. C.M.Carr, S.F.Ho, D.M.Lewis, E.D.Owen, M.W.Roberts, J. Text. Inst. 1985, 55, 419
15. A.P.Negri, H.J.Cornell, D.E.Rivett, Aust. J. Agric. Res. 1991, 42, 1285
16. D.J.Peet, R.E.H.Wettenhall, D.E.Rivett, A.K.Allen, Comp. Biochem. Physiol. 1992, 102B, 36
17. R.J.Ward, H.A.Willis, G.A.George, G.B.Guise, R.J.Denning, D.J.Evans, R.D.Short, Text. Res. J. 1993, 63, 362
18. D.J.Peet, R.E.H.Wettenhall, D.E.Rivett, Text. Res. J. 1995, 65, 58
19. To be published